The influence of high temperatures on the tribological properties of automotive friction materials

Savage, Luke

Award date:
1995

Awarding institution:
University of Bath

THE INFLUENCE OF HIGH TEMPERATURES ON THE TRIBOLOGICAL PROPERTIES OF AUTOMOTIVE FRICTION MATERIALS.

Submitted by Luke Savage
for the degree of PhD
of the University of Bath
1995

COPYRIGHT

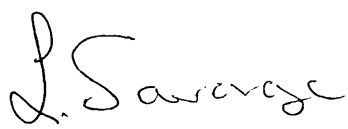

(Luke Savage)

ProQuest LLC
789 East Eisenhower Parkway
P.O. Box 1346
Ann Arbor, MI 48106-1346

Abstract

Temperatures of over 800°C can be generated at the frictional interface within the brake systems of large vehicles, such high temperatures result in severe wear at the frictional interface, and can also lead to a very dangerous condition known as brake fade, characterised by a sharp fall in the coefficient of friction between the pad and disc, resulting in a catastrophic loss of braking efficiency.
Common friction materials are very specialised composites often containing up to 15 components bound together within a phenolic resin matrix. The high temperature behaviour of the various constituents of friction materials were investigated using thermogravimetric analysis, focusing in particular on the thermal decomposition of the phenolic resin matrix material, where it has been firmly established that the thermal decomposition products of phenolic resin are the primary cause of brake fade. This has lead to the development of a novel approach for reducing fade in conventional resin based friction materials, involving a partial carbonisation to 400°C.

The high temperature wear characteristics of both modified and conventional friction materials were examined using standard dynamometer tests, as well as a 'continuous drag' type test machine, equipped with a heating facility. During this study a number of factors were identified as the main influences on the overall wear behaviour of friction materials. These included test temperature, sample test history, and the various effects of friction films, which were the subject of a detailed analysis.
The formation of friction films was found to be an important facet of a successful friction material, producing a reduction in wear at the frictional interface. Films were examined and analysed using EDX, SEM, and X-ray diffraction techniques, which revealed the presence of a high proportion of magnetite (Fe_3O_4), containing iron which originated from the disc surface. It was established that the incorporation of iron in friction material formulations encouraged film formation, thereby reducing disc wear substantially.

CONTENTS

Chapter Four

Chapter Five

(The development of improved friction materials)

==========

CHAPTER 1

General Introduction

1.1 Preface

Friction materials are used to provide the braking action in a whole variety of modern vehicles. As the brakes are applied, the friction material is pressed against a metal disc or drum, usually made of steel or fine grained cast iron. This action causes a frictional force to develop which resists the motion of the vehicle. Friction materials convert the kinetic energy of the moving parts, into heat energy within the friction material and surrounding brake assembly, this heat is then dissipated to the atmosphere.

Modern brake pads and linings are mainly resin bonded composites containing a range of fibrous reinforcements, friction modifiers, and fillers. Indeed, it is not uncommon for a particular friction material formulation to contain up to 15 different components. The reasons for this are that successful friction material formulations have been developed within the industry, using largely empirical methods. Different materials are added to the mix to adjust the physical properties for a specific application. This frequently results in over complicated formulations. Another reason for this is that friction materials require a diverse range of physical properties, which are not found in conventional materials, the more important of which are outlined below:-

a) Friction

The coefficient of friction of a brake material is the ratio of the applied force to the drag generated on the disc. The generally accepted standards [1] for the coefficient of friction (μ) of commercial friction material must:-

a) be no lower than 0.25 under "cold" conditions

b) be no lower than 0.15 under "hot" conditions

c) not fluctuate more than 20%.

Kragelskii [2] stated that the coefficient of friction (μ), must be reasonably stable (0.25 - 0.5), over a temperature range of -20°C up to 1000°C, (and up to 3000°C for aircraft). Also μ must not fluctuate with operating speed, or give rise to discontinuities in friction level (stick-slip).

b) Wear

Wear should be even across the frictionall surface, the amount of wear being kept to a minimum under all conditions, though not at the expense of the brake rotor or drum, which should not be worn, scored, or grooved, by the friction material.

c)Mechanical properties

Friction materials must have adequate compressive, shear, and fatigue strength, in order to cope with the compressive and shear forces generated each time the brakes are applied, so that mechanical strength and dimensional integrity are maintained during repeated brake applications.

d)Thermal properties

Frictional heating presents a serious problem to the friction material designer. Temperatures of 1000°C are known to have been reached at the brake interfaces of trains and large commercial vehicles. Such temperatures give rise to a phenomenon known as brake fade particularly in brakes containing phenolic resin systems. Brake Fade is characterised by a severe drop in the coefficient of friction during braking, and once the brake system has cooled the coefficient of friction returns to a higher level, this is termed "the recovery". This loss in coefficient of friction results in at best, a drop in braking efficiency, and at worst, total brake failure. The fade and recovery characteristics of friction materials is of particular importance to this work.

There is a large temperature gradient through the friction material thickness during operation, the form of the gradient depends on the rate of heat generation at the brake pad - rotor interface, and the thermal conductivity and thermal capacity of the friction material. If the thermal conductivity is too high, there is a danger that the hydraulic brake fluid will become heated and expand and even boil, resulting in total brake failure. Conversely if the thermal conductivity was too low, all the heat would be trapped at the interface, giving rise to high wear rates, and unstable friction levels.

Other temperature effects such as thermal expansion which cause thermal fatigue within the composite, should be minimised. Also the material must not ignite, soften, melt, swell, or grow.

In addition to the requirements listed, it is important that friction materials show low moisture/oil sensitivity, and must be corrosion resistant. On application the braking action should be free from judder, and brake squeal. The materials

themselves must be easily formulated, cheap to produce, and contain no potential pollutants or harmful substances.

Clearly there are many factors to be considered during friction material development, the improvement of one property may be detrimental to others, hence any changes made to a material to improve one particular property, must be accompanied by an investigation into how other properties are affected, and a balance struck to give the optimum set of material characteristics to suit the particular application.

Currently brake fade is one of the main causes of concern within the automotive brake industry. In lighter vehicles such as cars and vans, the effect is not common under normal conditions. However, recent trends in brake system design has seen a move towards the increasing use of rotor-pad combinations, as opposed to drums and linings. There is also a drive towards smaller, lighter brake systems to aid fuel economy, with an accompanying increase in power to weight ratio in modern vehicles. These changes will result in a reduction in the size of brake pads, with a relative increase in the amount of kinetic energy to be absorbed. Consequently there will be an increase in temperature per unit area of friction material, leading to increased fade problems.
Brake fade is a more serious problem in off-road industrial earth moving equipment used in quarrying, large juggernauts, and also in high performance motor cars and motorbikes. In these applications much higher temperatures are generated at the brake interface, due to the higher loads put on the brake system.

Kragelskii [2] proposed a mechanism for brake fade based on the decomposition of the resin matrix at elevated temperatures, the resulting products acting as lubricants between the sliding surfaces, thus causing a drop in the coefficient of friction (μ).
Herring [3] also stated that the breakdown of the phenolic resin matrix was the major contributor to weight loss in organic brake linings, the weight loss being due to gaseous products being given off at temperatures above 260°C. As higher temperatures were encountered, higher molecular species were evolved. Herring was primarily working on brake drum lining friction pairs, and concluded that the main reason for fade was due to a build up of gaseous products at the interface, causing back pressure opposing the load applied by the calliper on the lining, resulting in a drop in friction.
In the past anti-fade materials have been developed for specialist applications such as the aircraft industry where braking conditions are far harsher. For

instance, the energy which must be dissipated when braking a Boeing 707 weighing approximately 170,000 Kg, moving at 320 Km/h, is 670 MJ or the equivalent of 2000 cars travelling at 60mph. All this energy has to be dissipated within 30 seconds in the worst possible case. Consequently the temperatures reached at the brake interface can be as high as 3000°C [4].
Quite obviously special materials with frictional stability at high temperatures were needed. This criteria was fulfilled by carbon/carbon composites which have added advantages of a 40% weight saving over conventional steel based brakes, good thermal shock resistance, and high heat capacity (2.5 times that of steel) [4].

Carbon/carbon composite brakes are made by using carbon fibre as a reinforcing material in the form of fabric laminates, or semi-random chopped fibre mats. These are then impregnated with phenolic resin, pitch or CVD carbon to densify the composite. There is often more than one densification cycle carried out in order to achieve the desired density. Anti-oxidants can also be added, which blocks active sites preventing attack by oxygen. Carbon/carbon composite friction materials are also being used as disc, brake pad, and clutch materials in formula 1 racing cars and bikes, to take advantage of the low weight and the good frictional performance of these materials.
Heat dissipation is a problem in racing brakes, the repetitive brake applications does not allow the heat generated to escape. Disadvantages of carbon/carbon brakes and clutches are that the coefficient of friction was found to be unstable at low temperatures [5], and they are very expensive to produce, consequently they are only used in the specialist applications outlined above.
Another group of friction materials which have been developed without the use of a resin matrix are sintered metal friction materials, which show good thermal stability, and are used as the frictional components of high performance motorbikes. These materials contain metal powders such as iron, brass, and bronze, as well as lubricants, typical examples being graphite powder and molybdenum sulphide, and also friction modifiers such as particle abrasives (e.g. alumina, mullite or silica) [6]. The powder mix is then heated under pressure to temperatures below the melting points of the metals, until the powder particles coalesce forming diffusion bonds between the metal particles. There is no resin binder, or any other organic content, and so the material possesses high thermal stability and thermal rupture resistance, and hence shows negligible high temperature fade. However, sintered materials are known to exhibit poor low temperature performance, and under high temperature conditions, μ can climb to a dangerously high level, which can lead to local

melting, producing fade [7]. Again, a serious drawback of these materials is that production is expensive.

Clearly the removal of the volatile organic constituents from friction materials, imparts fade resistance. The primary aim of this work is to investigate the possibility of producing an economic, fade resistant, friction material which could be easily formulated using similar equipment and production techniques, presently being used to make conventional brake pads. It is proposed that this could be achieved by pre-carbonising existing friction material formulations, as well as other specially developed materials. The result of this would be a partial or complete removal of the volatile components, from within the phenolic resin binder and other organic constituents, which have been identified as the root cause of fade.

This study investigated the tribological characteristics of pre-carbonised friction materials using a B.I.C.E.R.I universal wear machine, (commonly referred to as a pin on disc machine) situated at the University of Bath. Promising formulations were tested on an automobile inertia dynomometer situated at European Friction Industries (The industrial sponsors of this work).

1.2 The Development Of Friction Materials

Up until the twentieth century non-specialised materials such as wood, leather, and metal were used as brake materials, but as the automobile and aircraft industries advanced, larger vehicles which could travel at higher speeds were developed. Non-specialised materials could not cope with the higher work load, and hence temperatures, created during braking. Their friction surfaces would become carbonised which lead to a loss in coefficient of friction, hence there was a need to develop specialised heat resistant brake materials [8].

Herbert Frood started producing resin impregnated woven cotton brake linings in 1901 [9]. The woven cotton was superseded in 1908 by woven asbestos, a material which possessed greater temperature resistance, and retained a high strength up to 450°C, and thereby giving a more reliable coefficient of friction during use. It was also cheap, and possessed good mechanical properties. By the 1930's thermosetting phenolic resins were introduced. These resins which could withstand even higher working temperatures, were needed with the advent of disc brakes, as disc brake pads are smaller than drum brake linings, and so have to absorb more energy per unit area of friction surface.

In the 1970's the dangers of asbestos dust became apparent, which lead to legislation seeking the removal of asbestos from public places [8], and promoted investigations into possible asbestos contamination from disc pads and drum brake linings. Jacko [10] studied the gaseous and particulate emissions from automotive brakes, and put the asbestos content of these emissions at 1.65% or less. Despite this, brake manufactures have striven to develop a suitable replacement fibre for asbestos. This has not been easy due to the unique set of properties asbestos possesses. Amongst the fibres tried have been steel [11], potassium titanate fibre [12], glass fibre [13], carbon fibre [14], organic fibres such as aramid [15], and various ceramic fibres [16], [17]. As a result, currently 85 - 90% of new European passenger cars are fitted with asbestos free brakes, with commercial vehicles moving in the same direction [8].

Modern automotive brake pads contain a large range of component materials which can be categorised according to the function each performs:-

The Matrix

Phenol - Formaldehyde resins are universally used to form the matrix in brake pads and linings. There are two main methods of producing phenolic resins, a one stage process or a two stage process, which differ in the end product that they produce.

The one stage process involves phenol being reacted with excess formaldehyde, so that the P:F ratio is < 1. This mixture is heated together with an alkaline catalyst, to produce a liquid resin called Resol. If this resin is further heated to higher temperatures, an insoluble hard solid is produced.

The two stage process involves the same mixing of phenol and formaldehyde, but with the P:F ratio > 1. The mixture is heated with an acid catalyst, the result being a solid known as Novolac, which is normally ground to a powder and mixed with hexamine, which produces methylene bridges within the final resin structure, and leads to a higher degree of cross linking.[18]. Novalac-hexamine resin powders are the type used to produce modern friction materials.

The phenolic resin powder is mixed with other powdered ingredients, making up typically 6 - 15% wt, of the final composite. The mix is then moulded using a heated die under a pressure of 4000 p.s.i. The die temperature is maintained at approximately 150°C, which allows the Novalac resin to melt and flow, forming a matrix binding all the other constituents together.

Fibres

Fibres provide increased strength, stiffness, and a higher resistance to thermal shock. The rapid fluctuations in temperature at the surface of friction materials during braking result in high surface stresses, which may lead to thermal cracking. Fibrous reinforcement, dissipates the energy at the crack tip, so curtailing its propagation into the body of the material.

Modern friction materials are categorised according to the type of fibre reinforcement they contain. Firstly there are the non-asbestos organics, which utilise a combination of aramid fibres, glass fibres, and mineral fibres produced from rock and other mining by-products, which are melted and then spun into fibres. The other group of materials are the semi-metallics, which utilise a metal fibre reinforcement, the most common being steel wool.

Friction Modifiers

Solid lubricants are added to produce uniform levels of friction at the interface, and also to keep the coefficient of friction from rising above approx. 0.7, which will help keep operating temperatures and wear rates low. A blend of lubricants is generally preferred, as operating temperatures cover a wide range. Graphite powder, coke, and molybdenum disulphide are most effective at low temperatures, and calcium fluoride, lead or antinomy sulphide, lead oxide, and low melting metals give higher temperature lubrication.

Abrasives are also added in small amounts in order to increase the level of friction and reduce the wear rate of the friction material. The proportion added as well as the particle size, and morphology, are factors which should be carefully considered, so that brake rotor damage by ploughing or scoring is avoided. Examples of typical abrasives used are refractory oxides, silicates, and magnesium oxide.

Fillers

Fillers are generally low cost materials which are added in relatively large amounts. However they are seldom totally inert in tribological terms, and often play an integral part in the overall properties of the friction material. The most commonly employed are barytes (barium sulphate), perlite (an expanded volcanic glass), and vermiculite (a naturally occurring form of mica).

Metal fillers in the form of powders or chippings are added to improve the thermal conductivity of the friction material, which in turn improves thermal resistance. Typical examples of these are copper, bronze, brass, and zinc. Semi-

metallic friction materials frequently contain larger quantities of metal fillers such as sponge iron.

Organic fillers include rubber from ground up tyres, and "friction dust" derived from cured and powdered cashew nut resin. Organic fillers impart flexibility to the friction material, this increases the surface contact between the brake pad and rotor during operation. They also have the ability to absorb vibration and so reduce brake noise generation. However, organic fillers are the least thermally stable and consequently contribute to brake fade at high temperatures.

1.3 Theories of tribology

1.3.1 Introduction

Since civilisations began, such as those in Sumaria and Egypt 5000 years ago, man has been aware of the frictional and wear phenomena associated with contact between surfaces moving relative to one another. In some cases this was found to be beneficial, e.g. carpenters used hard materials such as bone or stone to fashion wood boring drills. The more undesirable frictional effects were also encountered when moving heavy stones or carvings on rollers. Pictorial evidence from the time of the Egyptians, clearly shows the use of oils as lubricants to ease the path of heavy loads, during construction work[19].

Aristotle (330 BC) wrote of the force of friction and recognised that it was related to the shape of objects. Leonardo da Vinci (1470 AD) recorded the fact that heavier objects required more effort to make them slide along a surface than lighter ones. The first scientific work on friction was carried out by Guillaume Amontons (1663 - 1705).

1.3.2 Theories of friction and contact between surfaces

Amontons (1699) elucidated a simple model for friction based on two laws:-

i) Frictional force (F) is directly proportional to the applied load (L)

$$F = \mu L$$

where μ = Coefficient of Friction. This is the Amontons equation.

ii) Frictional force (F) is independent of apparent area of contact (a).

Amontons knew that the surfaces he worked with were not perfectly flat, and other workers such as Desagulier (1740) found that on polishing surfaces, frictional force was found to rise. He attributed this behaviour to adhesion effects between the surfaces. This theory was rejected by Coulomb (1781) as he argued that if friction was due to adhesion between two surfaces, then the adhesive forces involved would rise if the surface area between two objects was increased. His experiments showed him that this was not so. He also stated a third law :-

The coefficient of friction is independent of sliding speed[20].

The third law is less stringent than the other two, and has been founded on the observation that the coefficient of static friction (μ_s) is greater than the coefficient of dynamic friction (μ_d), but once sliding has been initiated μ_d is found to be independent of sliding velocity, up until very high velocities are encountered, of the order of hundreds of metres per second [21].

For a complete understanding of the causes of friction a closer look at surface contact was required. Bowden and Tabor [22] proposed that when two surfaces touch they make contact only at the tips of the surface asperities, resulting in the real area of contact (A), being very much smaller than the apparent area of contact (a). It was argued that since the asperities supporting the load have such small cross sectional areas, plastic flow would occur even at very low applied loads. The promontories would yield plastically until their areas of contact were large enough to support the applied load (L) thus :

$$\sigma_y = L / A \qquad (1.1)$$

where σ_y = Yield Stress of the softer material in compression.
A = Real area of contact.

This plastic deformation results in localised adhesion of the surfaces. If relative sliding occurs, a resisting frictional force has to be overcome, in order for sliding to continue. This resisting force develops from two sources, a

deformation force (Fdef), which resists the ploughing action of hard asperites, through a softer material, and an adhesion force (F_{adh}), which must be overcome, in order to break the adhesive junctions which exist at points of real contact between the two surfaces. Both the adhesive force and the deformation force contribute to the measured value of μ. It has been shown experimentally that the deformation contribution to coefficient of friction, μ_{def}, is less than 0.1, while the adhesive contribution provides the main resistance to sliding, and hence the major contribution to μ. The force F_{adh} required to shear these junctions, can be represented by the following equation:

$$F_{adh} = A\,\tau_y \qquad (1.2)$$

where τ_y = Shear Stress of softer material

A = Area of real contact.

now combining equations (1.1) and (1.2).

$$F_{adh} / L = A\tau_y / A\sigma_y = \mu_{adh} \qquad (1.3)$$

hence $F_{adh} = \mu L$

which is a statement of Amonton's first law of friction. Now that it has been shown that plastic deformation resulting in localised adhesive bonding produces the main resistance to sliding in metals, early observations within frictional systems can be explained.

If the apparent area of contact is increased the load on the surface is spread over a larger number of asperities, hence lessening the plastic deformation at each of the asperities with no increase in the real area of contact, and hence no increase in friction. If however the real area of contact (A) is increased, e.g. by polishing surfaces or by increasing the load on the surface, friction rises.

In practice the ratio of τy: σy in most metals is 1 : 5 and from the simple relationship:-

$$\tau_y/\sigma y = \mu_{adh} \qquad (1.4)$$

A value in the order of 0.2 would be expected for the adhesive contribution to μ, and together with the deformation contribution (μ def < 0.1), a maximum of 0.3 for μ could be possible for metal-metal combinations in air. However experiment has shown that many metal combinations in air give values of $\mu >$ 0.5. This indicates that the real area of contact between metals must increase during sliding, to explain the higher value of μ found in practice.

Bowden and Tabor [22]. suggested an extension to the simple theory which states that the tangential force evolved in the shearing of asperity junctions, adds to plastic deformation at the junction, producing junction growth and increased real area of contact (A). In some cases (A) can be increased to such an extent that it equals the apparent area of contact (a). Frequently when this occurs the applied tangential force is no longer sufficient to shear the two surfaces, resulting in seizure and the principle behind the technique of cold welding in metals.

The Bowden and Tabor theory explains the two fundamental laws of friction, and gives coefficients of friction of the correct magnitude for metals, but the theory relies solely on the breaking of adhesive bonds, to explain the shear forces required to produce sliding in a frictional system.

Kragelskii [2] suggested that the mechanism of friction was a dual molecular - mechanical interaction of asperities. Similarly Edwards and Halling [23] considered the effect of junction angles on friction, and concluded that the coefficient of friction (μ) is dependent on junction angle, and that the Bowden and Tabor theory is a special case where the junction angle equals zero. This theory is based on the premise that asperities interact, leading to ploughing effects where hard asperities penetrate into a softer metal substrate, thus inducing plastic flow in the softer metal.

The above treatment assumes the tips of asperities in contact, deform plastically under loading, and from equation (1.3):-

$$L \alpha A \ \alpha \mu$$

For contact between metal surfaces finished by conventional engineering processes, this assumption is valid [21]. However, many polymers differ fundamentally from metals in that the deformation of their asperities is predominantly elastic.

Hertz (1881) studied the elastic behaviour of an elastic sphere in contact with a

Figure 1

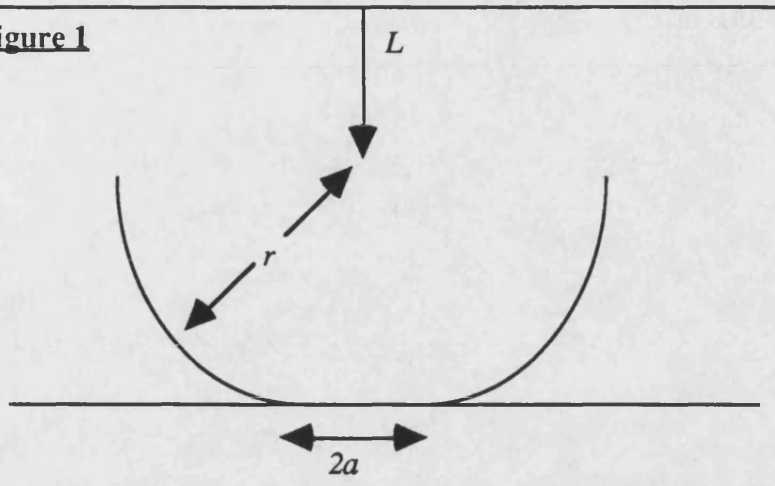

Elastic deformation of a sphere of radius r, pressed against a plane surface under a load L.The diameter of the contact circle is 2a [21].

flat plane under a load (L), see fig 1.

Contact occurs over a circular area of radius (a), where:-

$$a = \left(\frac{3Lr}{4E}\right)^{1/3} \tag{1.5}$$

Here r is the radius of the sphere, and E is the elastic modulus, which is derived from the young's moduli of the two materials E_1, and E_2, and also ν_1 and ν_2, the Poisson's ratios, for the two materials:

$$\frac{1}{E} = \frac{(1-\nu_1^2)}{E_1} + \frac{(1-\nu_2^2)}{E_2} \tag{1.6}$$

From eqn. (1.5) the area of contact between the sphere and plane is approximately:-

$$\pi a^2 = 0.83\,\pi\left(\frac{Lr}{E}\right)^{2/3} \tag{1.7}$$

Hence for elastic deformation of asperites:

$$A \propto L^{2/3}$$
$$\mu \propto A/L \propto L^{2/3}/L \propto L^{-1/3}$$

This indicates that while μ stays proportional to the real area of contact (A), when load (L) is increased, there is a fall in μ as the real area of contact is no longer proportional to (L).

In order to quantify the limit of plastic behaviour for all materials, Greenwood and Williamson [24] defined the term "plasticity index" (ψ), in the form:

$$\psi = \frac{E}{H} \cdot \left(\frac{\sigma}{r}\right)^{1/2} \qquad (1.8)$$

Where E is defined in Eqn. (1.6), H is Vickers indentation hardness and $(\sigma/r)^{1/2}$ is approximately equal to the average slope of the asperities, where (σ) is the standard deviation of the asperity hights, and (r) is the average radius of an asperity. If $\psi < 0.6$, then the asperities will behave elastically under most conditions. If $\psi > 1.0$, then plastic flow occurs most commonly. Most metals have a plasticity index larger than 1.0, while a ψ of <0.6 is found in a wide range of polymers including high and low density polyethylene, PTFE, PMMA, rubber, and some epoxy resins [21].
Polymers also exhibit viscoelastic behaviour, where the deformation of asperities and flow stress is dependant on strain rate. In practice polymers have coefficients of friction between 0.2 - 0.4, when sliding upon themselves, with the notable exception of PTFE which has a μ value approaching 0.05.
Generally friction between two solids can be affected by a number of different parameters, such as the plasticity index, which changes with temperature, sliding velocity, material surface finish, and the materials themselves, and the presence of oxide films. The value of μ is constant only for a given pair of materials under a certain set of conditions.

1.3.3 Mechanisms of Wear

Wear is defined by the Institute of Mechanical Engineers as " The progressive loss of substance from the surface of a body brought about by mechanical action". Burwell [25] defines it more simply as " The unwanted removal of solid material from rubbing surfaces". Both these definitions encompass a range of phenomena which may occur during relative sliding of two surfaces e.g. abrasion, adhesion, corrosion, galling, surface fatigue (fretting). Any number of

as there are for friction, although the work carried out in the field has been extensive.

Generally wear increases with greater sliding distances, higher loads, and within softer materials. Bowden and Tabor [22] make the distinction between surface damage, and wear, where the former may well occur with the absence of the latter. This indicates that the formation of wear particles is the area of importance when considering different types of surface damage phenomena. Adhesive and abrasive wear are the dominant wear mechanisms in brake materials, and will be discussed in detail.

i) Adhesive Wear

Cold welding at specific asperity junctions, plus tangential motion at these points leads to shearing and reformation of these junctions. This process leads to wear. The amount of wear generated in this way is governed by the way in which the junction is sheared. This may occur at the interface between the two materials, leading to little wear, but if the junction is stronger than one of the materials, shearing will occur within the body of the softer material. If both materials are softer than the interface, then again failure will occur within the material bulk. It was seen earlier that all junctions contribute to friction, but not all contribute to adhesive wear, i.e. to the formation of a wear particle.

Archard [26] used a k factor to represent the fraction of friction junctions which produce wear. Burwell [24] derived a similar function $k' = k/H$ where H is the indentation hardness of the softer material, and called it the adhesive wear coefficient. The Archard equation for adhesive wear assumes that the area of asperity contact $(a') = \pi r^2$ and each contact supports a load L where:

$$L = \sigma_y \pi r^2 \qquad (1.9)$$

where σ_y = Yield stress of the softer material.

r = Radius of asperity.

If a junction is sheared during sliding, a distance of $2r$ will have been travelled. Assuming the wear fragment produced is hemispherical, then each will have a volume of $2/3\ \pi r^3$. If the total wear volume / unit sliding distance is (Q) then :

$$Q = \Sigma \frac{\frac{2}{3}\pi r^3}{2r} \qquad (1.10)$$

or

$$Q = \Sigma \frac{1}{3} \pi r^2 = (\frac{\pi r^2}{3}). \qquad (1.11)$$

If each contact supports a load of $\sigma y\, \pi r^2$ then total load $L = \sigma y\, \pi r^2 n$ .where n equals the number of contacts, and it follows that:-

$$n \pi r^2 = \frac{L}{\sigma y} \qquad (1.12)$$

From eqn. 1.11 : $Q = \frac{L}{3\sigma y}$ (1.13)

If k = the number of asperities contributing to wear particle formation then:

$$Q = k\frac{L}{3\sigma y} \qquad (1.14)$$

Clearly Archard has related wear volume to $1/\sigma y$ the reciprocal of yield stress. Burwell said volume of wear was proportional to $1/H$ the reciprocal of hardness, hence both these results are essentially the same. Adhesive wear is affected by the condition of the surfaces, with clean surfaces greatly enhancing the formation of adhesive junctions, so increasing wear. A vacuum environment also promotes strong adhesion and hence greater wear. The operational conditions such as temperature have a pronounced effect, this is most apparent when the melting point of one of the friction pairs is reached, then adhesive wear becomes very severe.

Bowden and Tabor [22] found that load (L) had a profound effect on the wear of metals and that when the load was increased above a certain limit the wear rate suddenly jumped, increasing by a factor of 100 to 1000 times. This jump from mild to severe wear is illustrated by figure 2, a characteristic plot of wear coefficient (k/H), against average pressure (~load), for steels of different hardnesses:

FIGURE 2

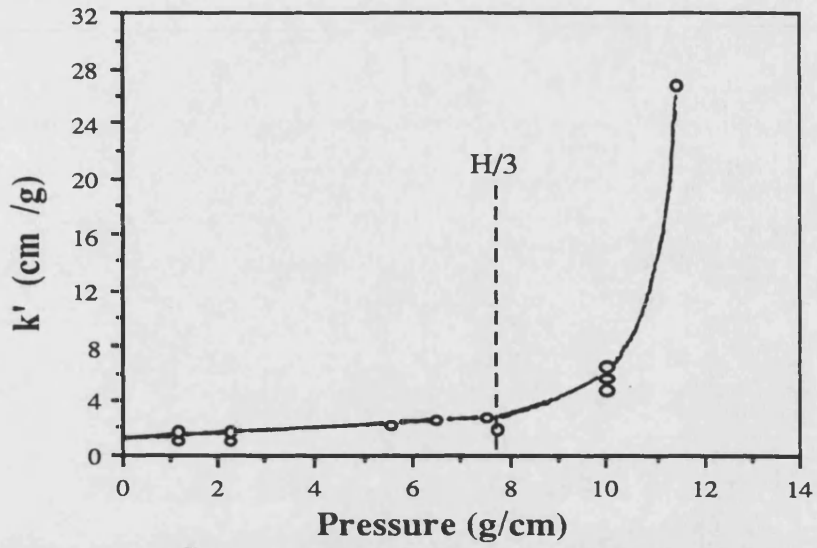

Value of wear coefficient k' vs the average stress for steel having a hardness of 233 Brinell. slider: 120° cone; steel S.A.E 1095; speed: 20cm/second.[25].

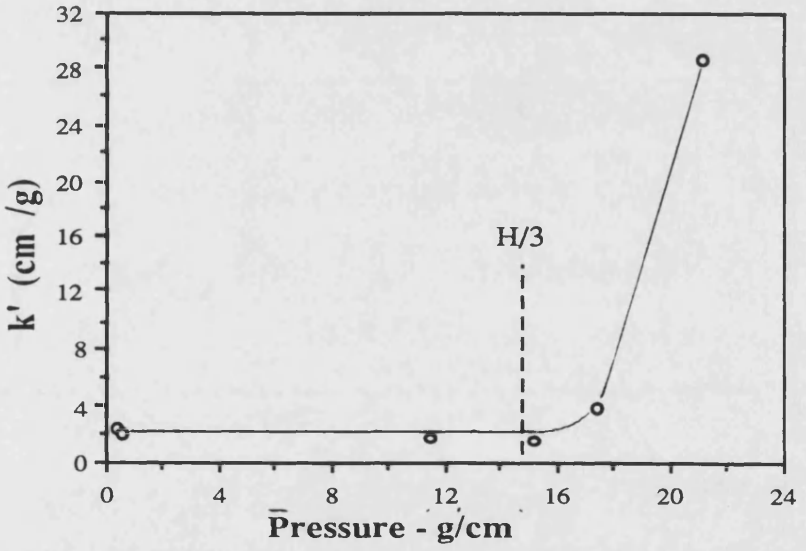

Value of wear coefficient k' vs the average stress for steel having a hardness of 430 Brinell. Slider : 120° cone; steel: SAE 1095; speed 20cm/second [25].

The wear coefficient remains fairly constant for a time, up to a critical pressure of about $H/3$ (H = hardness of steel), after which there is a rapid increase in the wear coefficient. Bowden and Tabor explained this phenomenon indicating that the critical pressure value $H/3$ represented the point at which the surface oxide present on the metal was penetrated resulting in larger adhesive junctions.

ii) Abrasive Wear

Burwell [25] identified two mechanisms of abrasive wear, both of which result in a loss of material from a softer surface due to a ploughing or scoring action of a harder surface. The first of these mechanisms involves two surfaces in rubbing contact, the asperities of the harder material ploughing a track through the softer material. The second mechanism involves a small hard particle which acts as a third body between rubbing surfaces. This third body could be grit or even environmental airborne dust, it could also originate from other wear processes, such as a product of corrosive wear which can often possess higher hardness than the materials which produced them, or it could be a work hardened wear particle.

In general abrasive wear increases as the dissimilarity of hardness between surfaces increases, and is also accentuated when there is a definite amount of roughness in the harder of the two surfaces.

There is no specific law governing the extent of abrasive wear, though abrasive wear can involve plastic flow or brittle fracture. Both types of behaviour have been modelled independently of each other, whereas in reality both mechanisms can occur in the same system, at the same time. Halling [27] has proposed a quantitative expression for abrasive wear involving the removal of material by plastic deformation. The model is based on two surfaces in contact, one consisting of hard conical asperities possessing a semi angle q (see Figure 3).

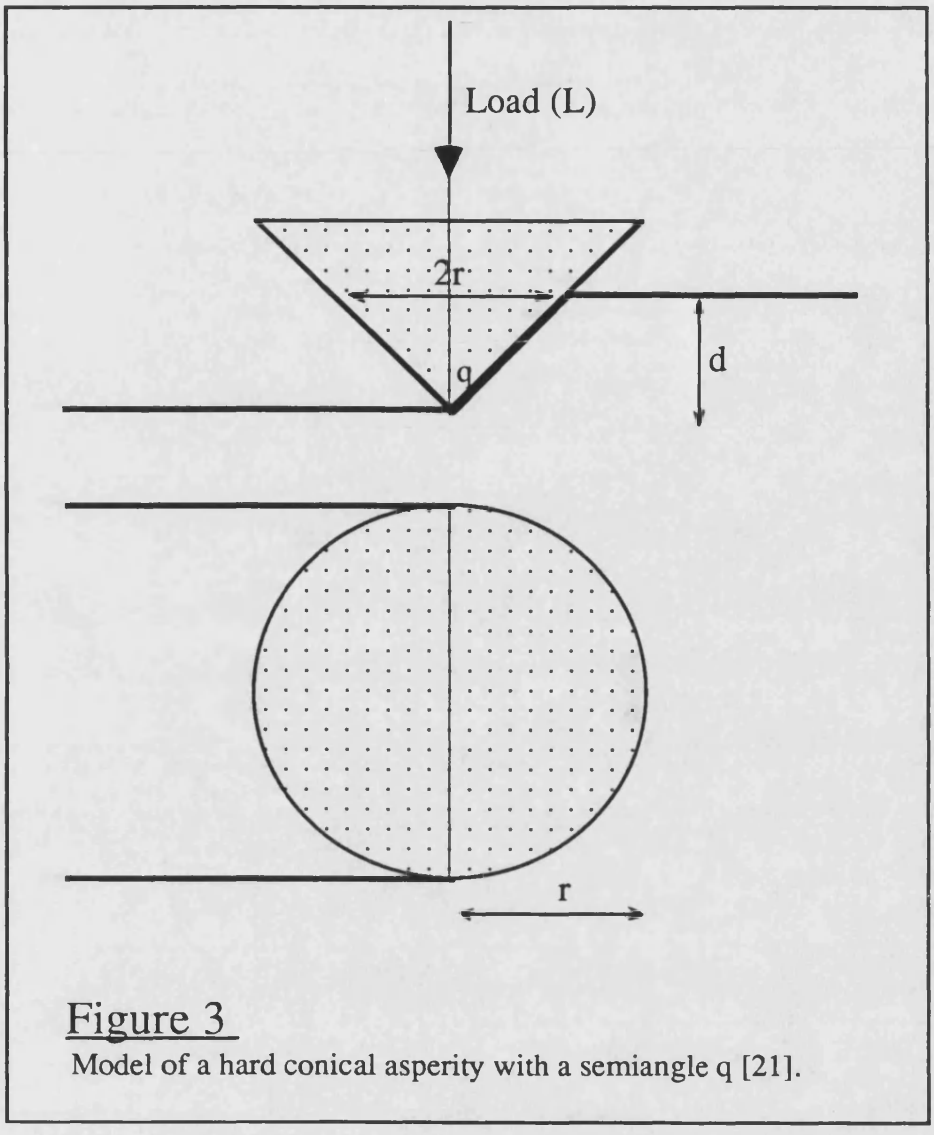

Figure 3

Model of a hard conical asperity with a semiangle q [21].

If the volume of material removed in a unit distance of sliding is *rd*.
where *d* = depth of penetration of the asperity, and *r* = asperity radius, then:

$$d = r \,.\, 1/\tan q = r \cot q$$

If (*Q*) equals the volume displaced in unit sliding distance

$$Q = nr^2 \cot q \qquad (1.15)$$

where *n* is number of asperity contacts.

If the asperity supports a load $L = \pi r^2 \sigma_y$
where σ_y is the yield stress of the softer material.

$$\text{Total } L = n\pi r^2 \sigma_y \qquad (1.16)$$

Eliminating n by combining eqns. 1.15 and 1.16 :

$$Q = \frac{L \cot q}{\pi \sigma_y} \qquad (1.17)$$

This can be simplified if hardness $H \sim \sigma_y$ the yield stress of the softer material, and by introducing (ka) a constant :-

$$Q = ka\, L/H \qquad (1.18)$$

(H = hardness of softer material)

This indicates that the wear rate should be directly proportional to sliding distance, and the load on the sample (L), which agrees with experimental observation [21]. Wear resistance has been shown to be proportional to the hardness of the softer material, which is in agreement with the work of Oberle [28] who indicated the importance of modulus of elasticity on abrasive wear. If a material can deform elastically to allow the passage of a harder asperity or particle, then wear will be kept to a minimum, and the hardness / elasticity (H/E) ratio, for a material can be used to indicate its wear resistance relative to others.

The second mechanism of abrasive wear is by brittle fracture. When a material surface is indented by an asperity under a high load, local plastic deformation can occur at the contact point, These intense stresses are relieved by plastic flow at the asperity tip, as illustrated in (a) Figure 4:

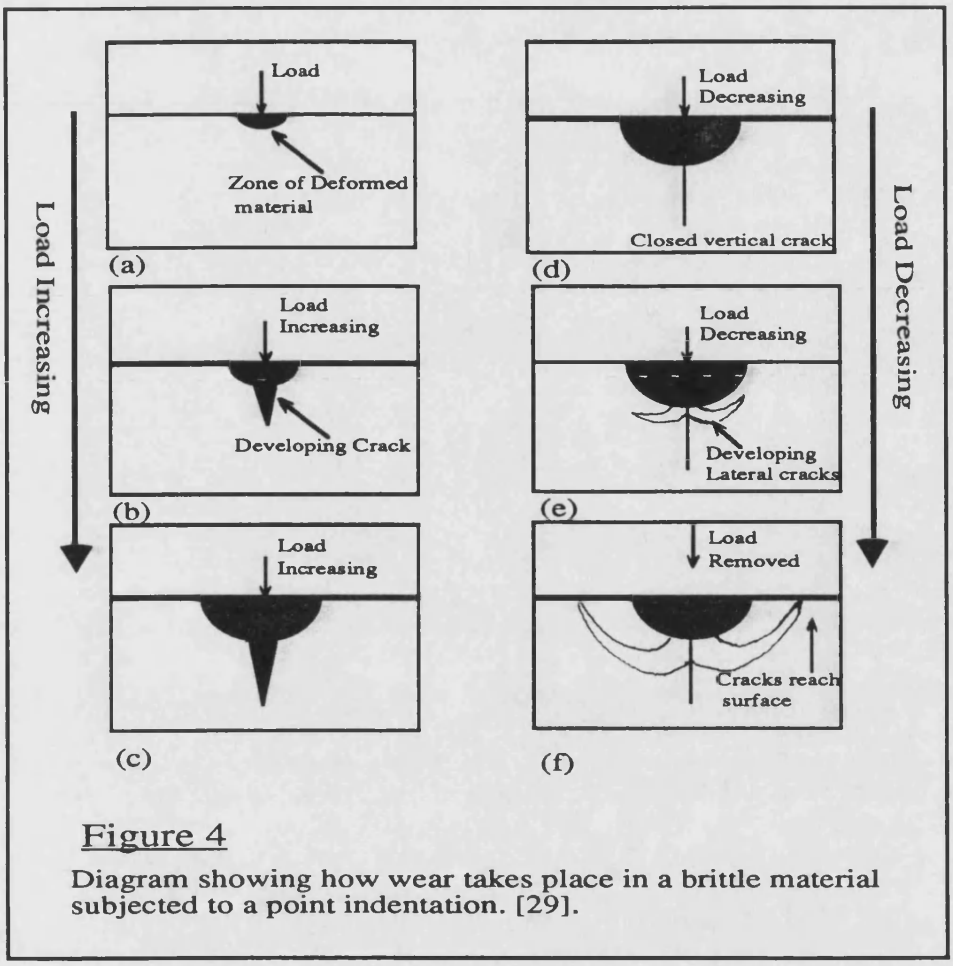

Figure 4

Diagram showing how wear takes place in a brittle material subjected to a point indentation. [29].

If the load on the indentor reaches a critical value a vertical crack initiates, (Fig 4b). As the load increases the crack grows (Fig. 4c). On reducing the load, the crack closes, and lateral cracks develop (Fig. 4d-f) The energy for the formation of these lateral cracks comes from the residual elastic stresses, induced by the relaxation of deformed material under and around the crack tip. Lateral cracking only proceeds once a critical load (w) has been exceeded. The value of (w) is determined by the fracture toughness Kc, and the hardness H of the material:

$$w \approx \left(\frac{Kc}{H}\right)^3 Kc \qquad (1.19)$$

The ratio of H/Kc is referred to as the brittleness index, and is a useful guide to the brittleness of a material, a low value, corresponds to a high value of w, which indicates that the material is resistant to fracture on indentation. A range

of other models for wear by brittle fracture exist, but all show Q to be dependant on w, H, and Kc.

A model for the brittle fracture of grey cast iron is of particular interest to this work, as it is commonly used for the fabrication of brake discs, and so shall be detailed here. Grey cast irons contain flakes of graphite, as the abrasive particle slides over graphite lamellae, cracks open up within the planes lying perpendicular to the sliding direction of the abrasive particle. (Figure 5):

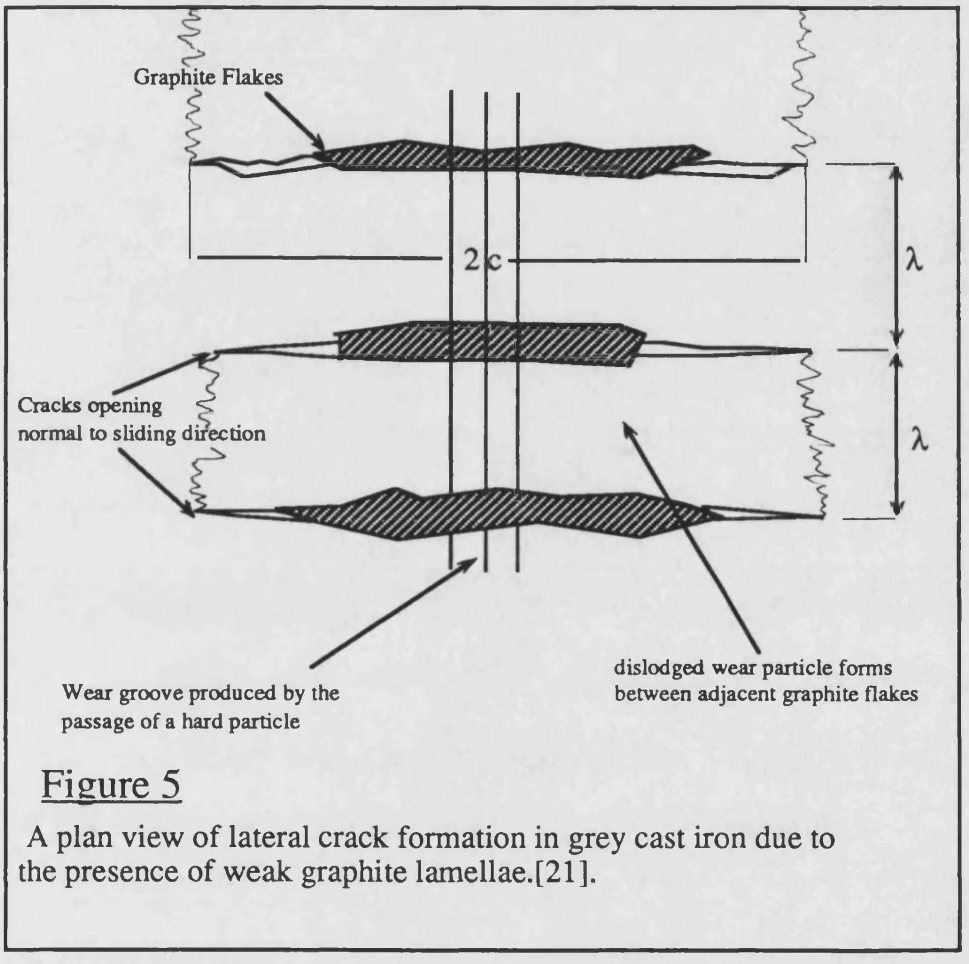

Figure 5

A plan view of lateral crack formation in grey cast iron due to the presence of weak graphite lamellae.[21].

The size of the wear particle produced is determined by the depth of penetration of the abrasive particle, the width of the cracks in the graphite flakes, $2c$, and the mean separation of the adjacent flakes (λ). It can be shown that this model gives an expression for the wear rate Q thus:

$$Q = \alpha_6 \, N \frac{w^{3/2} H^{1/2}}{K_C^2} \qquad (1.20)$$

Where N is the number of particles causing wear, and α_6 is a factor dependant on μ for the system, the geometry of the abrasive particle, and the spatial distribution of the graphitic lamellae. Once again Q is found to have the same functional dependence on w, H, and Kc.

iii) Abrasive wear in polymers

Lancaster [30] Examined abrasive wear of polymer surfaces sliding against rough metal surfaces, abrasive papers, and metal gauzes, and concluded that because the elastic moduli of polymers is lower than that of metals, elastic deformation will occur much more frequently than plastic deformation, during relative sliding of polymer surfaces. Two distinct mechanisms of abrasive wear were identified:-

Plastic deformation and cutting by hard asperities into the polymer, is a type of wear caused by asperities which are very sharp, whilst elastic deformation and fatigue is due to more rounded asperities. Rigid polymers showed rapid wear rates in comparison with most metals, due to the main wear mechanism being plastic deformation and cutting. In polymers where elastic deformation of asperities predominates, far lower wear rates occurred. Lancaster [30] also attempted to correlate wear rates of polymers with their physical properties, such as elongation and breaking strength. (figure 6). The results showed that polymers which are able to deform to allow the passage of a harder asperity, show a lower wear rate than those which show more brittle behaviour.

FIGURE 6

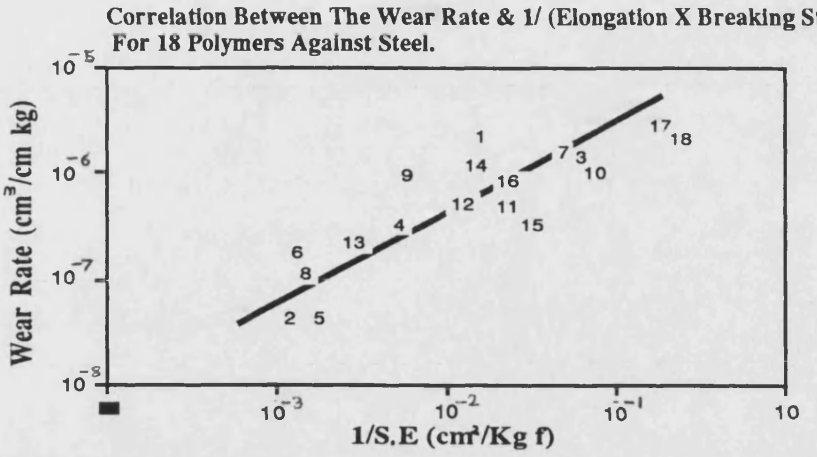

Correlation between wear rate during single traversals on 47 min. c.l.a. steel and 1/ (elongation x breaking strength) for 18 polymers. 1- Polymethylmethacrylate; 2- polyethylene (low density) ; 3- polystyrene; 4- acetal copolymer; 5- nylon 6.6; 6- polypropylene; 7- epoxy (828); 8- P.T.F.E. 9- PMMA-acrylonitrile copolymer; 10- polyester (17449); 11- P.T.F.C.E.; 12- polycarbonate; 13- nylon 11; 14- A.B.S. 15- polyphenylene oxide; 16- polysulphone; 17- P.V.C.; 18- polyvinylidene chloride [30].

Halling [27] discusses how generally the wear in polymers is low and can be predicted, for differing conditions of load and speed, using PV factors where P is the pressure and V is the velocity at the sliding surface. It can generally be shown that PV ~ linear rate of wear. (This assumes volume wear rate is proportional to the rate of energy dissipation).

As the steady state wear rate Q is proportional to PV, a wear coefficient K may be introduced :

$$Q = K\,PV \qquad (1.21)$$

If the wear rate Q is known for one PV value, then K can be calculated and used to find wear rates at other PVs for the same material and conditions.

iv) Summary

Wear may involve plastic deformation of material or brittle fracture. The occurrence of one or the other is dependent on the severity of the contact conditions, and the nature of the particular materials involved. For example in systems where there are large, hard, angular asperites, rubbing under high loads, against material with a low fracture toughness, wear by brittle fracture is

favoured. Under less severe conditions and within materials with high fracture toughness values, abrasive wear by plastic deformation predominates.

Abrasive wear by brittle fracture can give higher wear rates than by plastic deformation, as wear by brittle fracture can increase more rapidly than linearly with load, whereas the Archard equation for wear gives a linear relationship with increasing load.

Generally, wear resistance is governed by Kc, during brittle fracture, and by hardness during abrasive wear by plastic deformation. There are important exceptions however, polymers show a poor correlation between material hardness and abrasive wear, but a much better one when plotted against ultimate tensile strength and elongation, (Fig. 6).Also some ceramics and metals have comparable hardnesses but very different wear rates. This is because the plasticity index (or more simply E/H where E is Youngs modulus and H is hardness) is different for the materials. This is important because the ratio of E/H, dictates whether material deformation occurs by cutting or ploughing. A low value as found in ceramics, indicates that cutting will predominate rather than ploughing, and hence a higher wear rate will result. Ploughing is the dominant mechanism in metals, and this explains why they have a greater resistance to abrasive wear compared to ceramics of the same hardness [20].
Clearly, modelling wear even in the simplest systems is a complicated task, involving the consideration of both the physical properties of the materials involved, and the conditions under which wear is taking place. In automotive brake systems, the situation is further convoluted as it involves two dissimilar materials, one of which is an in-homogeneous composite containing hard abrasive particles, fibres and lubricants all held together by a polymeric matrix. Also the operating conditions of the system are vary variable, this means that the overall energy generated by the system which manifests as frictional heating, can vary greatly. Temperatures from -20°C to 1000°C may be encountered [2]. Such temperature variations will have a marked effect on the physical properties of the friction material and cast iron disc, which in turn will affect both the type of wear taking place and its severity. The effect of high temperatures on friction material operation is of particular interest to this work and is discussed in detail in chapter 2, together with empirically derived wear models proposed by other workers, as well as a discussion of other associated tribological phenomena which can occur in brake systems.

CHAPTER 2

Tribological characteristics of brake materials

2.1 Introduction

A typical disc-pad type braking system found on most modern vehicles is illustrated in figure 7. The rotors are conventionally made from pearlitic grey cast iron, the diameter of which depends on the braking force required, and ranges form 250mm for a saloon car, to 600mm for a large off road earth moving vehicle. The friction material part of the pads are between 12-18mm thick and also range in size depending on the particular application.

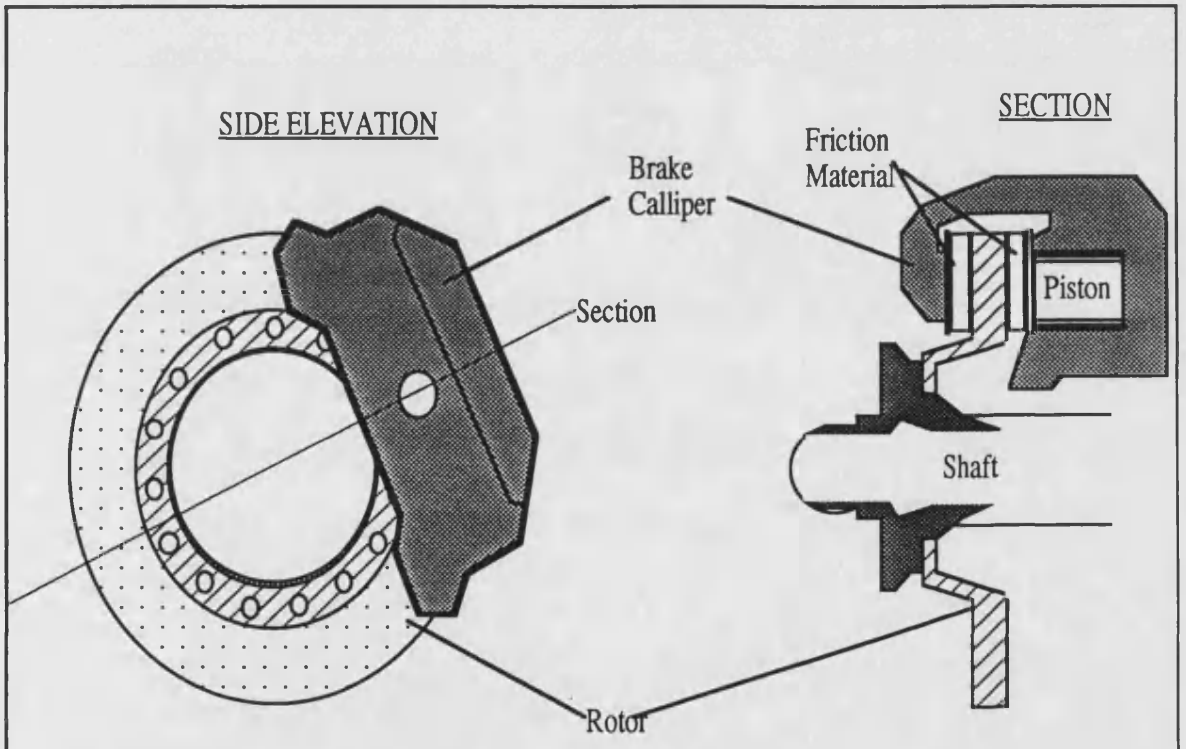

FIGURE 7

Conventional single piston disc brake, showing the calliper and rotor.

As with most tribological systems, the friction and resulting wear of brake materials during operation, is governed by the load or pressure exerted at the frictional interface, the relative sliding speed of the two surfaces, the braking duration, and also the physical properties of the disc and friction material used. The fact that friction materials convert the kinetic energy of vehicle motion into heat is an intrinsic part of the way brakes operate, however this means that the operating temperature can climb to 1000°C, which will result in major physical and chemical changes in both the rotor and pad material.

Microstructural changes can occur within the cast iron rotor, which can affect wear behaviour, and lead to embrittlement and cracking [31]. Friction materials can also undergo dynamic changes in physical properties such as hardness, and elasticity, whilst chemical changes occurring within the pad material, and the degree of cure of the phenolic resin binder, will all affect the tribological behaviour of the system, and are of particular importance to this work. In addition, the generation of a friction film at the interface between the pad and rotor is a common phenomenon during high temperature operation. The existence of a friction film, provides another level of complexity to the tribosystem, all of which must be considered when attempting to model brake performance.

For the reasons outlined above, hypotheses of friction and wear have not yet provided a sufficient theoretical model for the prediction of frictional performance, or wear life of brake materials under all conceivable working conditions. A number of investigations into brake material performance have however been published, where an attempt has been made to predict friction and wear, using relations based on empirically derived data.

2.2 Wear

Rhee proposed a relationship between wear ΔW (mass wear), and load (L), sliding speed (V), and time(t), for a phenolic resin friction material reinforced with firstly asbestos [32], and later with steel [33], rubbing against cast iron. In both cases the relation took the form:

$$\Delta W = K L^a V^b t^c \qquad (2.1)$$

Where a,b,and c, are a given set of parameters for the friction pair, the values of which were found by experiment.

Rhee also found that the temperature reached during testing had a strong influence on the wear rate for both friction materials, Both isothermal and transient temperature tests were conducted, which showed that above 200°C, wear was found to increase exponentially with rising temperature.

Liu & Rhee also conducted an investigation into the higher temperature wear (250 - 300°C) of firstly asbestos reinforced friction materials[34], and later semi-metalic friction materials [35]. In both materials wear data can be correlated using Arrhenius plots, and eqn. (2.1) may be modified to allow for high temperature effects:

$$\Delta W = K L^a V^b te^{-E/RT} \qquad (2.2)$$

where T is the brake interface temperature expressed as absolute temperature, and E is directly related to the activation energies involved in the wear process. A linear relationship was shown to exist between the wear rate and the reciprocal of absolute temperature,(see figures 8 and 9). The slope of the experimental curve was found to be characteristic of each material, and unaffected by differing loads and sliding speeds.

The activation energies from the slopes of the Arrhenius plots for each material ranged from 16 to 40 kJ/mole. It was concluded that wear at higher temperatures was clearly a temperature activated process, this process being the pyrolysis of the resin matrix, rather than oxidation, where the activation energy required is much higher (125 -209kJ/mole).

FIGURE 8

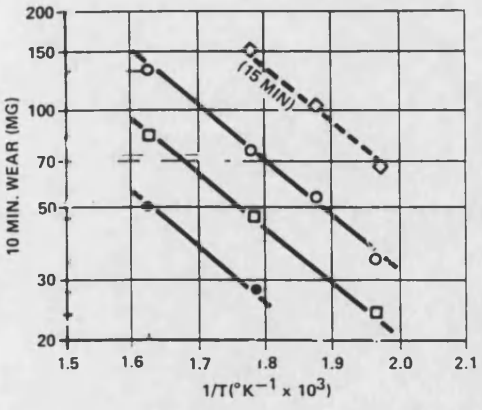

Fig. 8. An Arrhenius plot for the wear of specimen A: O - 90Kg x 300 rpm; □ - 90Kg x 150rpm; ● -45Kg x 150rpm [35].

FIGURE 9

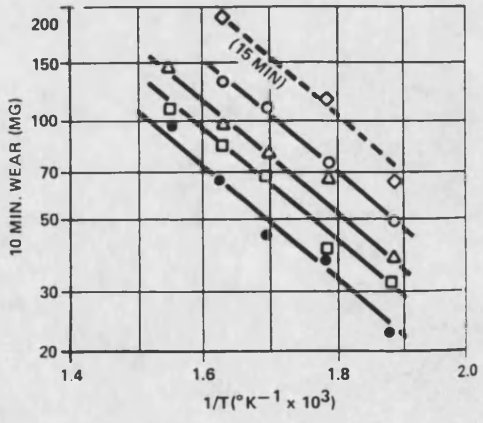

Fig. 9. An Arrhenius plot for the wear of specimen B: O - 90Kg x 300 rpm; □- 90Kg x 150rpm; ● -45Kg x 150rpm; Δ - 45Kg x 300rpm [35].

Todorovic [36], and Duboka [37], proposed a model for the prediction of brake lining life and coefficient of friction based on speed, pressure, and temperature, at the interface. Numerous influential factors contributing to friction material performance were outlined, these factors were then classified into two groups:
a) Effects dependant on the physical working conditions, such as load (L), sliding speed (v), and temperature T.
b) Effects due to design of the brake system, the friction material properties, and the rotor/drum properties, all of which are represented by (C) in the following relations:

$$\mu = C1\, L^{\alpha 1}\, V^{\beta 1}\, T^{\chi 1} \qquad (2.3)$$

$$w = C2\, L^{\alpha 2}\, V^{\beta 2}\, T^{\chi 2} \qquad (2.4)$$

The pressure, speed and temperature exponents, and $C1$ & $C2$, can be evaluated, using experimental data. Todorovic then attempted to verify the above models, by comparing experimental results with those predicted by the model, and obtained a very close match, with average deviation below 4%. However, the model relies on the fact that the values of $C1$, and $C2$, do not alter. i.e. the model is only applicable for a specific test design, and requires that the friction material/rotor used, possesses a constant set of tribological characteristics. Also the temperature range under investigation only reached 300°C, whereas, under real braking conditions, much higher temperatures have been recorded.

Bros et al [38], investigated the factors influencing the tribology of a range of different material formulations, and showed that the amount of wear generated for a given material was also a function of the pressure per unit area (L), test temperature (T,) the sliding speed(v), and a quantity termed "the coefficient of reciprocal covering" (kw), which quantifies the size of the interface between pad and rotor. It was found that kw, L, and T, all affected wear significantly, while sliding speed had the smallest effect.
Bros also proposed that there is a relation between wear and the Brinell hardness (HK) and impact strength (U) of the friction materials tested, of the form:

$$J_g = \left(\frac{HK}{U}\right)^a L^b\, V^c\, kw^{\mathrm{d}} \qquad (2.5)$$

Where $J_g \approx$ wear/unit area.

Other authors however, have not found a correlation between the mechanical and tribological properties of friction materials.[39].

Harding [40], performed a comprehensive study of the wear life of brake pads fitted to automobiles throughout the U.K. This involved the measurement of friction material wear from over 150 pad sets, which had been subjected to mileage's ranging from 5 - 32 thousand miles. From these measurements a projected pad life (l) was calculated from the relation:

$$l = M.\, t/\Delta t \qquad (2.6)$$

where M = Recorded mileage
t = Pad thickness still available
Δt = Measure of pad wear.

It was found that projected values of pad life (l), were generally much higher than those achieved in reality, and there was only a very broad correlation between pad wear and mileage, this is because the pad wear rate increased with higher mileage. The reason suggested was that the wear of friction materials increases after repeated exposure to elevated temperatures.

From the work outlined above there is a clear correlation between the operating temperature and the wear rate of a friction material. The temperature reached during braking is decided indirectly, by the braking pressure applied, the sliding speed, and the braking duration. It has been shown that at temperatures above ≈230°C, wear rate increases exponentially with temperature rise, due to the onset of thermal decomposition of the organic constituents within the friction material [32-35]. In reality, a standard automobile brake system, operates at between 50 - 250°C, for 95% of the time [40], but higher temperatures of up to 500°C do occur, and cause a very large increase in wear rate. These higher temperatures, which are potentially so damaging, are found to occur far more frequently in large lorries and industrial earth moving equipment, where the frictional forces generated need to be much greater, due to the higher kinetic energies generated by these larger, heavier vehicles. Clearly, any improvement in high temperature stability will produce a marked improvement in the wear resistance, and hence operating life of these materials.

2.3 Friction

Rhee [41], set out to test the applicability of Amonton's first law to braking systems, and studied the frictional properties of a range of commercial "organic" friction

materials. He found that there was the a characteristic fall off in coefficient of friction with increasing severity of the operating conditions, known as brake fade, and attributed this to three interacting mechanisms, namely: load fade, speed fade, and temperature fade. From his results it was clear that temperature fade, caused a far larger drop in μ than the other two mechanisms suggested. From this work a general equation was proposed correlating frictional force (F), to the load (L), and the sliding speed(v) at a given temperature Ti.

$$F = \mu L^a v^b \qquad (2.7)$$

where a & b are parameters measured at temperature Ti, and μ is the coefficient of friction.

μ was found to be constant regardless of the load and sliding speed at the interface, and is only dependent upon temperature Ti, so it was therefore concluded that Amonton's first law is inapplicable to automotive brake systems at elevated temperatures.

Tanaka [39] examined the effects of frictional heating on the coefficient of friction of resin-asbestos based composites, rubbing against a cast iron rotor. Tanaka looked in particular at the consequence of firstly modifying the resin used, and secondly, the effect of adding various materials to the composite. It was found that oil modified phenolic resin lead to very low friction ($\approx$0.1) at temperatures around 300°C, which was attributed to the lubricating action of the liquid and gaseous decomposition products of the phenolic resin matrix. Also the addition of metallic powders as fillers, had the effect of reducing the friction coefficient at higher temperatures and producing greater wear. It was found that the metal particles would act as hot spots during frictional heating, the surrounding resin matrix would then decompose resulting in lubrication of the sliding interface, and dislodgement of the metal filler particle. Overall the greatest influence on μ was found to be temperature, although there was a slight increase in μ as the sample fully bedded in towards the end of a test, this was due to an increase in the real area of contact between the two surfaces.

The temperature reached during brake operation has once again been shown to have the major influence on the instantaneous tribological properties of friction materials. Temperatures above $\approx$ 200°C cause the onset of brake fade, resulting in a fall in μ. Kregelskii [2], proposed that brake fade was due to the lubricating action of the liquid and gaseous breakdown products of the organic constituents in friction materials at high temperatures. Herring [3], demonstrated the presence of an interfacial gas layer, by measuring the back pressure caused by it, in a modified dynamometer test rig. The

effect of this back pressure is to reduce the force holding the lining and brake drum in contact, and so reducing the real area of contact between the frictional pair, thus also reducing the coefficient of friction. Again it can be stated that any improvement in the high temperature stability of the friction material constituents, would result in a more stable value of μ, and hence a reduction in brake fade.

2.4 The Brake Rotor

It is important to consider the tribological influences of the brake rotor, which makes up the other half of the frictional pair in brake systems. Brake rotors are traditionally constructed of pearlitic grey cast iron containing approximately 3.2% carbon, in the form of graphite flake, 1.2% silicon, and 0.9% manganese, plus other trace elements [42]. Grey cast iron is used as a rotor material because it is cheap, easily cast, has a low modulus of elasticity, and is dimensionally stable well above 500°C [43]. One other important property is its high thermal conductivity, and excellent thermal shock resistance imparting the ability to accept rapid heating and cooling cycles. The only drawback is the low tensile strength of cast iron, the value of which drops by half at temperatures of 600°C [31]. The tensile strength can be improved by alloying with Cr or Ni, but this gives rise to localised variations in temperature at the frictional surface, or "hotspots", which cause brake judder, and transfer of friction material from the pad to the rotor surface. The addition of alloying elements also has the effect of lowering the thermal conductivity, which causes the rotors to "cone", (a radial and axial distortion, which leads to brake squeal), and can also lead to thermal cracking.
The effect of repeated high temperature exposure on the brake rotor has been investigated by Jimbo [31]. who found that a temperature difference of 330°C can exist between the surface, and interior of a rotor during braking. This causes thermal stress and leads to the development of hairline cracks. He found that if the thermal conductivity was improved by the addition of molybdenum and carbon, heat cracking was reduced.

Clearly high braking temperatures can produce microstructural changes in rotors, and these changes can alter the tribological properties of the rotor. Coyle et al [44], examined the effects of high temperatures on brake rotor performance, and found that when a pearlitic cast iron is subjected to temperatures of 700°C, the lamella Fe_3C can become spheroidized. It was found that once this had taken place, pad wear was increased by 15%, and disc wear rose by 50%, compared to a pearlitic rotor.

Another factor which must be considered when evaluating the wear of friction materials is the roughness of the rotor used. Chapman [45], compared the pad wear,

and coefficient of friction produced by both ground and turned discs with Ra values from 20 -200μm. and found that a coarser finish gave a lower coefficient of friction, after an initial run in period. Pad wear was very erratic during early testing, but after a series of heavy duty tests, pad wear became uniform. This work highlighted the importance of standardising the condition of the rotor surface, before attempting to evaluate the tribological properties of a brake pad material.

The adverse effects of high temperatures on the efficient operation of brake rotors have been addressed to some extent by vehicle body shell designs which promote air flow around the brake assembly. Also the development of ventilated discs have reduced thermal effects. Recently there has been much interest in the development of lighter discs to aid fuel economy, with designers now considering the use of aluminium alloy, and SiC reinforced aluminium. These materials are potentially even more susceptible to high temperatures, and will require the development of specialised friction materials, and a redesigned brake assembly, in order to keep thermal damage to a minimum.

2.5 Friction Films

a) Introduction

Material transfer occurs in nearly all tribological processes involving dry sliding of one surface over another. Very often this transferred material starts off life as wear debris, which can then become plastically deformed and compacted at the sliding interface, producing a friction film, on both the rotor and the friction material surface. The presence of a friction film obviously alters the morphology, and properties of the two surfaces in contact, which can lead to dramatic improvements in the wear resistance of the pad and rotor [46].

b) Friction film formation

A review of wear literature, shows that friction films have been produced using many different material combinations, and test conditions. For example, films have been found to form in polymer - metal combinations, (PTFE & steel [47,48,]), metal - metal systems (Cu - Ni, Cu - Fe,[49]), and even between ceramics [50]. The friction films which form between friction materials and cast iron brake rotors are of particular interest. Jacko [51] performed a series of dynamometer tests on organic friction materials against a cast iron rotor, and describes how at elevated test temperatures (100°C +), a dark shiny glaze formed on the surface of the friction material, this he termed the "frictional heat affected layer" (FHAL).

This film was analysed using energy dispersive x-ray analysis, which showed it to be made up of the various constituents of the organic friction material, namely:- residues

of phenolic resin, rubber, cashew nut oil, asbestos, and barytes (barium sulphate). This showed that friction films in brake systems formed from the wear debris of the friction material used, the debris becoming compacted and smeared across both the pad and disc surfaces. The phenomenon is greatly enhanced by raising the temperature at the pad-disc interface, causing increased flow within the phenolic resin matrix, and other organic constituents. Other workers have also found similar cases of friction film formation :- Liu et al. [52] examined films formed between organic friction materials and cast iron drums and rotors, using S.E.M and E.D.X. Again it was found that the films were produced from the wear debris of the friction material. The friction films also contained iron carbides and oxides due to a reaction with the cast iron rotor. This was in agreement with later investigations by Rhee et al. [53] who studied a semi-metallic friction material, and Sinha et al. [54], found that friction films formed from compacted wear debris, when a Kevlar fibre - phenolic resin composite was abraded against a cast iron rotor. This study also presented evidence that abraded lengths of fibre were being incorporated into the resulting friction film.
More recently the chemistry of friction films produced during braking have been examined using x-ray photoelectron spectroscopy (XPS), which is a very sensitive technique for examining the first 50A° of a surface [55 to 58]. It was found as above, that friction films possessed the same elemental composition as found in the bulk friction material. Wirth [55 - 58] attempted to relate the chemistry of friction films to the tribological behaviour of brake materials, and examined the effects of adding lubricants such as MoS_2 [56,57,58], SbS_2 [55], and PbS [56], and in each case, the lubricant was transferred on to the rotor surface in large quantities. It was also stated that the presence of a friction film reduces the wear rate, and stabilises μ. Also the stability of the friction film was found to be adversely affected by the addition of steel fibre[56], or Fe_3O_4 powder [57].
Clearly there is strong evidence to suggest that friction films form primarily, from wear debris of the softer friction material, which transfers onto the cast iron rotor. Different conditions and materials affect how the friction film forms, and its resulting morphology. In general, films have an ultra-fine grain structure which is often in a partly or wholly carbonised state [51]. These particles are a product of large plastic strains at the asperities [49], caused by plastic flow and fracture, the fine debris being either lost as wear particles, or adhere to one of the interface surfaces, by Van der Waals attractive forces and electrostatic attraction, as well as mechanical keying [50].

c) Temperature effects.

Jacko et al. [51], examined the effect of temperature on the formation of the F.H.A.L. in organic disc brake pads which consisted of phenolic resin, cashew nut oil, rubber, zinc, asbestos fibre, and barytes. Tests were performed on an inertia dynamometer

against a cast iron rotor, over a range of test temperatures (100 - 438°C). Optical microscopy on sectioned and mounted samples showed that the layer became thicker with increasing temperature (Fig. 10):

Figure 10
Variation of FHAL thickness determined by microscopy as a function of maximum exposure temperature [51].

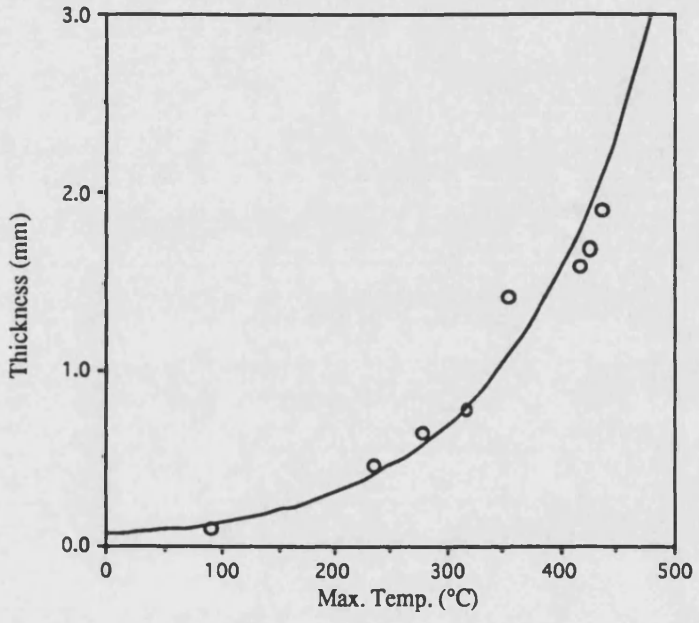

This increase in film thickness with higher temperatures was also noted by Liu. et al. [52] as well as by Rhee et al.[48], who studied a range of different polymers sliding against a stainless steel counterface, and found that friction films formed more easily under severe running conditions, i.e. if the input mechanical energy is higher, a higher temperature is generated at the rubbing interface, and a more extensive friction film is formed. Rhee et al. [48]. also found that a rougher counterface aided the friction film production, as wear debris is more easily retained at the interface. Jacko et al. [42], examined the friction films formed on the friction material surface, and showed that once a "glaze" had formed, stable friction levels and low wear rates could be maintained over a wide temperature range. It was also stated that the ease of film formation, was dependent on the ease of wear debris compaction. Compaction studies showed that cohesiveness falls as the friction material becomes more carbonised, so at higher test temperatures, the friction film breaks down and forms wear debris.

Figure 11a

Change in polymer content as a function of depth [51].

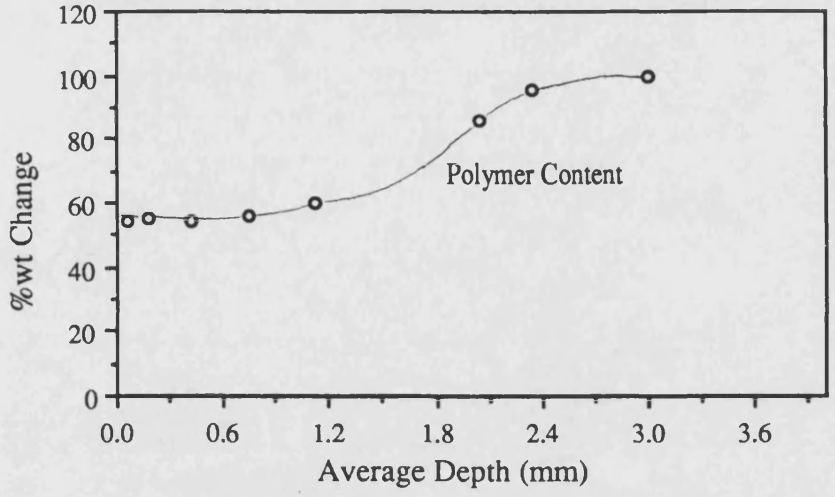

Figure 11b

Composition of FHAL as a function of depth [51].

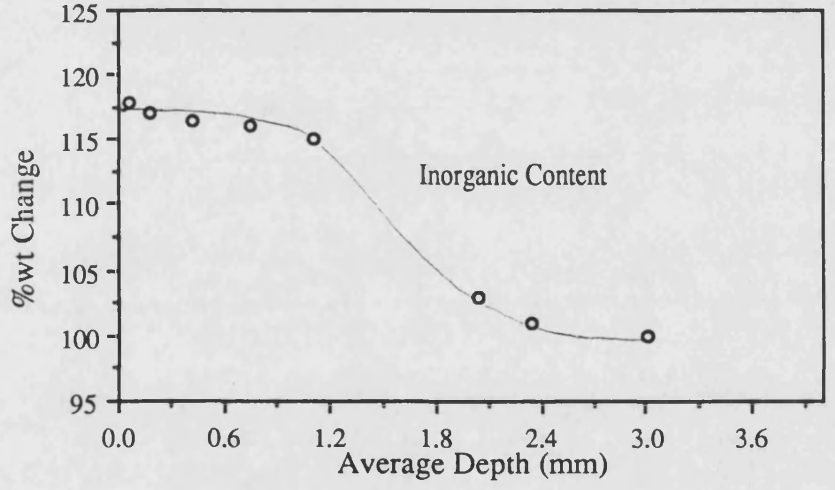

Phenolic resins were shown to be superior to polyimides at forming stable films at high temperatures.

In summary both interface temperature and surface roughness play an important role in friction film formation in braking systems .It is generally recognised that the presence of a friction film has the effect of reducing the wear rate of both the friction material, and the rotor. [46,48,49, 50,53,56]. Film thicknesses quoted for friction materials are between 1 and 7μm [59,60].Films are destroyed by the addition of abrasives [56,52,], and by prolonged exposure to high temperatures [56,42].

2.6 Chemical changes at the braking interface

From the above discussion, there is clearly evidence that the phenolic resin matrix undergoes a chemical change during high temperature operation. Jacko & Deucharme [61], investigated these changes using thermogravimetric analysis (TGA), and showed that the carbon concentration is higher at the rubbing surface than within the bulk of a friction material, and also that this concentration increases with higher temperatures, where organic constituents convert more easily to carbon. In a later paper Jacko found that the rubbing surface is constantly changing, and its composition is a function of the maximum temperature experienced. Samples of friction material taken through the thickness of a used brake pad, were examined using TGA, in an attempt to gauge the change in concentration of each type of pad constituent. It was found that there was a decrease in polymer content, and an increase in inorganic content, towards the rubbing surface (see Figure 11a, and 11b). These affects were attributed to the decomposition of phenolic resin and other organic constituents due to frictional heating. Optical microscopy supported these findings and also identified a glaze of melted and pyrolyzed products at the rubbing surface [51].

Bark [62], investigated chemical changes occurring in a phenolic resin based friction material, during high temperature braking using TGA, and pyrolysis gas chromatography (PGC). The rubbing surface of a brake pad was removed, to a depth of 0.125mm, and tested using TGA analysis, the results were compared to those from a sample of untested friction material. It was found that the organic content had changed from 15% found in the unused material, to 10% in the tested sample. This difference indicated that the phenolic resin had undergone partial degradation during high temperature testing. The identification of the volatile components produced by each material was made using PGC, the results are presented in table 1.

TABLE 1

Comparison of the pyrolysis products produced by used and unused friction materials [62].

VIRGIN MATERIAL	TESTED MATERIAL
Methane	Methane
Ethane*	Ethane
Ethylene*	Ethylene
Benzene	Benzene
Toluene	Toluene
m-Xylene	Ethylbenzene
p-Xylene	m-Xylene
o-Xylene*	p-Xylene
Phenol	o-Xylene
o-Cresol	
2,4-Xylenol	
2,6-Xylenol	

* These compounds were produced in trace amounts.

It was found that the used friction material contained much lower amounts of oxygen containing fractions: phenol, cresol, and xylenol, compared to the unused material, and only gave off hydrocarbons. This was further evidence that resin breakdown had occurred, and that the residual material left behind was in the form of an aromatic hydrocarbon.

2.7 Pyrolysis of phenol formaldehyde resin

The breakdown of phenolic resin at the frictional interface occurs in an oxygen deficient environment, where the resin becomes pyrolyzed. Fitzer, Mueller, and Schaefer [63] discussed the pyrolysis mechanisms and pathways of phenolic resins as outlined in figure 12.

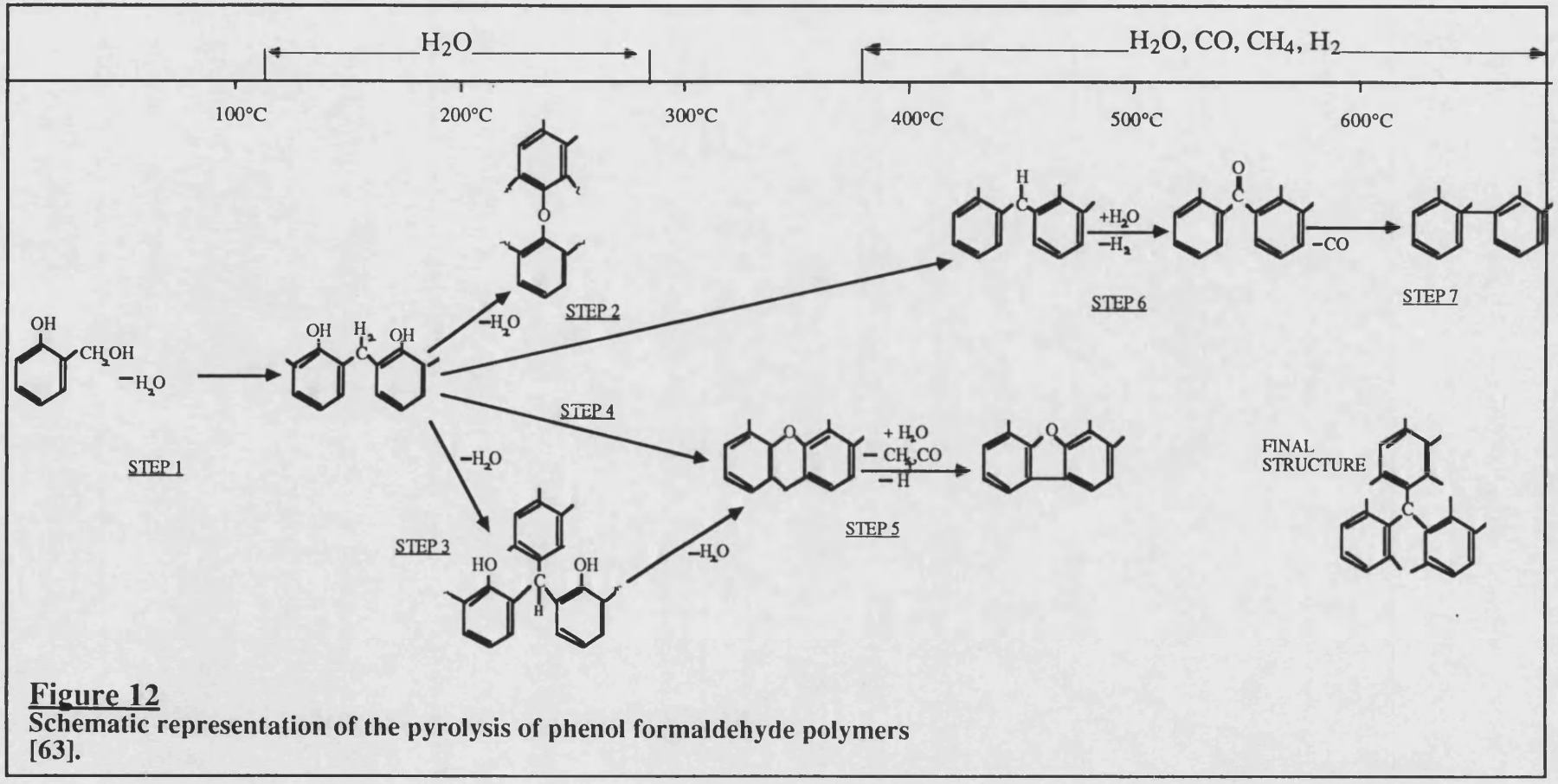

Figure 12
Schematic representation of the pyrolysis of phenol formaldehyde polymers [63].

Pyrolysis takes place in the solid state, involving condensation, oxidation, dehydration, and decomposition, which may occur as both parallel, and sequential reactions. Initially, the catalytic hardening reaction goes to completion with any residual water being driven off, with the further formation of methylene bridges (step 1, fig.12). Also any existing oligomers in the starting material will volatilise.
The first step in the pyrolysis is thought to be the formation of the ether bond (step 2), accompanied by the release of water, with the concurrent condensation of phenolic groups with a methylene bridge (step 3).
By 400°C ether diphenylpuran is formed (step 4), which subsequently goes to the furan ring structure (step 5). Within this temperature range, the resin starts to decompose to benzene, toluene, and xylene. Hydrogen may then be evolved as a result of the secondary oxidation of these products [64].

At temperatures above 450°C, it was proposed, that a self-oxidation of the remaining methylene bridges occurs, due to the presence of some residual water of pyrolysis (step 6). However in a later study by Morterra and Low [65] working on I.R. spectra of Novolac resins after heat treatment at different temperatures, it was stated that self-oxidation is not an important degradation pathway in Novolacs.

Above 460°C, ketone groups release carbon monoxide yielding a biphenyl structure (step 7). The polymer network remains intact up to 500°C, above which the aliphatic bridges holding the aromatic groups apart, are destroyed leading to the formation of polyaromatic domains, at temperature above 560°C [65]. This involves the evolution of H_2,CO, CO_2, and CH_4, as the resin is carbonised. The resulting structure is a series of aromatic layers which are turbostratically stacked and exist in small "crystallite" type packets which are angularly displaced relative to one another, reflecting the structure of the resin precursor. Jenkins and Kawamura [66] using x-ray diffraction techniques estimated the "crystallite" size of these turbostratic regions as La = 50A°, and Lc = 15A° (see figure 13).

FIGURE 13

Schematic structural model for a glassy carbon [66].

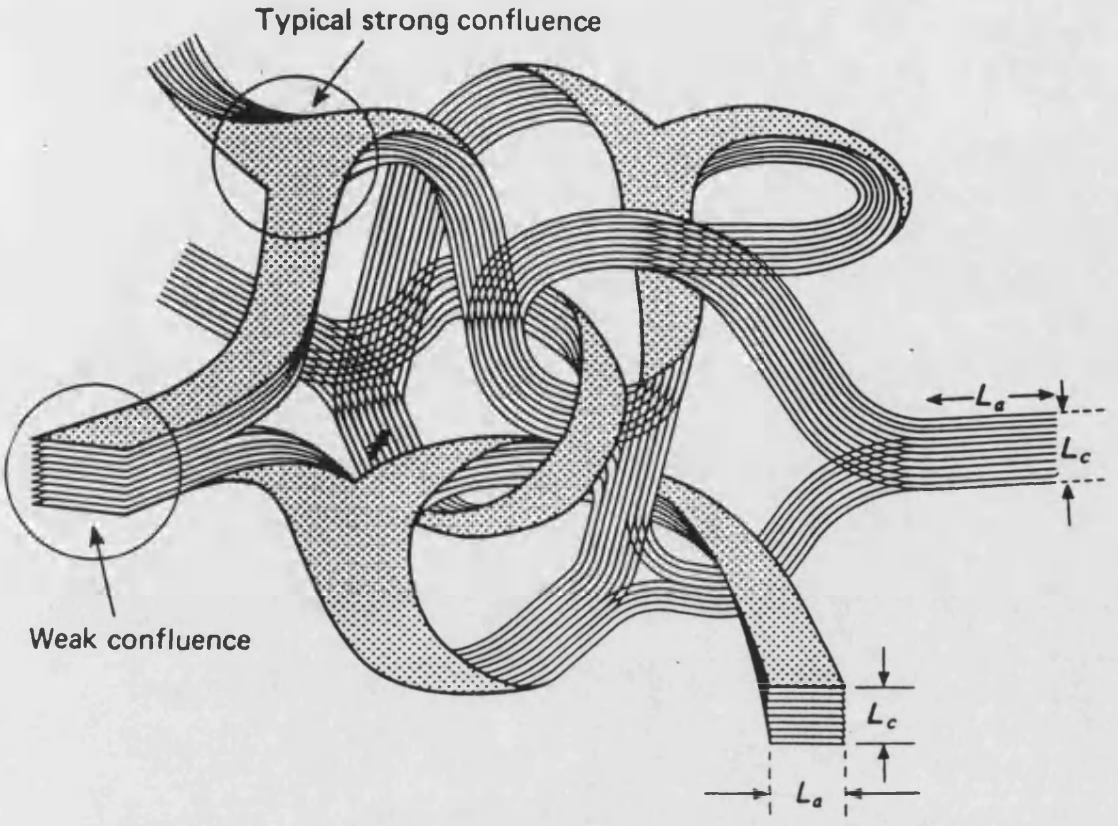

They also go on to suggest the existence of diamond like tetrahedral crosslinks within the amorphous structure. The structure of amorphous carbon prevents these materials from being annealed into graphitic structures. Further heating above 600°C brings little growth in the graphitic content because of insufficient molecular mobility.

Amorphous carbon is the matrix material in carbon/carbon fibre composite brakes used within the aircraft industry (see chapter 1 section 1.1), and the tribological properties of the material have been studied by a number of workers [67,68,69,]. Differences in the fabrication techniques and heating cycles used to produce amorphous carbon, has resulted in materials with different final microstructures, which is the probable cause of variations in the material properties reported. However, true amorphous carbon has been shown to have very good wear resistance due to its hardness [69]. The coefficient of friction has been shown to rise with

temperature [67], and there is also evidence that it does not possess the abrasive qualities of other ceramics [69]. Yoshida et al. [68] suggested that if a non-graphitic carbon can be made truly amorphous, there is a corresponding rise in hardness and wear resistance. Amorphous carbons are also very brittle however, and oxidise at temperatures above 500°C.

2.8 Summary

In this chapter the various tribological properties of friction materials have been discussed, also the way in which temperature effects, dominate all aspects of tribological behaviour during braking, has been highlighted. Chemical changes within the phenolic resin matrix as a result of frictional heating, has been identified as a major factor in determining the friction and wear of these materials, and these changes have been elucidated in some detail. The pyrolysis of phenolic resin is considered to be relevant for two reasons: firstly the volatile products of degradation produced during high temperature operation, give rise to brake fade, and secondly the residual carbonised polymer left behind, is weak and friable, and so the wear rate increases.

This investigation is concerned with improving the high temperature frictional performance of conventional friction materials, and it was postulated that this could be achieved by carbonising the material prior to testing. The material would then be free from the volatile components which cause fade. This necessitated a parallel study into how carbonisation would affect other tribological aspects of friction materials, namely: pad and rotor wear rate, and friction film formation.

CHAPTER 3

An investigation into the use of carbonised materials as a solution to brake fade

3.1 Preliminary study

3.1.1 Introduction

The thermal breakdown of the organic content of a friction material, and the accompanying production of liquid and gaseous products, gives rise to brake fade. If the volatile components of friction materials could be removed, then fade should not occur. A preliminary investigation was undertaken in which samples of commercial friction materials and phenolic resins, were carbonised under controlled conditions in order to remove any volatile constituents. The resulting weight losses, porosity increase, and density changes were measured.

3.1.2 Methods and materials

Below is a list of the materials tested :-

1) A1 commercial friction material (EFI).

2) A2 commercial friction material containing 6%wt resin (EFI).

3) A2 commercial friction material containing 10.4 wt% resin (EFI).

4) pure phenolic resin (CS318) (moulded under pressure).

5) pure phenolic resin (CS318) (straight moulded).

The A1 and A2 friction materials were supplied by European Friction Industries (EFI), the compositions of which are given in table 2. Two samples of A2 material were supplied, one sample containing 10.4%wt resin, and one containing 6%wt, so that any relation between resin concentration and the physical properties of the carbonised product could be identified.

Table 2

Contents of friction materials produced by European Friction Industries.

RAW MATERIAL	A1 Wt%	A1 Vol%	A2 Wt%	A2 Vol%
GRAPHITE POWDER	-------- -	-------- -	6.05	5.82
VERMICULITE	-------- -	-------- -	15.57	10.38
PHENOLIC RESIN	12.50	23.89	10.40	13.86
BARYTES	10.44	6.11	30.11	12.27
CALCIUM FLUORIDE	-------- -	-------- -	2.74	1.53
GRAPHITE FLAKE	11.09	12.64	-------- -	-------- -
LEAD SULPHIDE	15.66	5.56	-------- -	-------- -
ANTIMONY SULPHIDE	7.43	4.10	-------- -	-------- -
MINERAL FIBRE	15.52	14.26	-------- -	-------- -
PROCESSING AID	2.51	4.32	3.11	3.4
FRICTION MODIFIER	-------- -	-------- -	4.35	6.62
ABRASIVE	2.96	2.22	-------- -	-------- -
METAL POWDER	17.32	5.07	6.05	1.23
FILLER	4.57	21.83	21.62	44.89

In order to monitor the weight loss of the resin component of the friction materials independent of other brake pad constituents, moulded pure phenolic resin blocks using resin N° CS318 were also tested. The samples were moulded at a pressure of 2MPa, the same as the conditions under which the commercial friction materials were produced, and insured that the samples were free from trapped air bubbles. A second group of samples were moulded using a very low pressure

(≈4KPa), allowing much larger blocks of resin to be made, which were used as a control, in order to examine any size effects on weight loss.

Friction materials are commonly given a 6hr low temperature heat treatment in air, known as the post-bake, to ensure complete curing of the phenolic resin. One sample of each material was post-baked for 6hrs at 180°C, and one for 6hrs at 250°C, so any effects due to post-bake temperature could be assessed.

All samples were subjected to a 50hr high temperature heat treatment program, as outlined in figure 14. This schedule is commonly used to carbonise composites containing phenolic resin [70]. The carbonisation was carried out in a tube furnace under an argon atmosphere, to prevent carbon oxidation.

3.1.3 Results

A visual Inspection showed that all the A2 samples expanded and cracked during carbonisation, the samples with the lower resin content (6%), having completely disintegrated. The A1 samples remained intact, but contained small cracks. The phenolic resin samples suffered a noticeable volume change, and took on a shiny black lustre. Weight loss, density, and porosity changes are presented in table 3.

3.1.4 Discussion

An increase in porosity, and a corresponding decrease in density occurred in all the friction material samples carbonised. This was accompanied be a large volume increase. Conversely, the phenolic resin samples all exhibited an increase in density and contracted during carbonisation. The crack damage found in all the friction materials examined, can hence be explained. The matrix clearly wishes to contract during carbonisation, whilst the other constituents expand, thereby giving rise to internal stresses, leading to crack growth.

All A2 samples underwent a large expansion during carbonisation. This was because the samples contained crude vermiculite, which is a type of mica, or hydrous magnesium silicate with traces of iron and aluminium. When heated above 800°C, the structure can expand by a factor of ten, this process being known as exfoliation. The layered mica structure becomes separated, due to trapped water which escapes as steam.

Weight loss from the phenolic resin samples ranged between 26 and 36%wt, depending on the degree of post-bake and the sample size. Samples post-baked at the higher temperature of 250°C, showed on average 5% less weight loss, compared to samples carbonised at 180°C. Clearly a higher temperature post-bake will remove a larger amount of volatiles, prior to carbonisation. Also the smaller samples moulded under pressure, showed approx. 4.5% greater weight loss

Table 3

Weight loss, density and porosity changes due to carbonisation of selected friction materials and phenolic resins.

Sample	% Wt loss	(%) Orig. porosity	(%) Final porosity	Original Density (g/cm^3)	Final Density (g/cm^3)
A1 (P.C. 180°C)	20.4	2.7	13.4	3.01	2.71
A1 (P.C. 250°C)	19.9	1.6	14.2	3.01	2.68
A2 (P.C. 180°C) 6 wt% Resin.	Destroyed	----------	----------	2.15	---------
A2 (P.C. 180°C) 10.4 wt% Resin.	31.0	---------- --	---------- -	2.24	----------
A2 (P.C. 250°C) 6 wt% Resin.	30.5	12.9	45.0	2.18	1.55
A2 (P.C. 250°C) 10.4 wt% Resin.	30.0	5.2	34	2.25	1.60
Phenolic Resin (P.C. 180°C)	32.7	2.3	2.9	1.30	1.54
Phenolic Resin (P.C. 250°C)	26.4	2.4	2.5	1.24	1.60
Phenolic Resin * (P.C. 180°C)	36.1	2.7	0.9	1.27	1.41
Phenolic Resin * (P.C. 250°C)	32.1	2.9	3.9	1.22	1.44

Note: P.C. = Post cure temperature.

'*' = Pressure not used during moulding.

compared to the larger samples. Gaseous volatiles can escape more easily from a smaller sample, which possesses a larger surface area to volume ratio.
A1 samples were found to lose approximately 20%wt, whilst A2 samples lost approx. 30%wt. Comparing these values to the organic content of each material prior to carbonisation (table 2), it is clear that only approximately half the weight loss from each material could be attributed to organic breakdown, indicating that other constituents had undergone reactions resulting in weight loss.

3.1.5 Conclusions

The carbonisation of the commercial friction materials described, resulted in a weak and friable product. The main reason for this, was that high stresses developed within the material during carbonisation, leading to crack formation. The build up of trapped volatiles within the bulk of the material lead to increased internal pressure, in addition the resin matrix contracts as carbonisation proceeds, whilst other constituents (esp. vermiculite) expand, consequently stress levels are further increased, and the sample is damaged.
The problems outlined above could be prevented by using a heat treatment with a slower heating rate, which would allow volatiles to defuse away, and contraction to occur at a steady rate.
Conventional friction materials are clearly unsuitable for high temperature carbonisation involving temperatures as high as 800°C. Specialised materials need to be developed, containing only those constituents which remain inert at high temperatures.
Other findings are that phenolic resin monoliths were shown to lose 26 - 36%wt, over temperatures of up to 1000°C. These losses depended on the sample size and the post-bake temperature used.

3.2 The pyrolysis of phenolic resin

3.2.1 Introduction

In order to fabricate carbonised phenolic resin based monoliths free from cracks and flaws, which would be strong enough to be used as a friction material, a specialised heat treatment cycle was needed to firstly minimise the damage caused by escaping volatiles, and secondly to allow the resin matrix to contract slowly. This could be achieved by using a very slow heating rate, during the periods of greatest volatile evolution [71]. Thermogravimetric analysis (TGA), was used to identify temperatures over which greatest weight loss (Hence gas evolution)

occurs. From these studies a more suitable carbonisation regime was formulated. Sample blocks of cured phenolic resin were carbonised using this new regime, the carbonised products were examined using optical microscopy, and x-ray diffraction. Weight loss and volume changes were also recorded.

3.2.2 Methods and materials

Two commercially available phenolic resins were examined:-

Resin *A* - A high carbon yield novolac resin produced by Carborundum.

Resin *B* -- Resin N^{o} J1506H, produced by British Petrolium, which is already used in the production of friction materials.

Each resin was cured in an oven for 6hrs at 180°C, and then ground to a fine powder using a pestle and mortar, and analysed using a Setaram TGA. The work of Morterra and Low [65], Fitzer et al [63], and Jenkins et al[66], all state that the major pyrolysis reactions in phenolic resins have taken place by 800°C, where an amorphous char had formed, and weight loss approaches zero. For this reason 800°C was selected as the upper temperature limit for the TGA tests. Blocks of resin were moulded using a simple mounting press, as this method produced defect free blocks of resin. The moulded cylinders were then sawn into discs, ground flat, weighed, measured, and post-baked for 6hrs at 180°C. The samples were carbonised in a tube furnace in an argon atmosphere, up to a temperature of 800°C, using the carbonisation regime outlined in section 3.2.3.

The carbonised samples were monitored for weight loss and volume change, and examined for cracking, blistering etc, using optical microscopy.

X-ray diffraction traces of the carbonised samples were compared with samples of uncarbonised resin, to determine any changes in structural order which had taken place during carbonisation.

3.2.3 Results of TGA tests

The TGA results for resins *A* and *B* are shown in figures 15 and 16 respectively. Resin *B* lost approximately 65%wt, whilst the high carbon yield resin *A* only lost 44%wt. Both traces show that there is a gradual weight loss between 0 - 300°C, as water is driven off, due to further condensation reactions within the resin matrix. This is followed by the comencement of thermal degradation between 300-400°C, with a large weight loss between 400 - 700°C. These results match those published [75,77], and are consistent with the findings of Fitzer et al[63], who showed that H_2O, CO, CH_4, and H_2, were all given off within this temperature range, as polymer degradation proceeds. The derivative plot indicates that the highest rate of loss occurs between 500 - 600°C. From these findings, it was clearly beneficial to use the high carbon yield resin *A* in further tests, to minimise

shrinkage and volatile evolution. Based on these experiments the following carbonisation regime was proposed:-

100°C/hr	up to 150°C
50°C/hr	up to 200°C
20°C/hr	up to 300°C
7°C/hr	up to Finish Temperature.

Also a dwell of 4hrs at the finish temperature.

TABLE 4

Sample N°	%Wt Loss	%Volume Change
1	30.78	35.4
2	30.73	36.2
3	31.53	35.5
4	30.18	36.5
5	31.16	35.1
6	30.26	36.8
7	31.56	33.2
8	29.61	34.8
9	29.60	35.5
10	29.62	35.6
11	31.35	34.3
AVG.	30.5 +/- 0.5%	35 +/- 0.5%

3.2.4 Results of carbonising phenolic resin monoliths

The weight losses and volume changes which occurred during carbonisation are shown in table 4:-

All samples had a hard, black glass like lustre, and all contracted uniformly with no visible indication of cracks or blisters. Optical microscopy revealed that a few

cracks were present and the sample surfaces were covered with pits, originating from trapped air bubbles within the original samples. (See figure 17a and 17b).
Xray diffraction patterns of the phenolic resin samples before and after carbonisation are shown in figures 18 and 19, respectively.

3.2.5 Discussion

The high carbon yield Novolac resin *A* was shown to be superior to J1506H resin *B* in that it gave off proportionally less volatiles during carbonisation. This is an important advantage as sample damage by escaping volatiles, during preparation would be minimised.
The TGA on resin *A* showed a weight loss of 44%, whilst the block samples of resin *A* which were carbonised in a tube furnace, showed a weight loss of approx. 30%. The prime reason for this difference was that the sample used in the TGA experiment was powdered, and so, because of its larger surface area allowed volatiles to escape more easily, resulting in a greater percentage loss than from a solid monolith.
The suggested carbonisation regime allowed volatiles to escape and shrinkage of 35% to take place without catastrophic damage to the sample, demonstrating that slow heating rates over temperatures above 400°C, can be used to carbonise phenolic resin based friction materials without damage.
The peaks found on both the x-ray diffraction traces of phenolic resin samples where due to the presence of iron chromium oxide which is added to colour the resin. There is also a large background count in the uncarbonised sample (see figure 18), indicating that there is a large amorphous component associated with the sample. On examination of the pattern for the carbonised sample shown in figure 19, it is evident that there is a peak shift to the left indicating that a reduction in 'd' spacing has occurred, due to distortion of the crystal lattice as a result of sample contraction during carbonisation. Also the amorphous background signal is much reduced in the carbonised sample. This is a strong indication that the phenolic resin matrix becomes more ordered during carbonisation.

3.2.6 Conclusions

1) The high carbon yield resin *A* possessed greater high temperature stability than resin *B*, and hence proved more suitable for use with this work.
2) A weight loss of approx. 30% and volume decrease of approx. 35% occurred in block samples of resin *A* when carbonised to 800°C. Similar behaviour can be expected to occur within resin based friction materials when carbonised under the same conditions.

3) X-ray diffraction studies have indicated that phenolic resins undergo a structural change during carbonisation, resulting in a less amorphous and more ordered structure, which may affect material properties.
4) TGA measurements gave important information on the changing weight loss rate of phenolic resins, this information was then used to develop a specialised carbonisation regime, which was shown to reduce the damage to samples during carbonisation.

Figure 14 **Carbonisation cycle for a typical phenolic resin composite [70].**

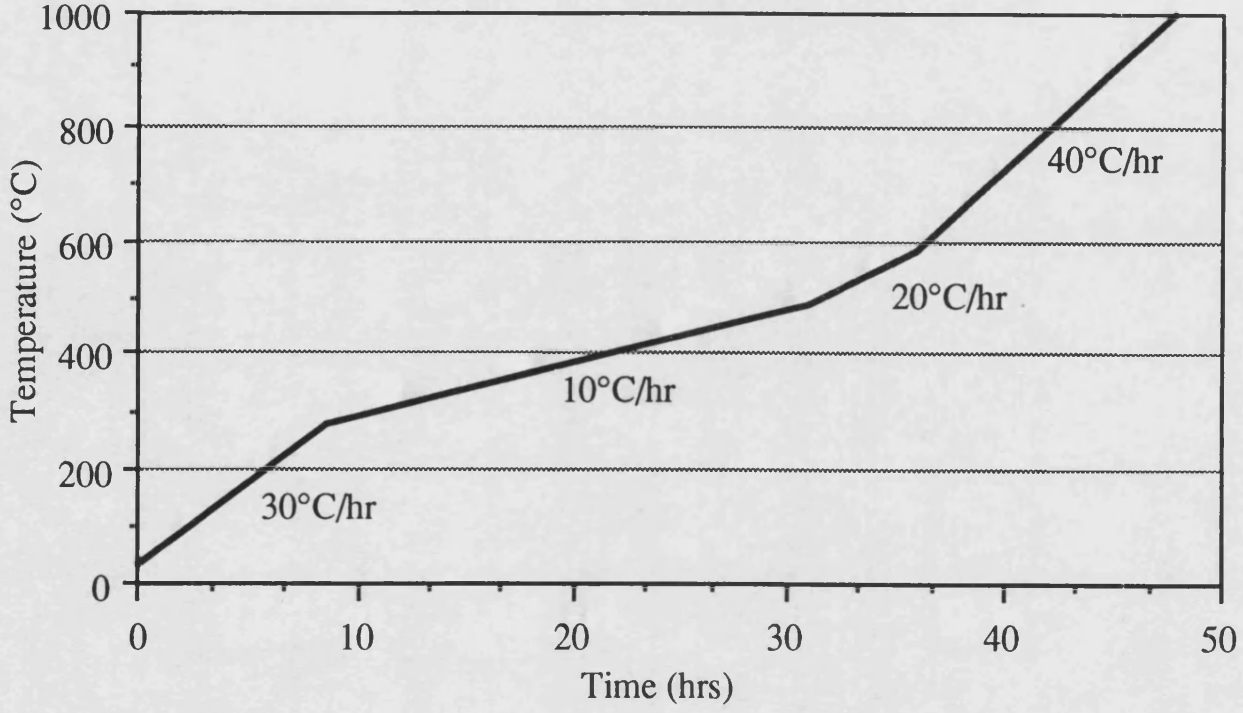

Figure 15

Thermogavimetric analysis of resin A.

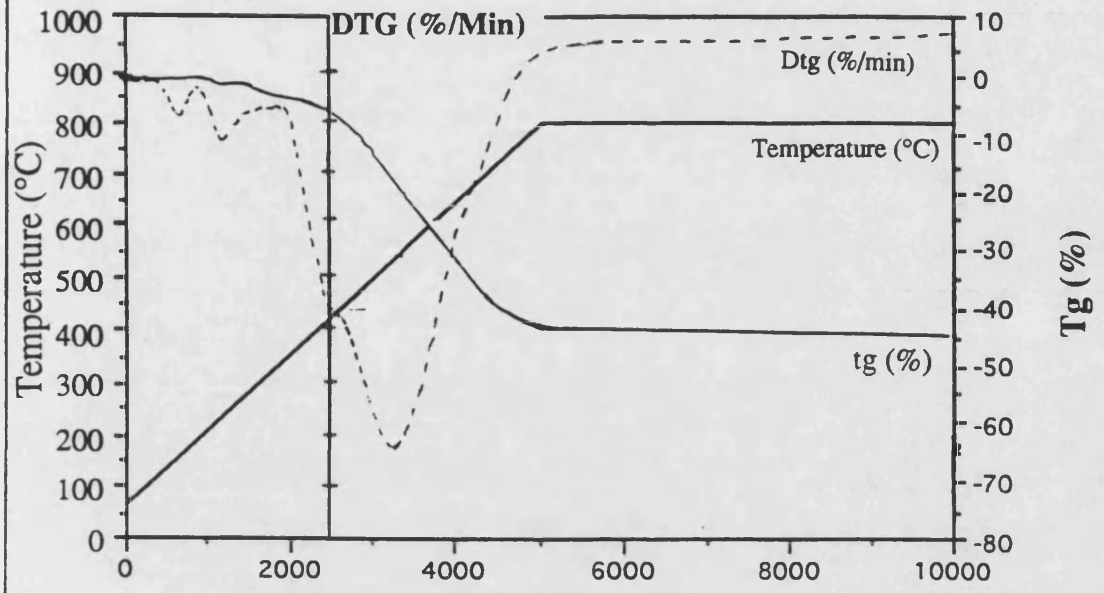

Figure 16

Thermogravimetric analysis of resin B.

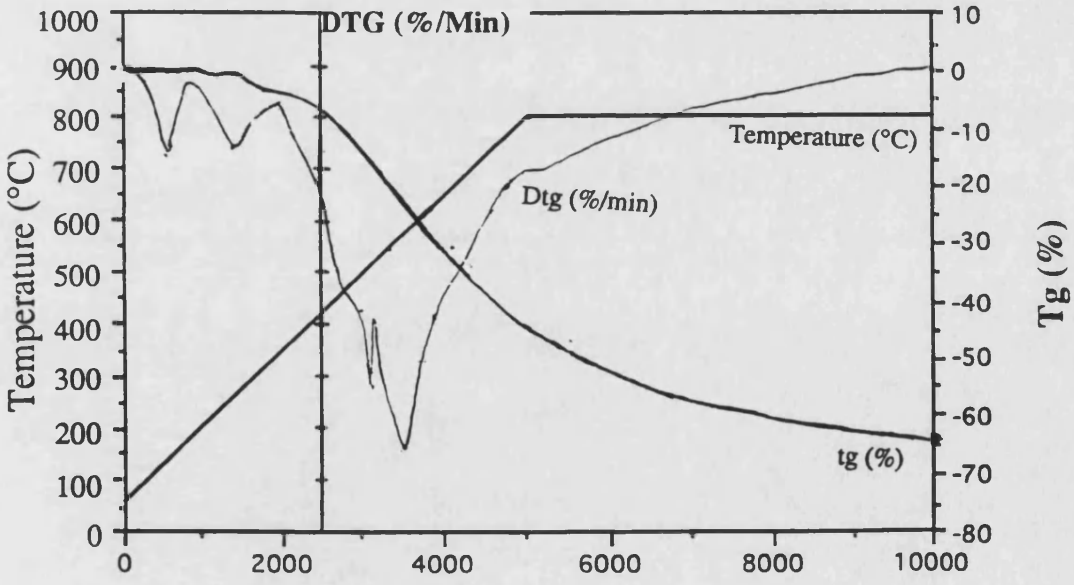

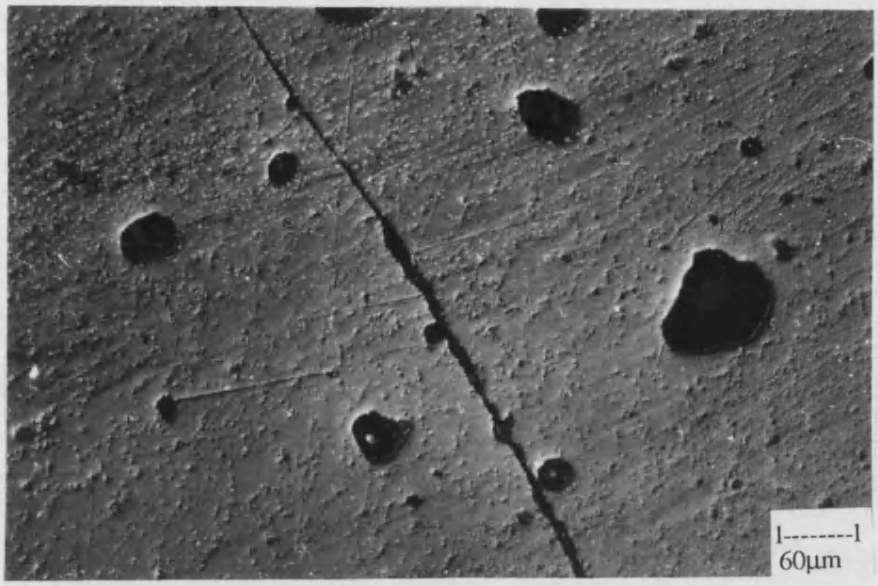

Figure 17a
Optical micrograph of a pure phenolic resin sample carbonised to 800°C, showing the cracked and pitted surface (x160).

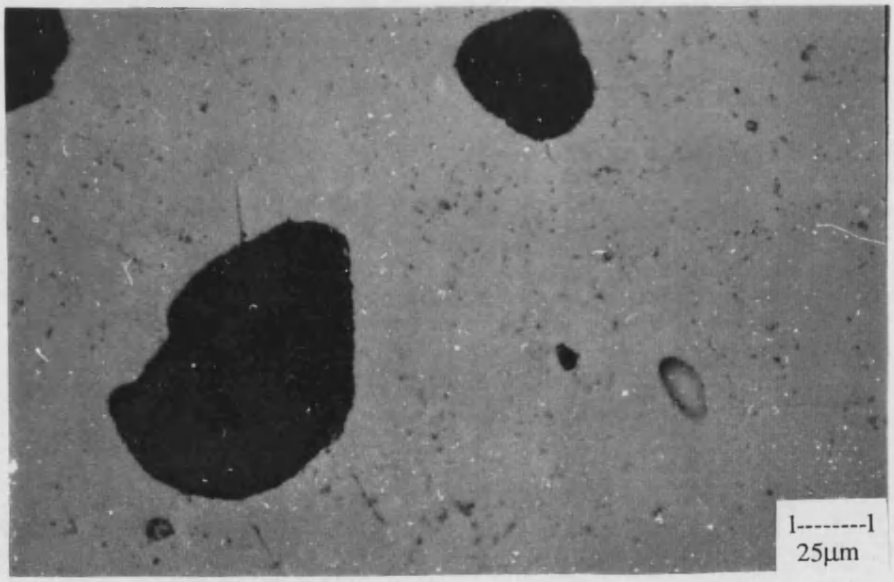

Figure 17b
Optical micrograph of pure phenolic resin sample carbonised to 800°C, showing a close-up of a pit on the sample surface (x400).

Figure 18
X-ray diffraction trace of uncarbonised phenolic resin.
The resin contains iron chromium oxide producing the peaks labled.

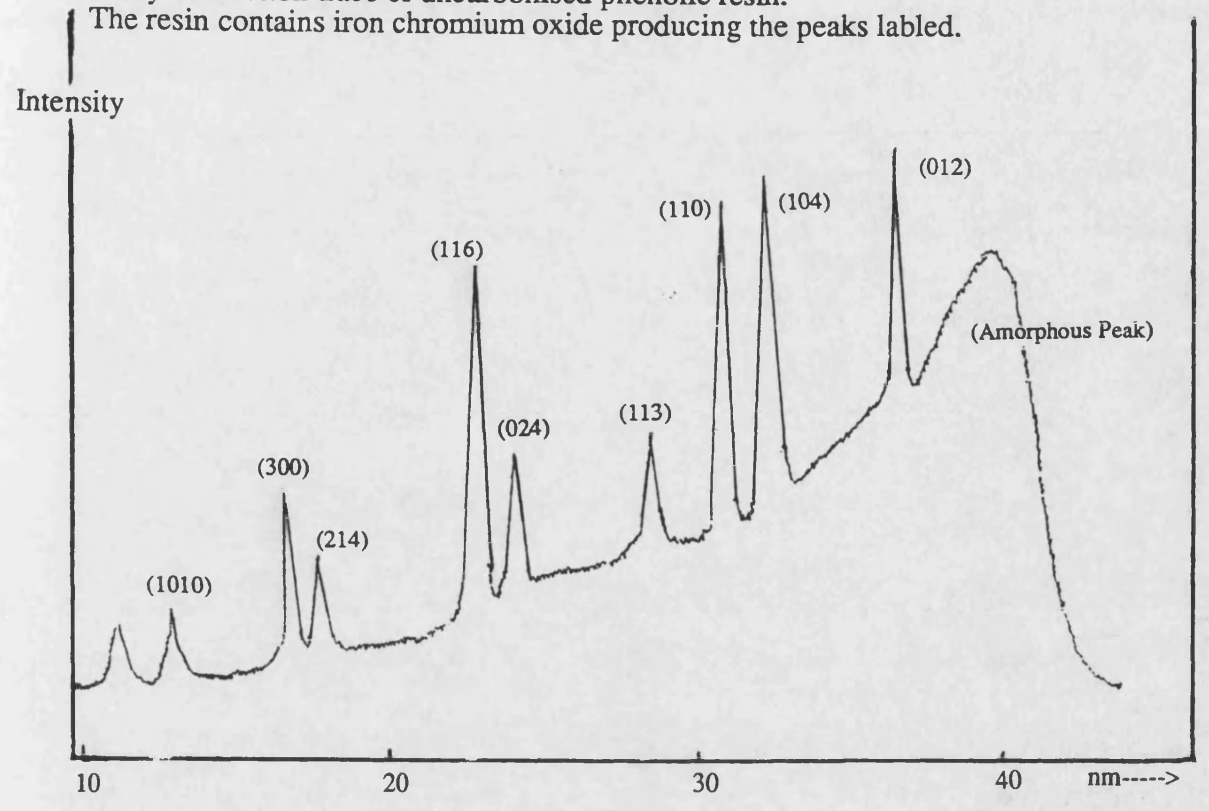

Figure 19
X-ray diffraction trace of phenolic resin carbonised to 800°C.
showing a peak shift and the absence of a large background signal.

3.3 The development of a specialised friction material to study the effects of carbonisation on tribological properties

3.3.1 Introduction

The work reported in this section examines the feasibility of using carbonised materials in brake systems, which involves the study of their friction, wear, and mechanical properties. In section 3.1 it was seen that conventional friction materials are made up of a large number of components, some of which will become reactive or expand at high temperatures. Unwanted expansion irrecoverably damaged samples, while internal reactions could lead to large weight losses, and may contribute to fade. It was therefore deemed necessary to develop a specialised material for this study. Consequently this section of work is based on a simple material, made up of only four components: a fibre (Rockwool mineral fibre), a lubricant (graphite powder), a filler (barytes) and high carbon yield novolac phenolic resin which acts as the matrix. Each component other than the resin, was selected because of its cheapness, availability, and more importantly, because it would withstand the necessary carbonisation regime involving temperatures up to 800°C, without thermal degradation, and would still be able to fulfil it's specific function afterwards.

Three point bend tests were used to measure the flexural strength and elastic modulus of each formulation. It is important that the individual constituents do not react or expand during carbonisation, measurements of volume changes and weight losses which occurred during carbonisation, as well as x-ray analysis, were used to give an indication of any reactions or expansions which had occurred. The friction and wear properties of each formulation, were measured using a continuous drag pin on disc test machine.

3.3.2 Methods and materials

In order to study the individual effect of each constituent on the properties of the final product after carbonisation, a matrix of 18 different mixes based on the four components listed above, were formulated. The contents of each sample are shown in table 5:

Table 5 Sample content (wt%)

Mix N°	Wt% Resin	Wt% Barytes	Wt% Rockwool	Wt% Graphite
1	10	60	30	0
2	10	40	50	0
3	10	20	70	0
4	10	55	30	5
5	10	35	50	5
6	10	15	70	5
7	10	50	30	10
8	10	30	50	10
9	10	10	70	10
10	20	50	30	0
11	20	30	50	0
12	20	10	70	0
13	20	45	30	5
14	20	25	50	5
15	20	5	70	5
16	20	40	30	10
17	20	20	50	10
18	20	0	70	10

Table 5 shows that 9 of the mixes contained 10%wt resin, and 9 contained 20%wt. Each of these two groups of 9 were sub-divided into three, containing different amounts of graphite powder: 0%wt, 5%wt, and 10%wt, which were further divided into three levels of fibre content, set at 30%wt, 50%wt and 70%wt.

150g samples of each of the 18 formulations were moulded into bars, under a pressure of 2MPa. The bars were slit and ground to give four $10mm^3$ cubes for wear testing, and four three point bend specimens, approximately 130mm x 10.5mm x 5.5mm.

All samples were post-baked at 180°C for 6hrs, weighed, measured, and carbonised using the regime outlined in section 3.2, plus a final dwell of 10hrs at 800°C.

After carbonisation all samples were measured for weight loss and volume change. The three point bend tests were carried out on an Instron 1185 machine,

using a support span of 100mm, and crosshead speed of 2mm/min. Four samples of each of the 18 mixes were tested and the flexural strength and elastic modulus were calculated according to ASTM D standard N^{o} 790 - 80 [72]. Four samples of A1 commercial friction material (See table 2), were also tested, for flexural strength and modulus comparison.

The assessment of coefficient of friction, and wear of each of the carbonised materials was carried out using a B.I.C.E.R.I. universal wear machine. This equipment was originally developed to study the tribological properties of materials in a variety of environments. It is commonly referred to as a pin on disc machine, because a loaded sample in the form of a $10mm^3$ cube of friction material is attached to a pivot arm, and rests on a rotating disc,(See Figure 20, and 40a -40d).

The pin on disc machine measures both wear and frictional force, via two force displacement transducers(see fig. 40a). The wear transducer is mounted on the pivot arm, and measures vertical movement, whilst the frictional force transducer rests against a calibrated stainless steel post, which bends (within its elastic limit), under the frictional force acting through the pivot arm (see fig. 40b). This deflection is measured by the pre-calibrated transducer, giving a measure of the frictional force between the pin and disc.

The outputs from the two transducers feed to a computer which converts the data to give the instantaneous coefficient of friction and wear between the sample and disc. The load on the pin and the velocity of the disc (P-V factor), can be set to a working maximum of 400N load, and 267 rpm, although at higher loads, vibration between the pin and disc becomes a serious problem. Grey cast iron discs were used during all tests similar to those used on most vehicles.

A load of 271N was used, which gives a pressure of 2.7MPa, in line with the pressures used in a heavy duty pad - disc brake system. An rpm of 170 gave a sliding speed of approx. 2.0m/s, during testing. The duration of each test was 2hrs, and each of the 18 compositions were tested four times, and the coefficient of friction and wear results averaged. A sample of A1 commercial friction material (the contents of which is given in table 2) was also tested under the same conditions, to provide a comparison.

3.3.3 Results

i) Visual and optical examination.

A visual inspection showed that all samples were found to be crack free and undamaged by the high temperature carbonisation used. Optical studies were used

to compare carbonised and uncarbonised samples, and revealed that there had been a change in the optical properties of the Rockwool mineral fibres during carbonisation. Prior to the heat treatment the fibres appeared transparent to light, and afterwards appeared translucent or opaque. E.D.X. (Energy Dispersive X-ray analysis) studies performed on fibres before and after carbonisation, (see figures 21 and 22 respectively), indicated that there had been no obvious change in composition. Further studies involving Vickers hardness tests revealed that the fibre hardness had not altered during carbonisation, and was approx. Hv400, (Although this figure can only be regarded in a comparative sense, as the indentor cracked the individual fibres during testing). A possible reason for the opaque appearance of the fibres could been due to crazing brought about by the thermal fatigue.

ii) Weight losses and volume changes.

The average weight losses and volume changes for each of the mixes are shown in table 6. Figure 23 compares the volume decrease which had occurred in each sample during carbonisation. Clearly the samples made with the higher resin content of 20%wt, experienced a greater decrease in volume, than those made with 10%wt. as expected In all samples the volume decrease occurred uniformly in each dimension, and samples retained their original uncarbonised shape.

iii) Three point bend tests.

Figure 24 gives the average flexural strength of each of the 18 compositions tested, while the average elastic modulus for each composition is shown in figure 25. The error bars represent the standard deviation giving an indication of the spread within each group of results. All samples failed in a brittle manner, under the central loading point.

iv) Friction and wear tests.

All 18 compositions were tested, and it was found that the compositions which contained no graphite powder (mixes 1,2,3,10,11,12) wore very severely during testing and consequently could only be tested once, so their data has not been presented. For all other compositions, the results of four repeat tests were averaged, and figure 26 and 27, illustrates the typical spread of wear and coefficient of friction data obtained from these materials. Each point represents the average taken over forty readings, the error bars represent the 95% confidence limits, which have been omitted from all other graphs to avoid overcrowding.

Figures 28a to 28d gives a comparison of the coefficient of friction of the remaining 12 mixes. The results have been grouped according to the resin and

TABLE 6

Weight loss and volume change in samples after carbonisation.

Mix N°	% Resin Content	Avg. Wt Loss	Avg. Volume Decrease
1	10	18.42	13.85
2	10	15.30	15.1
3	10	9.83	14.9
4	10	17.57	14.15
5	10	13.58	8.6
6	10	8.58	12.4
7	10	16.03	11.8
8	10	12.37	6.4
9	10	7.49	8.9
10	20	20.53	10.45
11	20	15.86	19.55
12	20	10.45	21.05
13	20	19.56	16.45
14	20	13.88	16.7
15	20	8.99	14.85
16	20	17.91	14.0
17	20	12.77	15.35
18	20	7.25	13.9

graphite composition of each mix. Wear data is presented in the same format in figures 29a to 29d.

Figure 30 shows the average coefficient of friction and wear values for A1 commercial friction material tested under the same conditions. Each point represents the average taken over forty readings, where the error bars represent the 95% confidence limits.

3.3.4 Discussion

ii) Weight losses and volume changes

All samples experienced a volume decrease during carbonisation, and were found to be free from visible crack damage. This is in contrast to the results presented in section 3.1 for conventional friction materials, where the material constituents expanded and wrecked the samples, rendering them useless as friction materials. It is clear from figure 23 that there is a greater volume decrease in samples containing a larger proportion of resin, as would be expected. Interestingly there is also a slight decrease in % volume change with rising sample number in each group of specimens. This may be related to the proportion of graphite powder within each mix, which increases with sample number, suggesting that specimens containing a greater proportion of graphite powder undergo a smaller volume change. Graphite is dimensionally stable over the carbonisation temperatures used, and may well inhibit contraction of the resin matrix.

From the results presented in section 3.2 on the carbonisation of pure phenolic resin, a weight loss of approx. 30% from the resin component was predicted, which means that the expected losses after carbonisation of the above samples, were 6% loss from samples containing 20% resin, and 3% loss from the samples containing 10% resin. However the results given in table 6 show that the losses were much higher. A plot of barytes content vs weight loss in figure 31, shows a direct relationship. Barytes is stable up to temperatures of 1600°C, where a weight loss of less than 1% was recorded during a TGA of pure barytes over the carbonisation temperature range used (figure 32). Such a loss would not account for the losses incurred in the carbonised samples. It was therefore concluded that a reaction must have taken place. The following reaction was proposed:-

$$BaSO_4 + 4C \rightarrow BaS + 4CO$$

In order to test for this, a mixture of barytes and graphite powder was prepared and analysed using the TGA, the resulting thermogram is shown in figure 33.

Evidently there is an increase in the weight loss, with the final loss being 7.5% after being held at 800°C for 1.38hrs. The TGA also shows that the reaction rate increases markedly at 800°C. The weight loss would have been greater if the samples were held at 800°C for 10hrs as were the furnace carbonised samples, and so it follows that the high weight losses reported were due to the reaction suggested above.

To further verify this high temperature reaction, x-ray diffraction traces of a typical composition was taken before and after carbonisation (Figures 34 and 35 respectively). The mix contained 50% barytes, 10% graphite powder, 10% resin, and 30% fibre. Clearly there is a very good match between the $BaSO_4$ peak pattern labelled in figure 34, and that predicted for a standard sample of barytes detailed in the accompanying table as expected. However, the trace shown in figure 35 taken after carbonisation, shows a major change in composition, where the pattern of peaks is totally different. The new pattern corresponds to that expected from a standard sample of BaS detailed in the accompanying table. (The graphite peaks have also been labelled for clarity). This result clearly proves that the $BaSO_4$ (barytes) in the uncarbonised sample, is reduced to BaS after carbonisation.

iii) Three point bend tests

The results of the flexural strength measurements on all 18 compositions are presented in figure 24, and on comparison, were shown to be weaker than conventional friction materials such as A1, whose flexural strength was found to be $39MN/m^2$. The elastic modulus of A1 friction material was found to be $9GN/m^2$, comparing this figure with the range elastic moduli measured in the experimental materials presented in figure 25, it is clear that even after carbonisation, these materials possessed a comparable or higher modulus than A1.

The addition of graphite powder caused a decrease in both flexural strength and elastic modulus. The % volume change results for each composition shown in figure 23 indicated that samples containing larger amounts of graphite powder underwent a lower shrinkage during carbonisation. Graphite is dimensionally stable over the carbonisation temperatures used and may well inhibit contraction of the resin matrix. This would then lead to a build up of internal stresses within the sample, lowering the flexural strength and modulus value. Graphite flakes are also known to behave as crack like voids in some solids, encouraging the build up of stress concentrations. This allows cracks to propagate through the material more easily, so reducing the strength of the sample.

Samples containing the 20%wt of resin, showed an increase in flexural strength of approximately a fifth, compared to the samples containing 10%wt resin. However, there was no clear improvement in elastic modulus with increased resin content.

Generally increasing the fibre content resulted in a higher elastic modulus, and a higher flexural strength in the samples containing no graphite, whereas in samples containing graphite powder, increased fibre content made little difference to the overall strength of the composite. This was probably due to the weakening effect of graphite powder overriding any strengthening effects imparted by the fibres.

iv) Friction and wear tests

Figures 28a -28d show the coefficient of friction results for each of the different formulations. In each case the coefficient of friction rose during the first 40 to 60 minutes of the test, after which it remained relatively stable for the duration of the test. This behaviour was also seen in A1 friction material shown in figure 30. This early increase in the coefficient of friction in each material was due to a bedding in effect where the real area of contact between the sample and disc increased, resulting in a rise in μ. The level of fibre or resin content had no clear effect on μ, but comparing 28a with 28c and 28b with 28d, samples containing high levels of graphite powder resulted in a slightly reduced μ .

Examination of the graphs shown in figures 29a to 29d, indicate that samples with a larger resin content of 20%wt were more resistant to wear than the samples containing 10%wt resin. The results of the flexural tests showed that a higher resin content, gave a stronger material, which could account for the increased wear resistance. Also as the resin becomes carbonised its structure becomes more ordered, (Section 3.2.6 x-ray diffraction data). The carbonised structure may possess planes of easy slip and have some lubricating properties, so that a higher resin content would have the effect of reducing wear.

The effects of fibre content are less clear, but materials containing 70%wt fibre, had a generally lower wear rate than those containing 30% fibre, due to the higher strength of these materials.

The lubricating properties of graphite powder were shown to be very important in reducing wear. This can be seen by comparing the wear rates of materials containing 5% graphite (Figures 29a and 29b) with the wear rates of materials containing 10% graphite (Figures 29b and 29d).

Many of the samples showed negligible wear during the first 40 minutes of testing, after which the wear rate increased. The same behaviour was seen in the test results for A1 friction material shown in figure 30. This increase in wear rate

coincides with the point at which the sample shows full contact with the disc surface, characterised by a constant coefficient of friction shown in figures 28a to 28d. Overall the wear rates shown by many of the compositions tested were of the same order as that of A1 commercial brake material.

3.3.5 Conclusions

The experiments described in this section were designed to explore the possibility of producing a simple experimental friction material, which in a carbonised form would retain sufficient strength, and the necessary tribological properties, to be used in a brake system. The properties of the experimental materials were measured and compared to those of a commercial friction material (A1) which was used as a bench mark. It was found that the experimental materials had a lower flexural strength, with some samples possessing only half the strength of A1, whilst elastic modulus was found to be same or higher. More importantly, the friction and wear behaviour of a large proportion of the formulations tested was comparable to that found in A1, tested under the same conditions.
The effects of each constituent on both the mechanical and tribological properties of the carbonised composite are summarised below:-

1) Graphite powder was found to act as an effective lubricant, and was unaffected in its action by the carbonisation process. It was found that the addition of graphite reduces both friction and wear rate as would be expected, but also reduces the flexural strength and elastic modulus. There was also some evidence that graphite powder could inhibit matrix contraction during carbonisation, resulting in high internal stresses within the sample. This could explain the lower flexural strength and modulus values found in samples with a high graphite content. It is also well known that graphite flakes can act like internal cracks, producing stress concentrations, which encourages cracks to propagate, producing a weakening effect on the composite.

2) The mineral fibres used were found to be unaffected structurally, and possessed the same hardness before and after carbonisation. Samples with a larger fibre content possessed a generally higher elastic modulus and flexural strength, whilst the level of fibre content was found to have little effect on the coefficient of friction. Samples with a high fibre content showed generally lower wear rates.

3) Materials with the higher resin content although accompanied with a higher weight loss, were as much as 20% stronger and showed greater wear resistance. However, there was no discernible effect on the coefficient of friction.
In addition to the above findings barytes ($BaSO_4$) which was previously regarded as an inert filler material, was shown to react with graphite powder to form barium sulphide (BaS) and carbon monoxide (CO) during carbonisation to 800°C.

Figure 20
Schematic diagram of a 'pin on disc' wear machine.

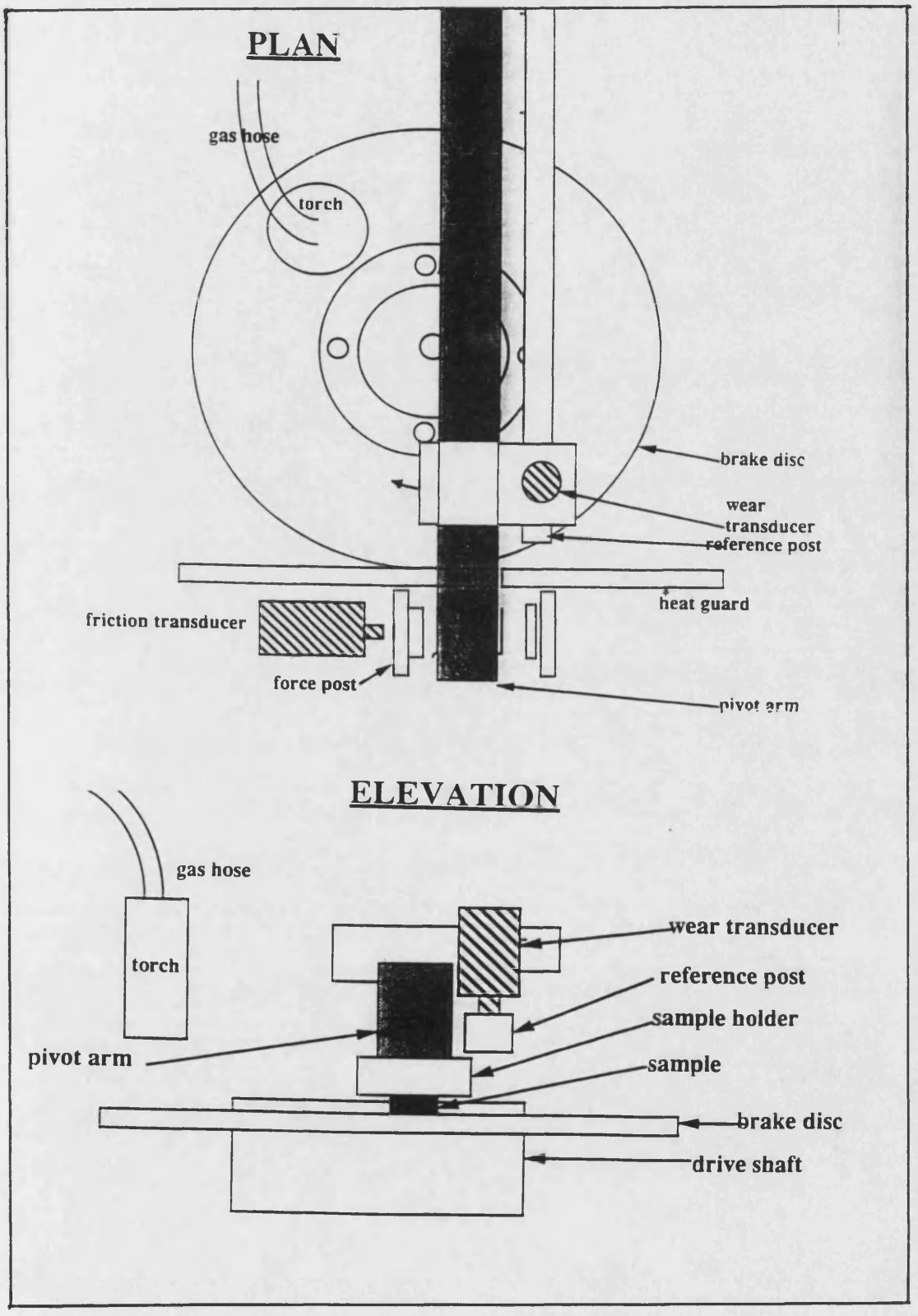

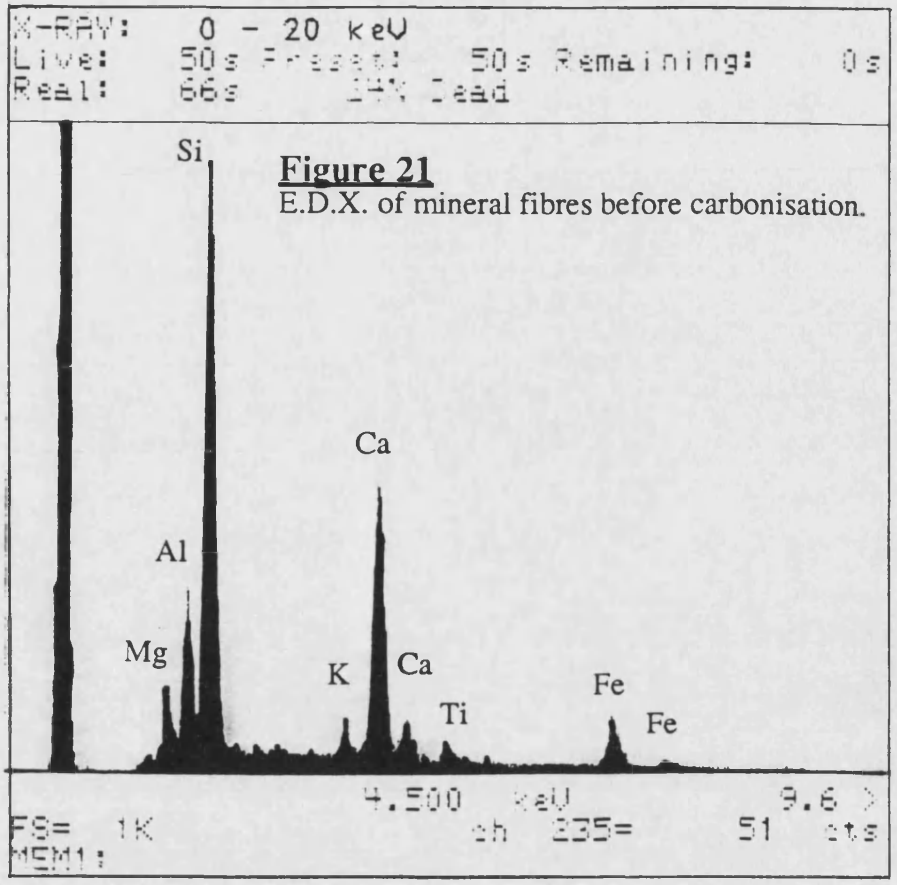

Figure 21
E.D.X. of mineral fibres before carbonisation.

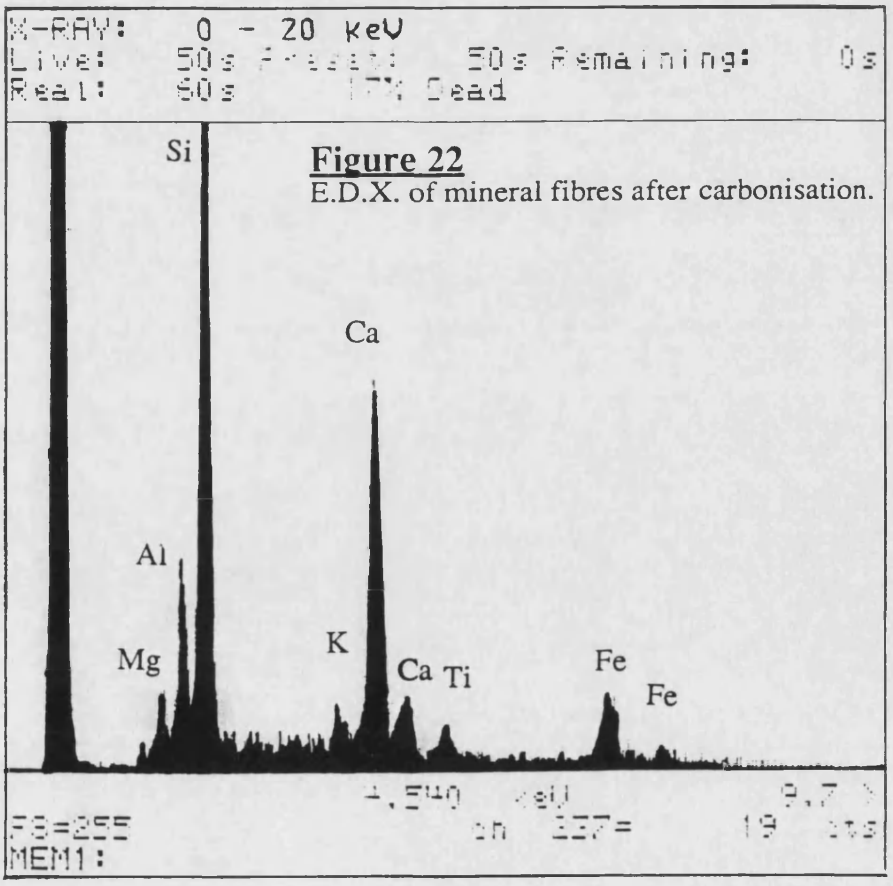

Figure 22
E.D.X. of mineral fibres after carbonisation.

Figure 23

The effect of resin content on volume change during carbonisation.

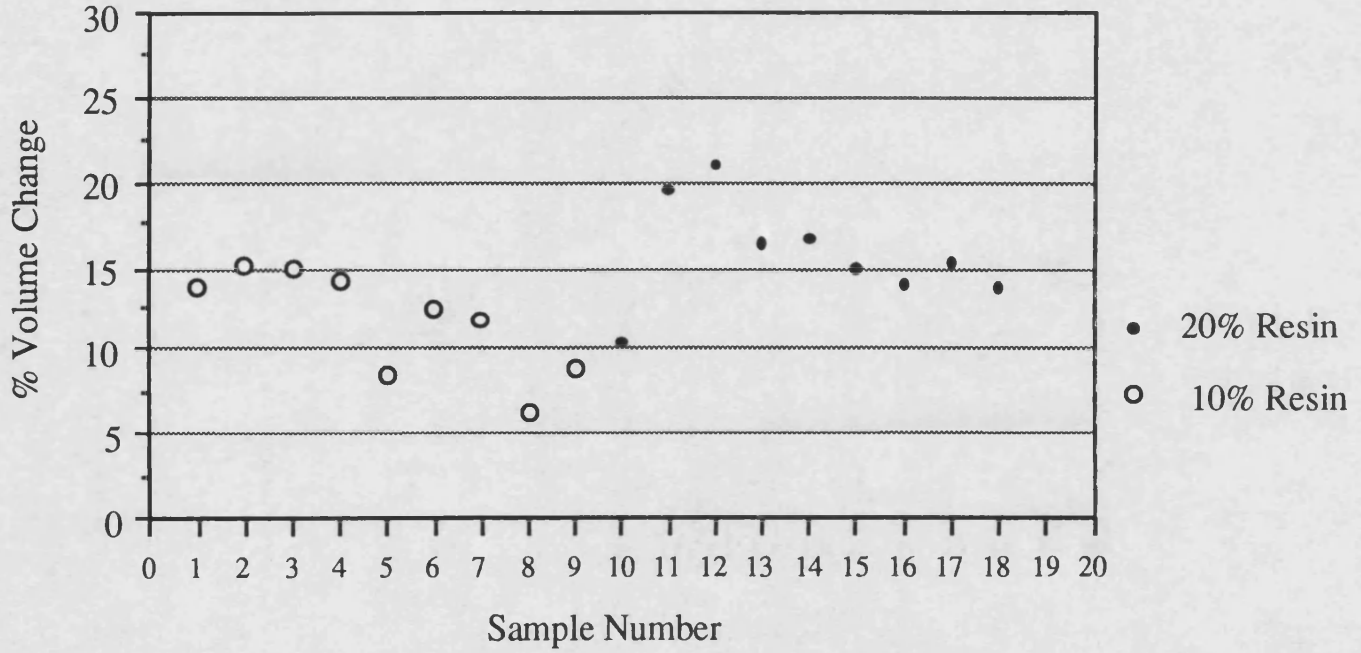

Figure 24 Variation of the average flexural strength with material composition.

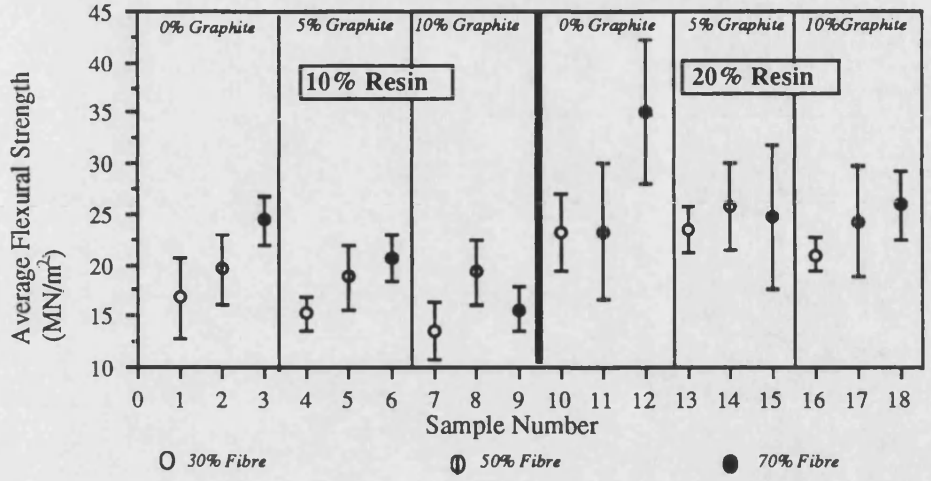

Figure 25 Variation of the average Elastic modulus with material composition.

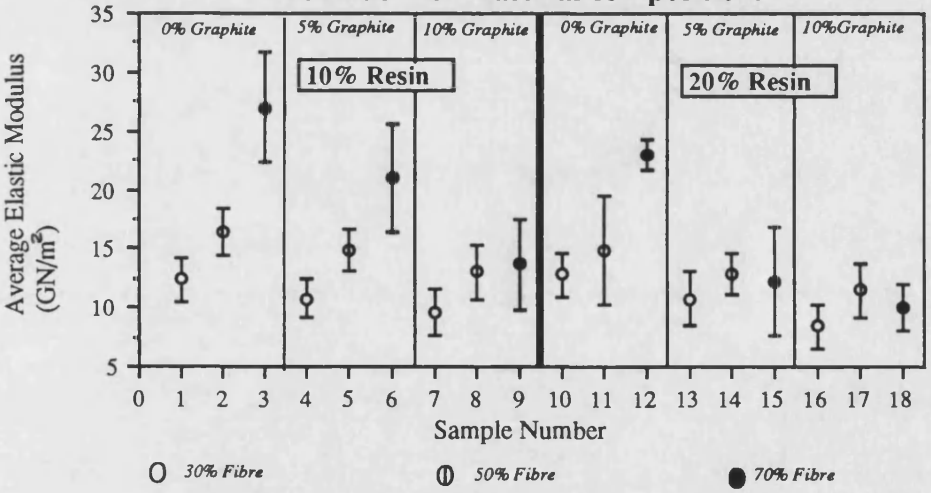

Figure 26

Typical wear data distribution from four tests using sample 17, (Each point represents 40 readings).

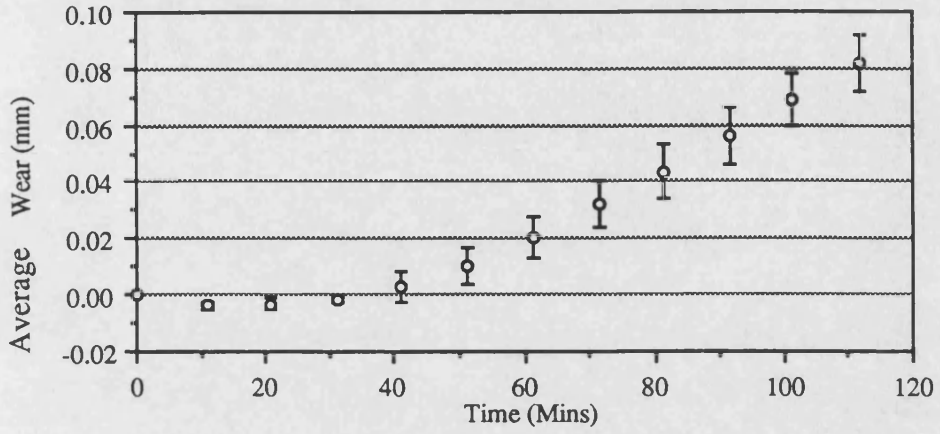

Figure 27

Typical distribution of coefficient of friction data from four tests, using sample 17, (Each point represents 40 readings).

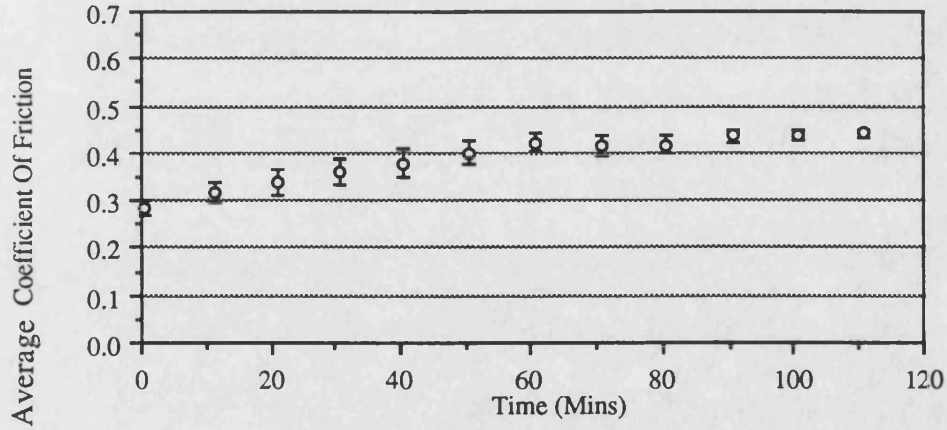

Figure 28a

Average coefficient of friction for samples containing 10% resin, & 5% graphite.

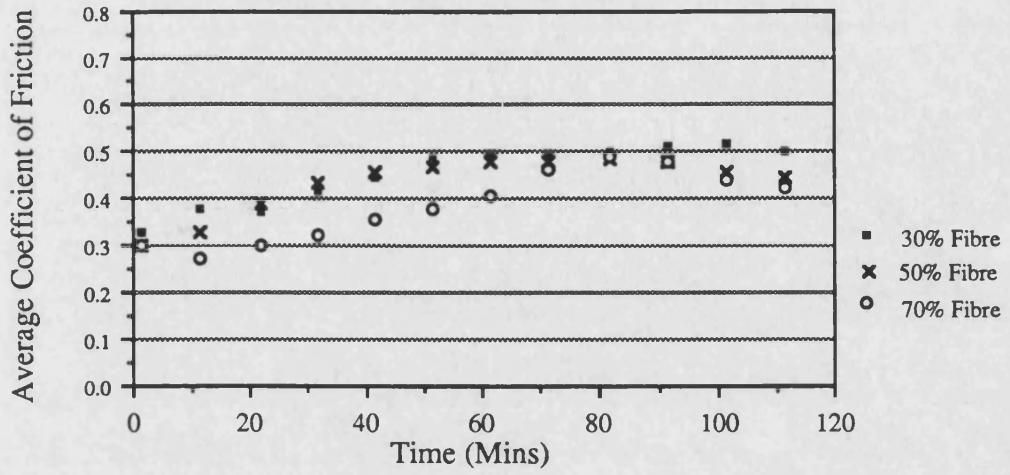

Figure 28b

Average coefficient of friction for samples containing 20% resin, & 5% graphite.

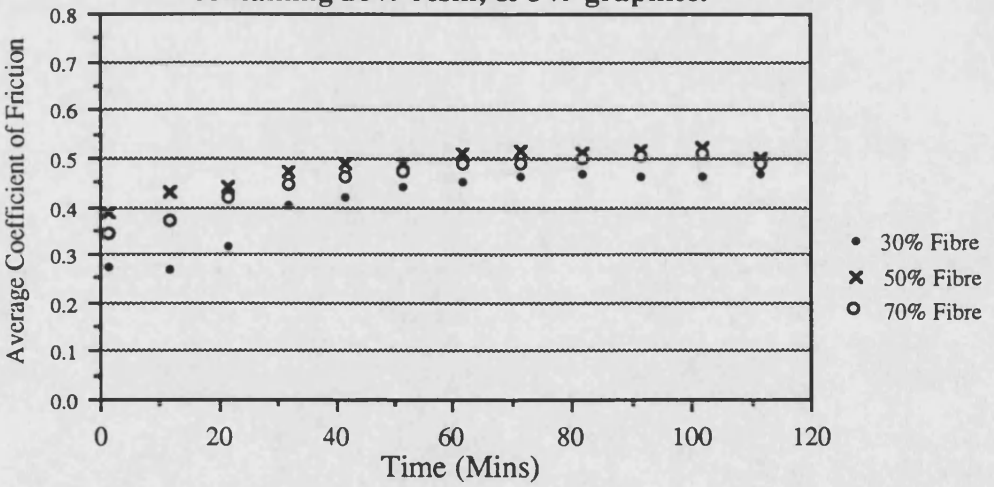

Figure 28c

Average coefficient of friction for samples containing 10% resin, & 10% graphite.

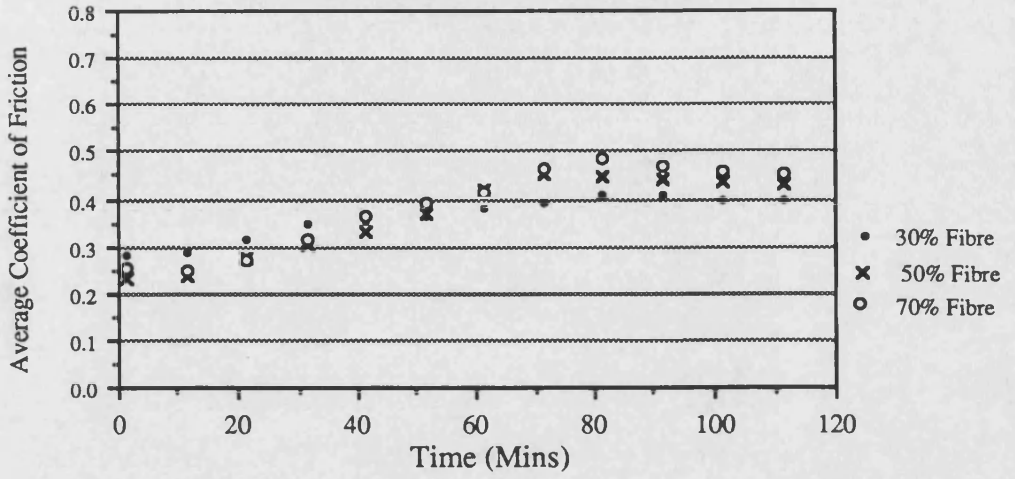

Figure 28d

Average coefficient of friction for samples containing 20% resin, & 10% graphite.

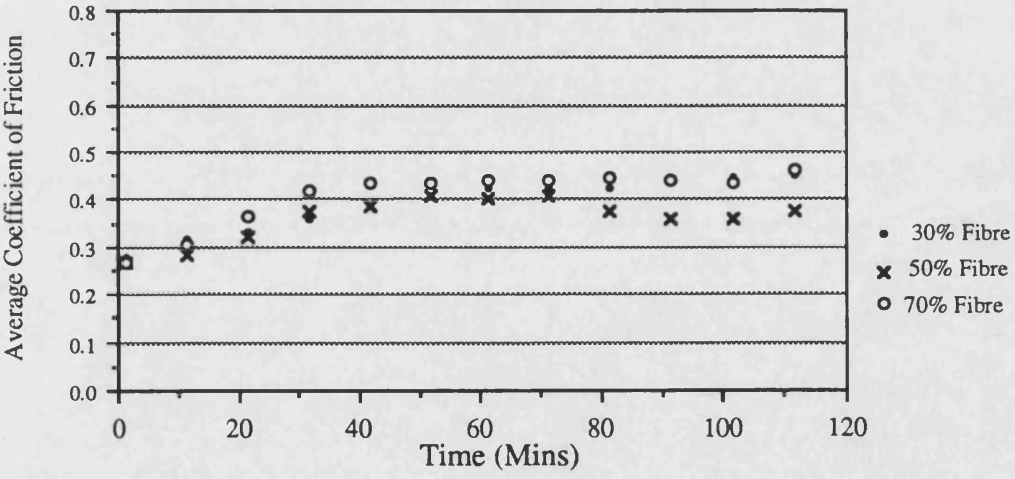

Figure 29a Average wear for samples containing 10% resin & 5% graphite.

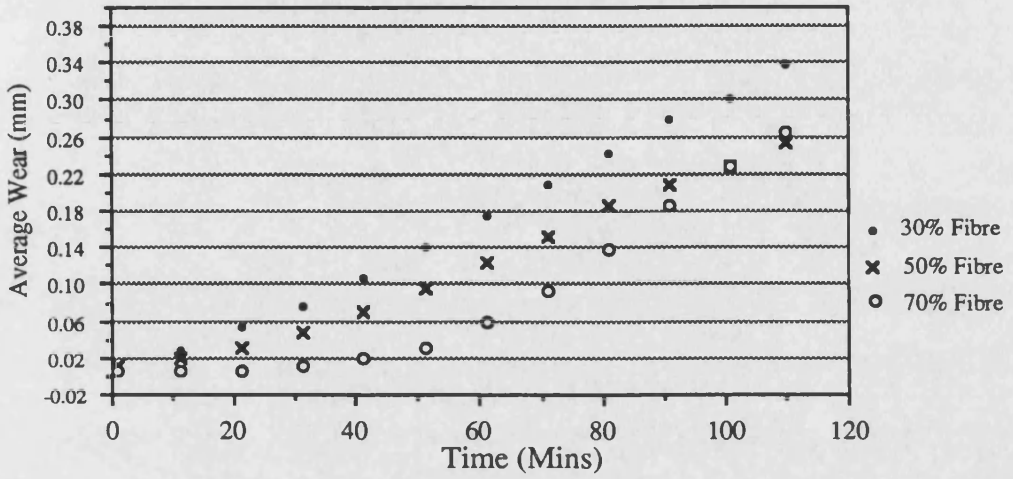

Figure 29b Average wear for samples containing 20% resin, & 5% graphite.

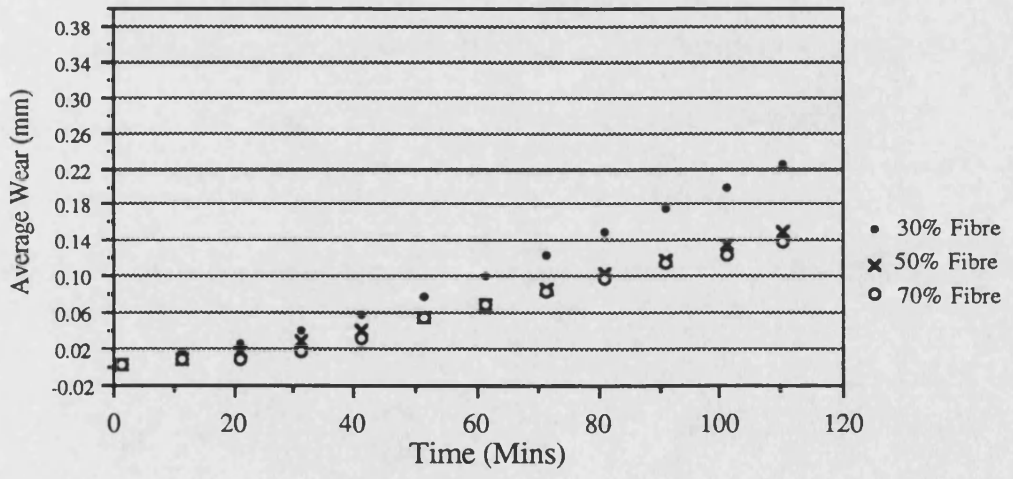

Figure 29c

Average wear for samples containing 10% resin, & 10% graphite.

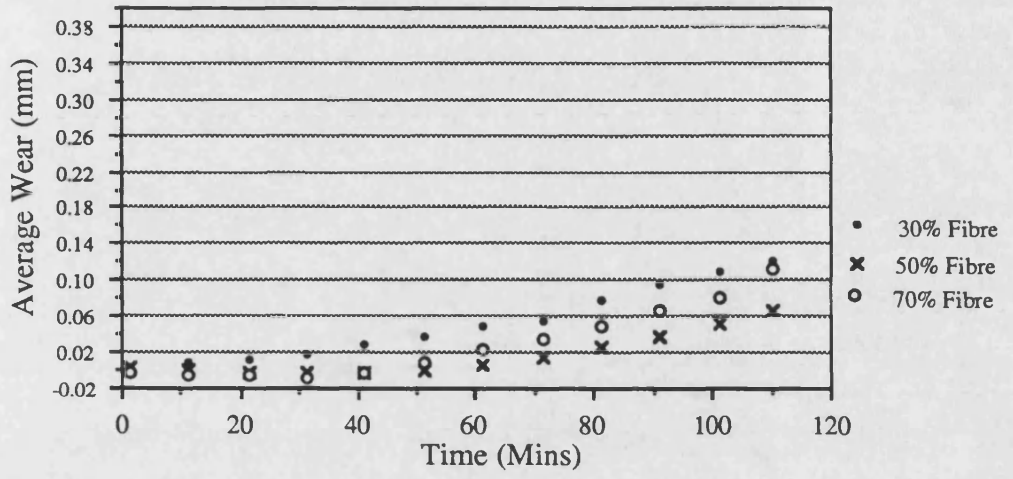

Figure 29d

Average wear for samples containing 20% resin, & 10% graphite.

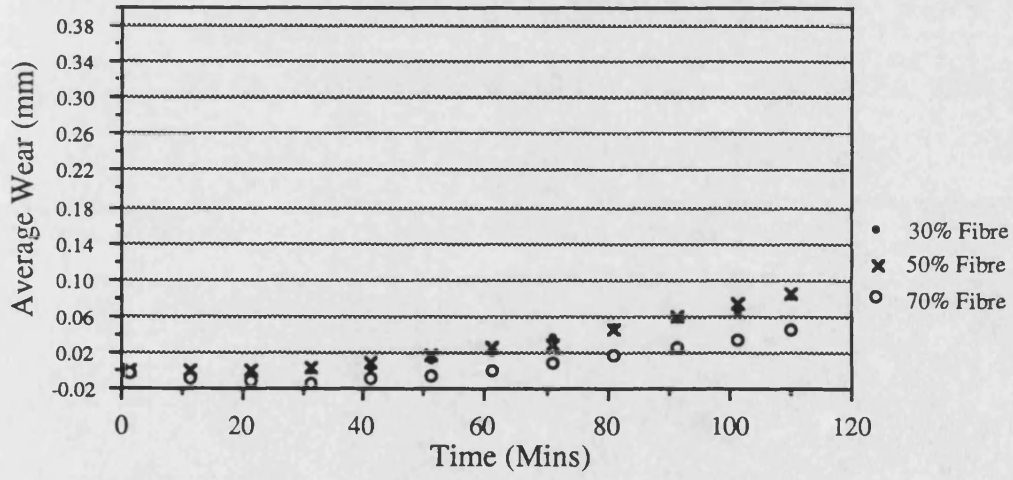

Figure 30

Friction and wear data for a conventional friction material (A1).

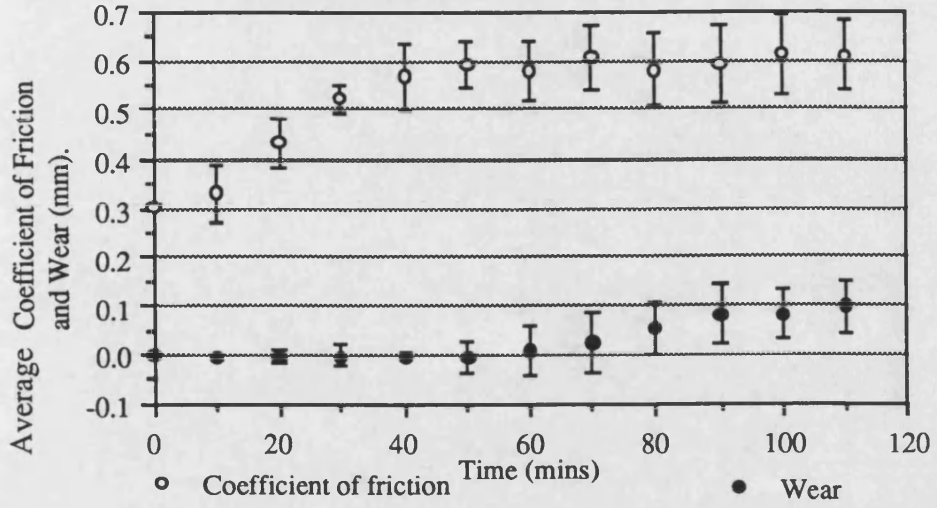

Figure 31

Variation of %wt loss during carbonisation with % Barytes content.

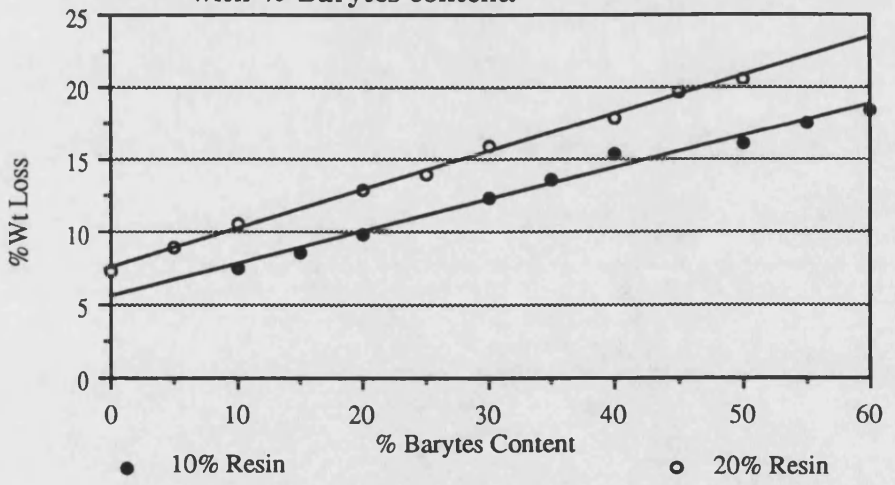

Figure 32

TGA of pure barytes (barium sulphate).

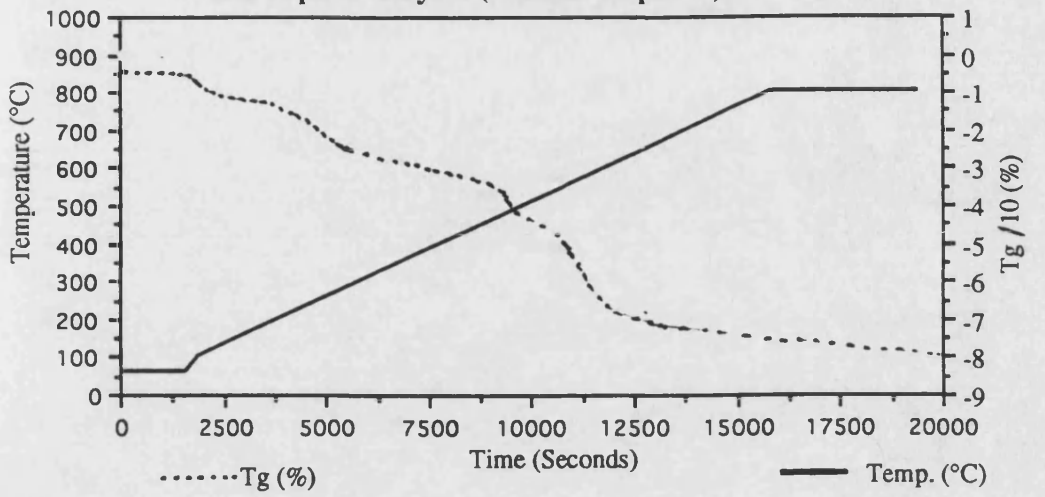

Figure 33

TGA of barytes plus graphite powder.

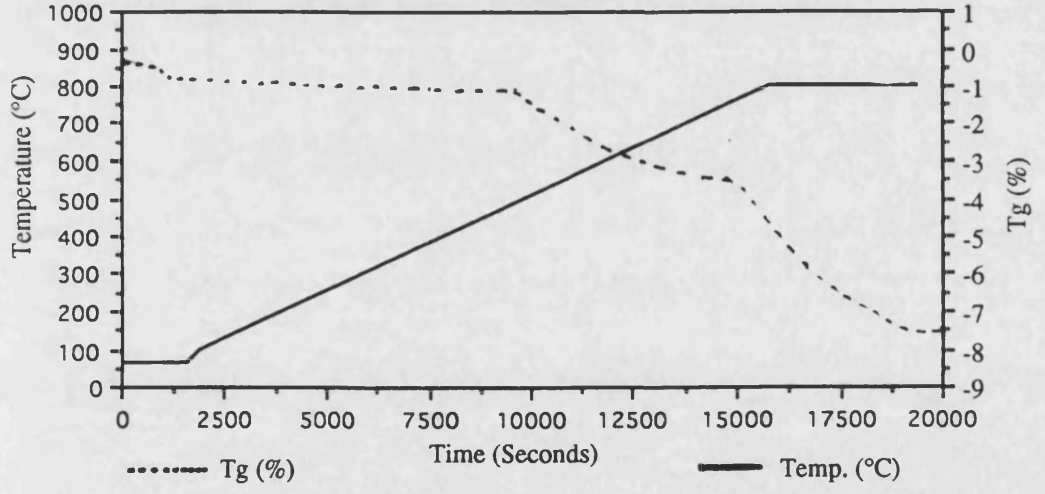

Figure 34

X-ray diffraction pattern of R1 friction material containing :- 50% barytes ($BaSO_4$), 10% Graphite, 10% resin, and 30% fibre. The trace was taken before carbonisation. (The accompanying table lists crystallographic data taken from a standard sample of $BaSO_4$, which was used to label various peaks in the trace with the correct *hkl* co-ordinates).

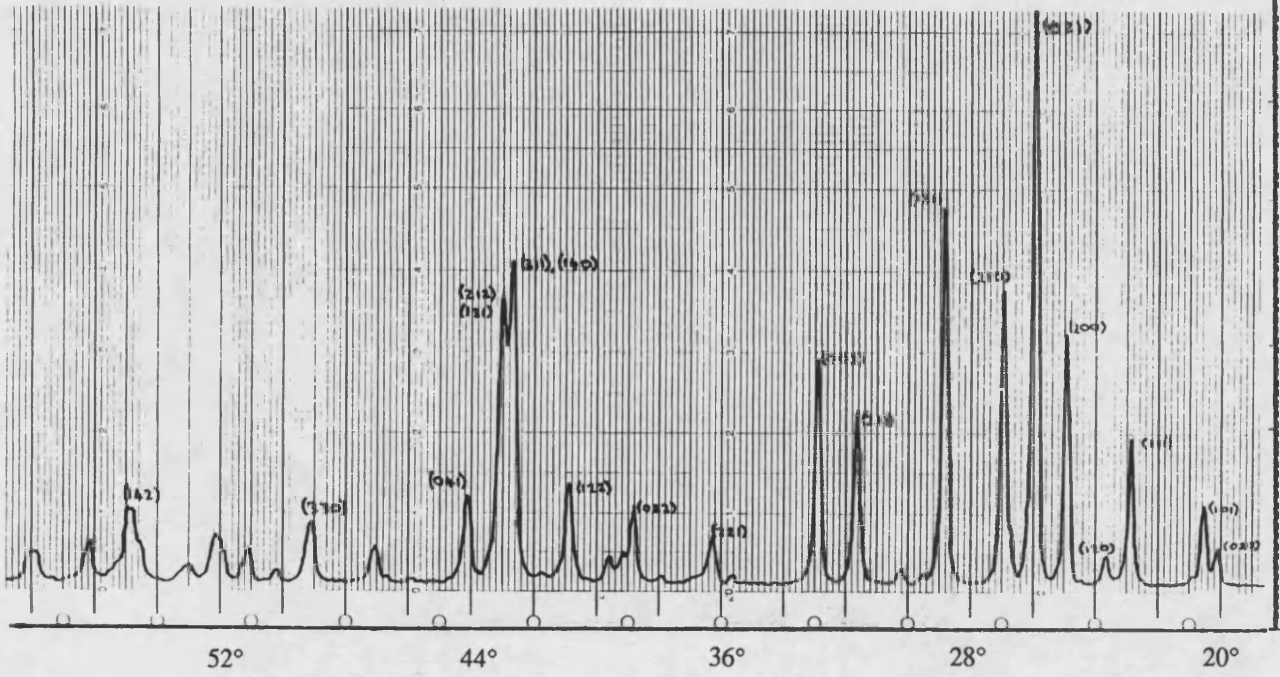

d Å	Int.	h k l
5.58	2	1 1 0
4.44	16	0 2 0
4.339	30	1 0 1
3.899	50	1 1 1
3.773	12	1 2 0
3.577	30	2 0 0
3.445	100	0 2 1
3.319	70	2 1 0
3.103	95	1 2 1
2.836	50	2 1 1
2.735	15	1 3 0
2.729	45	0 0 2
2.482	13	2 2 1
2.447	2	1 3 1
2.325	14	0 2 2
2.305	6	3 1 0
2.282	8	2 3 0
2.211	25	1 2 2
2.169	3	2 0 2
2.121	80	1 4 0
2.106	75	2 1 2
2.057	19	0 4 1
1.9486	1	2 2 2
1.9317	7	1 3 2
1.8575	18	3 3 0

Figure 35

X-ray diffraction pattern of R1 friction material containing :- 50% barytes ($BaSO_4$), 10% Graphite, 10% resin, and 30% fibre. The trace was taken after carbonisation. (The accompanying table lists crystallographic data taken from a standard sample of BaS, which was used to label various peaks in the trace with the correct *hkl* co-ordinates).

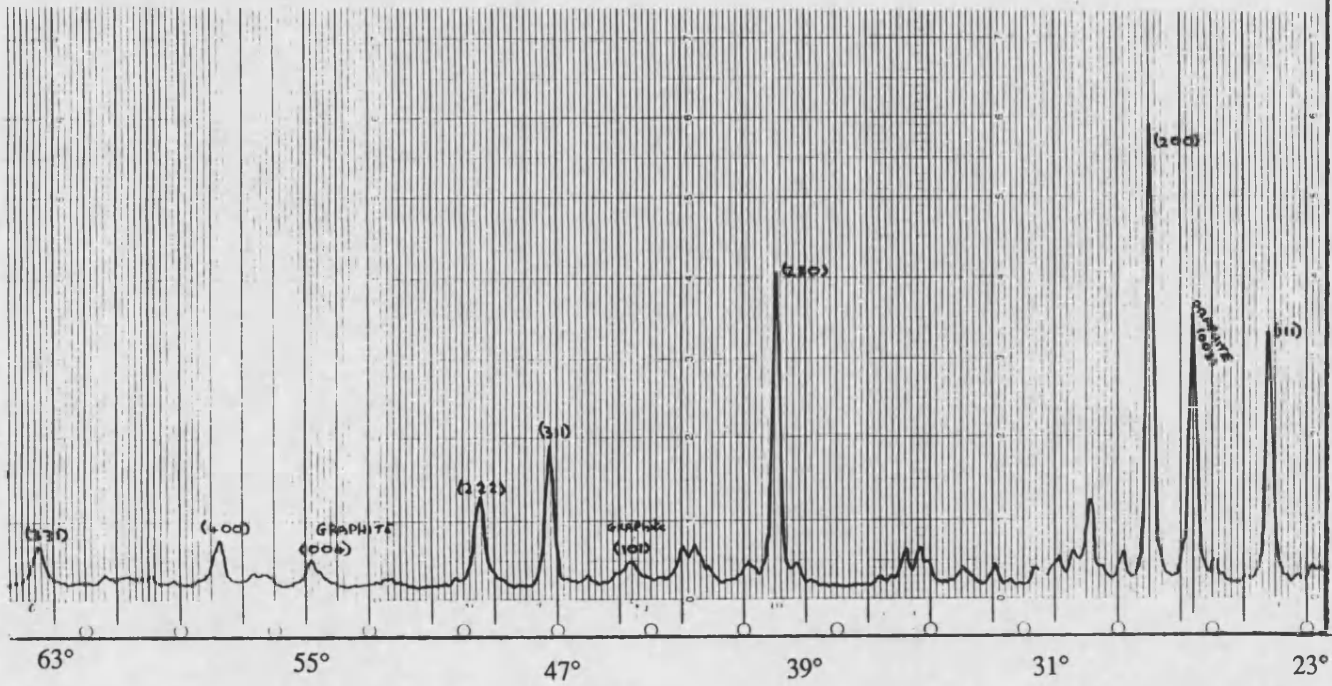

d A	Int.	h k l
3.688	70	1 1 1
3.194	100	2 0 0
2.258	80	2 2 0
1.9258	40	3 1 1
1.8433	25	2 2 2
1.5970	14	4 0 0
1.4652	12	3 3 1
1.4287	35	4 2 0
1.3037	20	4 2 2
1.2291	10	5 1 1
1.1286	6	4 4 0
1.0801	8	5 3 1
1.0641	14	6 0 0
1.0094	10	6 2 0
0.9734	6	5 3 3
0.9627	8	6 2 2
0.9217	<1	4 4 4
0.8941	6	5 5 1
0.8856	8	6 4 0
0.8534	12	6 4 2
0.8313	8	7 3 1
0.7984	<1	8 0 0

3.4 Fade Assessment Using An Inertia Dynamometer

3.4.1 Introduction

The pin on disc continuous drag test machine used in section 3.3, was useful for giving comparative information on the carbonised materials formulated, however it was unable to give information on the fade characteristics of the carbonised materials or simulate the real braking conditions, found in automobiles etc. To determine these latter properties testing is normally performed on an inertia dynamometer.

An inertia dynamometer simulates the inertia generated in the average automobile when in normal use. This is achieved by using a large flywheel, which is connected to a car brake disc. Testing involves halting the motion of the flywheel by disc pads, as normally found on a car. A diagram of a commercial dynamometer is shown in the appendix (page 230).
Temperatures generated during dynamometer testing are of the same order as those generated in a car under severe braking conditions. This means fade testing can be carried out, as well as friction material wear measurements.

3.4.2 Methods and materials

Four 70 mm diameter discs of the following mix were moulded:

20% Phenolic Resin

25% Barytes

50% Rockwool Fibre

5% Graphite Powder.

This particular formulation was selected from those tested in section 3.3, because it displayed a stable coefficient of friction, a low wear rate, and retained a high flexural strength after carbonisation.
Samples were post-baked at 180°C for 6hrs, and carbonised using the same heating program outlined in section 3.2. The carbonised samples were then cut and bonded to steel back plates to produce a set of brake pads for testing. The

material will hence forth be referred to as R1. A1 commercial friction material was also tested for comparison.

Dynomometer testing involves four test sequences, as follows:-
1) A bedding in cycle, of 250 stops, from 30mph, to monitor initial wear and to ensure good mating between the pad and disc surface.

2) An initial performance test, where coefficient of friction (μ), is related to calliper pressure (the pressure applied to a pad during braking). This test is performed at speeds equivalent to 30, 50, and 70mph, where four stops are made at each speed. The pad - disc assembly is cooled using air blowers so that each stop starts at the same temperature, thereby ensuring that each test is conducted under the same conditions.

3) Fade and recovery tests were performed at 30 and 50mph. This involves 40 stops in quick succession, thereby causing the temperature to rise to a level sufficient to induce fade. At stop 30, the air blowers are switched on, and temperature is reduced for the last ten stops. This is when recovery occurs.

4) After the fade and recovery test step 2 is repeated, this is termed the final performance test.

3.4.3 Results

The dynamometer test results for the R1 experimental material, were compared to those of A1 a heavy duty industrial brake pad material.
1) Bedding in results
During bedding in the R1 material lost 0.44mm of material, which is a factor of ten larger than that lost by A1 under the same conditions.

2) Initial performance
Figures 36 and 37 show initial performance test results for the R1 material and A1 respectively. The μ value of R1 was an acceptable level for use as a brake material. Also μ remained at a high level during initial testing. The results for A1 show a characteristic drop in μ with increased test speed, this trend was not so clear in the R1 material.

3) Fade and Recovery Tests

Unfortunately the R1 sample disintegrated during the 50mph test, making the results invalid, hence only the 30mph test results will be considered.
The 30mph fade tests for A1 material are shown in figure 38. Disc temperature rose to 400°C by stop 30, where the μ value faded to 0.25. The disc was then cooled to approx. 100°C allowing the coefficient of friction to recover to approx. 0.4.
Figure 39 shows the fade and recovery test for R1. The μ value did not fall below 0.3, but increased with rise in temperature. On cooling after stop 30, the R1 over recovered to a μ of 0.52, which subsequently dropped back to a level of 0.32.

4) final performance tests could not be performed as the R1 samples had disintegrated during the fade and recovery test.

Final wear results were that R1 lost a total of 2.0mm during all tests made, this was about a factor of ten larger than that of A1.

3.4.4 Discussion

The R1 material showed a promisingly stable coefficient of friction throughout the tests performed, showing significantly less fade than A1. This indicated that the carbonisation of the phenolic resin matrix prior to testing, imparts some fade resistance.
Dynamometer testing showed that R1 experimental material was susceptible to high wear rates, a factor of 10 higher than found in A1, whilst the pin on disc testing carried out in section 3.3, indicated that the two materials had similar wear rates. The reason for the difference in these findings is that dynamometer testing involves much higher sliding speeds, and consequently the temperature reached during testing is much higher, involving disc temperatures of over 500°C. In contrast during the pin on disc tests described in section 3.3 the recorded disc temperature reached a maximum of only 165°C. This fundamental difference in test conditions highlighted the need for a clearer understanding of the effects of test temperature on wear rate in friction materials.
The R1 composite proved to be too weak and friable to cope with the repeated brake applications involved in dynamometer testing, clearly a stronger and tougher material was needed.

3.4 .5 Conclusions

R1 showed a promisingly stable coefficient of friction throughout the tests displaying significantly less fade than a conventional friction material, indicating

that the theory of using a pre-carbonisation heat treatment to remove the volatile components which cause fade, is essentially valid. However, R1 showed a very high wear rate compared to A1, and lacked the mechanical strength and toughness to withstand the repeated brake applications made during use.

3.5 Summary

Phenolic resin based friction materials undergo carbonisation during high temperature braking, the volatiles produced being the cause of brake fade. This statement has been validated by the work described in this chapter, where it has been shown that brake fade can be reduced by the removal of the volatile components within friction materials, by subjecting the material to a carefully controlled high temperature carbonisation after fabrication.

A detailed study of the way the phenolic resin matrix behaves during carbonisation, showed that the resin undergoes a typical weight loss of 30%, and contracts by 35%. There is also a strong indication that the resulting structure is more ordered. Such a carbonisation regime involved temperatures up to 800°C, and under these conditions many of the usual constituents found in commercial friction materials undergo expansion and become reactive, which lead to higher weight losses and damage to the sample. As a consequence the resulting carbonised product was weak and unsuitable for use as a friction material.

The lack of strength of carbonised friction materials, was a serious drawback. The problem was addressed to some extent by using a gentler carbonisation regime, and by formulating friction materials from only those constituents which were thought to remain inert over the temperatures used. Low temperature laboratory tests gave promising low wear rates for these materials, whereas during industrial testing on an inertia dynamometer involving temperatures up to 500°C, the material once again showed an unacceptably high wear rate.

Clearly improvements in the strength and toughness of carbonised materials was needed, coupled with a greater understanding of how material strength changes with carbonisation temperature. Also an investigation into how conventional friction materials behave during high temperature testing, could give an insight into how the wear rates of carbonised materials could be improved.

Figure 36
Performance inertia dynamometer test on R1 experimental material.

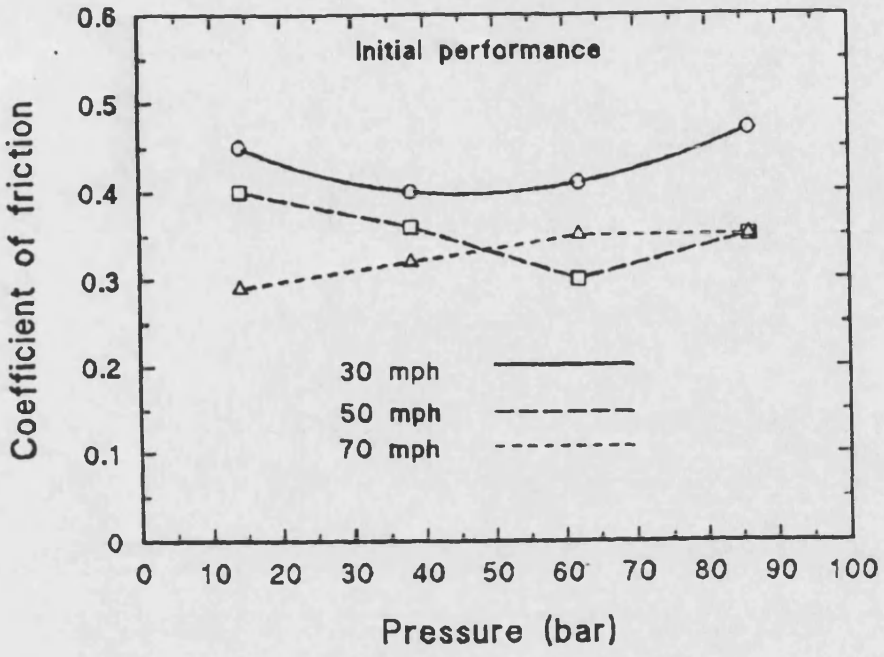

Figure 37
Performance inertia dynamometer test on A1 conventional friction material.

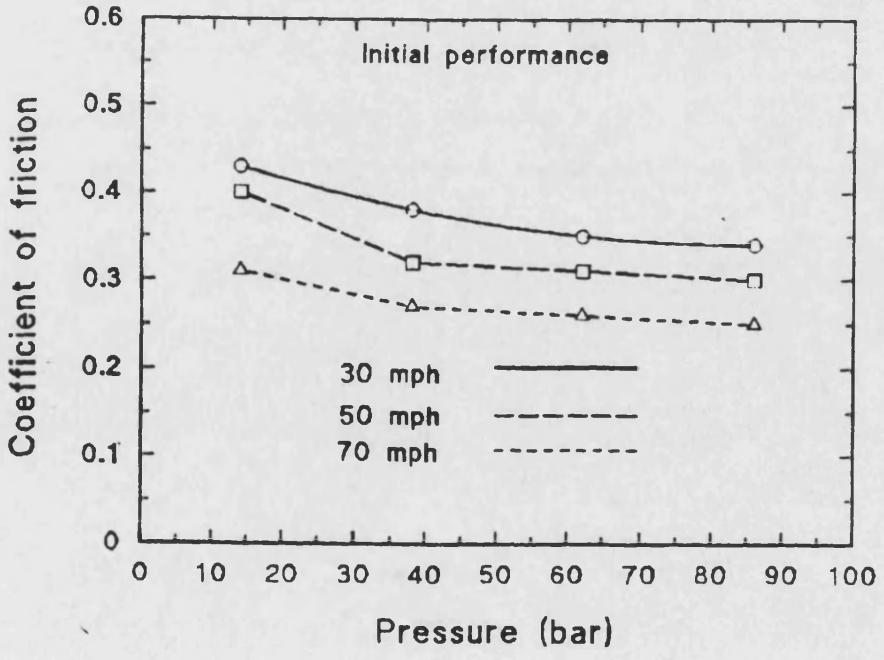

Figure 38
30mph fade and recovery dynamometer test on A1 conventional friction material.

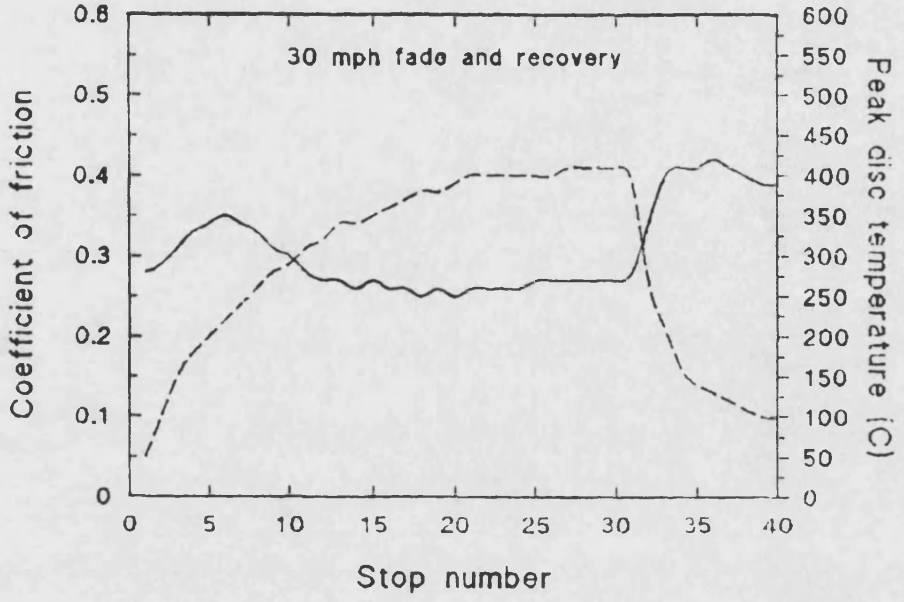

Figure 39
30mph fade and recovery dynamometer test on R1 experimental material.

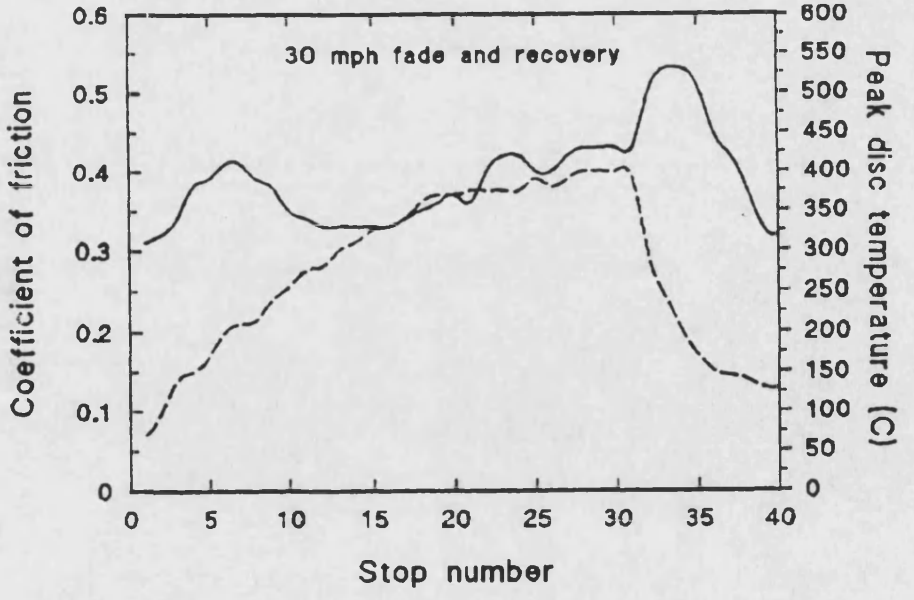

CHAPTER 4

4.1 An investigation into the effect of carbonisation temperature on the mechanical and tribological properties of friction materials

4.1.1 Introduction

The work presented in Chapter 3 concluded with the dynamometer testing of a carbonised experimental friction material, and it was found that the material showed promising fade resistance. However, the material was also severely weakened during the carbonisation process, and consequently wore heavily during dynamometer testing. In order to address this problem, detailed information was needed on how the mechanical strength and wear of friction materials changes as the carbonisation temperature is raised. In this study a simple friction material was formulated, and batches of samples were carbonised at different temperatures up to a maximum of 800°C, and the resulting flexural strength, coefficient of friction, and wear behaviour of each batch was measured and compared.

4.1.2 Methods & Materials

It is inevitable that the strength of a phenolic resin based composite will be reduced during high temperature carbonisation. In order to minimise this effect, it is important to select an experimental material which possesses a high strength in the "green form" or uncarbonised state, and which contains only materials that remain inert up to temperatures of 800°C. In Chapter 3 it was shown that the barium sulphate component of the R1 experimental material, reacted with carbon at elevated temperatures, producing carbon monoxide as a by-product. The internal build-up of gas within samples may have caused internal stresses to develop resulting in a weaker product, consequently barium sulphate was not used in further test materials. Preliminary flexural strength tests were performed on a range of different composites composed of materials typically used in brake pad formulations. The composite formulation chosen for its superior strength in the 'green' form, here after referred to as R2 was as follows:

25% Vol. Phenolic Resin (High carbon yield novalac),
10% Vol. Graphite Powder,
65% Vol. Mineral Fibre.

The mineral fibre used had a typical length of between 15 - 19mm, and an average diameter of 9μm, the chemical composition is shown in table 7.

Table 7 Typical composition of a mineral fibre

OXIDE	WEIGHT %
SiO_2	38 - 46
CaO	31- 40
Al_2O_3	9 - 12
MgO	8 - 15
Fe_2O_3	0 - 2

This mix was moulded into flat plates, using the procedure outlined in section 3.3.2-chapter 3. Flexural strength test specimens were prepared having the following dimensions:- 150mm long, 5mm thick, and 13mm wide. Pin on disc specimens were all $10mm^3$.

The specimens were divided into 8 groups, each containing 9 flexural test samples, and 6 pin on disc samples making a total of 15 samples in all. Each group was carbonised at a different temperature:- 150°C, 200°C, 300°C, 400°C, 500°C, 600°C, 700°C, and 800°C, using the heating schedule shown in table 8.

Table 8 Heating schedule used for the carbonisation of R2 friction material

RAMP	TEMPERATURE
100°C/hr	up to 150°C
50°C/hr	up to 200°C
20°C/hr	up to 300°C
7°C/hr	up to Finish Temperature
4hr Dwell	At Finish Temperature

Each sample was weighed before and after carbonisation, so that weight loss could be calculated. Three point bend tests were conducted in accordance with

ASTM standard N_O 790 - 80, and the flexural strengths of each specimen were determined. Friction and wear tests were carried out on the pin on disc apparatus (details of which are outlined in section 3.3.2 chapter 3), and each sample was tested under an applied pressure of 2.7 MPa, at a disc rpm of 170, for 3hrs. Samples were weighed before and after each test, so that wear/hr in grams could be calculated. In this way the wear data derived from the measurements made by the wear transducer mounted on the pin on disc machine could be verified. Dynamometer testing discussed in chapter 3 highlighted how the high temperatures generated under real braking conditions, can cause a large increase in the wear rate of friction materials. To study the effect of high braking temperatures on friction and wear, the pin on disc test machine was adapted to allow a propane gas torch to be used as a heat source (see Figures 40a to 40d). The flame was directed onto the disc surface and could generate disc temperatures of up to 500°C. This facility was used to test each sample of R2 at high temperatures by holding the disc surface at approximately 400°C during testing, to simulate the disc surface temperatures reached during standard dynamometer tests. The disc surface temperature was measured and recorded using a thermocouple sliding on the surface of the rotating disc (see Fig. 40d).

4.1.3 Results

The flexural strengths and accompanying weight losses for each of the groups of carbonised R2 materials are shown in figure 41. The error bars designate 95% confidence limits, and all samples failed in a brittle manner, directly below the central loading point. Clearly as the carbonisation temperature rises, weight loss rises, and flexural strength falls, until after 500°C where both weight loss and flexural strength start to level out.

Figure 42 is a typical set of friction and wear data for R2 friction material. This particular set of data is from a test on a sample of R2 material which had been carbonised to 150°C. Clearly, there is an approximately constant wear rate and coefficient of friction throughout the test, (this behaviour occurred in all the other R2 samples, irrespective of their individual carbonisation temperatures). No external heating was applied during testing, and the temperature rise shown was entirely due to frictional heating. This resulted in the temperature rising to 125°C in this particular test, (during the testing of other R2 samples, frictional heating resulted in maximum temperatures of between 115 - 165°C).

Each of the groups of R2 samples were also tested under high temperature conditions where the disc surface temperature was raised to 400°C, figure 43 is a typical set of data from a high temperature test. The disc was heated from room

temperature to 400°C in approximately 30 minutes, after which time the wear rate was high and the coefficient of friction was low. The transition to high wear and low friction coefficient occurred at approximately 325°C.
Similar data were obtained for each of the batches of samples, and from this data the average wear rate and coefficient of friction for each material was calculated and the results are shown in figures 44, 45, and 47.
The effect of carbonisation temperature on the wear rate of R2 friction material during unheated tests is shown in figure 44. Wear rates were very severe in samples that were carbonised at temperatures above 600°C, and for this reason the data has been omitted from the plot. The wear rates for each of the carbonised samples during high temperature testing, are also shown.

The wear data for R2 material presented in figure 44 was derived from wear transducer measurements, and those in figure 45, were found by measuring the weight changes in samples before and after each test. On comparison of the figures 44 & 45, the wear behaviour of R2 is essentially the same regardless of the method of measurement, and because the two methods are entirely independent of one another, it substantiates the wear data presented.
The change in the average coefficient of friction with carbonisation temperature is shown in figure 47, where the friction coefficient data from high temperature tests are also shown. For the reasons stated above, data for samples carbonised at temperatures above 600°C have been omitted.

4.1.4 Discussion

Figure 41 shows how weight loss rises with carbonisation temperature, reaching a maximum of 6.8% in samples carbonised to 800°C. This value is lower than that recorded from any of the R1 materials carbonised to the same temperature. (See chapter 3). The R1 materials all contained barium sulphate, which was shown to react with carbon producing gaseous by-products, which contributed to the overall weight loss from these samples during carbonisation. Barium sulphate was absent from all the R2 formulations, resulting in a lower weight loss.
It has been shown that the expected weight loss from a pure phenolic resin sample when fully carbonised up to a temperature of 800°C is 30%wt. All the R2 samples contained 25%wt of resin, which would have given an expected overall weight loss of 7.5%wt, on full carbonisation up to 800°C. It was found that the weight losses of the 800°C samples, ranged from 6.4 - 7.3%wt, which is approximately equal to the predicted figure. This is a clear indication that the weight losses

which occurred in all the R2 samples, was solely due to the breakdown of the phenolic resin matrix.

The simultaneous fall in flexural strength of R2 samples, with rising carbonisation temperature, is also shown in figure 41. For carbonisation temperatures up to 500°C, samples became progressively weaker as more weight was lost. As volatiles escape from the resin matrix, pores are left behind, and so in samples carbonised at higher temperatures the accompanying weight loss is greater, resulting in a more porous material. It is well known that the nature and extent of porosity in amorphous carbon materials has a major influence on strength [91], where strength falls as the porosity increases. This explains why the strength of carbonised R2 materials falls when higher carbonisation temperatures are used. The average flexural strength of A1 commercial friction material was found to be $38MN/m^2$, which serves as a benchmark in terms of the flexural strength required of a friction material, Figure 41 shows that samples carbonised to temperatures above 400°C, are too weak to be of use as friction materials, whilst those carbonised to 400°C, possess adequate strength, and may also show improved fade resistance, although only about half of the total volatile content would have been removed by carbonising to this temperature.

Fitzer, Mueller, & Schaefer [63], conducted an analysis of the products of phenolic resin pyrolysis, which are illustrated in figure 46. The dashed lines show how the relative portions of gaseous products are divided indicating that up to 400°C the gaseous products consist exclusively of water vapour, which forms from the rupture of methylene bridges. At temperatures above 400°C, larger molecular weight species containing carbon are evolved, indicating that the carbon network is starting to degrade. On comparison of the weight loss curves shown in figures 41 and 46, it is evident that both curves have generally the same shape, although the actual percentage weight loss is much greater in figure 46, because a pure resin sample was used, rather than a composite material as in figure 41. Both curves also indicate that there is a drop in the rate of weight loss after 500°C. Coincidentally the degradation of the carbon matrix reaches a maximum at 500°C after which the rate levels off, as shown in figure 46.

A typical set of pin on disc wear data is presented in figure 42, the temperature rise shown was measured using a sliding thermocouple in contact with the disc surface (See Figure 40d), which showed that disc temperature rose to approximately 125°C, however, it must be stated that this method can only provide bulk disc temperatures, and can not give an indication of the true temperatures being reached at the frictional interface. As yet there is no method which can accurately measure temperatures generated at the brake interface. However, some experiments were performed using thermally activated paints,

which undergo a colour change when exposed to a certain temperature. The paint was applied to the non-contacting faces of a sample, which indicated that during a test where the disc temperature reached approximately 150°C, the temperature reached within the sample near to the sliding interface was 210°C, and microscopic examination of painted areas immediately adjacent to the interface showed that small areas of the interface region had a brownish white tinge, indicating that that these areas had experienced temperatrures as high as 340°C. How these isolated high temperature areas, or "hotspots" influence the overall behaviour of the friction material is uncertain.
Figure 43 shows a typical set of data from a high temperature test, in which the test only ran for 47 minutes, after which the wear transducer went off scale, and further increases in wear could not be measured. These high wear rates occurred in all other high temperature tests performed on R2 material, irrespective of the individual carbonisation temperatures used on each batch.

The change in wear rate with increasing carbonisation temperature is presented in figures 44 and 45. The wear rate of R2 samples carbonised up to 500°C remains constant, after which there is a large increase in wear as the samples become progressively weaker with increasing carbonisation temperatures. Figures 44 and 45 also clearly illustrate the dramatic effect of raising the test temperature. When the disc surface temperature was raised to 400°C (to simulate those temperatures generated during heavy duty dynamometer testing), wear rates were very high and far in excess of the acceptable levels of wear found in commercial friction materials under similar braking conditions.
A partially carbonised friction material may well show a greater resistance to brake fade but these materials must also display acceptable wear characteristics, so it is clearly important to improve the wear resistance of these materials when they are subjected to high test temperatures, so that they display the same degree of wear resistance shown by conventional friction materials. For this to be achieved, a greater understanding of how conventional friction materials behave under high temperature conditions is needed.

Friction coefficient data for R2 material is presented in figure 47, and shows that for the unheated tests there is no clear relation between the average coefficient of friction and the carbonisation temperature used, however the friction coefficient data presented did show some fluctuation, particularly in samples carbonised at 300°C, (Some of the reasons for the more minor fluctuations will become apparent later, during the discussion of figure 48). There was also a marked decrease in μ when the R2 samples were tested at 400°C. This effect could be

linked to the very high sample wear associated with high temperature tests. During heavy wear a large quantity of debris is formed at the frictional interface. This can act as a third body lubricating the interface which effectively reduces the coefficient of friction, similar behaviour has been found by other workers, [60,53].

Also of interest was the fact that during the low temperature pin on disc testing of R2 samples, frictional heating caused a rise in the disc surface temperature which could fluctuate by as much as 50°C from test to test, although the test conditions were identical. This can be explained by comparing the average coefficient of friction value with the temperature attained during each test, (see figure 48). There is clearly a direct correlation between the two. This is not surprising as it follows that a higher coefficient of friction indicates that the frictional force resisting sliding at the interface is greater, (the load applied to the sample being the same in each test). So in samples which display higher coefficients of friction, a greater force is required for sliding to continue, this extra energy produces extra heating, and hence higher disc temperatures. Referring back to figure 47, samples which were carbonised at a temperature of 300°C showed unusually high average coefficients of friction, which resulted in the highest disc temperatures of 160°C+ shown in figure 48. Why these samples showed such high levels of friction is uncertain.

4.1.5 Conclusions

1) Weight losses which occurred during the carbonisation of in the R2 samples tested were solely due to the breakdown of phenolic resin.

2) Weight loss rose and flexural strength fell with increasing carbonisation temperature. The strength of samples carbonised to temperatures beyond 400°C were too low to be of use as friction materials. 400°C has been identified as the temperature above which carbon containing species are evolved during pyrolysis, indicating that the matrix is starting to breakdown. Also the wear rate of R2 samples remains constant in specimens carbonised up to 500°C, above which it increases markedly. Clearly it is beneficial to use lower carbonisation temperatures to gain increases in composite strength, but lower carbonisation temperatures remove less of the volatile components which cause brake fade. There may well be a "middle ground" however, where adequate material strength is retained, and a sufficient quantity of the volatiles are removed from the phenolic resin matrix, to gain some fade resistance. It is suggested by the work in this section that a carbonisation temperature of 400°C, may well produce a

composite with the aforementioned properties. This theory is explored further in the next chapter.

3) The coefficient of friction of R2 material in unheated tests was unaffected by the carbonisation temperature used, however, when the same samples were tested under high temperature conditions, there was a dramatic fall in μ, which was attributed to the lubricating action of the large amounts of wear debris produced.

4) High test temperatures of 400°C+ resulted in large increases in wear for the R2 material. In order to improve the high temperature performance of carbonised materials, a greater understanding of the various effects of high temperatures is needed. Since some conventional friction materials perform well under high temperature conditions, a detailed study of the behaviour of these materials, would give a better understanding of high temperature wear.

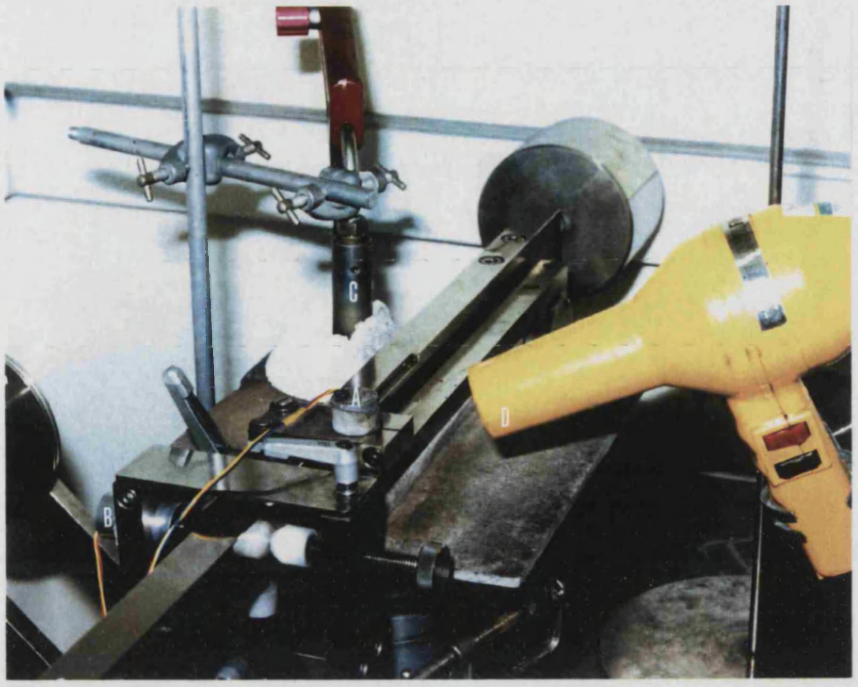

Figure 40a
Showing the pin on disc machine used. The position of the linear displacement transducer used to measure wear is marked by (A), the friction transducer is marked (B). The rig is also equipped with a propane gas torch used for generating high disc temperatures (C), and an air blower to reduce the temperature the wear transducer.

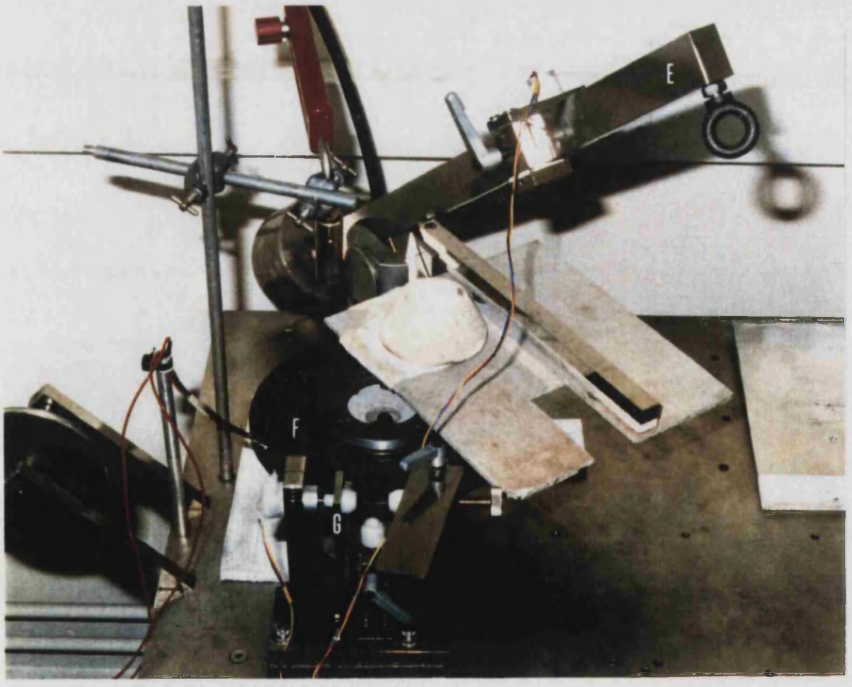

Figure 40b
Showing the pivot arm in the raised position (E), and the car brake disc exposed (F). The force post upon which the pivot arm pushes can also be seen clearly (G).

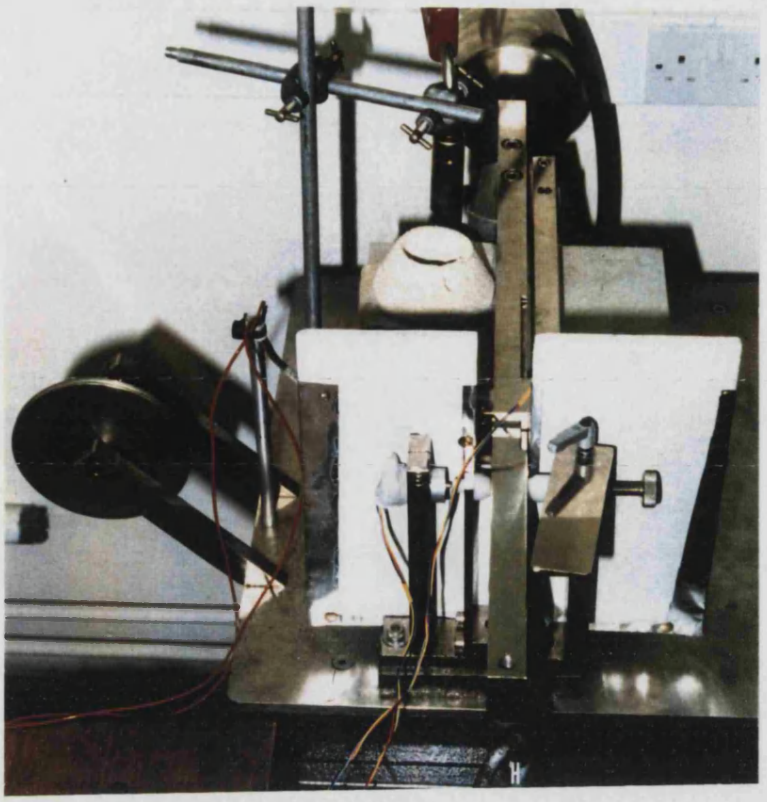

Figure 40c
Showing the machine during operation, with the pivot arm down and loaded at one end (H).

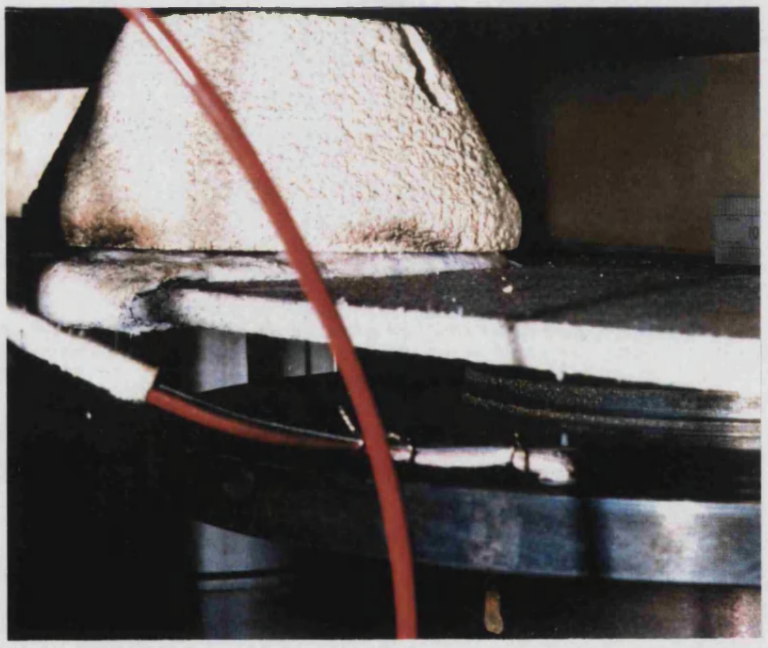

Figure 40d
Showing the thermocouple arrangement on the pin on disc machine. The thermocouple is sprung loaded against the disc surface.

Figure 41

The change in weight loss and flexural strength with carbonisation temperature R2 friction material.

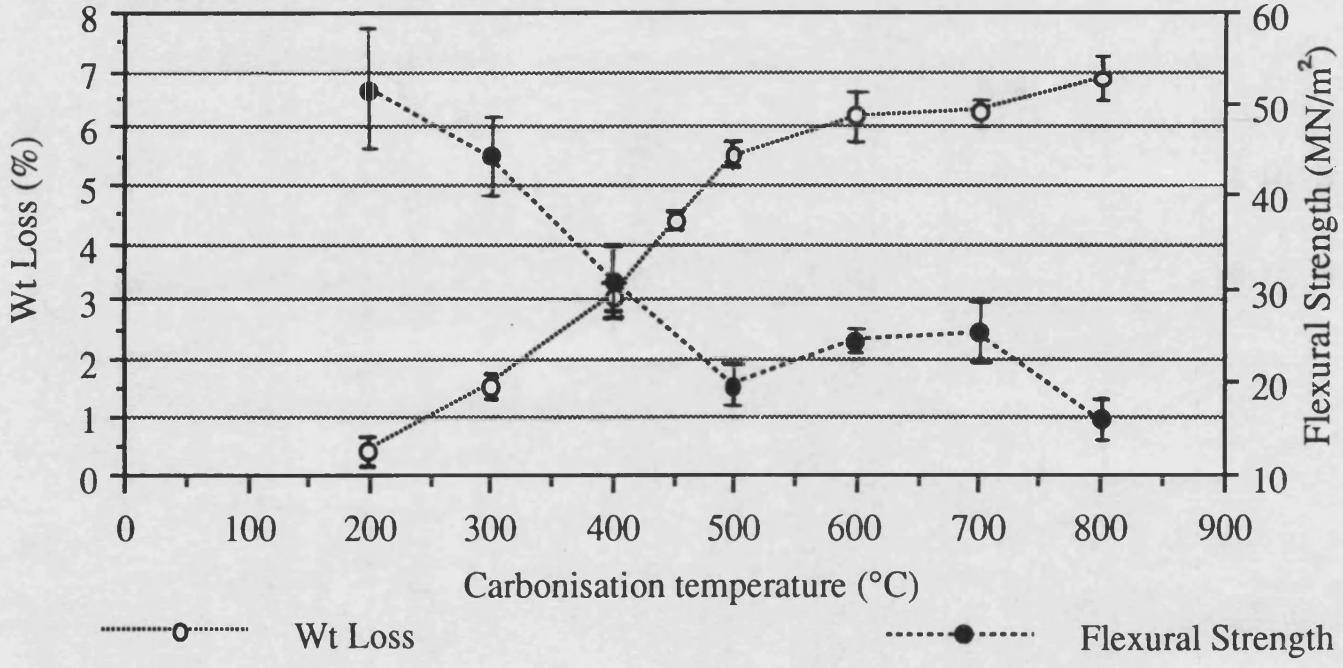

Figure 42

Typical set of friction and wear data for R2 friction material during an unheated test.

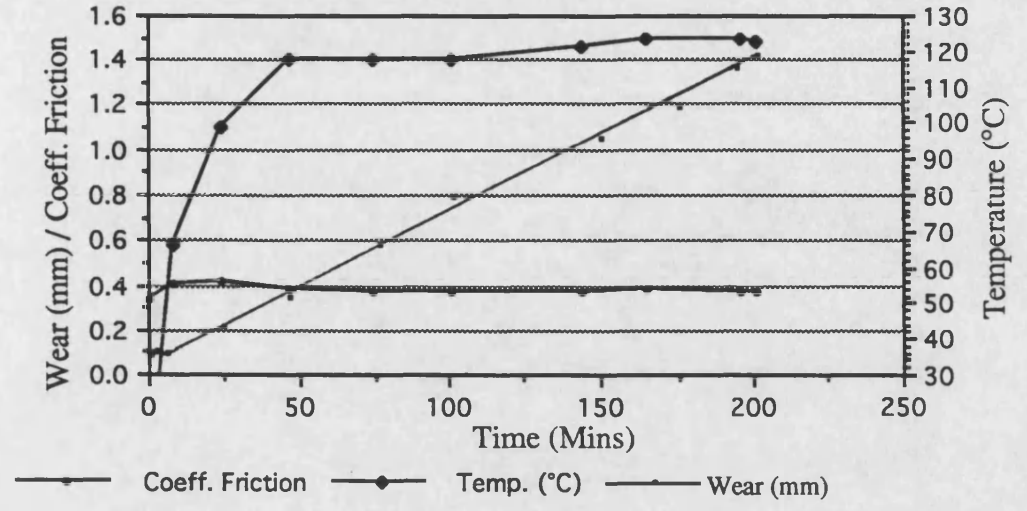

Figure 43

Typical set of friction and wear data for R2 friction material subjected to high temperature testing up to 400°C.

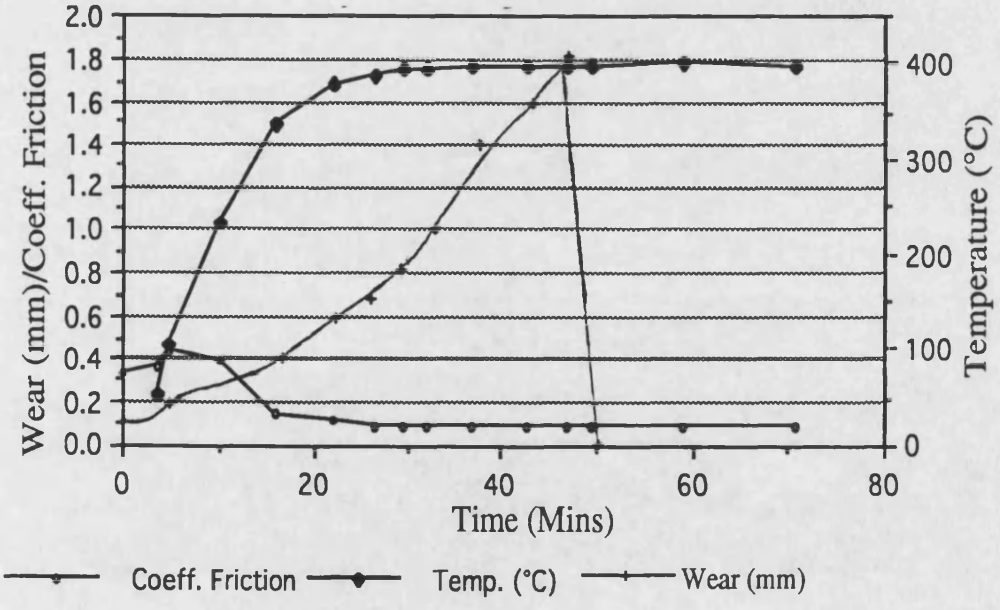

Figure 44

Effect of carbonisation temperature on the wear rate of R2 material (expressed in mm/hr), for heated and unheated tests.

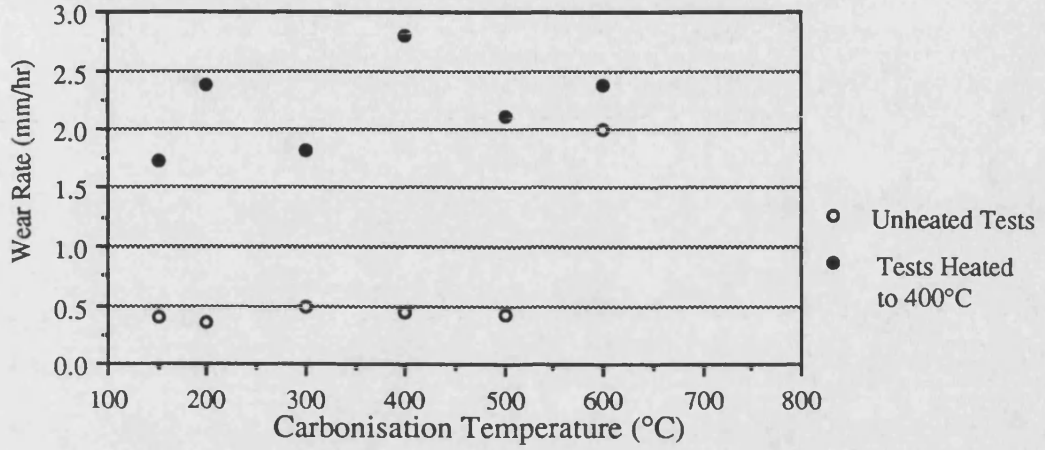

Figure 45

Effect of carbonisation temperature on the wear rate of R2 material, (expressed in Grams/hr), for heated and unheated tests.

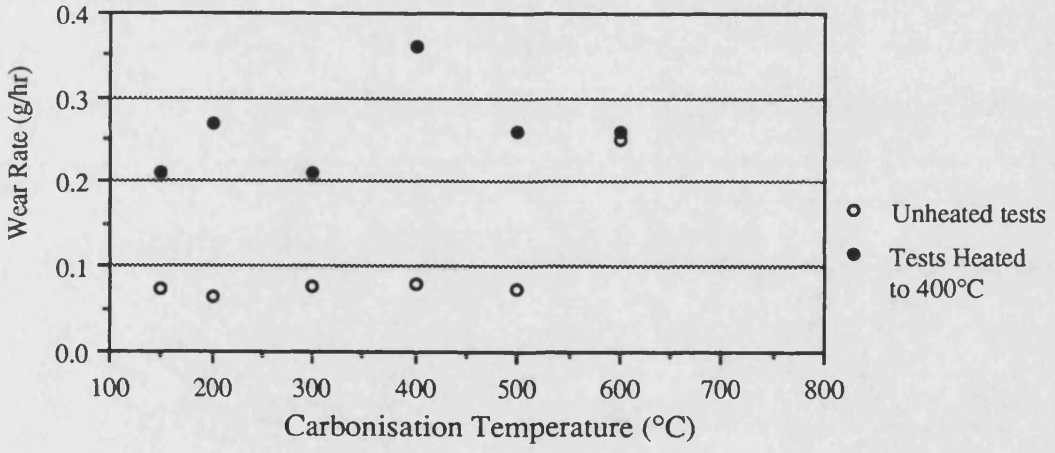

Figure 46

Thermogravimetric and gas analyses for the pyrolysis of a phenol-formaldehyde polymer [63].

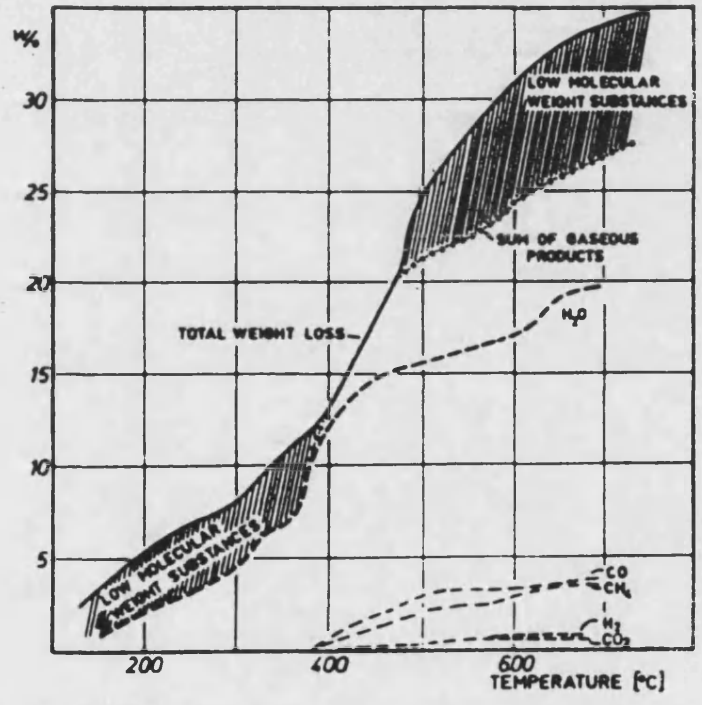

Figure 47

Effect of carbonisation temperature on the coefficient of friction of R2 material for both heated and unheated tests.

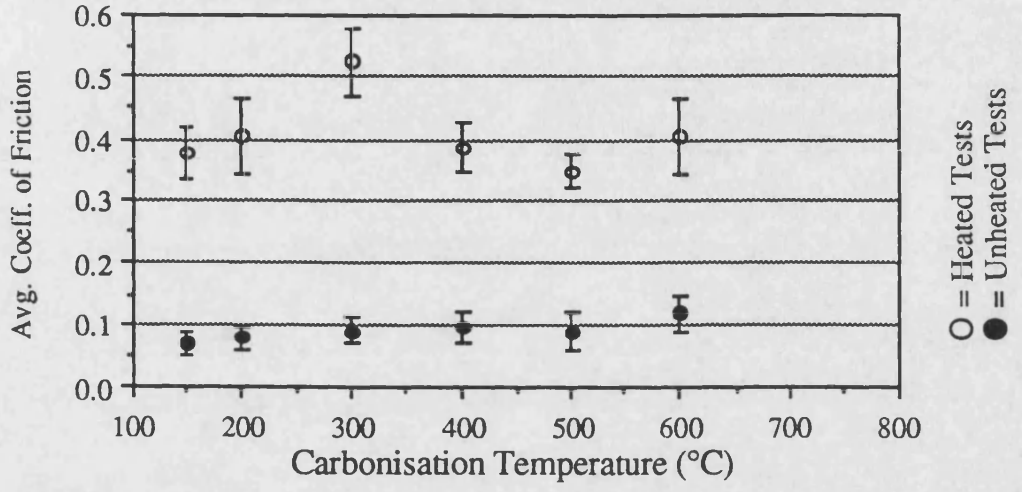

Figure 48

The relation between coefficient of friction and the test temperature reached during testing of R2 friction material.

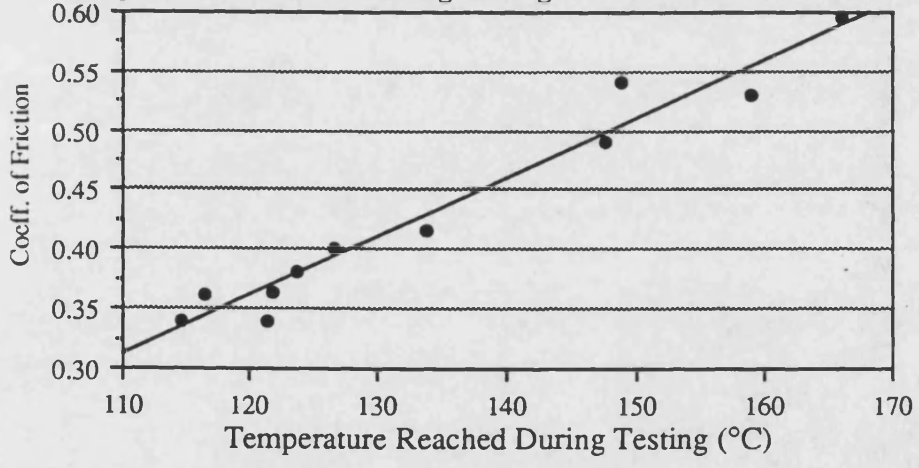

4.2 An investigation into the tribological behaviour of commercial friction materials under high temperature test conditions.

4.2.1 Introduction

Previous work reported in section 4.1 has shown that a heat treatment involving partial carbonisation may well improve the fade resistant properties of friction materials. However, this heat treatment also produces a weaker material which is susceptible to heavy wear, this being most severe during high temperature testing. Conventional commercial friction materials are tested over a whole range of test conditions using an inertia dynamometer. During some tests, the temperature can climb to 400 - 500°C, and under such conditions conventional materials display far superior wear resistance, compared to carbonised materials. In order to learn why this is so, a detailed study of the high temperature wear behaviour of two commercial friction materials was undertaken. One material was known to exhibit very low wear at high temperatures, and was designed to be used under heavy duty conditions, such as on large trucks and industrial earth movers, whilst the second cheaper material was designed for light vehicles, such as cars and vans. Both materials were tested using the pin on disc wear test machine, which had been adapted so that high temperature tests could be carried out (see figures 40a -40d), and the behaviour of each material was compared. It was hoped that a greater understanding of how these materials behave at high temperatures may lead to the improvement of the high temperature wear resistance of carbonised materials.

4.2.2 Methods & Materials

Part 1

A1 and A2 are commercially available friction materials the composition of which is outlined in Table 2 chapter 3. A1 is a heavy duty friction material used on large vehicles, whereas A2 is a material designed for use within the automobile industry. Samples of each of the two formulations were hot moulded into plates using a pressure of 2MPa, and a temperature of 150°C. The moulded plates were then post-baked for 6hrs at 150°C, in line with the standard production route used to produce conventional brake pads. The plates of each were then machined to produce $10mm^3$ wear test specimens.

Testing was performed on the pin on disc wear machine which had been adapted to allow high temperature wear tests to be performed, as outlined in section 4.1.2. The first series of tests were designed to examine how the wear rate of each

material is affected by test temperature. Samples of each of the two materials were tested at different disc surface temperatures, with a fresh sample being used for each new test. The tests were all conducted under the following conditions :- 2.7MPa pressure at the sliding interface, a disc sliding speed of 2.06 m/s, and a test duration of 3- 5hrs.

Each sample was run against the disc for 1 hour, during which no external heating was applied, this ensured that each sample was properly bedded-in before the commencement of the high temperature part of the test, where the gas torch was used to raise the disc surface to a certain discrete temperature, and once the desired temperature was attained it was held for the duration of the test. Tests were conducted on each sample at temperatures ranging from 150 - 400°C.

Part 2

The second set of tests were designed to examine how repeated high temperature tests affect the wear of each friction material, and also the wear of the disc. Testing was carried out using the same materials, and test procedure as described above, except that the disc surface was first skimmed on a lathe, to remove any residual wear tracks from previous tests. Samples of each material were then run against different areas of the newly turned disc surface, as illustrated in figure 49, (the necessary adjustments to the sliding speed and sample load were made to ensure test conditions for both materials were the same).

Figure 49

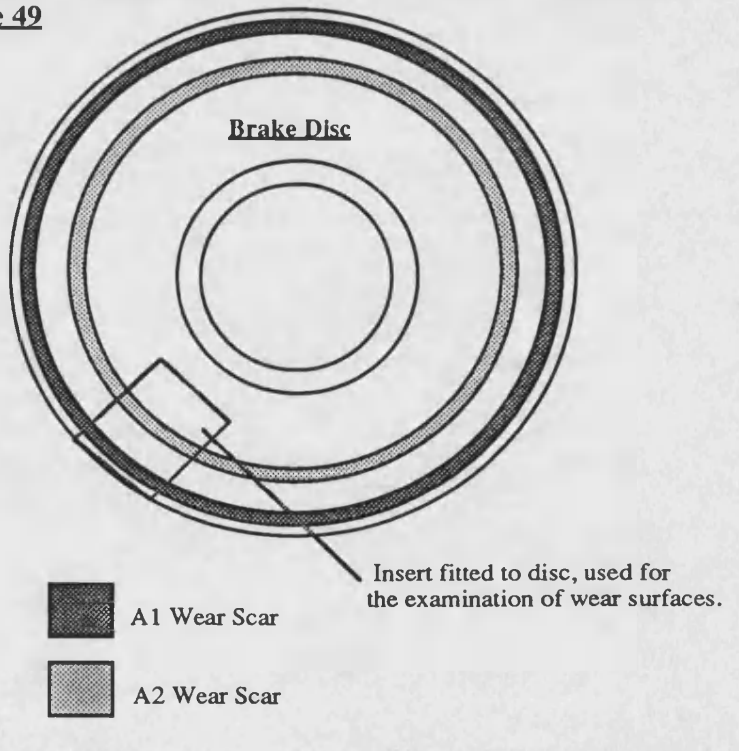

A recess was cut into the disc surface and a removable cast iron insert was machined from another brake disc and fitted in to the recess. The disc surface was then reground to make it uniform. In this way the wear tracks on the disc surface could be examined more easily. After each test the insert was removed and the roughness or Ra value and the amount of disc surface wear was measured using a Rank Taylor Hobson Talisurf machine. Ra values were measured both perpendicular and parallel to the sliding direction along the wear scar, as shown in figure 50. Disc wear was measured by running the stylus across the full width of the wear track, from which a depth profile of the wear scar could be obtained, and from this, disc wear could be measured. All measurements were made in the centre of the insert at the same location, and checks showed that Ra values and wear profiles differed very little from one location to another. Figure 51 shows a typical depth profile of a wear scar obtained after test N_o4, using A1 friction material. The test regime involved firstly three unheated tests which allowed the sample to bed in and the disc surface roughness to become constant, this removed any effects that disc roughness might have on sample wear. Then each material was subjected to the high temperature testing described above, where the disc surface was heated to approximately 400°C, and held for 1hr. A total of four consecutive high temperature tests were performed on each material.

4.2.3 Results

Figures 52 and 53 are typical examples of high temperature test data for A1 and A2. It can be seen that in both the sets of data shown, the disc temperature reached was 400°C. Data was extracted from curves such as these, for the different disc temperatures used and plotted on the same axis for comparison, producing summarised graphs for both A1 and A2 shown respectively in figures 54 and 55. Each curve plotted on these graphs represents the actual cumulative sample wear which occurred during a 60 minute period where the disc temperature was kept constant.

The wear rate at each test temperature has been plotted in figure 56 for both A1 and A2 friction materials, and shows the trends in wear behaviour of the two materials more clearly. Up to 300°C the A1 material has a very low wear rate compared to A2, then the wear rate of A1 rose as the disc temperature was increased to 350°C during the next test, and by 400°C it is comparable to that of A2.

The results of the experiments described in part 2 dealing with the effect of repeated high temperature tests on the wear of A1 and A2, are summarised in

figures 57 -60. The cumulative disc and pad wear results for A1 friction material which occurred during testing are shown in figures 57 and 58 respectively, whilst the data for A2 friction material is shown in figures 59 and 60. Figure 61 illustrates the way in which the disc surface roughness altered as each test was performed.

The average coefficient of friction for each material during all the tests performed in this section are summarised in figures 62 and 63 for A1 and A2 respectively. The data are plotted against the disc surface temperature attained during each test, the error bars designate the 95% confidence limits. It was noted that during the testing of A1 material described in part 1, a dark glaze or friction film was seen to form on the disc surface during the high temperature tests. Consequently the disc surface was examined using a scanning electron microscope, and micrographs were taken after the first four tests on A1 during part 2. Figures 64 - 67 show how the wear track on the disc surface changed during the first four tests.

4.2.4 Discussion

The curves illustrated in figure 54 shows the change in wear with increasing disc surface temperature for A1 friction material, and indicate that as the disc temperature is raised above 300°C there is a corresponding increase in the cumulative wear rate. A similar plot for A2 friction material (see figure 55), shows that the cumulative wear rate increases at the lower temperature of 200°C. The wear rates of the two materials are compared in figure 56, which showed that the A2 material had a high wear rate, which increased with rising temperature, whereas the wear rate of A1 was very low at temperatures below 300°C, but then showed a sharp rise in wear rate at higher temperatures. Other workers [12, 32-35], have found that wear increases exponentially with increasing temperature above about 230°C, which was attributed to the onset of the breakdown of the phenolic resin matrix. In the case of the A1 material, there was indeed a sharp rise in wear rate which may have been exponential, but which did not occur until disc temperature of above 300°C was reached. From the TGA results presented in chapter 3, showing the thermal decomposition of various phenolic resins, it is clear that resin breakdown increases markedly at approximately 300°C, which coincides with the increase in wear rate seen in A1 material, so both the work in this section, and studies by other workers, have indicated that there is a link between the increasing wear rate of a brake material, and the onset of thermal breakdown of the phenolic resin matrix. The wear rate of both A1 and A2 friction materials can be expressed in an Arrhenius form such as:-

$$\Delta W = Ae^{-E/RT}$$

Where ΔW is the wear rate of the friction material in mm/hr, T is the absolute temperature, R is the universal gas constant, and E is the derived activation energy for the particular material. A plot of log ΔW vs 1/T should be linear if the process is thermally activated, such plots for A1 and A2 friction materials over temperatures of 200 - 400°C are shown in figures 68 and 69 respectively. Both plots do appear to be linear suggesting that wear is controlled by a thermally activated process. The slopes of the plots can be used to calculate an activation energy (E), for the wear of each material as follows:-

For A1 friction material: E = 5.56 kcal/mole.----(23.3 kJ/mol).

For A2 friction material E = 2.62 kcal/mole.----(10.9 kJ/mol).

These values are of the same order as those found by Liu and Rhee[34,35], who obtained activation energies from 4 to 9.6 kcal/mole for three asbestos based friction materials, and activation energies of 8 to 8.8 kcal/mole for semi-metallic friction materials. In a similar treatment using materials containing potassium titanate fibres, Halberstadt [12] found that the Arrhenius plots obtained were not linear over the entire temperature range studied, but two distinct regions of linearity could be distinguished, one at low temperatures, and one at temperatures of 200°C and above. This high temperature region gave typical activation energies of 8.3 and 8.9 kcal/mole for the two materials studied.

Rhee [73] attempted to correlate the activation energies reported above with the activation energies reported for the thermal decomposition of phenolic resin, quoting Nelson [74], who stated that the activation energy for the initial stages of thermal decomposition of phenolic resin lay between 8.9 and 10.8 kcal/mole, agreeing well with the findings of Liu and Rhee. Much higher activation energies of between 50 and 72 kcal/mol were reported by Friedman [75], during a study on the kinetics of thermal degradation of a glass reinforced phenolic resin ablation material. In a later investigation by Henderson et al. [76], involving a comprehensive study of the effects of heating rate on the kinetic parameters for the thermal decomposition of phenolic resin based composites, where heating rates ranging from 10°C/min to 160°C/min were considered. Activation energies of 62 and 74 kcal/mol were found for the two materials examined. Heating rate was found to have a negligible effect of the activation energies obtained. In a similar study by Farmer [77], who considered an even greater spread of heating rates from 8°C/min. to 430°C/min. reported activation energies of between 11.4 and 12.05 kcal/mol. However it was noted that the activation energy did not

remain constant over the entire temperature range, and that the values reported were averages. Clearly there are large differences in the literature values quoted, the pyrolysis of phenolic resins involves multiple reactions, where more than 40 molecular species have been identified from the thermal decomposition of these materials [78]. There is also a number of intermediate products formed during the decomposition of phenolics to volatiles, coupled with the fact that some of the reactions occur consecutively, whilst others occur simultaneously. There is also evidence that the kinetic parameters change with heating rate. For these reasons a single set of kinetic parameters has been unsatisfactory in predicting the pyrolysis reaction rates of phenolic resins [78]. Therefore to attempt to correlate the activation energies derived above, directly with those proposed for the thermal degradation of phenolic resins seems unjustified.

Activation energies associated with processes in the solid state are generally linked to the onset of bond breakage, and it follows that bond breakage is an integral part of the wear process. The partially carbonised matrix of a friction material typically contains carbon-carbon bonds and hydrogen-carbon bonds. The average dissociation energies for these bonds are 414 and 343 kJ/mol respectively, far higher than the activation energies quoted above. Evidently there is no simple process upon which the derived activation energies for wear can be pinned, and it is far more likely that the wear rate of a particular material is governed by other factors. Therefore the difference in the wear rate shown by A1 and A2 friction materials cannot adequately be explained by the fact that A1 has a higher activation energy than A2. The reason for the greater wear rate shown by A2 is probably due to the fact that the material contains only approximately half as much resin per unit volume as the A1 material. It follows that the A2 resin matrix will have a larger surface area to volume ratio than the A1 material, and so will contain a larger number of available sites for thermal attack. This will result in a proportionally greater loss of volatiles, with an accompanying increase in porosity of the matrix, leading to a fall in material strength and an increased wear rate.

On comparison of the wear characteristics of the two materials, it is evident that A1 would be a harder wearing material than A2, as the onset of heavy wear only occurs at temperatures above 300°C, whereas A2 displays generally higher wear at the lower test temperatures. Also in real braking systems, the operating temperature fluctuates between 50 & 250°C for 95% of the time [40], indicating that A1 would only experience heavy wear for 5% of the time, whilst A2 will experience heavy wear far more regularly.

Upon examination of Figures 52 and 53, which show typical wear data for both materials when tested at 400°C, there is an important difference in wear behaviour. The wear rate of the A2 material shown in figure 53, rose sharply as the disc surface was heated, and remained constant. When the heat source was removed, the temperature reduced to approximately 200°C, this reduction made little difference to the wear rate of the A2 sample which remained constant at its previous level, even though the disc surface temperature had dropped. In a similar test on A1 shown in figure 52, the wear rate was again seen to rise sharply during the heated phase of the test, but when the heat source was removed there was an immediate fall in the wear rate of the sample. These effects were also seen in other tests on the same materials, and indicate that high temperatures of 350°C+ are needed to induce a high wear rate in the A1 friction material, and that any reduction in temperature below approximately 350°C results in a drastic fall in the wear rate. In contrast the A2 material shows far greater temperature sensitivity and continues to wear heavily at temperatures above 200°C.

The experiments reported in part 2 of this section examine the effect of repeated high temperature tests on the wear rate of both the friction material and the cast iron disc. Figure 57 shows the cumulative wear of A1 friction material, over the 8 successive tests performed. The first three tests were run with no external heating applied, during which, the wear increased steadily with each test. During the fourth test the disc surface was heated to 400°C, resulting in a large increase in wear, as expected. However, during further heated tests which followed, the wear rates were very much reduced. Figure 58 shows the accompanying cumulative wear of the disc surface measured after each test, which again shows a drop in the disc wear rate to virtually zero after the first high temperature test (No 4).
Figures 59 and 60 show the results of similar tests on A2. The friction material wear data presented in figure 59, shows that again there is a large increase in wear during a high temperature test (Test N^{o} 4) as expected, however the following high temperature tests also result in large wear rates, this is in contrast to the behaviour of A1. Figure 60 shows the accompanying disc wear data for the A2 tests. The increase in disc wear is constant during each test regardless of whether or not the tests were conducted at high temperatures. Again this is in contrast to the behaviour of A1, where the wear rate fell after the first high temperature test.
There are clearly fundamental differences in the way in which each material behaves, A1 displays better wear resistance when tested repeatedly at high temperatures, and also causes far less disc wear. During testing, it was noted that a friction film developed on the disc surface during high temperature tests but films developed with A2 material were quickly removed during the unheated

phase of the following test, whereas the films produced by A1 remained on the wear track surface throughout the tests which followed. The photographs presented in figures 64-67 illustrate how the appearance of the wear track on the disc surface altered during the first four tests on A1. Figure 64 shows the roughened surface of a newly turned disc, which is then polished to a smoother finish by the first test with A1 (figure 65), where the individual graphite flakes within the cast iron are clearly visible. Figure 66 shows the same wear track after test N°3, showing an even greater degree of surface polish. The situation changes dramatically however, during the first high temperature test (N°4), where the graphite flakes are no longer visible, indicating that a film has been deposited upon the disc surface, (see figure 67). The effects of the friction film produced by A1 during test N°4 are clear, both disc and pad wear are reduced (see figures 57 and 58). This behaviour does not happen with A2 material, as the film is removed (figures 59 and 60).

Figure 61 shows the changes in surface roughness or Ra value of the wear scar produced by each material on the brake disc surface. It can be seen that there is a large reduction in the surface roughness of the disc during the first wear test in both A1 and A2, which then remains level until the first high temperature test (N°4). At this point the Ra value associated with A1 rises, as a transfer film forms on the wear track. During the first high temperature test using A2 (test N°4), there is a drop in the Ra value, this difference in behaviour is because no permanent film forms in A2, and the increased temperature promotes greater disc wear and hence a further smoothing of the disc surface resulting in a drop in the Ra value.
Figures 62 and 63 show that the friction coefficient varies little in each material at temperatures above 150°C. On comparison of the two sets of data, A2 shows a slightly higher coefficient of friction, than A1. These results also indicate that fade effects either can not be produced, or are not detectable with the pin on disc apparatus used. This may be due to the sample being too small to produce and trap enough volatile breakdown products, to cause a lubricating effect at the interface. It must also be stated that although it is possible to replicate the typical disc temperatures generated during heavy braking with the pin on disc apparatus, it is not possible to replicate the large amount of energy which is absorbed by the brake pad of an automobile during a brake stop lasting 30 seconds, where the disc sliding speed could be as high as 23 m/s. The pin on disc machine is only capable of a disc sliding speed of 2.5m/s, and in order to examine fade effects an inertia dynamometer is needed.

4.2.5 Conclusions

The work in this section was directed towards establishing the physical changes which occur in conventional friction materials when subjected to high test temperatures, in order to gain a better understanding of how these materials are able to operate under such conditions. To achieve this, the tribological properties of two very different friction materials were compared, namely A1 and A2. A1 is an industrial brake material designed to operate under heavy loads and high energy conditions, whereas A2 is a more conventional automobile brake material. The following conclusions can be drawn from the tests performed:-

1) Both materials showed a marked increase in wear rate when the disc surface temperature was raised to temperatures above 300°C, which coincides with the onset of thermal degradation of the phenolic resin matrix.

2) Arrhenius plots for the wear rates of A1 and A2 materials showed a linear relationship, indicating that the increase in wear rate of each material was a thermally activated process. The derived activation energies where 5.56 and 2.62 kcal/mol, for A1 and A2 respectively.

3) A1 showed a much lower wear rate at temperatures below 300°C, which would result in the material lasting far longer when actually in use on a vehicle.

4) A1 shows superior wear resistance during repeated high temperature tests, and also caused far less disc wear.

5) It was found that A1 formed a stable friction film on the disc surface during heated tests, the formation of a film coinciding with a drop in both disc and pad wear, and therefore believed to play an important role in the high temperature wear resistant properties of A1. A2 also produced a film at high temperatures, but it was quickly removed during subsequent testing.

6) The average coefficient of friction values for both materials showed little fluctuation with disc surface temperature. This indicates that fade effects either cannot be produced or measured using the pin on disc wear machine, and dynamometer testing must be used to explore these properties.

7) The beneficial effects of a friction film could be utilised to help improve the high temperature wear of carbonised friction materials, but for this to be achieved more information is required on what conditions are necessary, and what materials should be used to promote film formation, and also why are some films more tenacious than others? The solution to these problems is the objective of the work presented in the next section.

Figure 50

Schematic diagram of a section of brake disc showing how talisurf measurements relative to the wear tracks were made.

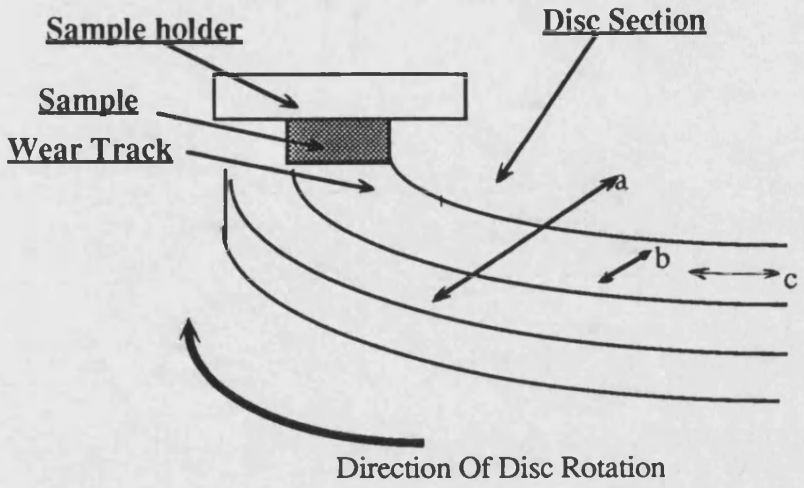

a) Talisurf traverse used to measure the depth of the wear scar.

b) Talisurf traverse used to measure the Ra value perpendicular to the sliding direction.

c) Talisurf traverse used to measure the Ra value parallel to the sliding direction.

Figure 51

A typical Talisurf traverse of a wear scar on the disc surface used to measure disc wear.

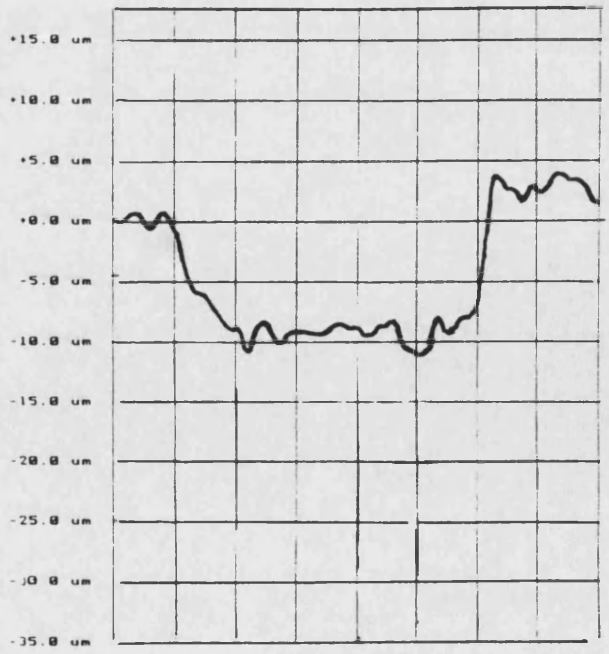

Figure 52
Typical friction and wear data for A1 where the disc surface temperature was raised to 400°C.

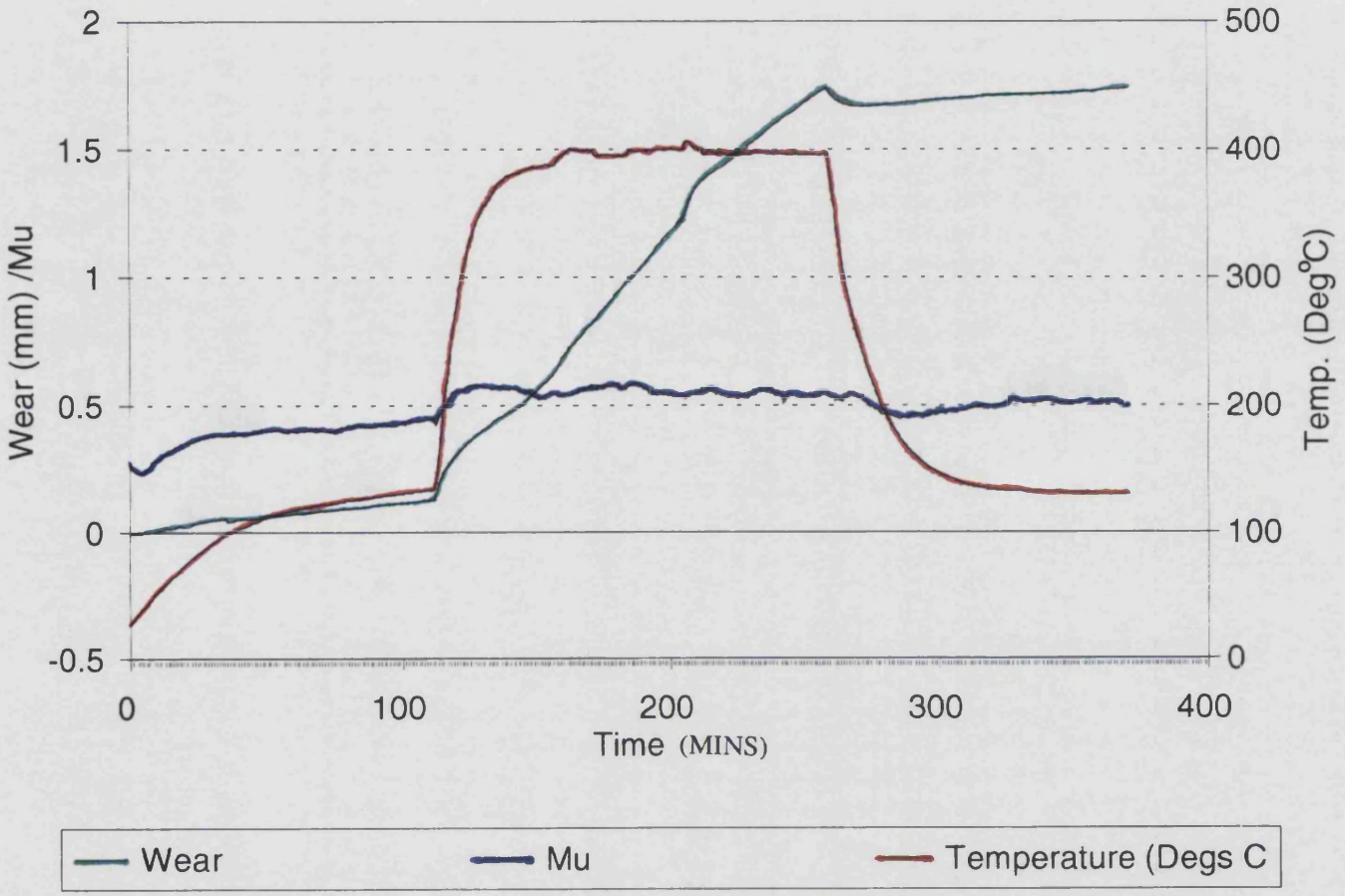

Figure 53
Typical friction and wear data for A2 where the disc surface temperature was raised to 400°C.

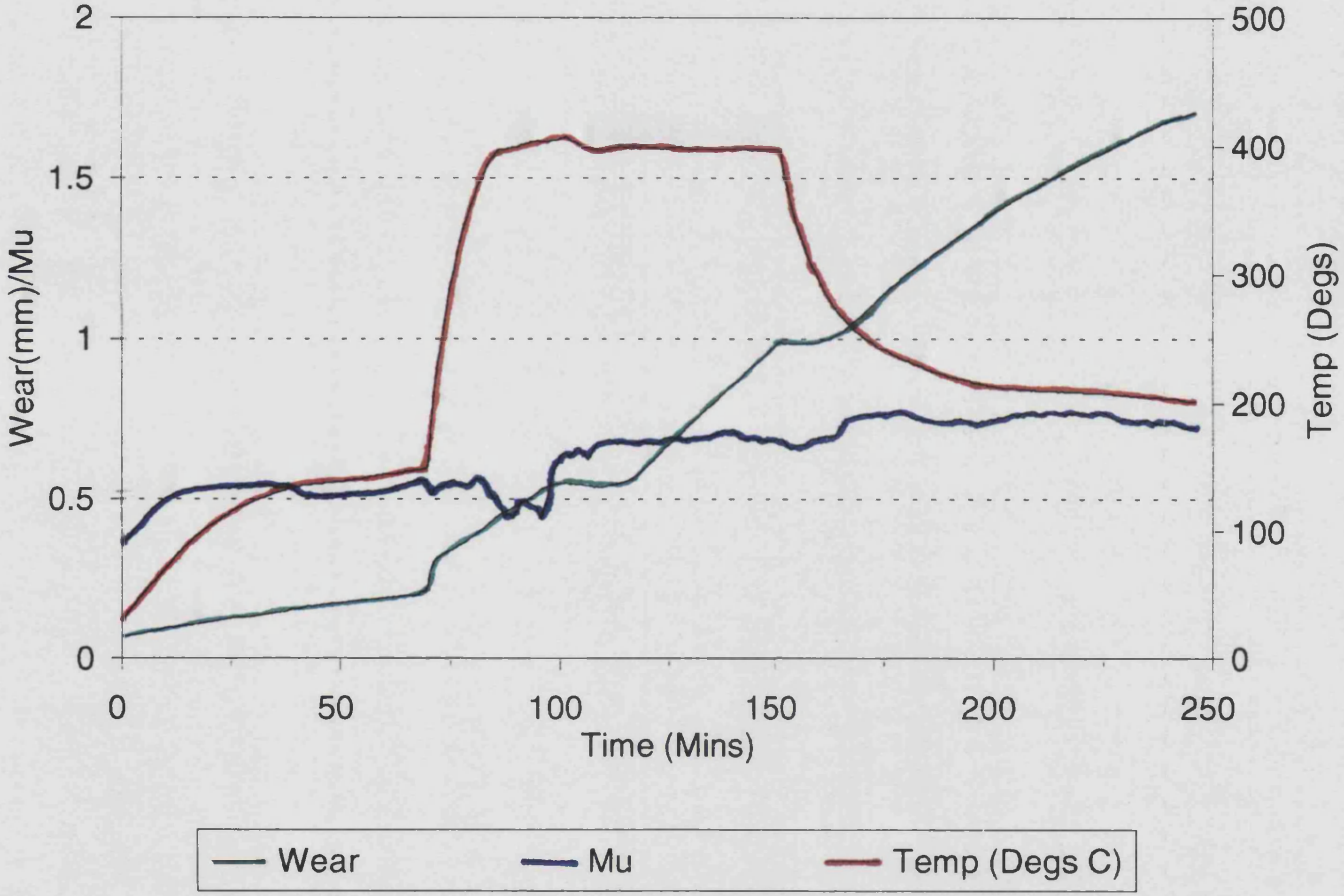

Figure 54

The effect of disc surface temperature on the wear of A1 friction material.

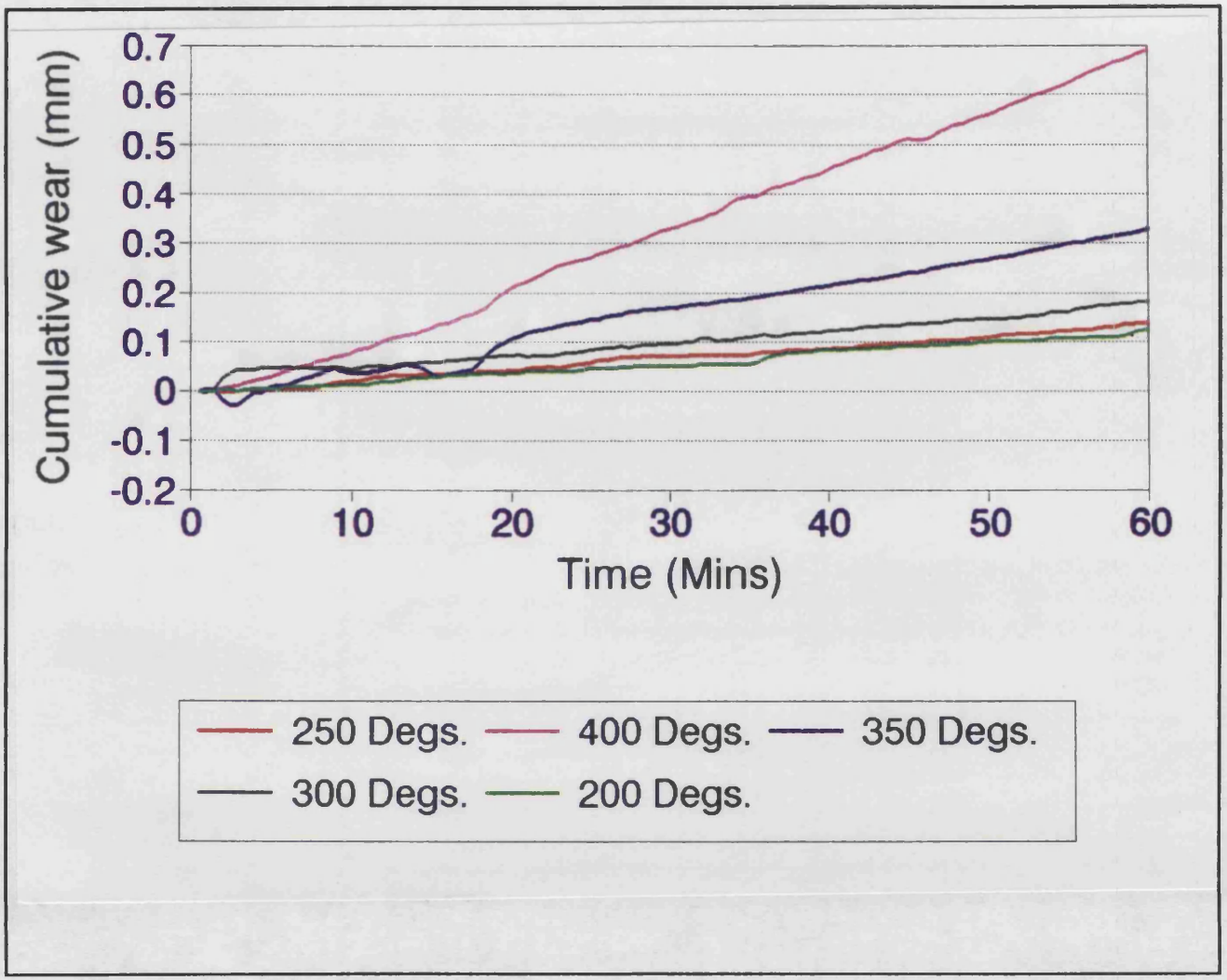

Figure 55

The effect of disc surface temperature on the wear of A2 friction material.

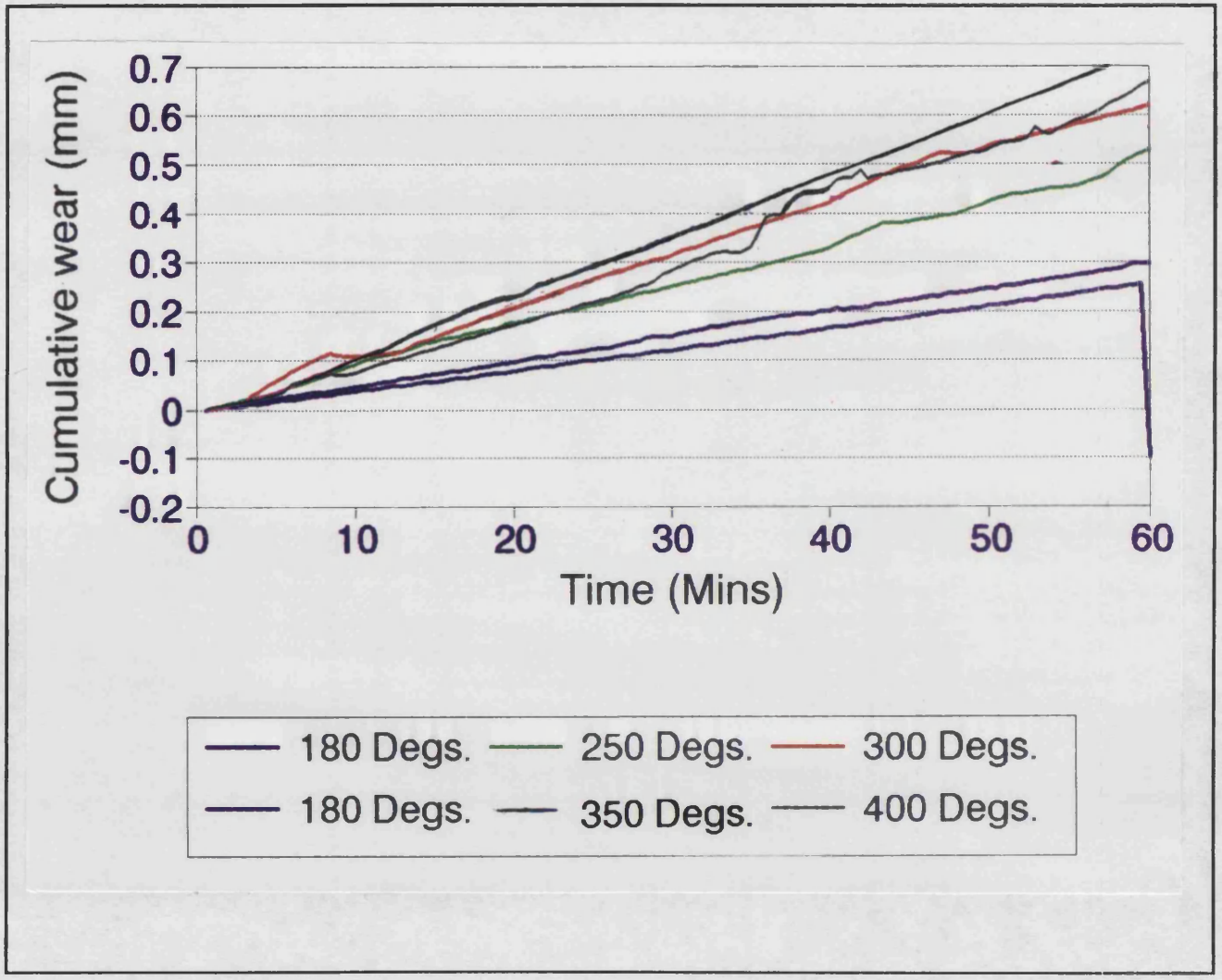

Figure 56

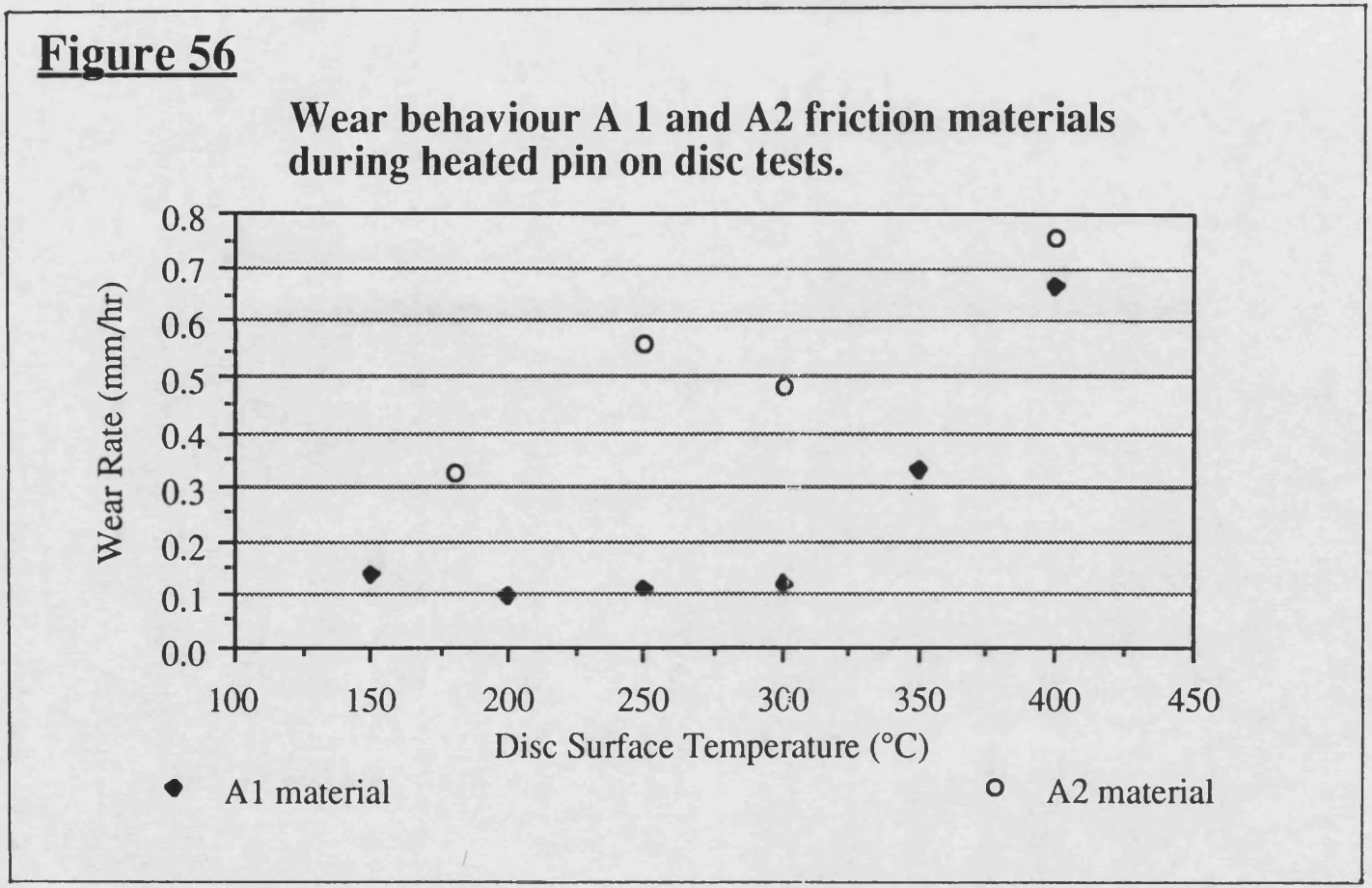
Wear behaviour A 1 and A2 friction materials during heated pin on disc tests.
Wear Rate (mm/hr)
0.8
0.7
0.6
0.5
0.4
0.3
0.2
0.1
0.0
100
150
200
250
300
350
400
450
Disc Surface Temperature (°C)
A1 material
A2 material

Figure 57

The change in wear of A1friction material during successive pin on disc tests.

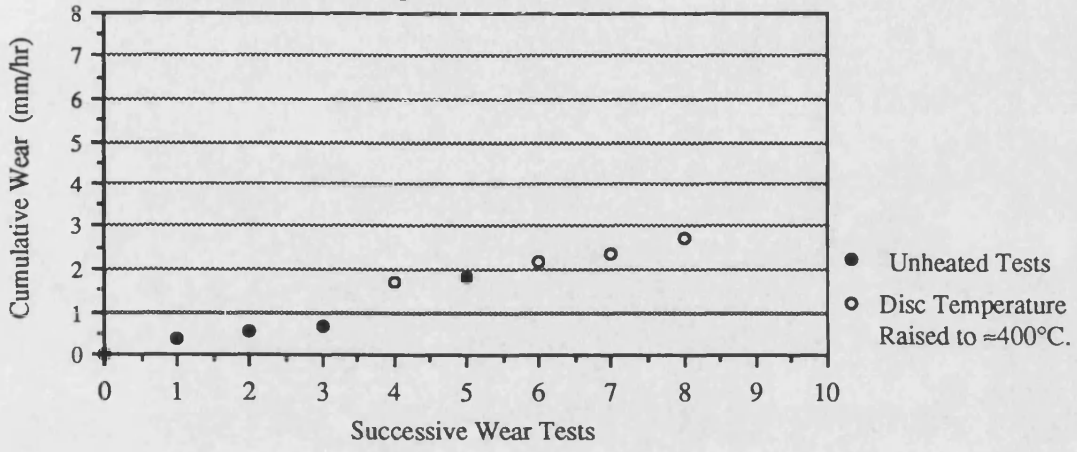

Figure 58

The effect of successive 2hr wear tests with A1friction material on the wear of a cast iron brake disc.

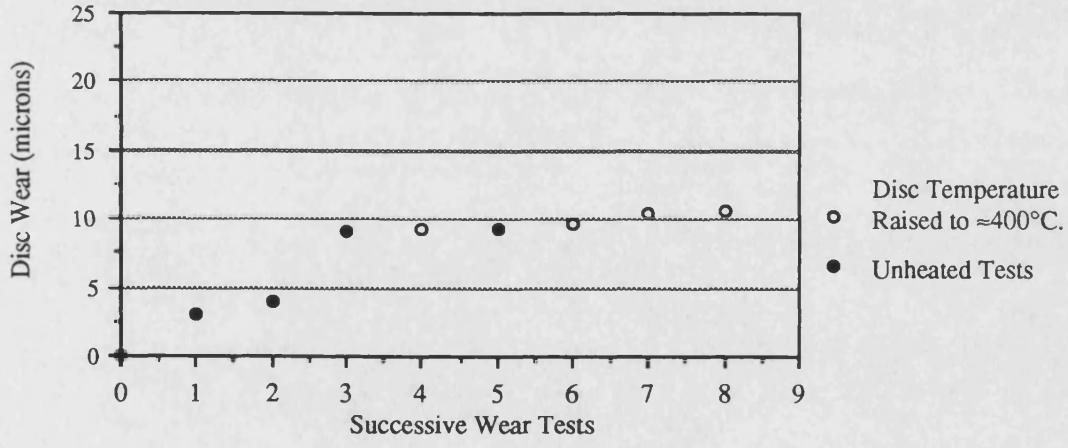

Figure 59

The change in wear of A2 friction material during successive pin on disc tests.

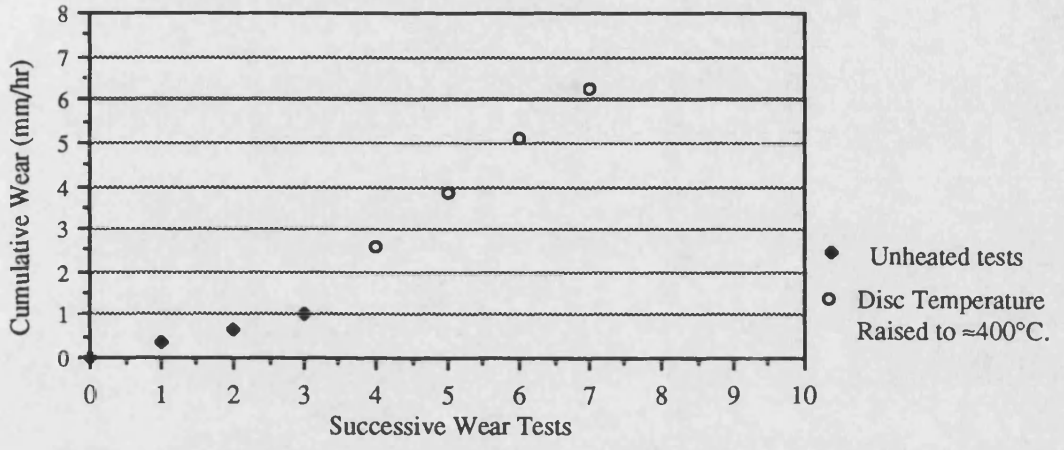

Figure 60

The effect of successive 2hr wear tests with A2 friction material on the wear of a cast iron brake disc.

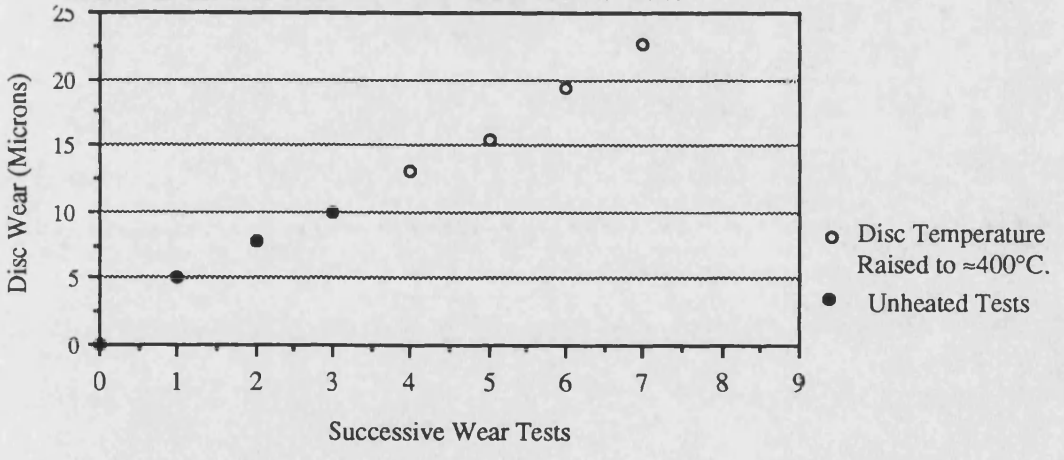

Figure 61

Variation of Ra value of a brake disc during a Series of wear tests using A1 and A2 friction materials.

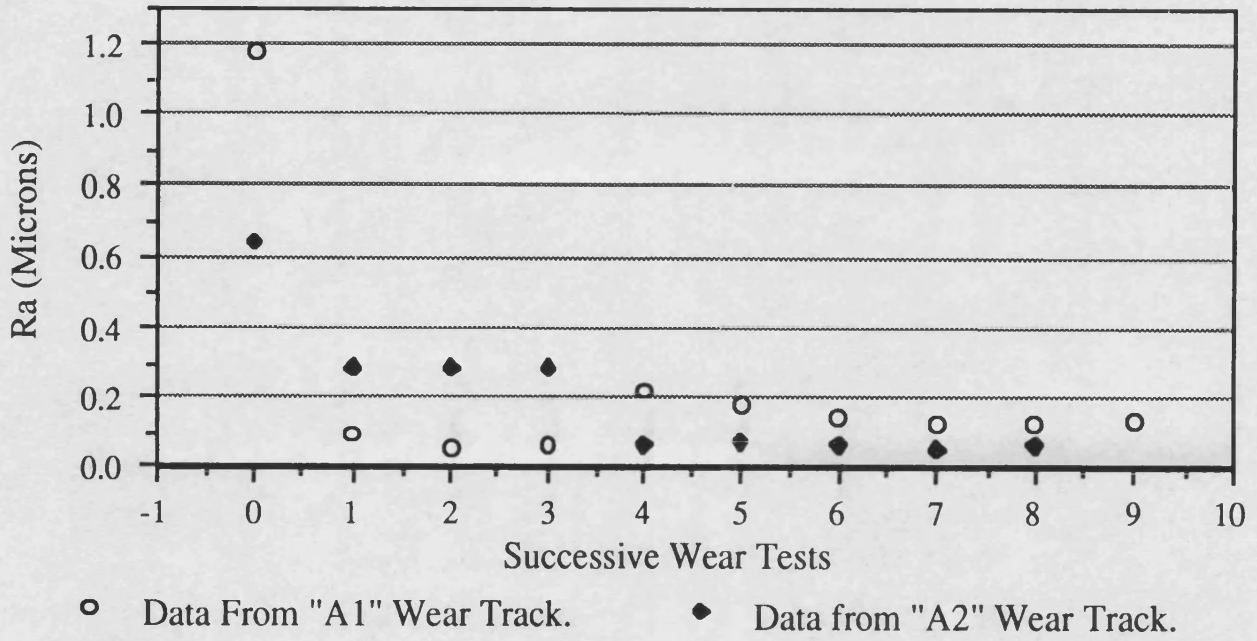

Figure 62

Variation of coefficient of friction with disc surface temperature for A1 friction material

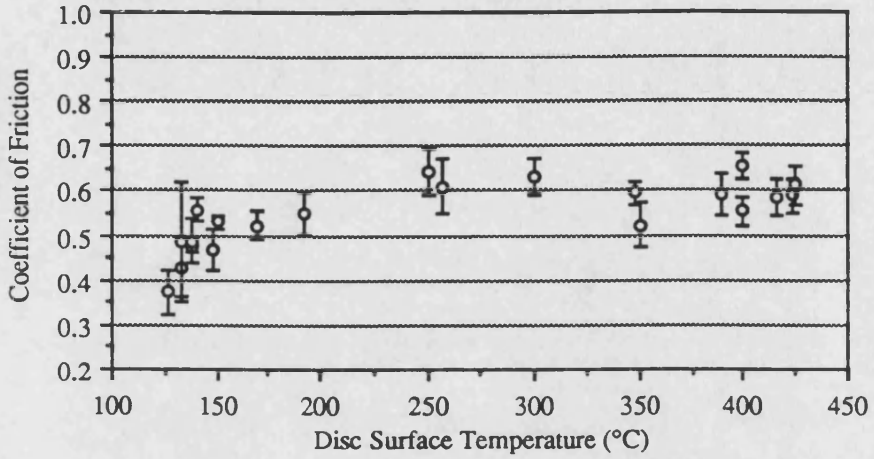

Figure 63

Variation of the coefficient of friction with disc surface temperature for A2 friction material.

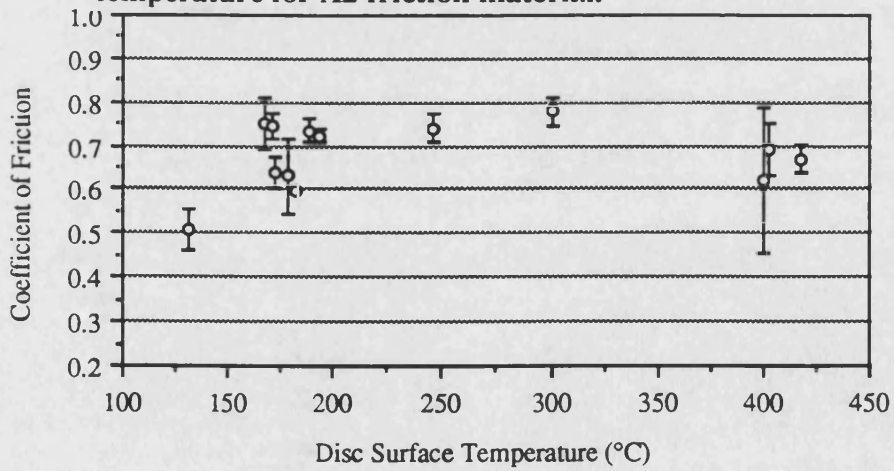

Figure 64
S.E.M. of the brake disc surface with a turned finish. (as received)

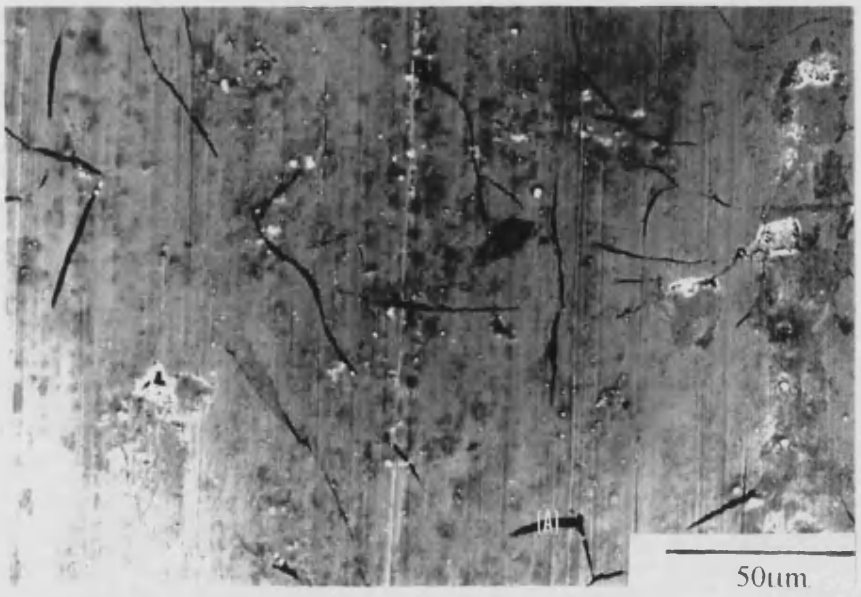

Figure 65
S.E.M. of the wear scar on the brake disc surface after test N° 1 with A1 friction material, The surface appears polished and the graphite flakes are clearly visible (A).

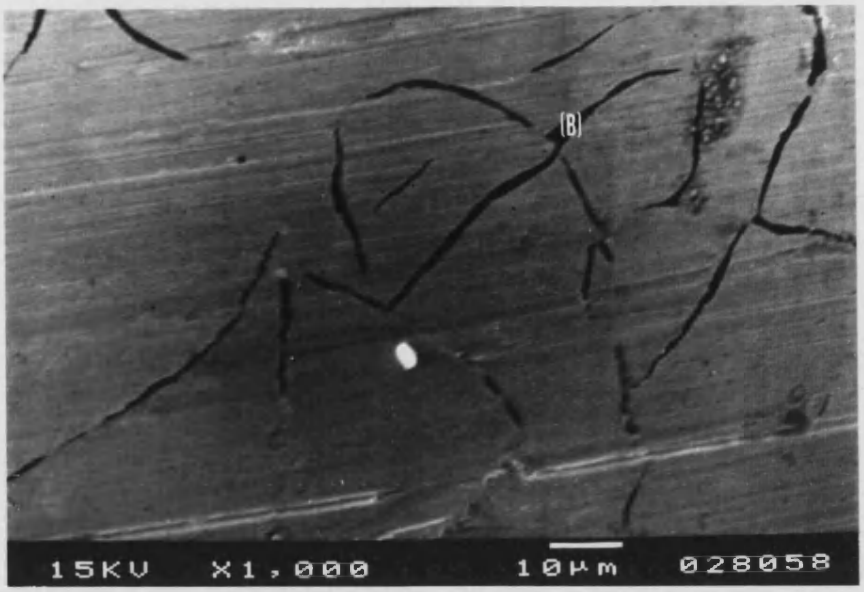

Figure 66

S.E.M. of the wear scar on the brake disc surface after test N^{o} 3 with A1 friction material. The surface is shown at a higher magnification to stress the degree of surface polish produced by low temperature tests. Once again the graphite flakes are clearly visible (B).

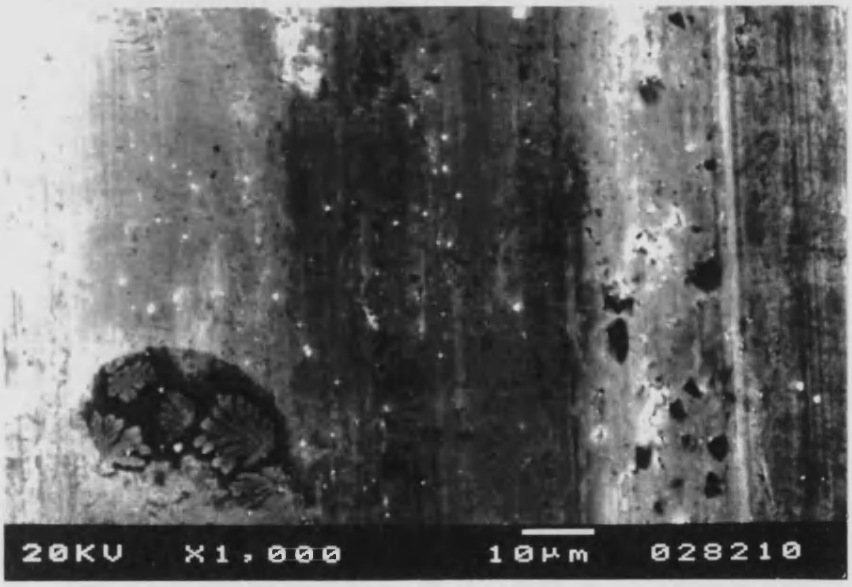

Figure 67

S.E.M. of the wear scar on the brake disc surface after test N^{o} 4, the first heated test where the disc surface temperature was raised to 400°C. Note that the polished surface finish and graphite flakes have disappeared, due to the formation of a friction film on the disc surface.

Figure 68

Arrhenius plot for A1 commercial friction material.
(derived from data presented in figure 54.)

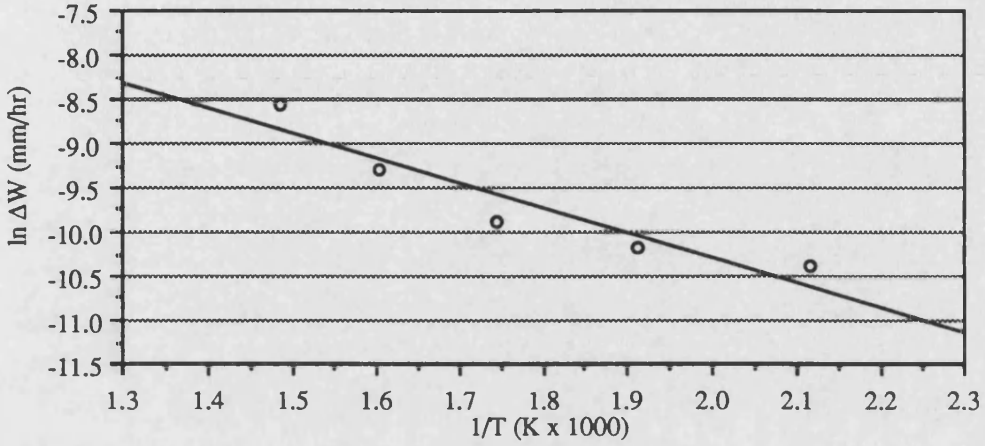

Figure 69

Arrhenius plot for A2 commercial friction material.
(Derived from data presented in figure 55.)

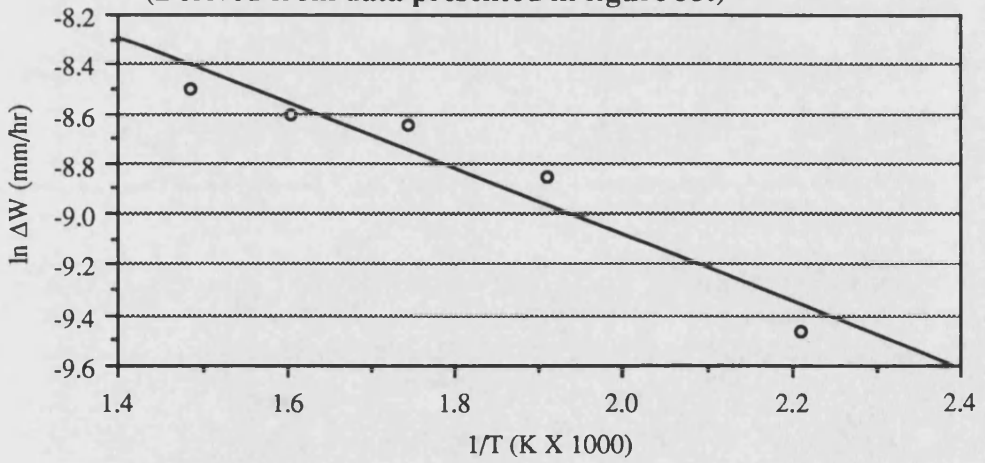

4.3 An investigation into the formation and composition of friction films produced by commercial friction materials.

4.3.1 Introduction

Earlier work (section 3.4) showed that by carbonising friction materials their fade resistance can be improved, however, carbonisation also reduces strength and consequently high wear rates were found in carbonised materials, this effect being most pronounced at high temperatures. The wear resistance of conventional friction materials is far superior in comparison, especially at high temperatures. Subsequent studies (section 4.2) have shown that good high temperature wear resistance is most prevalent in materials which cause a friction film to form on the rubbing surfaces of the friction pair. This is because it has the effect of reducing the wear rate of both the friction material, and the cast iron brake disc. It follows that if film formation could be encouraged in carbonised friction materials, then the wear resistance of these materials would also be improved. In order to formulate materials which form friction films, more information is needed on the types of compositions that promote the formation of adherent friction films, and what operating conditions are required for film formation to occur.

In the previous section it was seen that A1 friction material forms a stable, adherent, friction film, whereas A2 material does not. The reasons for this difference in behaviour are explored in this section. The friction films formed by A1 material are further investigated, in order to determine the temperature at which friction films form, and identify the friction film composition using Electron Probe Microanalysis (EPMA), Energy Dispersive X-ray analysis (EDX), Scanning Electron Microscopy (SEM), and X-ray diffraction studies.

4.3.2. Methods and materials

i) Production and examination of a friction film from A1 material.

The following series of experiments were designed to establish at what temperature friction films formed between the disc surface, and A1 friction material. The disc surface was firstly skimmed on a lathe to remove any wear scars from previous tests, then a series of pin on disc wear tests were carried out using the same methods and test conditions described in section 4.2.2. In order to ascertain the temperature at which a friction film forms, tests were run at progressively higher disc surface temperatures, and the wear scar surface was photographed after each test so that a record of film formation could be made. In this way the relation between film formation and disc surface temperature could

be studied. The photographs were taken using a Zeiss ICM 405 optical microscope.

ii) Production and examination of a friction film from the A2 material.
A2 friction material was also tested in a similar manner to that described above, however, it was quickly found that the films which formed with A2 material were removed once the disc surface temperature fell below approximately 200°C, whereas the films formed by A1 material remained intact at all temperatures tested. There were two possible explanations for the difference in behaviour of the two materials, either the friction film produced by A2 material was less adherent than that produced by A1, or that A2 was a more abrasive material than A1, and hence removed the film more rapidly. The abrasiveness of A2 could be compared to that of A1 by performing a test where a sample of A2 friction material, was run against a wear track covered with a thick film produced by the A1 material. If the A2 sample removed this film, then it would indicate that A2 was indeed more abrasive than A1. This test was performed under standard conditions, where no external heating was used during testing, and photomicrographs of the disc surface were taken before and after the test.

iii) Friction film analysis by EPMA.
A section of the disc surface was cut away and removed so that the friction surfaces produced by A1 friction material during testing could be examined using a JEOL 8600 Electron Probe Microanalyser (EPMA). This would give qualitative information on the elemental makeup of the friction film produced. The technique examines the X-ray emissions from the top 1- 5 μm of the surface of a material when it is bombarded with electrons. The X-rays produced are analysed by allowing them to impinge upon the surface of a crystal with a known lattice (d) spacing, the X-rays are then reflected by an angle (ø) (the Bragg angle), which is measured and from the Bragg equation:

$$n\lambda = 2d \sin \phi$$

where n is an integer, and λ is the wavelength of the incident x-rays. By measuring ø the wavelengths of the x-ray emissions produced can be found, and as these are characteristic to each element, the elemental composition of the sample can be identified. A total of four crystals each with a different lattice spacing, are needed in order to scan the entire spectrum of the possible wavelengths which could be emitted [79].

The polished disc wear surface which resulted from the testing of A2 material, was also examined and analysed by EPMA, although there was no visible film on the surface, this was done to provide a suitable control sample. The results of the two traces could then be compared.

iv) Friction film analysis by EDX.

It has already been stated that when A1 was tested at elevated temperatures, a black glaze forms on the rubbing surfaces of the disc, and the surface of the friction material. The glaze which formed on A1 samples during the tests described above, was also found on brake pads formulated from A1 material, that had been tested using a dynamometer. Samples of these brake pads and the film covered wear track on the cast iron disc, were examined using a JEOL 6310 scanning electron microscope, equipped with a LINK AN10000 energy dispersive x-ray analyser (EDX), which could give a qualitative analysis of the friction films which formed on each surface, and could also provide x-ray elemental maps of areas of the friction film. This facility was used to map the distribution of the various elements in the films found on the surface of the A1 brake pads.

EDX systems use a solid state Li - Si detector which produces a voltage pulse when x-rays impinge on the detector surface. The charge produced by a typical x-ray is proportional to the x-ray energy and can be amplified to give a measure of the energy of the x-ray. The data is collected using a multichannel analyser, which allows all the elements down to carbon (Z= 6) to be detected. The advantage of EDX is that the whole spectrum of elements present can be displayed at once, where it is shown as a function of intensity versus energy. The technique is also fast and is insensitive to specimen geometry [80].

v) Friction film analysis by X-ray Diffraction.

An attempt was made to remove some of the friction film from the surface of each brake pad for analysis, the film proved to be very adherent and difficult to remove, but by scraping the surface sufficient sample was collected. The scrapings were then ground to a fine powder in order to produce smooth continuous diffraction lines. The sample was analysed using the Debye - Scherrer powder camera method, which involves the diffraction of monochromatic x-rays by a powder specimen. This method was used because only a very small sample is required for analysis. x-ray diffraction analysis can yield a great deal of structural and chemical information about the contents of the friction film [81].

4.3.3 Results

i) Examination of the wear tracks and friction films produced by A1 material.

Figures 70 - 75 are optical photomicrographs of the wear track surface. Each test was conducted at progressively higher disc temperatures. Figure 70 shows the wear surface after the first test conducted at a maximum disc temperature of 145°C, where it is clear that the disc surface has been polished, giving it a metallic lustre which is the typical appearance of the wear tracks produced during low temperature testing. The graphite flakes within the cast iron disc are also clearly visible.

Figure 71 shows the same surface after the next 2hr test conducted at a maximum disc temperature of 277°C, again a polished metal surface containing graphite flakes is evident. The polished surface has also become straw coloured due to oxidation. The contrast between the appearance of the polished wear track and the rest of the disc surface is clearly shown in figure 72. The wear track appears bright, as it has been effectively polished during testing (labelled 'A'), while the normal disc surface remains dark due to its roughness (labelled 'B'). When the disc surface temperature is raised to 310°C, a film starts to form on the surface (shown in figure 73), however, the graphite flakes in the cast iron surface are still visible in some areas, indicating that the film is still thin at this stage. At progressively higher disc temperatures of 350 and 450°C, a thicker, more complete film was formed, (see figures 74 - 75).

ii) Examination of the wear tracks and friction films produced by the A2 material.

Figures 76 - 78 are optical photomicrographs showing the wear scar on the disc surface produced by the A2 friction material. Figure 76 shows the disc surface prior to any testing, where the disc has a turned finish. The same surface after three tests each lasting 2hrs where no external heating was applied is shown in figure 77. Again unheated testing resulted in a polished surface where the graphite flakes within the cast iron disc can be seen. The next wear test was at a higher temperature, where the disc surface was heated to approximately 400°C. This caused a film to form as shown in figure 78.

The high temperature test described above was then repeated, and it was noticed that during the first hour of testing the friction film was removed. With reference to figure 53 (section 4.2), which shows how a typical heated test is conducted, it can seen that each sample is run against the disc for an hour to allow it to bed in properly, then the temperature is raised. Clearly the friction film due to A2 was removed during the bedding in phase of the test, when no external heating was applied. This effect is clearly illustrated in figures 79 and 80. Each micrograph

shows the edge of the wear track on the disc surface, and three separate regions can be distinguished, firstly there is the unworn disc surface (labelled 'A'), next to this there is a narrow band of residual friction film from the previous test (labelled 'B'), and thirdly there is the new wear track due to the repeat test described above (labelled 'C'). During the repeat test the sample size was slightly reduced, in order to demonstrate the film removal shown in figures 79 and 80. This provided the sharp contrast between the film covered wear track produced during the first high temperature test ('B'), and the following test ('C'). clearly illustrating film removal. Figure 81 shows the wear track after a heated test with A1, where a thick friction film has been deposited on the surface. The same track is shown in figure 82, after an unheated test using A2, evidently the friction film has been stripped away from the surface in many areas.

iii) Friction film analysis by EPMA.

The results of the Electron Probe microanalysis of the A2 wear track are shown in figure 83, four traces are shown, each one corresponding to the reflections from each one of the four crystals used to examine the entire spectrum of the possible x-ray wavelengths. As there was no film on the disc surface, this trace effectively represents analysis of the bulk of the cast iron disc. This can be compared with those for A1 which are shown in figures 84 and 85. The peaks present on each trace have been identified and labelled with the appropriate elemental symbol.

iv) Friction film analysis by EDX.

Figure 86 shows the spectral analysis of an area of friction film on the disc surface, produced by A1 friction material. For comparison an unworn part of the disc surface was also analysed, the results of which are given in Figure 87. An analysis of the dark glaze found on the surfaces of A1 pads is also shown in figure 88. The peaks in each spectrum have been labelled with the relevant elemental symbols.

Figures 89 and 90 are SEM micrographs of the dark glaze which had formed on the surface of the A1 brake pads. An area of film was then selected for x-ray mapping, shown in figure 91. In the area examined some of the film had been scraped away to provide a contrasting background.The scraped area is marked as 'PAD', while the film covered area is marked as 'FILM', the area to be examined using x-ray mapping is also highlighted in the centre of the picture. Figure 92 shows the secondary electron image of the area under examination in close up, where the friction film (marked with an 'A'), lies over a brass chip (marked with a 'B'). which provides a contrasting background for the analysis. Figures 93,94, and 95 are micrographs of elemental scans for iron, copper, and silicon, respectively.

The concentration of an element is measured on the thermographic scale, where white areas indicate the regions which contain maximum concentrations of the element in question, and the black areas correspond to minimum concentrations. Maps for the other elements which appeared in the spectral analysis were also made, but the concentration of these were much lower than the concentrations of the elements shown, with the exception of oxygen which was omnipresent.

v) Friction film analysis by x-ray diffraction.
Figure 96 shows the x-ray diffraction pattern produced from a sample of film taken from the surface of a used sample of A1 brake pad. Figure 97 shows the x-ray pattern produced by a sample of pure magnetite powder, this clearly indicates the presence of magnetite on the surface of the A1 brake pad.

4.3.4 Discussion

i) Friction film formation by A1 and A2 friction materials.
Figures 70 to 75 illustrate how disc surface temperatures affect friction film formation in A1. Clearly no film has formed as a result of the test carried out at 277°C, however, at 300°C a friction film had formed. From this it can be concluded that film formation is a temperature activated process, which is initialised by a disc surface temperature of between 277°C and 300°C.

The micrographs shown in figures 76 to 78 of A2 clearly show that this material readily produces friction films at high temperatures, but will also remove them during subsequent unheated tests. This contrasts with the behaviour of A1, which does not remove its own film so easily.
The fact that A2 will also remove an A1 friction film, indicates that A2 material is more abrasive than A1, and explains why it removes its own friction film. Consulting table 2 in chapter 3 (section 3.1), where the contents of each material are listed, it can be seen that A2 contains two lubricants; Calcium Fluoride which is thought to possess lubricating properties at high temperatures up to 1000°C, and graphite powder a lower temperature lubricant, which has limited lubricating properties above 500°C, because it decomposes due to oxidation [82]. In comparison A1 contains lead sulphide which is only effective above 500°C, and two lower temperature lubricants; antimony sulphide, and a large proportion of graphite flake. Interestingly, A1 friction material contains four times the amount of lubricating components (by weight) than A2, which explains why A1 acts less abrasively towards its friction film.

iii) Friction film analysis by EPMA.

The typical composition of a cast iron disc is approximately 95% iron, 3.2% carbon, 1.2% silicon, and 0.9% manganese and other trace elements [42]. The trace shown in figure 83 was an analysis of the wear track of A2, which had a polished film free surface, and was used as a control sample providing a representative analysis of the brake disc composition, where all the peaks detected were due to the elements in the cast iron disc. This further verifies that no film was present on the surface of the A2 wear track. In comparison, the traces of the wear track due to A1 give additional peaks for Barium, Antinomy, Lead, Sulphur, Copper, and Calcium. All of these elements can be found in A1 friction material, and so indicates that some of the friction material is transferred on to the disc surface.

iv) Friction film analysis by EDX.

Comparing the EDX spectra of the unworn disc surface in figure 87, with that of the worn disc surface or wear scar due to A1 in figure 86, shows that once again the film present on the wear surface is made up of constituents from the friction material, and shows a similar composition to that found with the EPMA technique. It was also noted that iron was detected strongly, which was thought unsurprising at the time, and was attributed to the underlying iron matrix.

An analysis of the glazed surface of the A1 friction material sample was also carried out, shown in figure 88, and again the spectra produced contained a typical set of elements which would be expected from a friction material such as A1, except for the one important exception that, the large iron peaks found in the disc surface spectrum, were also present in the surface spectrum of the friction material. This indicated that the dark glaze on the surface of the friction material contained a significant proportion of iron in some form. This was surprising as the friction material contained no iron, and so the iron found, must have originated from the disc surface.

The micrographs shown in figures 89 and 90 illustrate how the surface of A1 friction material becomes encrusted with a friction film. The film has a homogeneous appearance, and has been scored and grooved by the disc surface. The elemental maps taken of the friction material surface clearly indicate that the film contained a large proportion of iron. Oxygen was also found in large quantities in areas of friction film, which suggests that the iron is present in the form of an oxide. Other friction material constituents were mapped, but were

found only in traces, with the exception of silicon whose distribution is shown in figure 95.

v) Friction film analysis by x-ray diffraction.
The powder camera x-ray diffraction patterns presented in figures 96 and 97, clearly indicate that the friction material surface film consists of magnetite (Fe_3O_4). Other lines can be attributed to the presence of carbon, and silicon.
There is clear evidence that the friction film which forms on both the disc and the friction material surfaces, contains some material originating from the brake pad, but consists predominantly of iron oxide in the form of magnetite (Fe_3O_4), which originated from the cast iron disc. The oxidation state of iron is dependant on the availability of oxygen, and a typical oxide layer may contain iron in two or even three different oxidation states [83].
Wustite (FeO) is a highly oxygen-deficient oxide which forms closest to the metal surface. However, wustite is unstable at temperatures below 570°C, and it disproportionates to iron and magnetite. Magnetite formation is encouraged in oxygen deficient environments, as would be found at the interface between a friction material and disc under a high load. Haematite (Fe_2O_3) is the most oxygen-rich oxide and forms next to the gas phase [83], but a gas phase as such, does not exist at the sliding interface of a brake system, and it is suggested that the haematite oxide does not form during braking, and no evidence for its formation has been found during x-ray diffraction analysis.

A number of workers have stated that the friction films in brake systems consisted of compacted wear debris which initiated from the friction material, [48,51,52,53,54,]. More recently the chemical composition of friction films has been investigated by Borjesson [84], and Wirth et al [55,56,57,58], who employed EDX and x-ray Photoelectron Spectroscopy (XPS), a very sensitive technique used for examining the first 5nm of a surface. These studies also concluded that friction films in brake systems originated from the wear debris emanating from the friction material, and gave no mention of a high iron concentration within the friction film. This was because all of the above studies involved analysis of films deposited on the cast iron disc surface, and any iron signal which appeared in the individual analyses, was attributed to an emission from the underlying cast iron substrate, and not to the friction film. It was stated by Wirth [57], that the iron Lα x-rays have low energy and could only penetrate a thin oxide layer, but not a thick film, so when these lines were detected in the EDX spectra from such a film, they could not be accounted for. However, it was suggested that the films could be thin or patchy, or could contain significant quantities of iron. The thickness of each of

the friction films was then examined and compared, this involved increasing the penetration of the incident electron beam by raising the accelerating voltage from 10Kv to 25Kv. This had the result of increasing the relative height of the iron peaks in the spectra of each of the films examined, It was argued that this increase was due to a greater contribution from the underlying iron matrix. Samples which showed the greatest relative increase in the iron signal, were deemed to have thinner films than others. However, this did not account for the presence of low energy Lα x-ray peaks found in the spectra of all the films examined and their presence was left unexplained. The findings of this study show that friction films do contain iron in the form of iron oxide, the presence of which could explain the results found in the investigation described above, because if significant quantities of iron where present at the film surface then the low energy Lα x-rays produced could escape from the sample and be detected.

Other workers have noted the presence of iron in friction films. Liu et al [52], examined the friction films which formed on the rubbing surfaces of brake drums using Scanning Auger Microscopy (SAM), and EDX. A cross-section of the drum perpendicular to the rubbing surface was examined, and an in-depth elemental profile of the friction film cross section was made. From these studies a measurable amount of iron was found in the friction film, and it was concluded that these friction films not only contained components of the friction material, but also contained fragmented pieces of oxide and carbide originating from the drum. Scieszka [64], examined the films which formed on the surfaces of brake materials when rubbed against a steel surface. Again it was found that as a result of friction against a steel counterface, a metallic layer with a high content of α-Fe and iron oxides formed on the friction material surface, which was termed "the metallization of friction linings". Scieszka went on to suggest a mechanism for iron layer formation, where he states that for metallization to occur, plastic deformation of the steel surface must take place, and the temperature generated at the interface must be high enough to initiate the degradation of the organic components of the friction material. This is important because it is suggested that this degradation of the organics will evolve quantities of hydrogen, which will reduce the mechanical properties of the steel counterface. It was proposed that this strength reduction occurs because the hydrogen diffuses through the cementite crystals in the steel surface, and effectively removes carbon from the cementite by the following reaction:

$$H_2 + Fe_3C \rightarrow 3Fe + CH_4$$

This leaves behind spongy ferrite with extremely poor mechanical properties. The spongy ferrite then becomes plastically deformed leading to strain hardening, and by a fatigue process detaches from the disc surface and is incorporated into the film on the friction material surface. It is interesting to note that at normal pressures the decarbonisation of cementite by hydrogen takes place at ≈300°C [85], which coincides with the disc temperature at which friction films started to form in the above study (See section 4.3.4 (i)). Scieszka [64] states that the metallization of the friction material surface causes a reduction in the coefficient of friction at the interface, and an increase in the wear rate of the steel counterface, whereas in the work presented in this section, friction film formation effectively reduced the wear of the cast iron disc. Also x-ray diffraction studies performed in this work have shown that the iron present on the friction surfaces of brake pads is in the form of magnetite (Fe_3O_4), and not ferritic iron. This is in agreement with the findings of Eyre and Dutta [86], who performed SEM studies of the wear surfaces produced by cast iron on steel, and concluded that under low loads and low sliding speeds, an α-Fe_2O_3 (haematite) film formed, but at higher loads as would be found in a brake system, magnetite formation predominates. Eyre & Dutta also found that the formation of an oxide layer coincided with a reduction in the wear of the steel counterface, which is in agreement with the findings in this section. Also microhardness studies have indicated that iron oxide layers have almost double the average microhardness of ferritic and pearlitic steels [64]. The higher hardness value of the adherent oxide layer would give a higher wear resistance than cast iron, and so it was not surprising that disc wear was reduced by the presence of such a film.

From the above study it is clearly advantageous to encourage the formation of magnetite on the contacting surfaces in brake systems. This could be achieved by incorporating iron powders into the friction material itself, which would provide a ready source of iron from which oxide films could form. The beneficial effects of iron powders is not unknown to brake manufacturers, who are beginning to incorporate them into friction material formulations. The tribological behaviour of friction materials containing iron powders are examined in detail in the following chapter.

4.3.5 Conclusions.

The experimental work described in this section has established the following:-

1) Film formation in A1 does not occur until disc surface temperatures of between 270 -300°C approx. are reached.

2) A2 friction material was shown to remove its own friction film during subsequent unheated testing. It was also shown to remove a friction film formed by A1, indicating that A2 friction material is more abrasive than A1. The reason for this is that A1 contains a larger proportion of lubricants than A2.

3) EPMA studies of the wear tracks on the disc surface showed that friction films do contain some components of the friction material used. The same findings were also made using EDX analysis of worn and unworn disc surfaces.

4) The EDX elemental analysis of the surfaces of brake pads showed that the film on the surface of the pad contained a large proportion of iron, which was shown to originate from the cast iron disc.

5) x-ray diffraction studies showed that the iron content of the friction films found on the surfaces of brake pads, was in the form of magnetite (Fe_3O_4).

6) Magnetite is harder than cast iron and so its formation slows the rate of disc wear, and there is also evidence that pad wear is reduced. For these reasons, the formation of an iron oxide friction film should be encouraged to reduce wear at the braking interface. It is suggested that this could be achieved by adding iron powders to the friction material, which would then serve as a readily available source of iron from which friction films might form.

Figure 70
Micrograph of the disc wear track after the First 2hr test with A1 friction material where the maximum disc temperature attained was 145°C (x200).

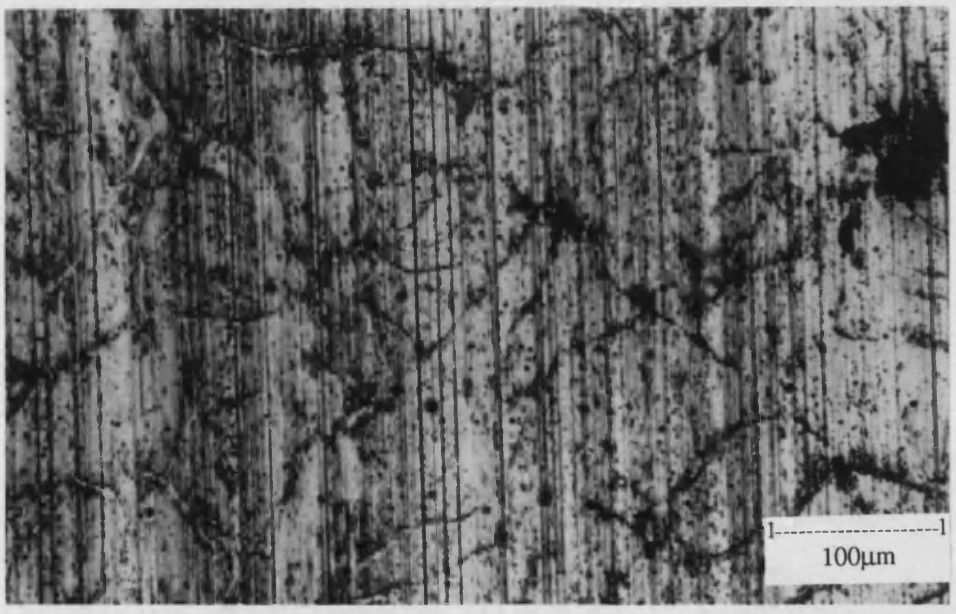

Figure 71
Micrograph of the disc wear track after the second 2hr test with A1 friction material where the maximum disc temperature attained was 277°C, note that the graphite flakes in the surface are visible (x200).

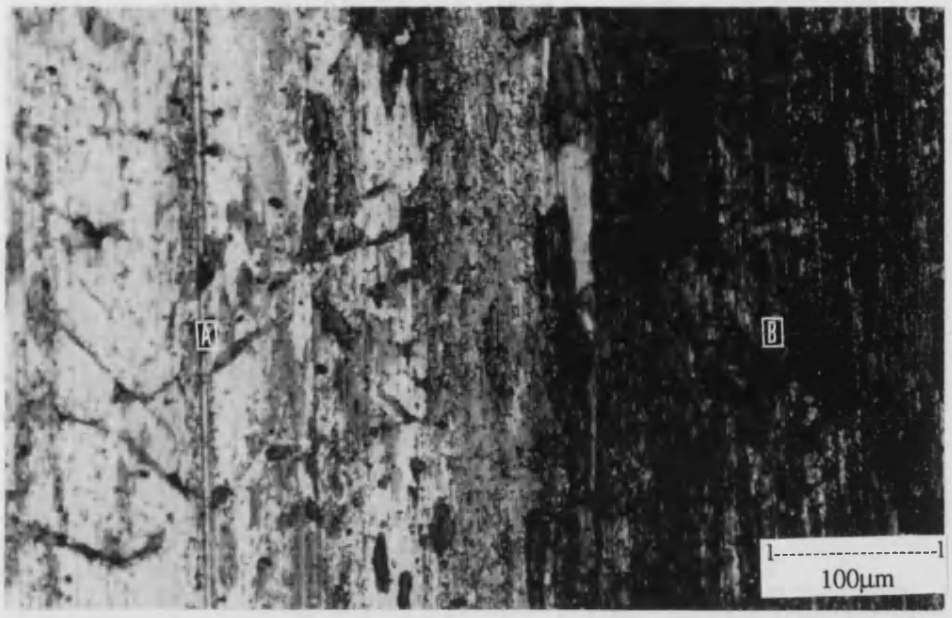

Figure 72
Micrograph comparing the unworn turned disc surface (labelled 'B') and the wear track (labelled 'A') after the second 2hr test with A1 friction material where the maximum disc temperature attained was 277°C (x200).

Figure 73
Micrograph of the disc wear track after the third 2hr test with A1 friction material where the maximum disc temperature attained was 310°C (x200).

Figure 74
Micrograph of the disc wear track after the fourth 2hr test with A1 friction material where the maximum disc temperature attained was 350°C (x200).

Figure 75
Micrograph of the disc wear track after the Fifth 2hr test with A1 friction material where the maximum disc temperature attained was 450°C (x200).

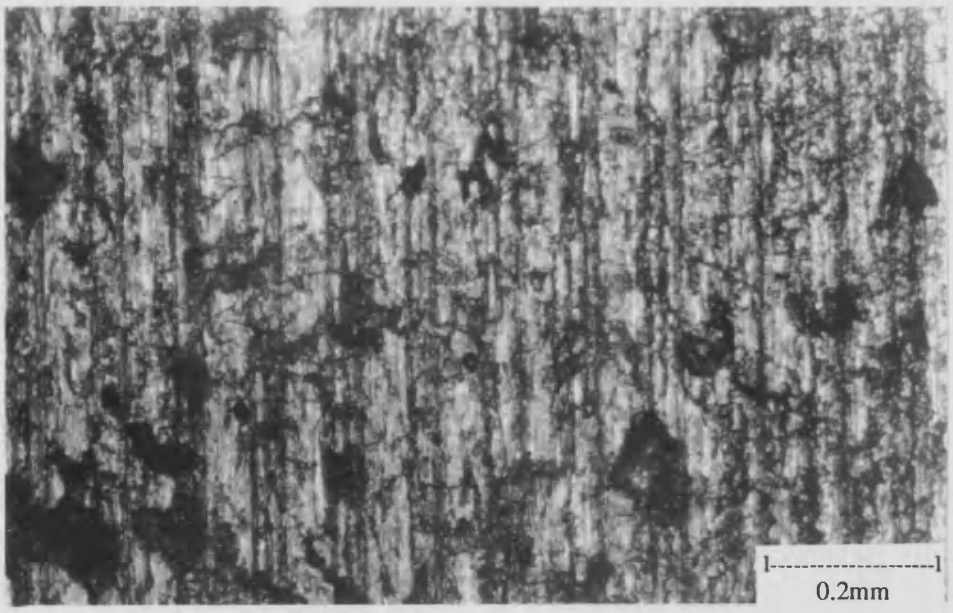

Figure76
Micrograph of the unworn cast iron brake disc where the surface has a turned finish, (x 100).

Figure77
Micrograph of the disc wear track due to A2 material, after a 6hrs of unheated testing, where the maximum disc temperature attained was 180°C. Note the polished appearence of the disc surface where the individual graphite flakes can be seen (labelled 'G') (x100).

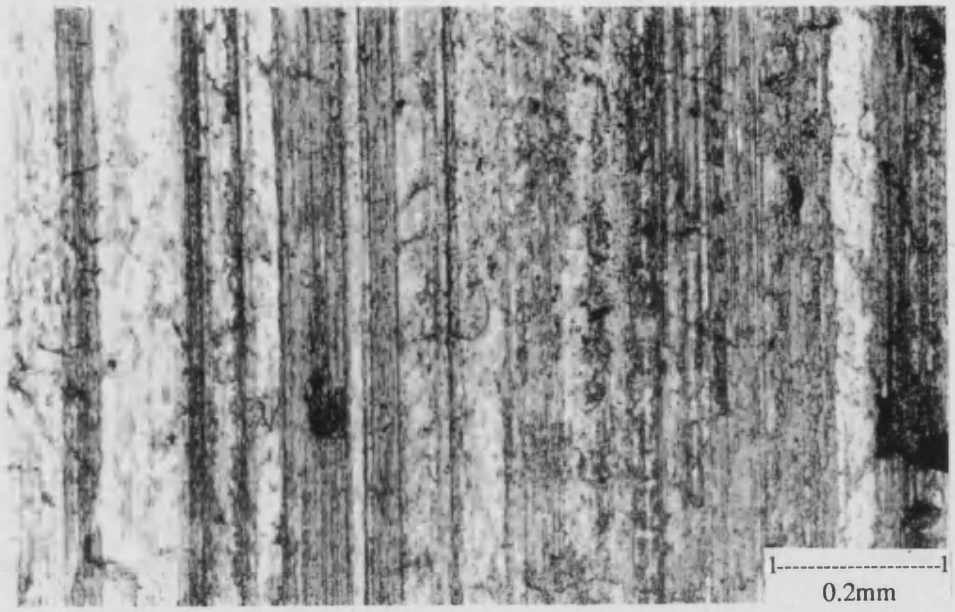

Figure78
Micrograph of the disc wear track due to A2 friction material, after a 2hr heated test where the maximum disc temperature attained was r400°C (x 100).

Figure 79
Micrograph of the disc wear track due to A2 friction material, showing friction film removal. Three seperate areas can be distingished:- The unworn disc surface (labelled 'A'), the wear track still covered with friction film produced during a high temperature test (labelled 'B'), and the 'polished' wear track where the friction film was removed during the following unheated test (labelled 'C'), (x50).

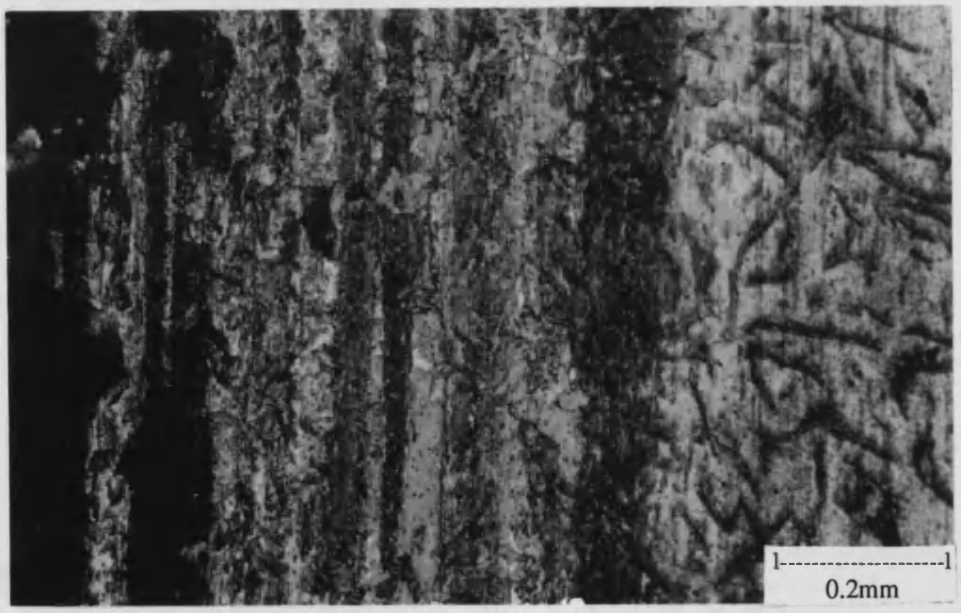

Figure 80
Micrograph of the disc wear track due to A2 material, showing friction film removal as in figure 79 (x100).

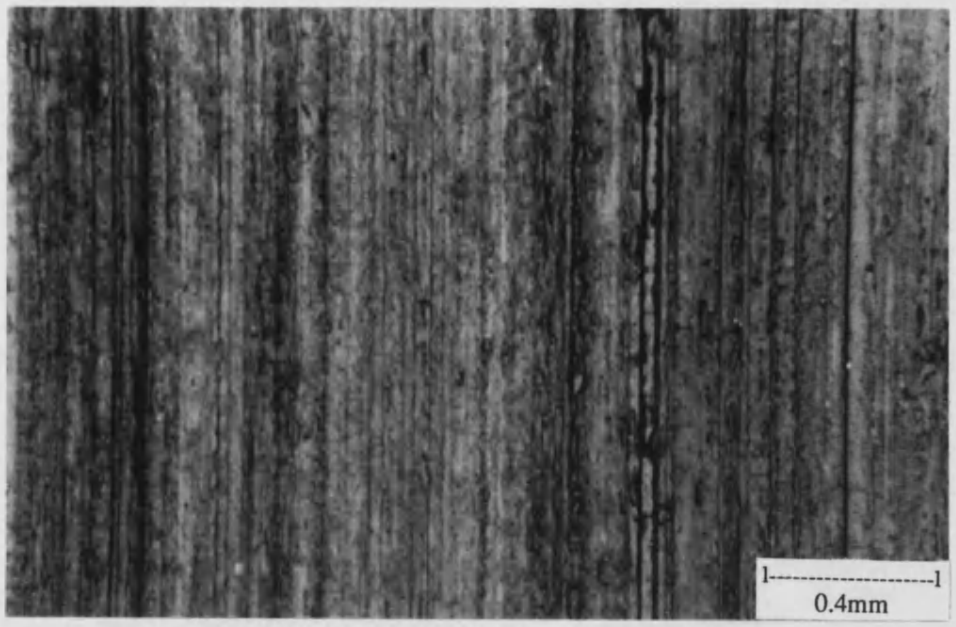

Figure 81

Micrograph of the film covered wear track on the disc surface, produced by A1 friction material, during high temperature testing, (x50).

Figure 82

Micrograph of the same area of wear track as shown in figure 81 after an unheated test with A2 friction material. The light areas indicate where the friction film has been stripped from the surface, (x50).

Figure 83
E.P.M.A. Qualitative analysis of the polished wear track which formed on the cast iron disc surface during testing with A2 brake material.

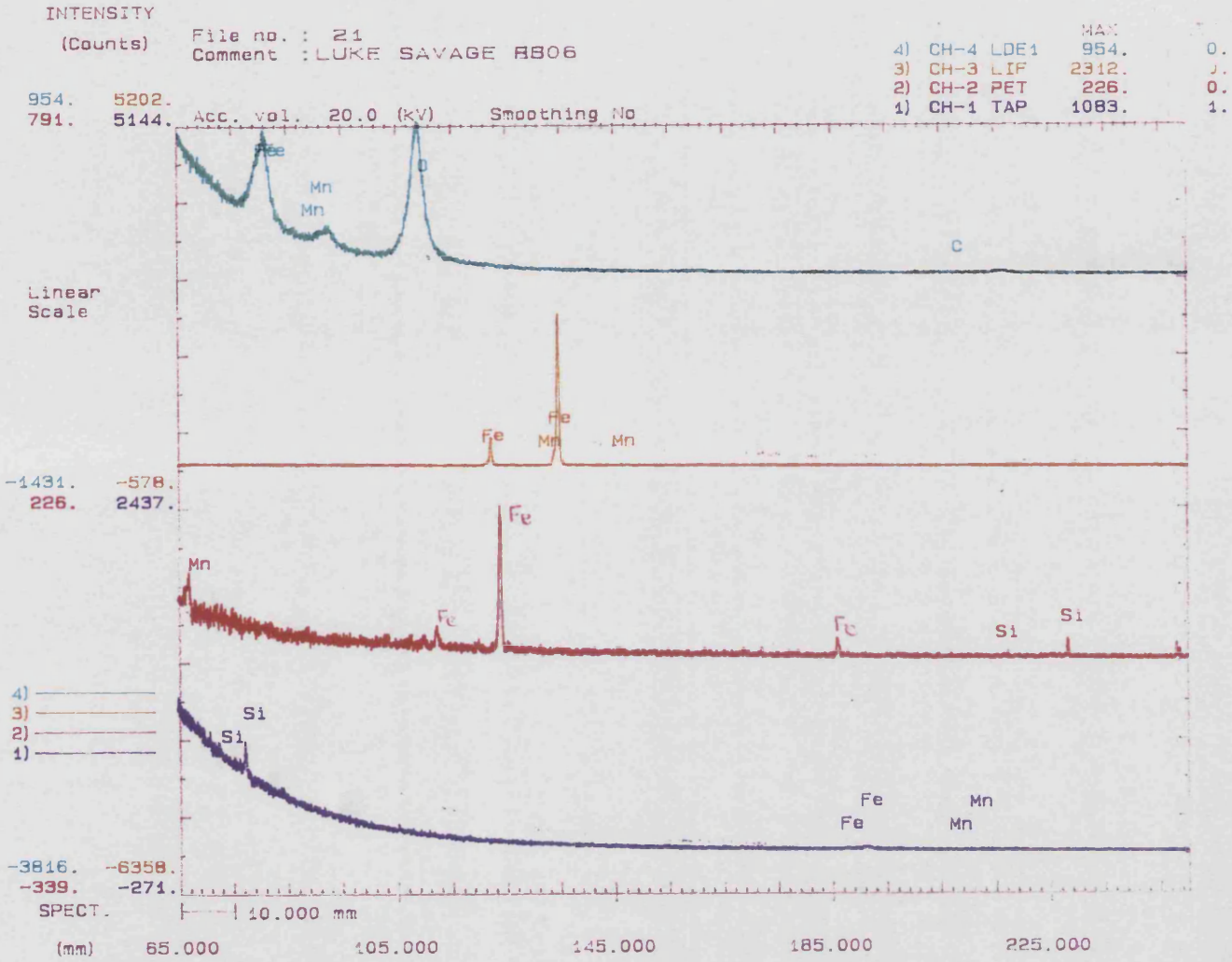

Figure 84
E.P.M.A. Qualitative analysis of the film covered wear track which formed on the cast iron disc surface during testing with A1 brake material:- shows traces due to the LDE & LIF crystals.

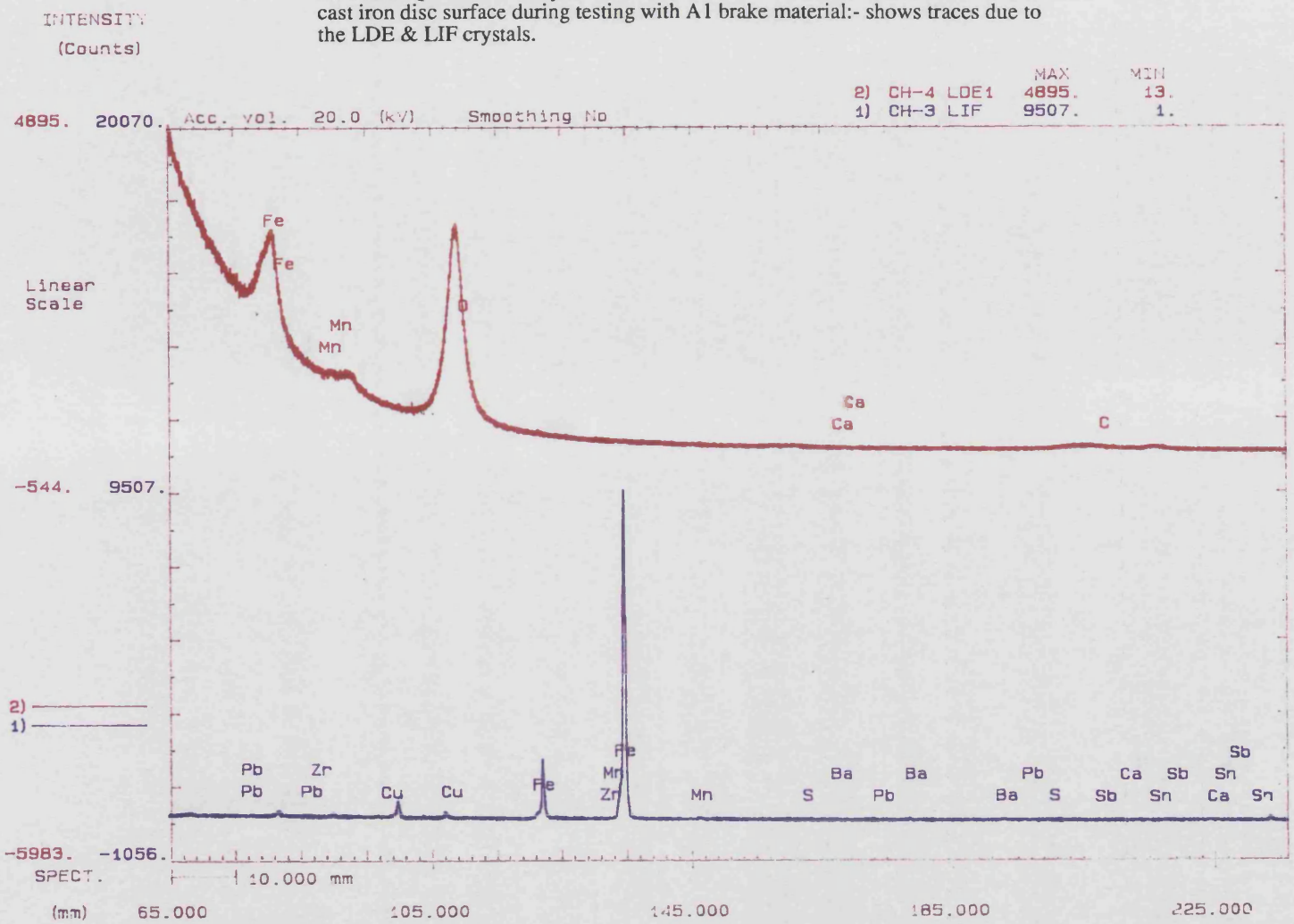

Figure 85
E.P.M.A. Qualitative analysis of the film covered wear track which formed on the cast iron disc surface during testing with A1 brake material:- shows traces due to the PET & TAP crystals.

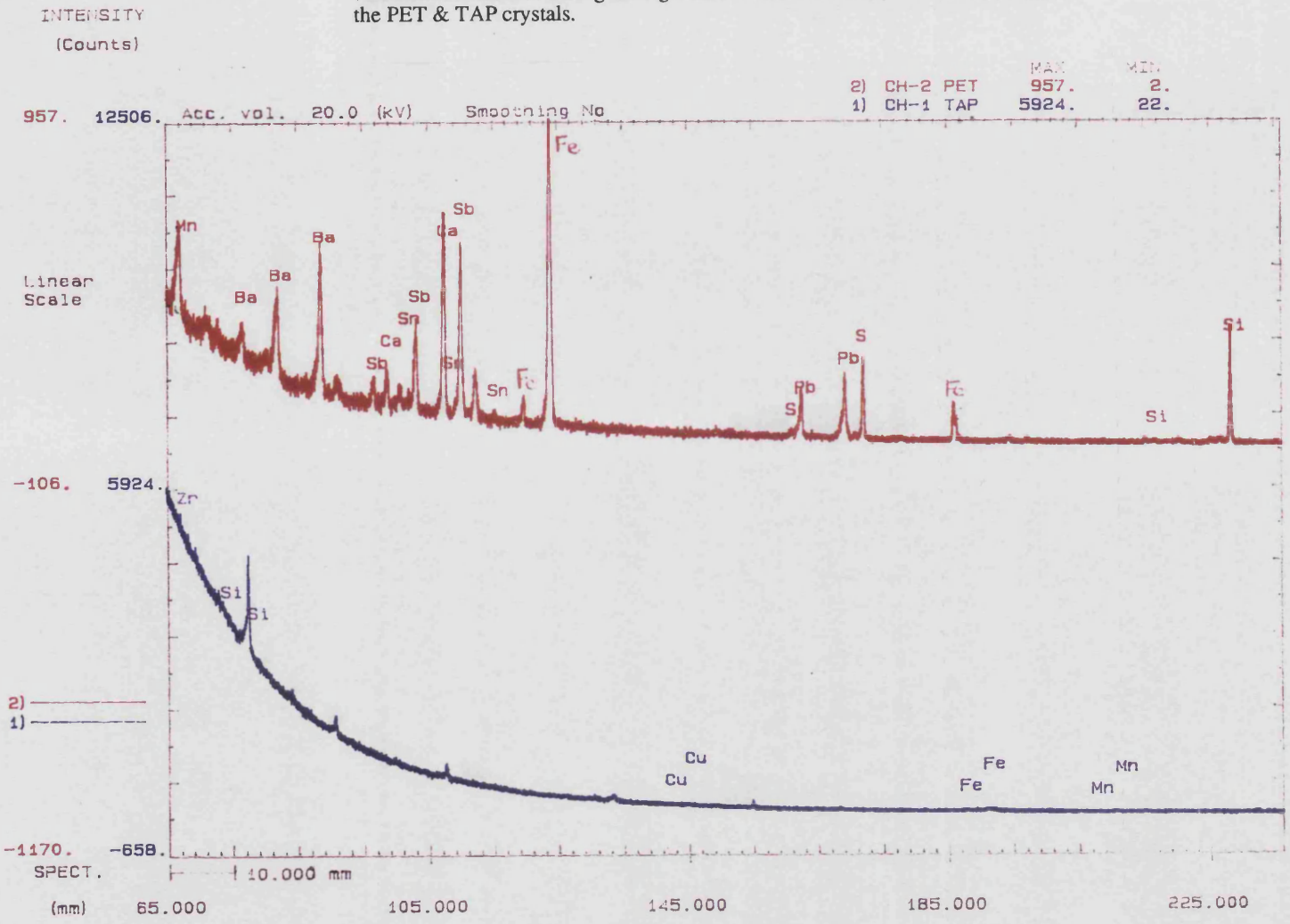

Figure86
E.D.X. Spectral analysis of the film covered wear track which formed on the disc surface during testing with A1 brake material.

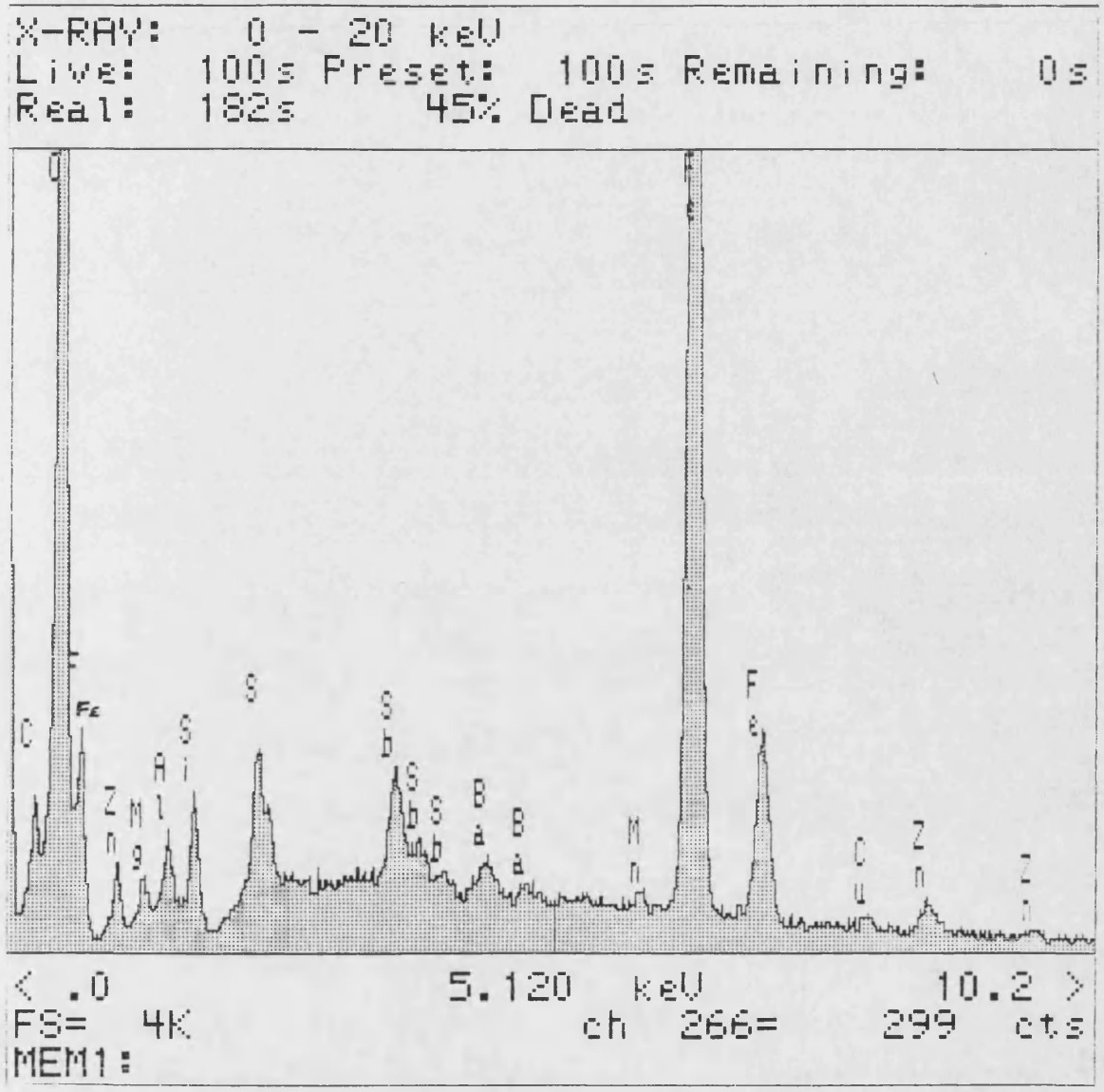

Figure87
E.D.X. Spectral analysis of an unworn cast iron brake disc surface.

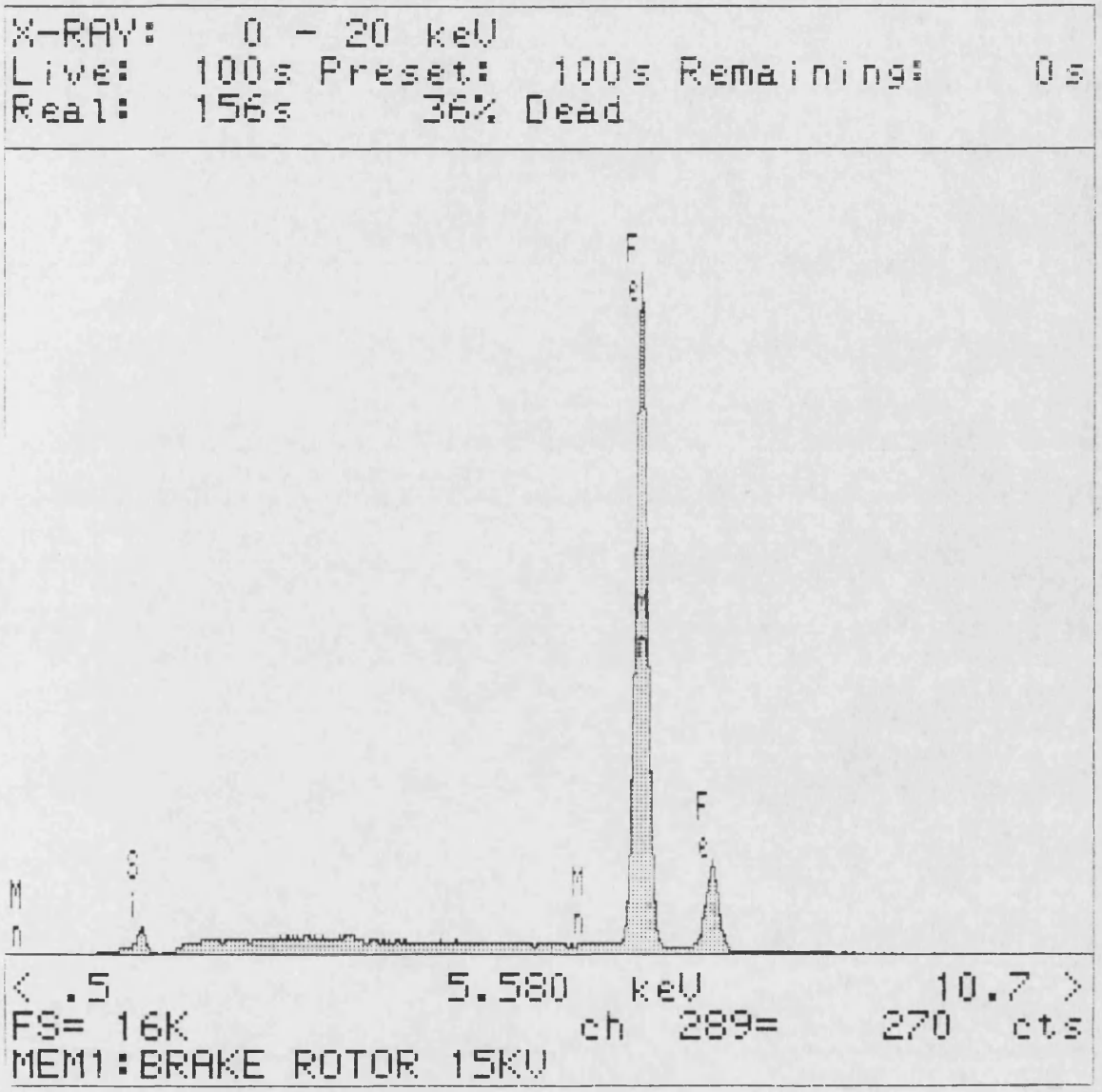

Figure88
E.D.X. Spectral analysis of the friction film on the surface of an A1 brake pad.

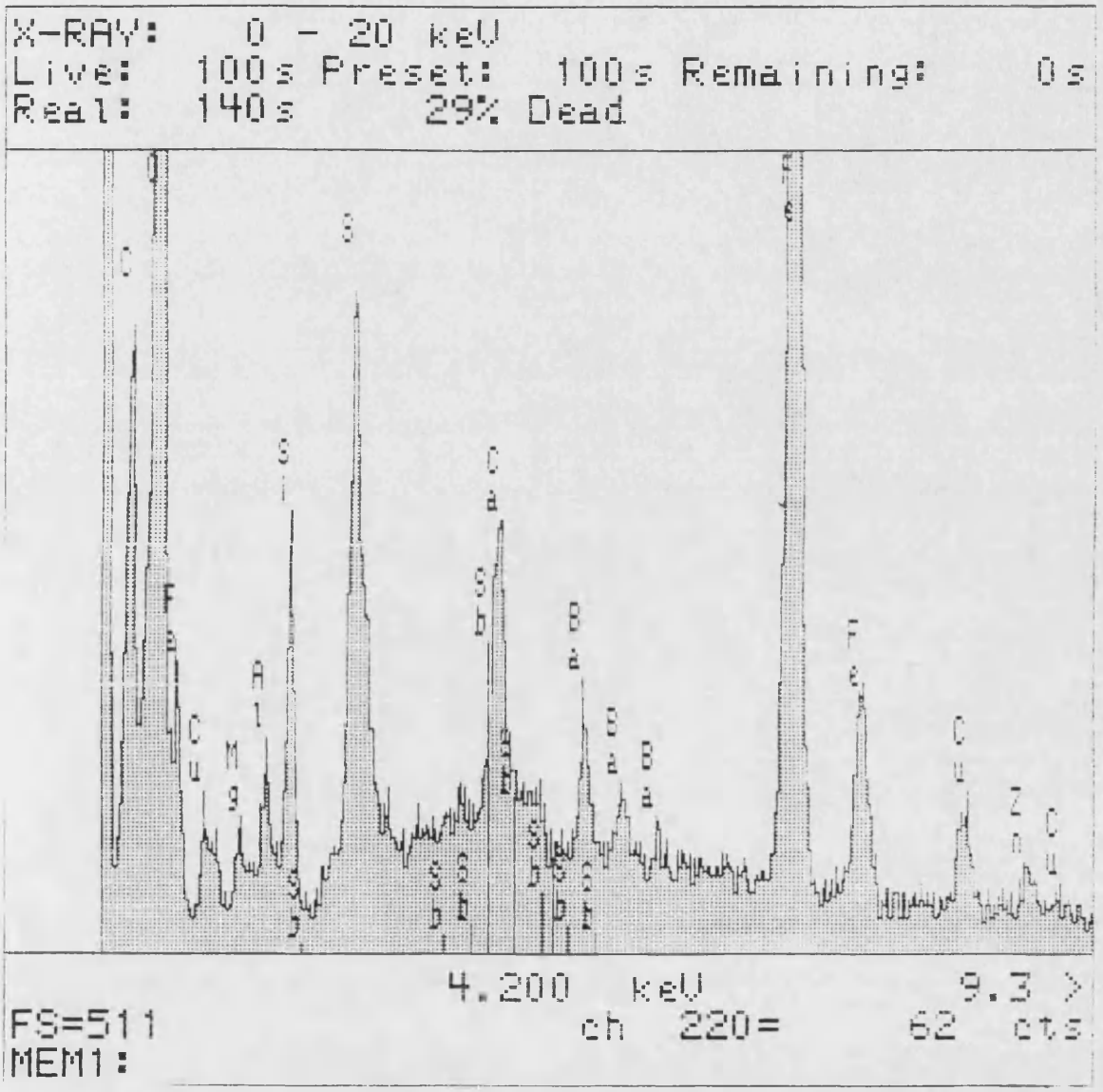

Figure 89
S.E.M. micrograph of the friction film on the surface of an A1 brake pad (x550).

Figure 90
S.E.M. micrograph of the friction film on the surface of an A1 brake pad (x1400).

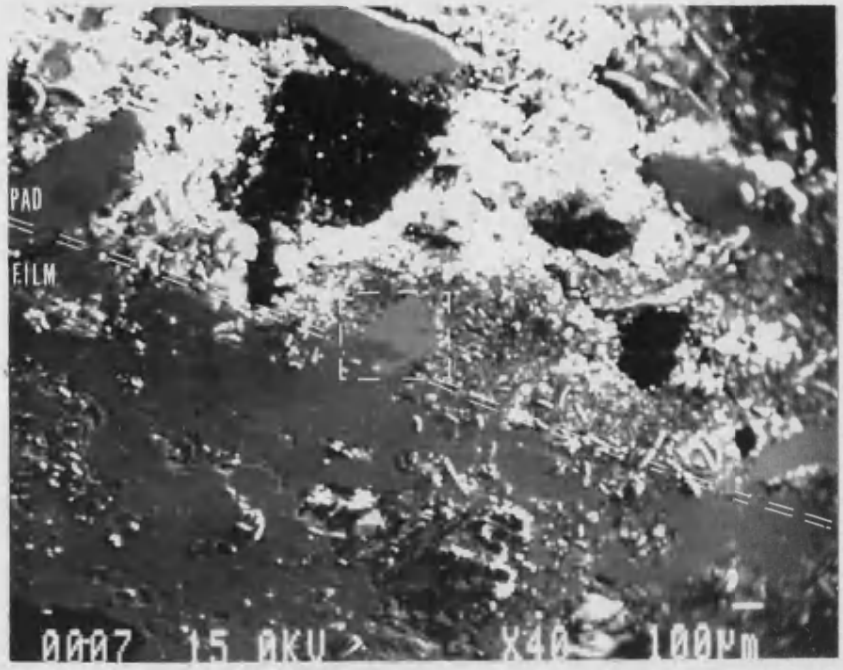

Figure 91
Micrograph of the friction film on the surface of an A1 brake pad, showing both the film and underlying pad areas (labelled 'FILM' and 'PAD'). The squared area was chosen for elemental mapping, (x40).

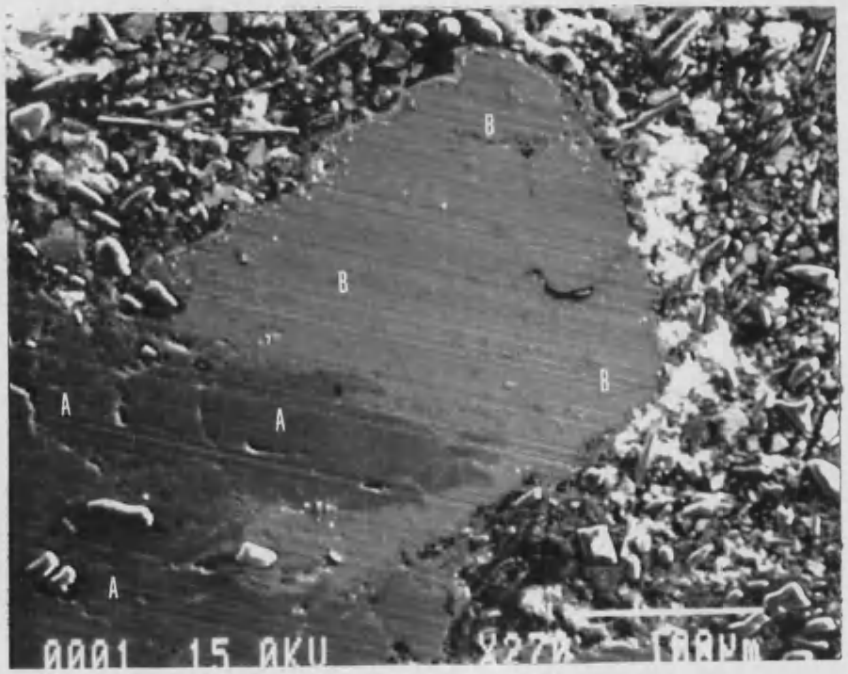

Figure 92
Micrograph of the friction film on the surface of an A1 brake pad, showing the secondary electron image of the area to be mapped. The film covered area (labelled 'A') and the underlying brass chip (labelled 'B') can be clearly distinguished, (x270)..

Figure 93
E.D.X. of the friction film on the surface of an A1 brake pad:-Mapping for Iron.

Figure 94
E.D.X. of the friction film on the surface of an A1 brake pad:- Mapping for Copper.

Figure 95
E.D.X. of the friction film on the surface of an A1 brake pad:-Mapping for Silicon.

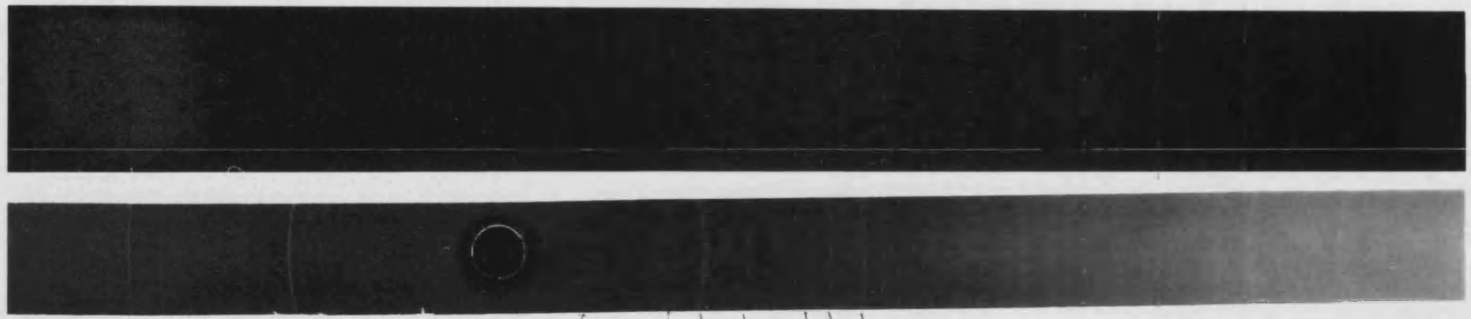

Figure 96
X-ray diffraction pattern of pure magnetite.

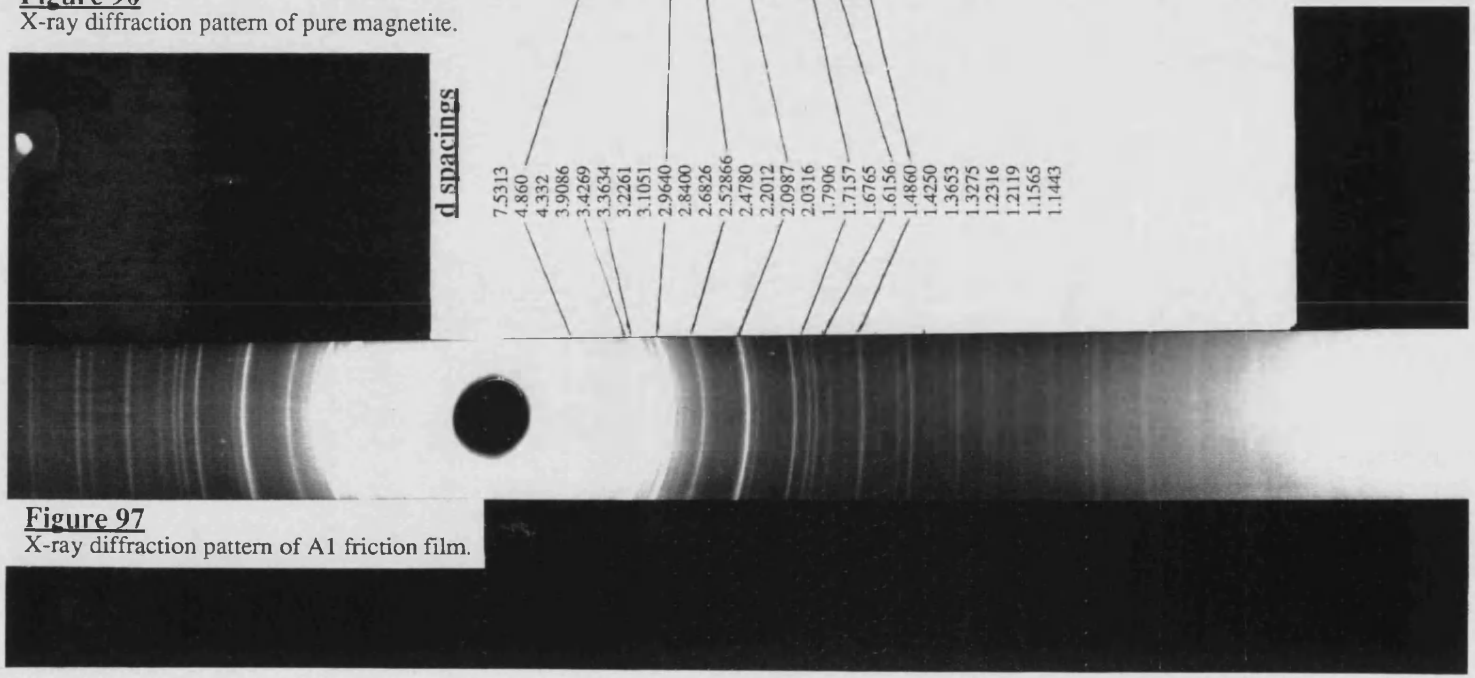

Figure 97
X-ray diffraction pattern of A1 friction film.

4.4 A further investigation into the high temperature wear behaviour of A1 friction material

4.4.1 Introduction

The investigation described in section 4.2. examined the high temperature friction and wear behaviour of A1 friction material sliding against a cast iron brake disc. These studies showed that A1 was a comparatively wear resistant material at high and low temperatures, and also produced minimal disc wear. It was seen that during high temperature operation, the friction surfaces of both the pad and the disc were shielded from heavy wear damage by the formation of a friction film. Analysis of the films on each surface indicated that they contained a large proportion of magnetite (Fe_3O_4) where the iron originated from the disc surface, together with traces of the friction material used during the test.

The work reported in this section is in two parts, where part 1 is a continuation of the work outlined above, involving a further investigation into the protective properties of the friction films produced by A1 friction material. This study compares the wear rates of two samples of A1, one of which was tested against a clean disc surface, and the other against a disc surface which was covered with a friction film. The results of these tests lead to the investigation detailed in part 2, where a relationship has been shown to exist between the wear rate and the number of high temperature tests performed on a sample.

4.4.2 Methods and Materials

Part 1

The objectives of the tests performed in this section were to further investigate the effects of friction films on the wear rates of friction materials and brake discs. A1 friction material was rubbed against a cast iron disc using the continuous drag 'pin on disc' wear machine as described in chapter 3 section 3.3.2. In order to explore any effects due to the presence of a friction film, a sample of A1 was repeatedly tested against a film covered area of the disc, and as a control, an identical sample was tested in the same way against a 'clean' area of the disc which had been conditioned by previous tests and was consequently smoothed and polished, but was not covered with a friction film.

Before testing could be started the brake disc surface was firstly conditioned by running a series of 5 bedding-in test cycles on each wear track, (A bedding in

cycle involves running a sample of A1 friction material against the unheated disc surface for 1 hour). This was important because new brake discs have a turned finish which can have an Ra (average roughness) value an order of magnitude higher than a run-in disc, so the disc surface must be standardised to give a constant surface. Figure 98 shows how the disc surface roughness reduces with the number of bedding-in cycles. Clearly the Ra values of both tracks has been reduced to a similar value, so removing any effects due to differences in disc surface roughness. Figure 99 shows the arrangement of the wear tracks on the disc surface. A friction film was deposited on the inner wear track during cycle N^{o} 5 of the bedding-in phase, this achieved by heating the disc surface to 400°C during the test. As a control experiment the outer track was bedded-in in a similar manner except that cycle N^{o} 5 was unheated so that no film formed on the wear track. The disc surface was prepared in this way so that the properties of a film covered disc could be compared with a plain disc surface of a similar roughness.

Testing was conducted using two new samples of A1 friction material which had been drawn from the same source, and prepared using the standard industrial production methods as described in section 4.2.2. Sample (I) was run against the film covered track, and sample (II) against the 'clean' track, under identical pressures and sliding speeds, namely 2.7MPa, and 2.06m/s. This was achieved by compensating the load on the sample, and the r.p.m. of the disc used during each test, depending on whether the test was run on the inner or outer track. Each sample was subjected to a series of 9 tests each lasting approximately 2hrs, the first four were low temperature tests where no external heating was applied during testing, whilst the remaining five were high temperature tests where the disc surface temperature was raised to approximately 400°C. The wear which occurred during each test was logged, and from this data a wear rate for each test was calculated. In this way the wear rates due to each wear track could be compared.
After the initial 9 tests described above, a further 6 tests were run on the film covered wear track using sample (I), until the sample had been completely worn away. This was done to investigate the effects of prolonged high temperature exposure on sample wear.

Part 2

During high temperature testing frictional heating can generate very large temperatures at the braking interface, and large amounts of heat are conducted away from the interface through the friction material, so that a thermal gradient exists through its thickness. The temperatures involved are often high enough to

cause the onset of thermal decomposition of the organic constituents of the friction material. The following study was designed to investigate how the degree of carbonisation of a friction material changes with distance from the rubbing surface, and also to compare the carbonisation profiles of an untested sample, with samples tested at approximately 400°C for 1, 3, and 6 hours.
A1 friction material was used in this study, four samples of which were prepared and conditioned as described above. The first 750μm of the rubbing surface of each specimen was sampled, this was done by removing 250μm of material from the surface using a milling machine, and as each layer was stripped off, the debris was collected using a vacuum hose, the end of which was covered with a clean tissue. In this way all the debris produced was sucked onto the tissue surface, giving a powdered sample of each 250μm layer of friction material. The process was then repeated in 250μm steps down to a depth of 750μm. The sampling technique is summarised in figure 100. Samples of the powdered wear debris produced during the high temperature pin on disc testing of the A1 described above, were also collected and analysed. The volatile content of each of the powdered samples was measured using thermogravimetric analysis, where each sample was heated up to a temperature of 800°C in an inert argon atmosphere at a rate of 160°C/hr.

The resulting weight loss indicated how the volatile content of the friction material changed with increasing distance from the rubbing surface. A large weight loss would indicate that the sample had suffered little thermal damage, whilst a small weight loss would indicate that the volatile components of the friction material had already been removed during testing, and that the material had undergone pyrolysis. Comparison could be made of the weight loss profiles produced by each of the different samples listed above. In this way any carbonisation effects caused by repeated testing at high temperatures could be explored.

4.4.3 Results

Part 1

Figure 101 compares the wear rates of A1 samples tested on each of the wear tracks described. The wear behaviour of each sample was very similar during the 9 pin on disc tests performed. During the first 4 unheated tests, the wear rate stayed relatively constant from test to test. The first high temperature test resulted in the formation of a friction film on the outer wear track, and also the wear rate in

both samples were much higher. The wear rates of both samples then fell during subsequent high temperature tests. Figure 102 shows the corresponding disc wear produced by each sample during testing. The film covered wear track showed negligible disc wear, while the clean track wore by approximately 1.5μm during the unheated part of the test regime. Heated testing resulted in a large increase in disc wear in both samples of A1 material, where the clean surface showed the greatest wear, reaching a maximum of 4.5 μm.

Figure 103 shows the wear results from the extended wear test carried out on the film covered inner track. Interestingly the wear rates in both the unheated and heated tests started to rise as more heated tests were made, reaching very high rates by tests 14 and 15. These results prompted the study described in part 2, the results of which are presented in figure 104, which shows how the weight loss of the surface layers of used friction materials, change with distance from the rubbing surface. The measurement of weight loss can be used to gauge the degree of carbonisation which has occurred within each sample, a low loss indicating a high degree of carbonisation. The figure indicates that samples of wear debris had the lowest weight loss which indicates that a large proportion of the volatile components of these samples had been removed during testing. When the weight loss profiles of three different samples are compared, it is evident that samples which have been tested more often at high temperatures, have lost more weight and have become carbonised to a greater degree. In each of the three samples the weight loss falls with increasing distance from the surface, until it reaches the same value as found from a virgin sample of A1 friction material.

4.4.4 Discussion

The results presented in figure 101 show that the wear rate of A1 friction material during unheated testing was very low irrespective of presence or not of a friction film on the disc surface. The first high temperature test lead to high wear rates in both (I) and (II) samples, however, the wear rate then fell during subsequent high temperature tests. This fall in the high temperature wear rate is due to the build up of a friction film at the sample - disc interface during the first high temperature test, which then effectively reduces the wear rate of the friction material during the subsequent tests.

The cumulative disc wear for each sample in figure 102, show that during unheated tests, the disc wear was effectively zero in tests run against a friction film covered area of the disc, whereas the clean disc surface wore by 1.5μm under the same conditions. Disc wear increased markedly in both samples during high temperature testing, where the overall wear of the clean surface was generally

higher than that of the film covered surface. These results show that the presence of a friction film reduces disc wear during both heated and unheated tests.
Figure 103 shows how the wear rate rose during extended testing under both heated and unheated conditions. This behaviour has been found to be a typical characteristic of friction materials when exposed to a large number of high temperature tests, occurring because the friction material sample was becoming progressively weakened by frictional heating, resulting in an increase in wear rate.
The experiments conducted in part 2 were designed to examine the extent to which the surface layers of a friction material become carbonised during repeated high temperature testing. The results of these tests are summarised in figure 104, where each sample tested was shown to have a reduced volatile content at the surface, the volatile content then rose with distance away from the rubbing surface and into the bulk material. This clearly shows that during high temperature tests the temperature gradient that exists through the sample, results in a corresponding concentration gradient of volatiles through the thickness of the friction material. Comparing the weight loss profiles of each of the samples tested, it is evident that the effects of frictional heating increase as samples are exposed to high temperatures for longer periods. These findings support the hypothesis that frictional heating causes a rise in wear rate in friction materials with increasing exposure to high temperatures, as illustrated in figure 103.
This effect is known to occur in brake pads in service, Harding [40], performed a study into the operational wear life of brake pads, in an attempt to model and so predict the ultimate wear life of friction materials when in use. He found that the ultimate life actually achieved was considerably less than that predicted from the model, and it was suggested that one reason for this was the fact that brake pads tend to exhibit an increased wear rate as their thickness decreases. This observation can be explained by the findings reported above, where the wear rate of a friction material increases as more tests are performed (or put another way "pad thickness decreases"). The explanation for this being that the material suffers increasing thermal degradation with increasing exposure to high temperatures, leading to an increase in wear rate.

4.4.5 Conclusions

1) The wear rate of A1 friction material was very low during unheated testing irrespective of the presence of a friction film on the disc surface. However, the presence of a friction film did reduce disc wear, especially under unheated test conditions.

2) Weight loss profiles of the first 750μm from the rubbing surface of friction material samples, showed that a weight loss gradient existed, between the rubbing surface and the bulk friction material beneath. Weight loss was found to be highest from the bulk samples, which then gradually reduced towards the rubbing surface, being lowest in samples of wear debris. This effect was caused by the thermal gradient which exists between the rubbing surface and the interior of the friction material. The high temperatures generated result in thermal degradation resulting in weight loss as the volatiles produced by the degradation escape from the material.

3) TGA studies of the surface layers of tested samples showed that friction material samples which had been subjected to high temperature tests more often, underwent a greater degree of carbonisation, resulting in the thermal damage of a larger volume of the remaining friction material, extending from the rubbing surface further into the sample bulk. These findings support the ideas put forward in (4) below, to explain the increased wear rates found in samples which have been repeatedly exposed to high temperature tests.

4) The wear rate of A1 friction material was found to rise after prolonged testing at high temperatures. This behaviour was believed to be due to the cumulative heating effect of repeated high temperature tests, which lead to the thermal weakening of the sample, leaving it more susceptible to heavy wear during subsequent tests. Similar behaviour is also known to occur in brake pad in service.

4.5 Chapter Summary

The preliminary experiments described in chapter 3 indicated that brake fade could be reduced by the removal of the volatile components within friction materials by careful carbonisation up to 800°C. However, such a heating regime weakened the friction material, and consequently the material wear rate was greatly increased. This increase was most severe during high temperature tests. These findings highlighted the need for further research into the relationship between material strength, and the carbonisation heating cycle used. Also a better understanding of how commercial friction materials behave under high temperature conditions was needed, because such knowledge would aid the development of a carbonised fade resistant material with improved wear properties at high temperatures.

The first part of the work presented in this chapter researched the relationship between the strength of a carbonised material and the carbonisation temperature used, and it was found that as the weight loss from samples rose with increasing carbonisation temperature, the flexural strength of the composite was reduced, and at temperatures above 500°C retained insufficient strength to be of use as a friction material. It was quickly realised that the high carbonisation temperatures of 800°C used in the preliminary studies described in chapter 3, where not necessarily needed to improve the fade resistance of a friction material, and a lower temperature of 400°C could be used instead. The use of a partial carbonisation involving a lower carbonisation temperature gave the added advantage of producing a stronger, more wear resistant product. These findings have lead to experiments on partially carbonised friction materials, the findings of which are reported in chapter 5.

The latter part of chapter 4 was directed towards obtaining a better understanding of how conventional friction materials behave during high temperature testing. The study examined the behaviour of commercial materials, namely A1 material, which was designed to be used under heavy duty braking conditions, and A2 material, which is produced for the automobile market, where service conditions are much less severe. It is well known that A1 material is "harder wearing" than A2 material, but the actual reasons for this difference had not been sufficiently expounded.

Heated pin on disc tests revealed that both materials showed a substantial increase in wear rate at high temperatures. This increase occurred at temperatures above 200°C in the A2 material, whereas the A1 material did not show an increase until temperatures of over 300°C were reached. The results suggested that wear was controlled by a thermally activated process, this was substantiated by arrhenius plots of the wear process where a linear relationship was obtained for both materials. The associated activation energies obtained from these plots were as follows:-

5.56 kcal/mole for the A1 material.
2.62kcal/mole for the A2 material.

Repeated testing at high temperatures revealed that there were fundamental differences in the way in which each material behaved. A1 material showed much less disc and pad wear at high temperatures, because a friction film formed on both rubbing surfaces at a temperature of between 277 - 300°C. Once formed this film reduced the high temperature wear of both the pad and the disc. A2 also produced films at high temperatures, but they were not as adherent and were removed during further tests, which allowed the pad and disc to wear more

rapidly. The reason A2 removes its friction film has been shown to be due to its abrasive nature.

The analysis of friction films produced by A1 material showed them to contain not only components found in A1, but also to contain a large proportion of iron oxide, in the form of magnetite (Fe_3O_4). The iron oxide was shown to originate from the cast iron disc surface, and deposited not only on the disc wear track, but also on the rubbing surfaces of the friction material as well. Magnetite is twice as hard as ferritic iron, therefore reducing the wear of the pad and disc.

A further study on A1 friction materials looking at the effects of repeated high temperature tests on wear rate, showed that wear was found to rise in samples after repeated testing at high temperatures. This was attributed to the cumulative effects of frictional heating on the friction material, which caused it to carbonise and loose volatiles resulting in a weaker material, which lead to the increased wear observed. TGA studies showed that samples were indeed becoming heat treated in this way, and that the volatile content of samples existed in a concentration gradient from the sample surface into the material bulk. The effects of frictional heating grew more severe the more often a sample underwent high temperature testing, resulting in a greater loss of volatiles and a steepening of the concentration gradient.

These findings highlight the complexities involved in determining the wear behaviour of friction materials, aside from all the individual effects produced by differences in the physical test conditions, such as sample load, sliding speed, and the temperature of the system, there is also the added consideration of whether the material produces a friction film, and if so what effect it produces, and how long-lasting are these effects. Also the test history of individual samples has been shown to play a significant role in determining the final wear rate of these materials.

The work presented in this chapter has shown that there is a clear improvement in the high temperature resistance in materials which produce thick, stable, iron rich friction films. Film formation could improve the high temperature wear resistance of carbonised friction materials. This behaviour could be encouraged in these materials by the incorporation of iron powders, and the increased use of lubricants to reduce film removal. Such materials have been formulated and tested, the results of which are reported in chapter 5.

Figure 98

Graph showing the drop in the surface roughness or Ra value, during bedding-in of the disc surface, measured parallel to the sliding direction.

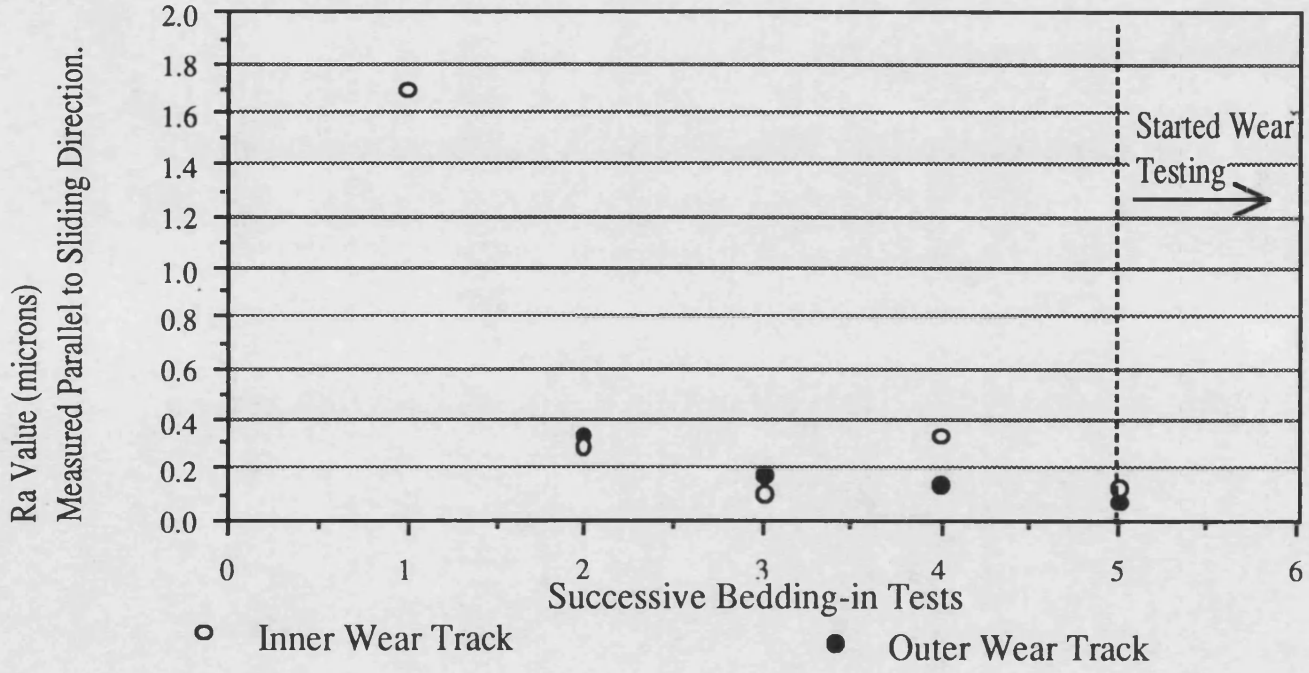

Figure 99

Figure 100

Schematic diagram showing how the friction surfaces of A1 friction material were sampled for T.G.A. analysis.

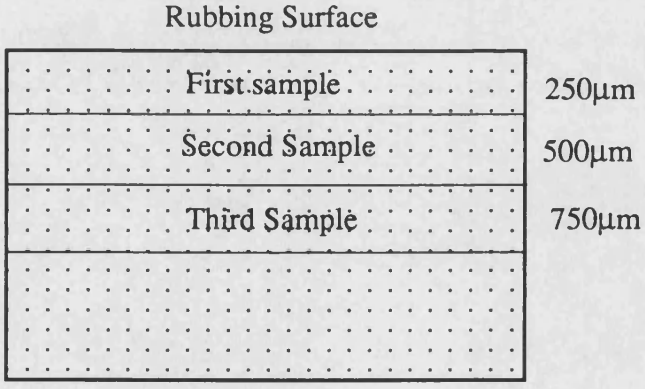

Figure 101

The fluctuation in wear rate of A1 friction material during successive wear tests.

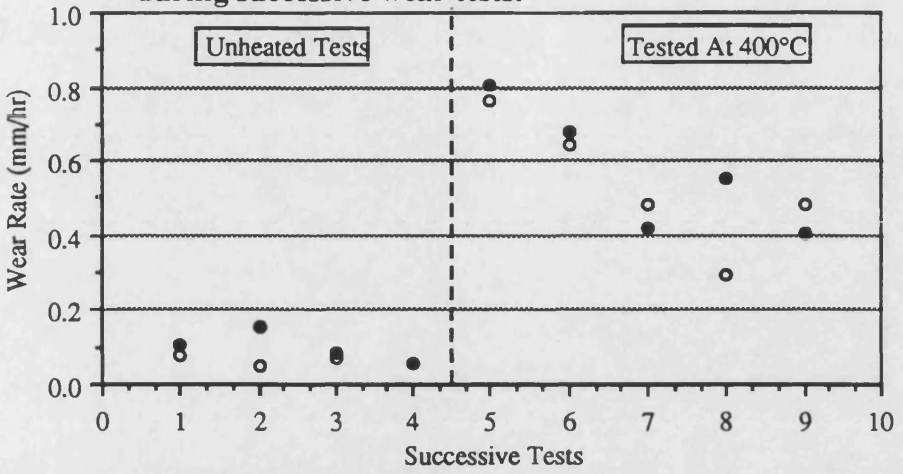

Figure 102

Graph showing the brake disc wear due to successive tests with A1friction material.

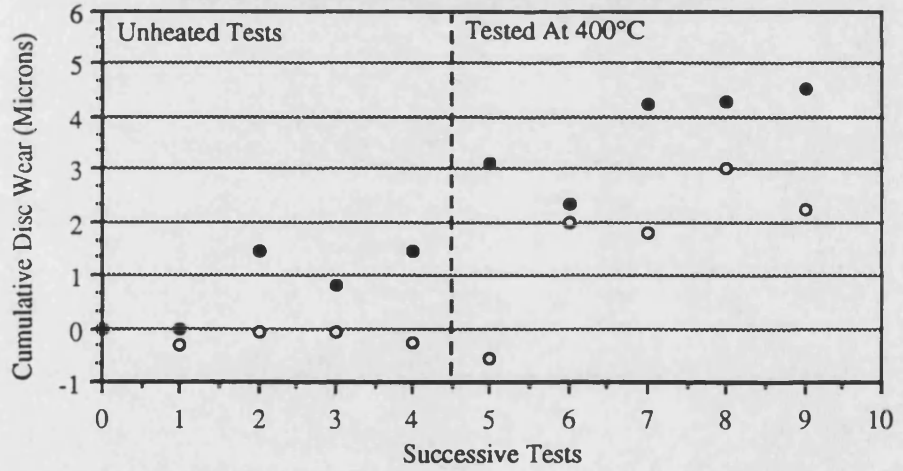

Figure 103

The fluctuation of the wear rate of A1 during successive pin on disc testing.

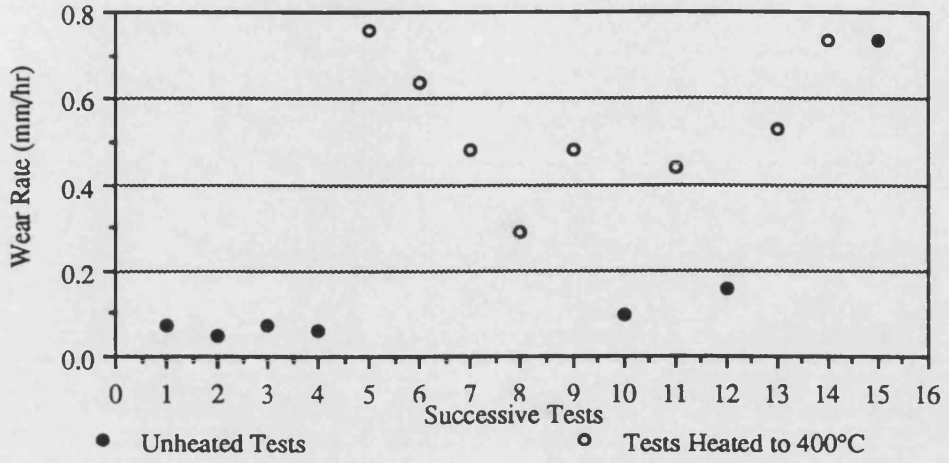

Figure 104

Graph showing how the volatile content in terms of wt loss changes through the thickness in samples of A1friction material which have been tested at high temperatures for different lengths of time.

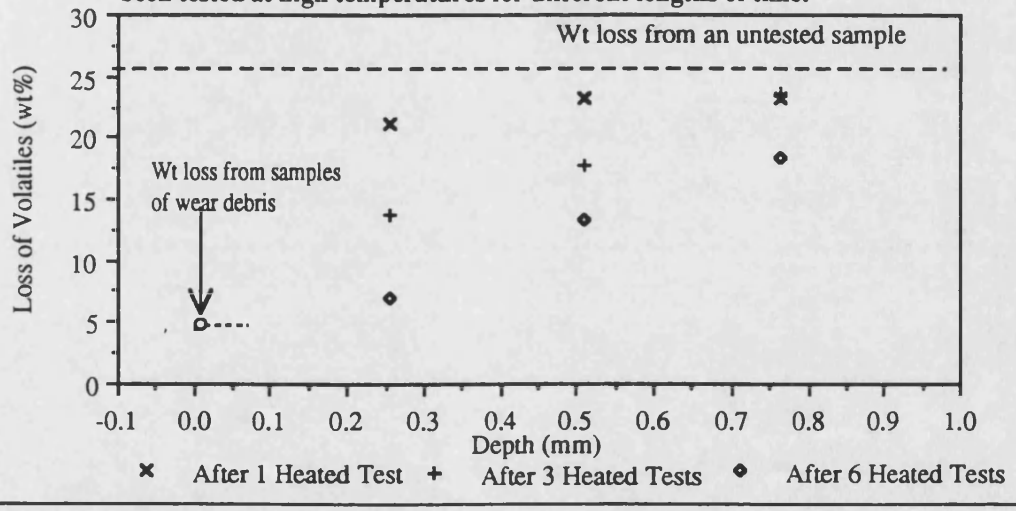

CHAPTER 5

The Development of Improved Friction Materials

5.1 The partial carbonisation of A1 friction material

5.1.1 Introduction

The studies detailed in chapter 3 indicated that the technique of carbonising friction materials to improve their fade resistance had some potential. However, a full carbonisation up to 800°C, which guaranteed the total removal of all volatiles from the friction material, also resulted in severely weakened samples with low wear resistance. Further studies of the effects of carbonisation temperature on material strength reported in chapter 4, showed that a significant proportion of the volatile components within a friction material had been removed in samples carbonised up to 400°C, whilst samples carbonised to this temperature retained sufficient strength to be used as brake linings. The work reported in this section is a continuation of the previous investigation, and examines the tribological properties of samples of A1 friction material which have been partially carbonised to 400°C. The wear behaviour and formation of friction films were studied using a pin on disc wear machine, and as a result of these findings, a full dynamometer test was run on the carbonised material to explore its fade resistant properties.

5.1.2 Methods and materials

i) Heat treatment

Three sets of motorcycle brake pads made of A1 friction material were used as samples for the carbonisation experiments described in this section. The steel backplates were carefully removed before heat treatment, and each sample was post-baked for 6 hours at 150°C, in line with standard production methods. This gave a total of 6 samples of A1 material, each having the following dimensions: 50mm x 35mm x 10 mm. This smaller sized brake pad was selected because conventional automobile pads were too large to fit into the tube furnace used. Carbonisation was conducted under an inert argon atmosphere using the heating schedule outlined in table 9 :-

Table 9 Heating schedule used for the carbonisation of A1 friction material

RAMP	TEMPERATURE
100°C/hr	up to 150°C
50°C/hr	up to 200°C
20°C/hr	up to 300°C
7°C/hr	up to 400°C
4hr Dwell	At 400°C

Each of the samples were weighed and their individual dimensions measured before and after carbonisation, so that weight losses and volume changes due to the carbonisation could be calculated.

ii) Pin on Disc Testing.

Two of the carbonised samples were sectioned into 10mm cubed wear specimens using a diamond tipped circular saw. The carbonised A1 samples were then exposed to a series of pin on disc wear tests, performed at progressively higher disc temperatures similar to those described during the testing and characterisation of conventional A1 samples in chapter 4, section 4.2. In this way the wear behaviour of A1 in the carbonised form, could be directly compared to that of standard uncarbonised A1 material. Optical photomicrographs of the disc wear surface were taken after each test so that any surface changes due to film formation could be monitored and recorded.

iii) Dynamometer Testing

Dynamometer testing is required to fully assess the stability of the friction coefficient of a brake material. A description of the car dynamometer test schedule has been given in section 3.4.2, however, the remaining pairs of carbonised brake pads were tested on a motorcycle dynamometer, where the testing schedule is sufficiently different to warrant a full description of the different test stages as given below:-

a) Bedding Performance.

This test is designed to allow the new set of pads to fully contact with the disc surface while the initial friction behaviour of the material can be assessed. The

test consists of 75 brake stops each from an interfacial sliding speed of 15m/s, (this is equivalent to a stop from approximately 90mph) and an initial disc surface temperature of 150°C. The coefficient of friction (μ) is measured throughout the duration of each stop, so that any 'in-stop' fade, (i.e. the decrease in μ during a stop), can be assessed.

b) Initial Performance.

The initial level of μ for the brake material is assessed at four different sliding speeds, and over a range of pressures. The sliding speeds used are 5, 10, 15, and 20m/s, (equivalent to 30, 60 ,90 and 120 mph) and 8 stops are made from each of these speeds using line pressures ranging from 50 to 400psi. The pressures quoted are line pressures, i.e. the hydraulic pressure delivered to the calliper, and not the pressure on the brake pad. The line pressure values quoted may be converted into pad pressures by the following formula:-

$$\text{Pad Pressure} = \frac{\text{Line Pressure x Piston Area}}{\text{Pad Area}}$$

Where - Piston Area = $1140mm^2$

- Pad Area = $1588mm^2$

c) 1st and 2nd Fade Tests.

Fade and recovery tests each involve the measurement of μ over 32 stops performed in quick succession, from 15m/s, thereby causing the temperature to rise to a sufficient level to induce fade. At stop 24 air blowers are switched on, to provide cooling, allowing the value of μ to return to its original level, this phase of the test is termed the recovery. The entire test is then repeated to give the second set of fade results.

d) Final Performance.

This test is essentially a repeat of test 2, and gives a comparison of the stability of μ after the material has been conditioned during the fade tests.

e) Cold Test.

This test repeats the first 10 stops of the bedding Performance test, so that the cold behaviour of the material can be assessed after the material has undergone fade tests. This is done because the results from the first ten stops during the bedding performance test, were affected by the fact that the sample and disc were as yet not fully in contact, which produces a lower value of μ.

A set of standard uncarbonised A1 motorcycle pads were also tested to provide comparative data, so that any improvement in fade resistance induced by the carbonisation process could be assessed. All the tests were performed using a steel motorcycle brake disc which is the common material used for their construction. The thickness and weight of each pad was measured before and after dynamometer testing, so that the wear rates of each of the materials could also be compared.

5.1.3 Results

i) Heat treatment

All samples were undamaged by the heat treatment, and underwent a negligible volume change, whilst the weight loss ranged between 2.80% and 3.14%.

ii) Pin on Disc Tests.

The results of the pin on disc testing of carbonised A1 samples are shown in figure 105, where the wear rate is plotted against disc surface temperature of each test. The graph also shows the wear rates produced by standard samples of A1 and A2 material when tested under similar conditions. The wear rate of the carbonised A1 sample shows similar behaviour to that of standard A1, with the wear rate remaining fairly stable up to 300°C, and then increasing markedly as the disc surface was heated to 350°C and above.

Figures 106 - 111 are photomicrographs of the disc surface taken after each test, and show how the appearance of the disc wear track changes with increasing test temperature. Figure 106 shows the wear track after a 2hr test where the disc surface temperature reached approximately 150°C by frictional heating alone. The wear track appeared polished with a metallic lustre, and the graphite flakes within the cast iron are clearly visible. During the next test the disc surface temperature was raised to 244°C, and once again the wear track appeared polished with no evidence of any film formation, a typical view of the wear track after this test is shown in figure 107. The dark areas correspond to a roughened surface which scattered light. Figures 108 and 109 shows the wear track surface after the following test, during which the disc surface was raised to 295°C. Evidently a friction film had formed over the majority of the wear track surface during this test, although there were some areas where no film was found, resulting in the bright bands of polished iron seen in figure 108 and 109. In the subsequent test conducted at a disc surface temperature of 350°C, the wear track was completely

covered with a friction film, (see figure 110), and this film was further thickened during the next test at 425°C shown in figure 111.

iii) Dynamometer Testing

The Results of dynamometer testing of both A1 material and carbonised A1 material, are presented together so that the behaviour of each material during the different stages of testing can be compared directly.

a) Bedding Performance.

Figure 112 shows the bedding performance, cold, and initial performance test results for uncarbonised A1 friction material. It can be seen that during the bedding-in process, the temperature rose to approximately 150°C and remained there for the duration of the test, (indicated by the red line on the graph). The blue line gives the average value of μ during each stop, while a square symbol shows the μ value measured at the beginning of each stop, and a circle shows the value of μ measured at the end of each stop. In this way the behaviour of μ during each stop can be assessed. In the A1-uncarbonised material the average value of the friction coefficient rises from 0.25 to 0.35 during the first 12 stops, this increase is due to an increase in the real area of contact between the pads and disc as bedding-in proceeds. These 12 stops were repeated for the same sample after completion of all other dynamometer tests, and the results of this repeat test are shown as "Cold", next to the bedding performance test results. On comparison, it is clear that μ remains fairly constant during the repeat "Cold" test and does not show the increase in μ seen in the bedding performance results. During the following stops the average friction coefficient remained reasonably stable at approximately 0.35. It was also noted that μ generally increased during each stop, going from approximately 0.35 to a maximum of approximately 0.5.

Comparing the bedding performance results for A1-carbonised shown in figure 113, there is a similar rise in the average μ during the first 12 stops, it then remains fairly constant at approximately 0.425 during further tests. The "Cold" test results show a similar behaviour as those for A1-uncarbonised material, where μ remains constant. The in-stop increase in μ for the carbonised material goes from 0.375 to maximum of 0.6.

b) Initial Performance.

The initial performance characteristics of A1-uncarbonised material, and A1-carbonised are shown in figures 112 and 113 respectively. On examination of the results for A1-uncarbonised, there is a drop in the average μ with increasing

sliding speed, from approximately 0.5 at 5m/s to 0.35 at 20m/s. The value of μ remains fairly constant with increasing line pressure for each sliding speed. The same results for A1-carbonised also show a drop in the average μ with increasing sliding speed, from a maximum of 0.55 at 5m/s, to 0.35 at 20m/s. The uncarbonised material shows a greater sensitivity to increasing line pressure, where there is a decrease in μ of approximately 0.1 when the line pressure was increased from 50 to 350 psi, in all but the 20m/s test.

c) 1st and 2nd Fade Tests.

The results of the first and second fade tests performed on each material are shown in figures 114 and 115. Temperature rise is represented by the red line, and in all the tests shown the disc surface temperature rose to a maximum by stop 23 of between 450 and 500°C. During the 9 tests which followed, air blowers were used to reduced the disc temperature to less than 100°C. In the first fade test on A1-uncarbonised (figure 114), the average value of μ started at approximately 0.35 and stayed reasonably constant up until stop 10 after which it starts to fall, the disc surface temperature was approximately 275°C at the end of stop ten. The average value of μ reached a minimum of 0.225 by stop 17, which is attributable to the fade effect. Once the air blowers were switched on, the average value of μ increases to 0.35, this is termed 'the recovery'. The positive difference between the final μ and the initial μ for each stop declines until stop 14 where the correlation then becomes negative, this is termed the "in stop fade". When cooling commences the trend is reversed, and the difference once again becomes positive. The 2nd fade results for A1-uncarbonised shows that the material characteristics have changed. The average coefficient of friction stays reasonably constant throughout the test, at a level of 0.35 - 0.375. Also the in-stop fluctuation is positive during all the stops made, indicating that there was no in-stop fade.

In contrast to the behaviour of A1-uncarbonised, the average coefficient of friction during the first fade test on A1-carbonised (figure 115), remained between 0.375 and 0.4 during the entire test. The in-stop μ fluctuation increased during each stop, showing no in-stop fade as seen in the A1-uncarbonised material. The average μ value during the second fade test also remained reasonably constant, fluctuating between 0.4 and 0.35. The in-stop fluctuation was also all positive.

d) Final Performance.

The results of the final performance test for A1 uncarbonised and A1 carbonised materials are shown in figures 114 and 115 respectively. The average coefficient of friction value for A1-uncarbonised material fell with increased sliding speed,

going from a starting value of 0.45 at 5m/s, to 0.4 at 20m/s. There was also a decrease in average coefficient of friction with increasing line pressure in both materials, falling by approximately 0.075 at each of the sliding speeds used. A1-carbonised showed less sensitivity to sliding speed, where the results for the 10, 15, and 20m/s tests were very similar. The overall drop in average coefficient of friction during the whole test was the same in both materials, and went from 0.45 to 0.325.

Comparing the final performance results with the initial performance results in both materials, there was a drop in the average coefficient of friction value particularly at sliding speeds of 5 and 10m/s. The A1-carbonised material shows less line pressure sensitivity during the final performance test, while the sensitivity of A1-uncarbonised is relatively unchanged.

The weight loss and thickness loss from each pad used in the dynamometer test described, are summarised in the table below.

Table 10

The weight and thickness loss from each pad during dynamometer testing.

Brake Pad	Wt Loss (g)	Thickness Loss (mm)
Left A1-Carbonised	0.677	0.192
Right A1-Carbonised	0.618	0.181
Left A1-Uncarbonised	1.816	0.208
Right A1-Uncarbonised	1.64	0.205

5.1.4 Discussion

The results of pin on disc testing of carbonised A1 shown in figure 105 demonstrated that the A1-carbonised material showed very similar wear characteristics to those of A1-uncarbonised. The micrographs shown in figures 106 -111, indicated that the carbonised A1 material formed a friction film at a disc temperature of approximately 295°C. Similar behaviour was also observed in uncarbonised A1 material.

This suggested that a carbonisation of 400°C, did not significantly effect the wear properties of the material or its ability to form adherent friction films, however, the volatile content of the brake material was reduced by approximately 3%wt. The contents of A1 friction material are listed in table 2 chapter 3, which shows that phenolic resin makes up 12.5%wt of the friction material. If it is assumed that

the entire 3% weight loss was the result of resin pyrolysis, then this translates to a 24%wt reduction in resin content by a carbonisation to 400°C. This figure can be compared with the results from earlier experiments on phenolic resin carbonisation reported in section 3.2 which showed that a maximum loss of approximately 30%wt can be expected from a phenolic resin sample fully carbonised to 800°C, suggesting that a 24%wt loss is reasonable, although probably inaccurate as it is doubtful that all the weight loss was a purely a result of resin degradation. It was thought that the reduced volatile content may well lead to a reduction in fade in this material, and in order to explore this further, dynamometer testing was undertaken.

Figures 112 and 113 show that the behaviour of each material was generally very similar during bedding performance and initial performance testing, the only differences were that A1-carbonised possessed a slightly higher average μ value, which tended to reduce with increasing line pressure, particularly at lower sliding speeds.

When the first 12 bedding-in stops in the bedding-in tests were repeated after all other tests had been performed giving the "cold" test results, it was seen that the average value of μ for both materials was far more stable and did not show the gradual increase found in the first 12 stops of the bedding performance tests. This is because the sample was fully bedded-in by this stage, and so the real area of contact between the pad and disc was constant, resulting in a stable friction coefficient.

The behaviour of the two materials during the fade tests (figures 114 and 115), show important differences. The uncarbonised sample experienced fade during the first test, indicated by a fall in the average value of the coefficient of friction. In-stop fade also occurred during high temperature stops, were the μ value is higher at the start of braking than at the end. During the second fade test on A1-uncarbonised the average value of the coefficient of friction remained relatively constant, and no in-stop fade occurred. This was because the friction material surface had become conditioned by the high temperatures generated at the interface during the first fade test, and consequently the volatile content at the rubbing surface was reduced, leading to a stable level of friction.

In comparison, the carbonised A1 material showed better high temperature stability, and there was no drop in the average value of μ, and no in-stop fade in either test using this material. This result indicates that a significant improvement in fade resistance can be achieved by the partial carbonisation of friction materials.

Both materials showed similar behaviour during the final performance test, where the average μ value for each material fluctuated less than in the initial performance tests. This was due to the conditioning effect of the previous tests.
The weight and thickness loss for each material presented in table 10, shows that the carbonised A1 brake pads had slightly less thickness loss than uncarbonised A1, and only approximately a third of the weight loss, although the carbonised pads had a lower density. This indicates that the carbonised material showed slightly better wear resistance than uncarbonised A1, further confirming that carbonisation up to 400°C, does not adversely affect the wear resistance of friction materials.

5.1.5 Conclusions

1) The wear properties of samples of A1 friction material which had been carbonised to 400°C, were compared to uncarbonised A1, and it was found that both materials possessed similar wear characteristics, indicating that carbonisation up to 400°C did not cause the material to wear any more than the uncarbonised A1. This was further confirmed in the wear results from dynamometer testing.

2) Carbonised A1 showed the same tendency to form a friction film on the rubbing surfaces of the friction pair as shown by uncarbonised A1, indicating that this behaviour was unaffected by the carbonisation process.

3) Dynamometer testing showed that carbonised A1 samples possessed a stable average coefficient of friction value at high temperatures, and did not undergo in-stop fade, whereas uncarbonised A1 showed a drop in the average coefficient of friction at high temperatures, and did show in-stop fade.

4) Although only 3%wt of volatiles were removed by carbonisation to 400°C, it can be assumed that a large proportion of this loss was from the phenolic resin matrix, which translates to a theoretical maximum loss of 24%wt of the resin content of the friction material. This was shown to be enough to produce a marked improvement in the fade resistance of a conventional friction material, and was found to cause no decrease in wear resistance.

Figure 105

Graph comparing the wear rate of A1 friction material which has been carbonised to 400°C, with the wear rates of conventional friction materials, A1and A2.

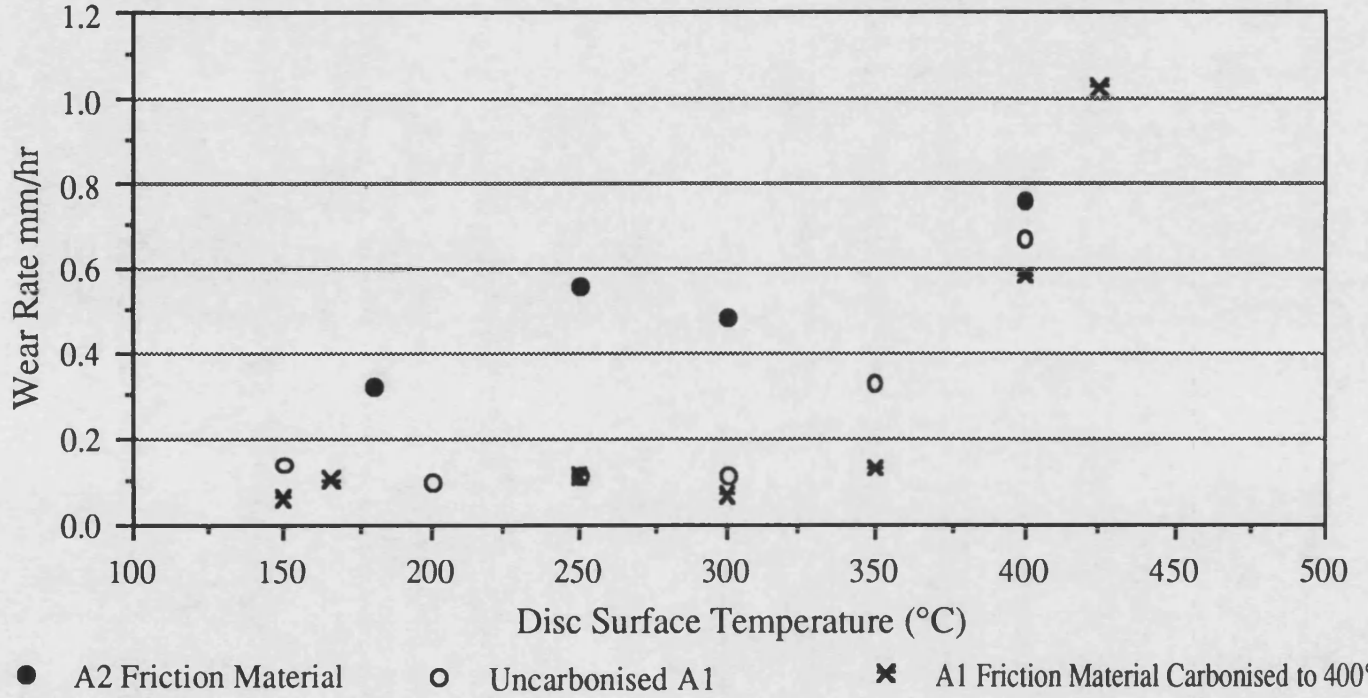

Figure 106
Micrograph of the cast iron disc surface after the first 2hr test using A1 friction material which had been carbonised to 400°C, where the disc surface temperature reached 150°C. The surface appeared polished and the graphite flakes within the cast iron are clearly visible (x200).

Figure 107
Micrograph of the cast iron disc surface after the second 2hr test using A1 friction material which had been carbonised to 400°C, where the disc surface temperature reached 244°C. The surface appeared polished and the graphite flakes within the cast iron are clearly visible (x50).

Figure 109
Micrograph of the cast iron disc surface after the second 2hr test using A1 friction material which had been carbonised to 400°C, where the disc surface temperature reached 295°C, showing a close up of the disc surface in an area which highlights the difference in appearence of film covered areas of disc (x200).

Figure 108
Micrograph of the cast iron disc surface after the second 2hr test using A1 friction material which had been carbonised to 400°C, where the disc surface temperature reached 295°C. Here a large proportion of the disc wear track surface was covered by a friction film (x100).

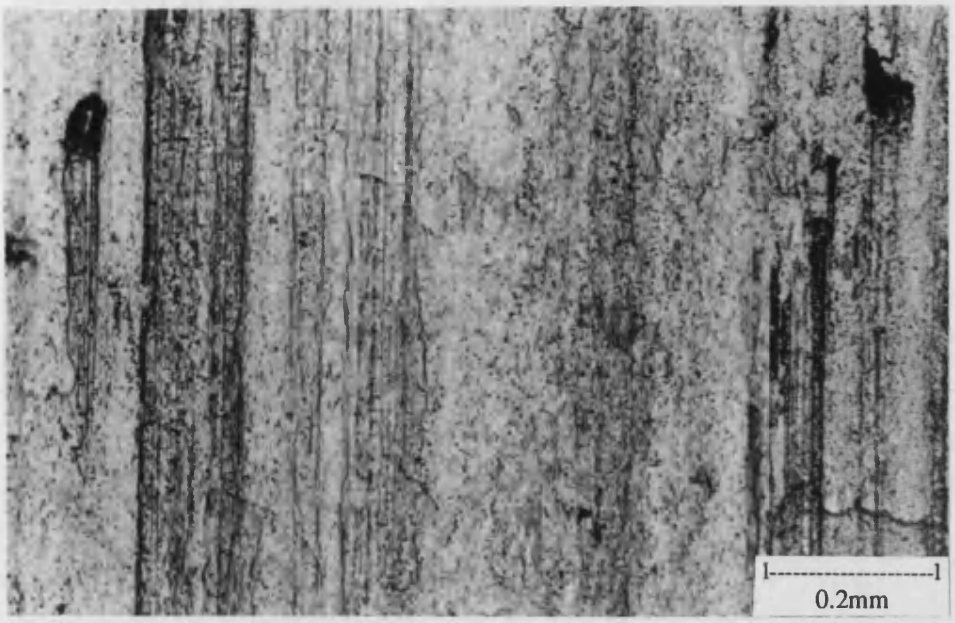

Figure 110
Micrograph of the cast iron disc surface after the second 2hr test using A1 friction material which had been carbonised to 400°C, where the disc surface temperature reached 350°C. At this temperature the friction film becomes more extensive, and completely covers the wear track surface (x100).

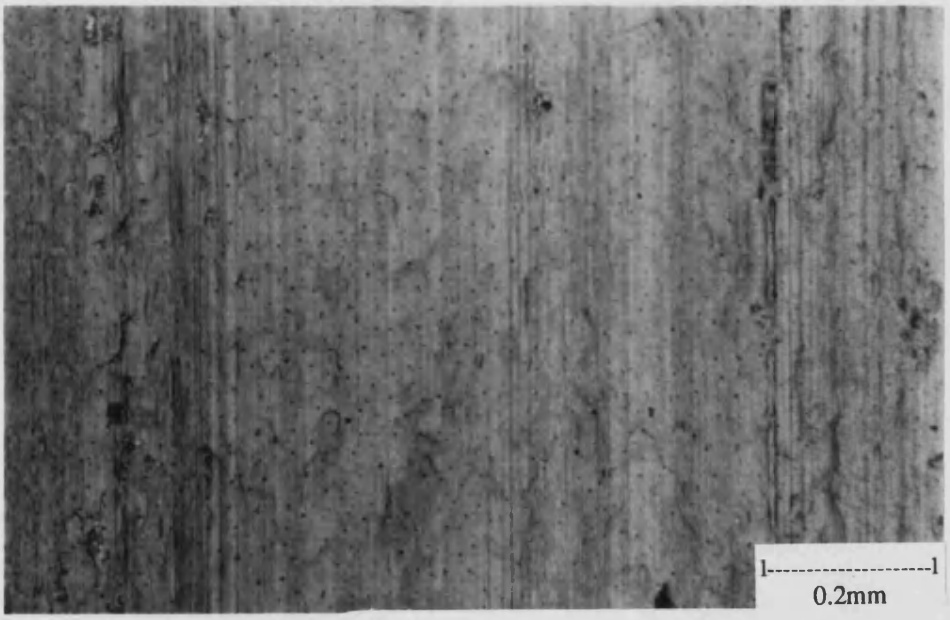

Figure 111
Micrograph of the cast iron disc surface after the second 2hr test using A1 friction material which had been carbonised to 400°C, where the disc surface temperature reached 425°C. This is a typical view showing the thick, adherent film produced at these disc temperatures (x100).

Figure 112

Dynamometer testing of samples of un-carbonised A1 friction material, showing the bedding-in, cold, and initial performance test results.

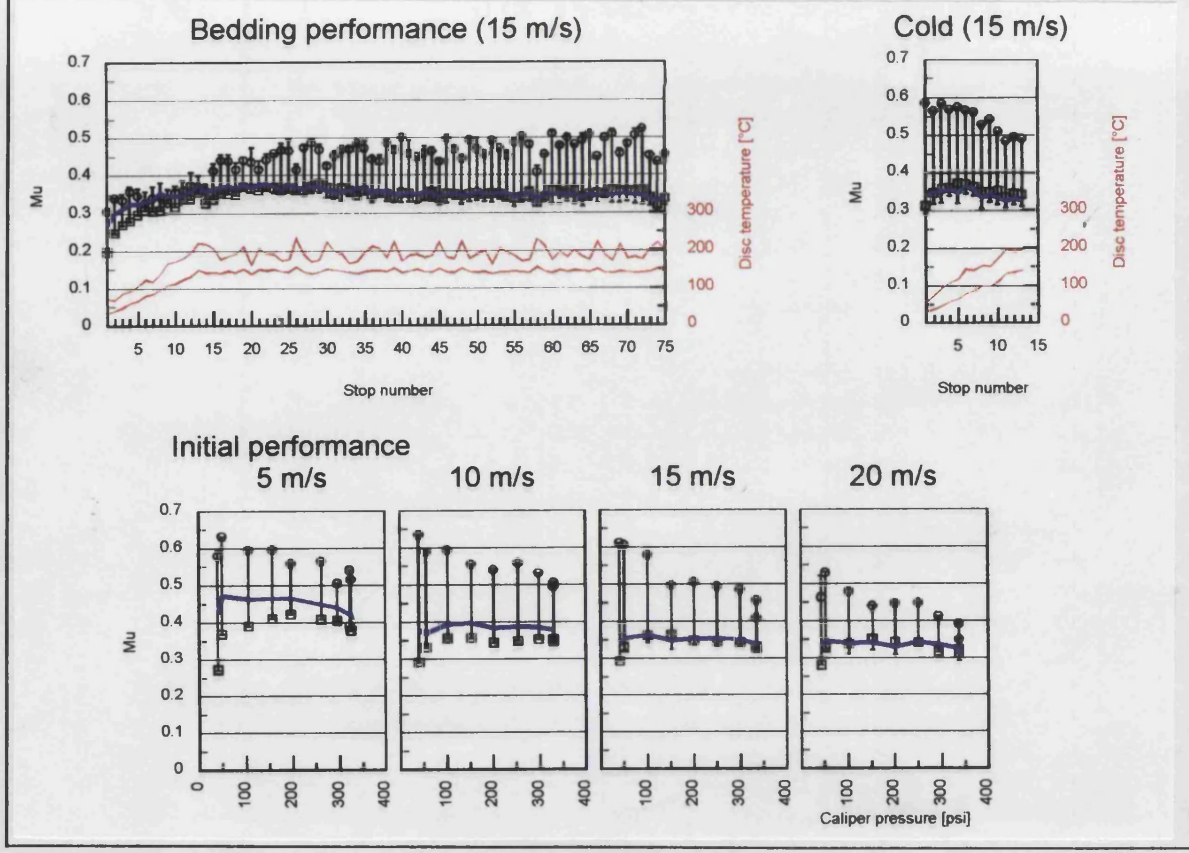

Figure 113

Dynamometer testing of samples of carbonised A1 friction material, showing the bedding-in, cold, and initial performance test results.

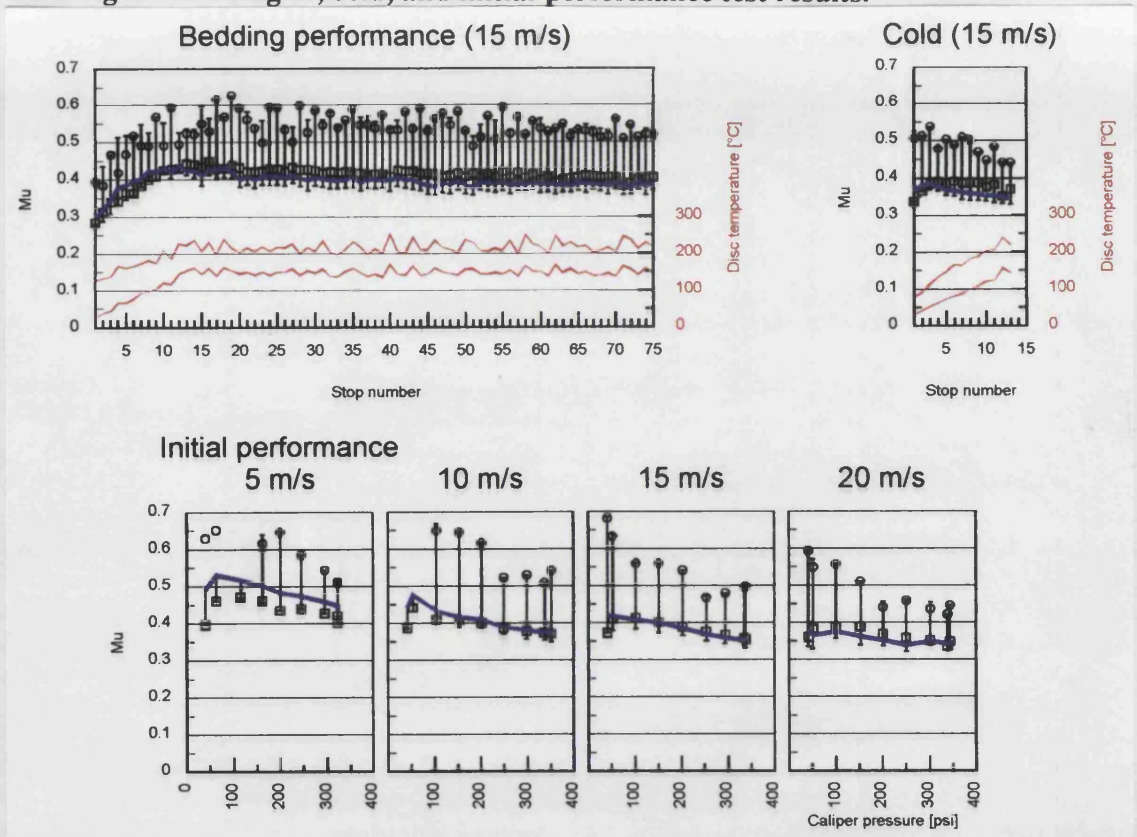

Figure 114

Dynamometer testing of samples of un-carbonised A1 friction material, showing the first and second fade tests and the final performance test results.

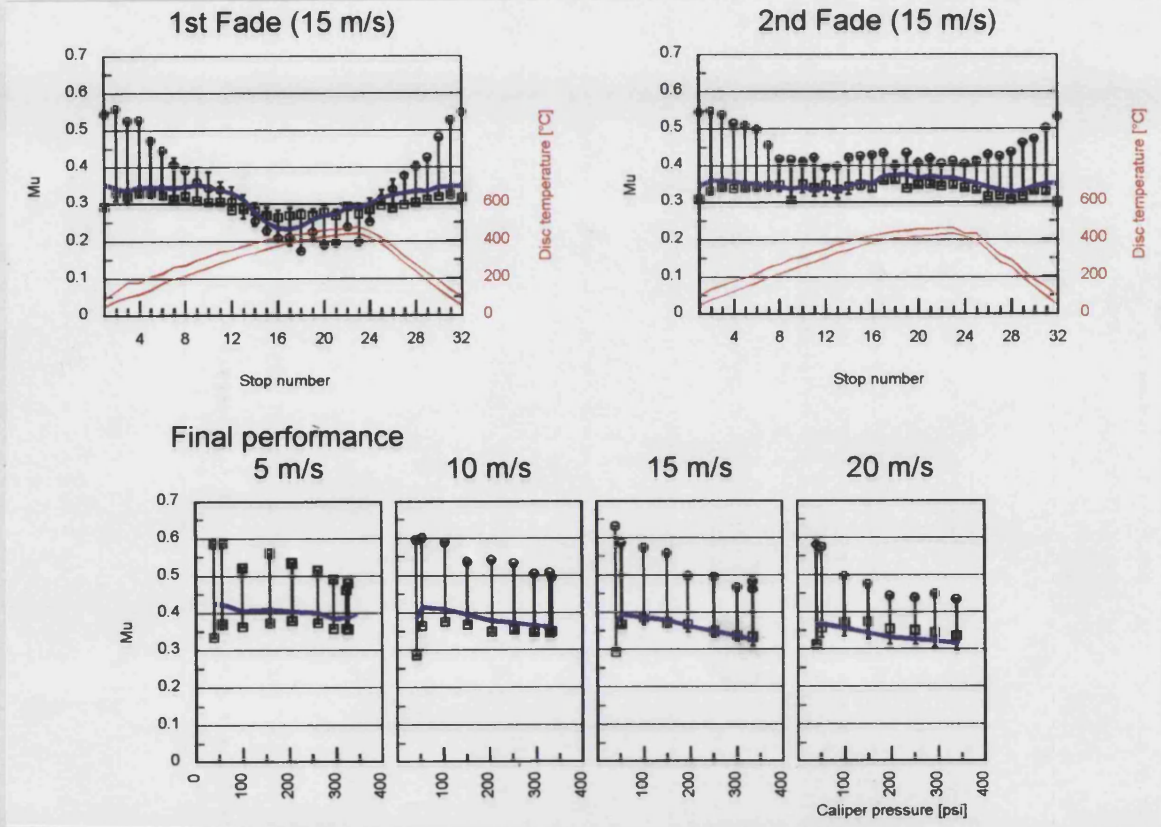

Figure 115

Dynamometer testing of samples of carbonised A1 friction material, showing the first and second fade tests and the final performance test results.

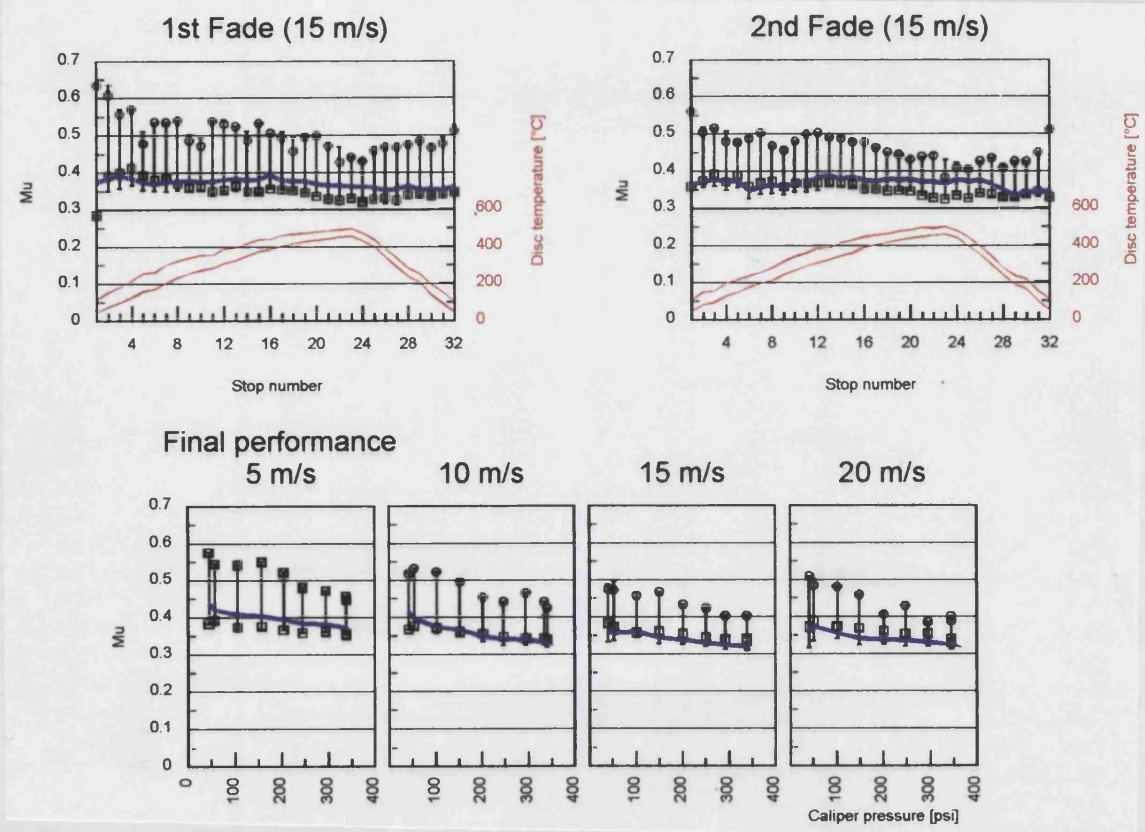

5.2 The optimisation of the carbonisation heating regime.

5.2.1 Introduction

In previous investigations (sections 3.3, 4.1) friction materials were carbonised to temperatures of 800°C involving a very slow heating rate of 7°C/hr. The reason for this was because the build up of gases within the sample bulk were thought to increase internal stresses, and result in a damaged sample with inferior mechanical properties. A slower heating rate would insure that volatiles are released gradually, and have a greater time to escape from the bulk of the sample. In this way thermal stress damage to the sample could be minimised. In Chapter 4 it was shown that a relatively low carbonisation temperature (400°C), produced a pronounced improvement in the fade resistant properties of a friction material, and that a full carbonisation up to 800°C is not necessary. It follows that a lower carbonisation temperature produces less volatiles, which reduces the danger of sample damage, consequently it was felt that the very slow heating rate of 7°C/hr used previously may not be needed during a 400°C carbonisation, where faster heating rates could be used without altering the resulting physical properties of the carbonised samples.

This is important as slow heating rates and long carbonisation times are expensive and too impractical to be incorporated as part of the production process of a commercial friction material, and so the work described in this section investigates the influence of faster heating rates and shorter carbonisation times on the physical properties of the carbonised samples of A1 material.

5.2.2 Methods and materials

a) Carbonisation Heating Rate.

In the carbonisation heating program used in work reported in section 5.1, the slowest part of the process occurs from 300-400°C, which takes place at 7°C/hr. The objective of this study was to use different heating rates for this part of the program ranging from 7 to 30°C/hr, and measure the weight loss, density change, and macro porosity change in the samples produced.

Slabs of A1 friction material were obtained from European Friction Industries and were sawn into blocks of 20.0 x 16.5 x 7.0mm. These samples were post-baked for 6hrs at 150°C in a muffle furnace, in line with standard production methods, and each block was weighed and measured. The samples in groups of three, were given identical heat treatments up to 300°C (table 11), after which they were

subjected to different heating rates during the slowest portion of the heating program (i.e. between 300 and 400°C). The heating rates used were 7, 10, 15, 20, and 30°C/hr. The heat treatments were carried out in a Carbolite tube furnace, under a flowing argon atmosphere.

Table 11 Heating schedule used for the carbonisation of A1 friction material.

RAMP	TEMPERATURE
100°C/hr	up to 150°C
50°C/hr	up to 200°C
20°C/hr	up to 300°C
Differing Rates	up to 400°C
4hr Dwell	At 400°C

After carbonisation the samples were re-weighed and measured, in order to determine weight losses and volume changes. Bulk density and apparent macro porosity measurements were made using the method described in BS 1902, part 1C, 1967, section 10.1 [87]. As this method does not give any indication of the type or size of macropores present, these latter characteristics were determined using the following methods:-

i) Impregnation with potassium permanganate solution [88].
This method establishes whether the macropores within the friction material are interconnected or closed pores. The method involves immersing samples in a beaker of potassium permanganate solution, under vacuum, to allow the potassium permanganate solution to displace air within the macropores of the samples, (Figure 116 {A}). After approximately 40 minutes the beaker was removed from the chamber and placed in a pressure vessel and left under pressure for approximately 18 hours to force permanganate solution into the samples. after impregnation the samples were dried in an oven, so that any potassium permanganate contained within the macro porous structure of the sample would crystallise. Each sample was sectioned through the centre, and mounted in Bakelite, with the sectioned face at the surface (figure 116 {B}). The sectioned samples were then examined using an optical microscope, where a small drop of water was placed in the centre of the sectioned face. Care was taken to ensure that the water drop remained in the centre, well away from the sample edges. If

interconnected macro porosity did exist within the sample, then the potassium permanganate solution would have been able to penetrate to the centre of the sample. This could be detected because the drop of water on the centre of the section will penetrate the underlying macropores and re-hydrate the permanganate crystals, some of which will diffuse from the macropores back up into the water droplet, turning it mauve. In this way interconnected macro porosity can be detected (see Figure 116 {c}).

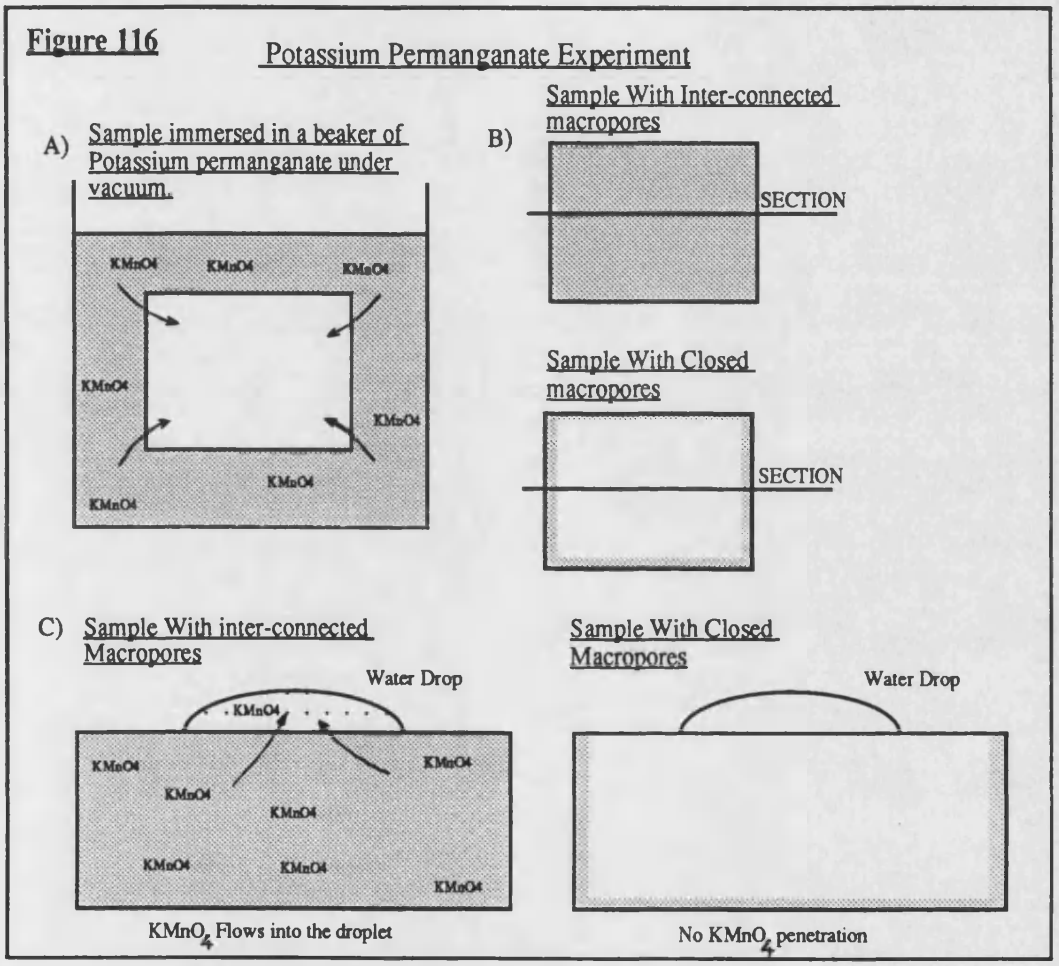

One sample from each group was tested using the method described above, in addition two samples of carbon/carbon brake material, which were known to have inter-connected macro porosity, and two samples of pure uncarbonised phenolic resin which were known to have a closed macropore structure, were examined in the same manner, to provide a control.

ii) Impregnation with florescent resin.

The types of porosity which can occur within a solid are categorised by size. Micropores are characterised by having a width of >2nm, mesopores have a width

of between 2 and 50nm, while macropores possess a width of 50nm or greater. It was important to study any effects that an increased heating rate may have had on the size, shape, and amount of macro porosity of the A1 samples, because macropores are the largest and so will have the greatest influence on the mechanical properties of the samples produced. Also the shape of the pores produced is important as there is a greater stress concentration around a crack shaped pore, than round a spherical pore, which will strongly affect the strength of the material.

The macropores that exist within a sample can be viewed by impregnating the sample with resin containing a U.V. florescent dye. Once the samples have been dried they are sectioned and the macro porosity revealed under U.V. light using an ultra-violet microscope. In this way the pore structure of different samples can be examined and compared.

The method for the impregnation and sectioning of the florescent samples was the same as that for the potassium permanganate samples described above. Impregnation was performed initially on samples that had been carbonised at 7°C/hr and at 30°C/hr, as any differences in macro porosity due to the heating rate used would be most apparent in these samples.

b) Carbonisation Dwell Time.

During previous carbonisation heating schedules,(section 3.3, 4.1, and 5.1), samples were heated to 400°C and then held at that temperature for some hours. The time at temperature is termed the dwell time. The work in this section was directed towards examining how different dwell times affect the final properties of the carbonised samples. 14 blocks of A1 brake material were prepared with dimensions of 20.0 x 16.5 x 7.0mm. All were post-baked for 6hrs at 150°C, and carbonised to 400°C as described in (a) above, (with a heating rate of 7°C/hr between 300 and 400°C). Once 400°C was reached the samples were allowed to dwell for 0, 5, 10, 20, 30, 50, and 70 hours. After each dwell time three samples were removed from the furnace for weight loss, volume change, bulk density and apparent macro porosity determination.

5.2.3 Results

a) Carbonisation heating rate.

Figure 117 shows the weight losses from each sample for heating rates ranging from 7°C /hr to 30°C/hr. There is a negligible difference in weight loss between the samples, indicating that the heating rate between 300 and 400°C has no effect on the weight loss. Also, no measurable volume change occurred in any of the

samples tested, indicating that the final density remained unaltered by the different carbonisation heat treatments used. This is confirmed in figure 118 which shows the bulk density of samples carbonised at the different heating rates, where there is negligible difference in the bulk densities of the samples tested, confirming that there was no change in the bulk density due to different heating rates.
Figure 119 shows the variation of the apparent macro porosity in samples carbonised using different heating rates, the percentage apparent macro porosity falls from a maximum of 5.8%, to a minimum of 4.5% in all the samples tested, where there is a slight decrease in percentage porosity with increasing heating rate.

Potassium permanganate tests for interconnected macro porosity, were firstly performed on the carbon/carbon brake materials, and pure phenolic resin control samples. A strong colour change occurred in the carbon/carbon samples as expected from a material with interconnected macro porosity, whereas no colour change occurred in the pure phenolic samples, because the sample contained only closed macropores. All of the A1 samples showed no colour change indicating that the material possesses only closed macropores.
Fluorescent resin impregnated samples of A1 were also sectioned and examined. It was found that the resin only penetrated the surface of each sample by a maximum of 0.5mm. There was no apparent difference in the size, amount, and structure of the macro porosity of samples carbonised at 7°C/hr, compared with those carbonised at 30°C/hr, suggesting that a faster heating rate had no appreciable effect on the resulting sample macro porosity. The pores present were generally spherical in nature, and had a maximum size of approximately 10μm.

b) Carbonisation Dwell Time.

Figure 120 shows the effect of increasing dwell time on the weight loss from samples of A1 friction material. It is apparent that there is negligible difference in the weight losses which occurred in any of the samples. Clearly increasing the dwell time had no discernible effect on the weight loss obtained from samples of A1 over the range of times tested. The samples also showed negligible change in dimensions or volume, suggesting that the density of the samples also remained unaltered. Figure 121 shows the bulk density of each sample after carbonisation. The results show some scatter, but there is no clear difference in the bulk densities of any of the groups of samples tested. This further confirms that the carbonisation dwell time had a negligible effect on the density of the A1 samples tested.

Figure 122 shows the effect of increasing the dwell time on the apparent macro porosity in each sample. The results do show a slight increase in macro porosity with increasing dwell time, rising from a minimum of 4.5% in samples which have been carbonised using no dwell, to a maximum of 6.5% after a 70hr dwell, although this effect may be due to natural scatter produced by such measurements.

5.2.4 Discussion

It is clear from the results presented that the use of faster heating rates during carbonisation has a negligible effect on the weight loss from samples of A1 friction material, where the weight loss was found to be approximately 3%wt. There was also no change in volume during carbonisation in any of the samples tested and from these results it follows that there was no difference in density between any of the carbonised samples. This was confirmed in the results from measurements of the bulk density. The results of potassium permanganate tests indicated that the carbonised samples contained only closed macropores, or if interconnected porosity was present the pore size was very much smaller than that found in carbon/carbon friction materials. The extent, size and shape of the macro porosity present in samples was unaffected by the heating rate. The apparent macro porosity showed a small variation among samples, where the macro porosity was slightly higher in samples carbonised at the slower heating rates, which could have been a result of the samples remaining at high temperatures for longer periods of time. A similar trend was seen in the figure 122 where longer dwell times lead to a slightly higher apparent porosity. It must also be stressed that the trend is slight and could be the result of scatter within the data. In any event, the macro porosity figures presented can only be assessed in a comparative sense, as it has been shown that A1 material contains only closed macropores, and so the macro porosity measured is not the true percentage macro porosity of the material, but rather a measure of the macro porosity present which is open to the surface of the sample.

The second set of tests which looked at the effects of longer carbonisation times on the amount of volatiles produced at 400°C. It was found that an increase in the dwell time from 0 to 70hrs, made no difference to the sample weight loss. There was also no volume change detected in any of the samples, and no significant difference in their density. Apparent macro porosity measurements showed that there was only a slight increase in macro porosity in samples with longer dwell times, although this observation may have been the result of scatter within the data.

The results described above show that during the carbonisation of phenolic resin based friction materials up to 400°C, the production and escape of the volatile by-products is not a time dependant process, and that further removal of volatiles can only be achieved by increasing the temperature of carbonisation (this behaviour was seen in the studies performed in chapter 4, section 4.1), or by performing the carbonisation in a vacuum environment. This indicates that the diffusion of volatiles from the bulk of the material to the surface is not the controlling factor during the release of volatiles at 400°C. The fact that there was little difference in the apparent density or macro porosity in all the samples carbonised to 400°C, irrespective of the type of heat treatment they received, suggests that the physical and tribological properties of the material are unaffected by the heat treatment used. This indicates that the safe carbonisation of friction materials up to 400°C can be completed in a much shorter time than previously thought possible. This increases the viability of the carbonisation process in terms of its use in industry, because a faster carbonisation would be less costly, and would increase the speed at which the finished product could be produced.

5.2.5 Conclusions

1) The effect of heating rates ranging from 7 to 30°C/hr during the carbonisation of samples of A1 friction material to a temperature of 400°C, had a negligible effect on the resulting weight loss, bulk density and apparent macro porosity of the samples produced.

2) Sample impregnation with potassium permanganate has indicated that carbonised samples of A1 friction material possess only closed macropores, whilst the use of florescent dyes have shown the that the size, shape and extent of the macro porosity was found to be very similar in samples carbonised at a rate of 7°C/hr and at 30°C/hr, further indicating that the macro porosity of samples was unaffected by the heating rate used.

3) Increasing the dwell time of samples carbonised to 400°C was found to have a negligible effect on the sample weight loss, bulk density, or apparent macro porosity.

4) These findings suggest that much faster heating schedules could be used during the carbonisation of friction materials up to 400°C, where such heating rates were previously thought to result in damaged samples with inferior properties. The use

of faster heating rates would result in a substantial saving in terms of the cost and time of production of carbonised friction materials.

Figure 117

Weight loss vs heating rate for samples of A1 friction material during carbonisation from 300 - 400°C.

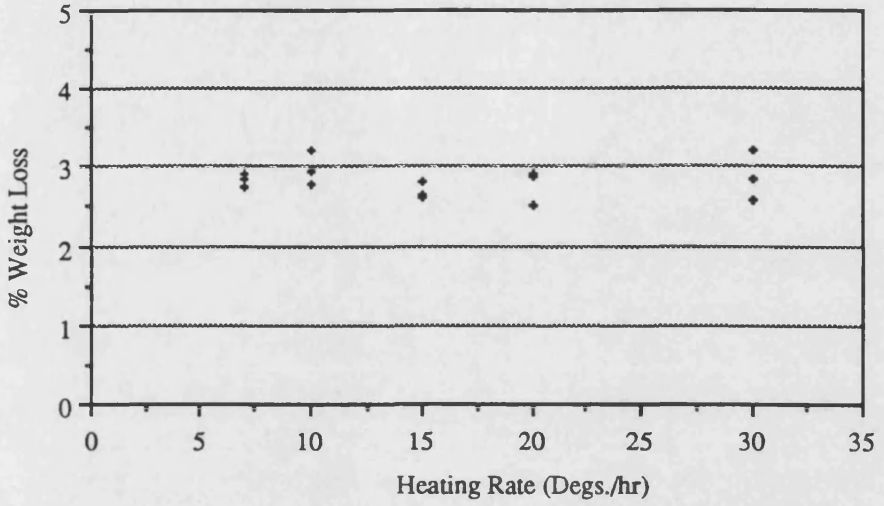

Figure 118

Bulk density vs heating rate for samples of A1 friction material during carbonisation between 300 - 400°C.

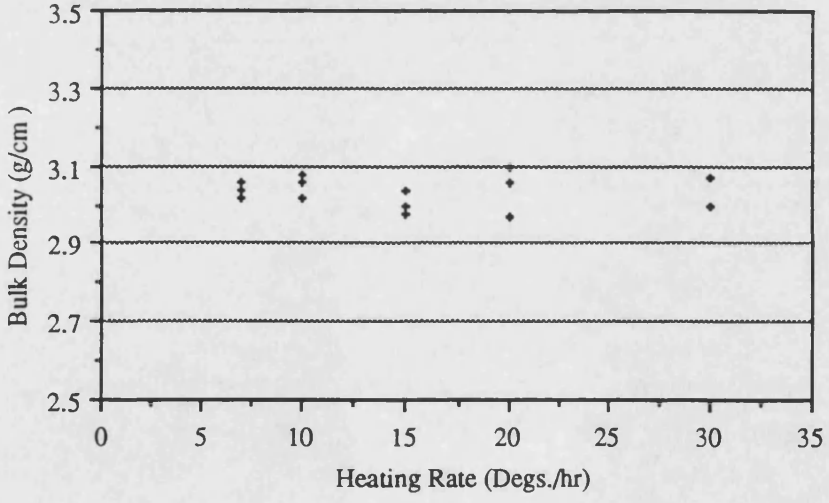

Figure 119

Apparent porosity vs heating rate when samples of A1 friction material were heated at different rates between 300 and 400°C.

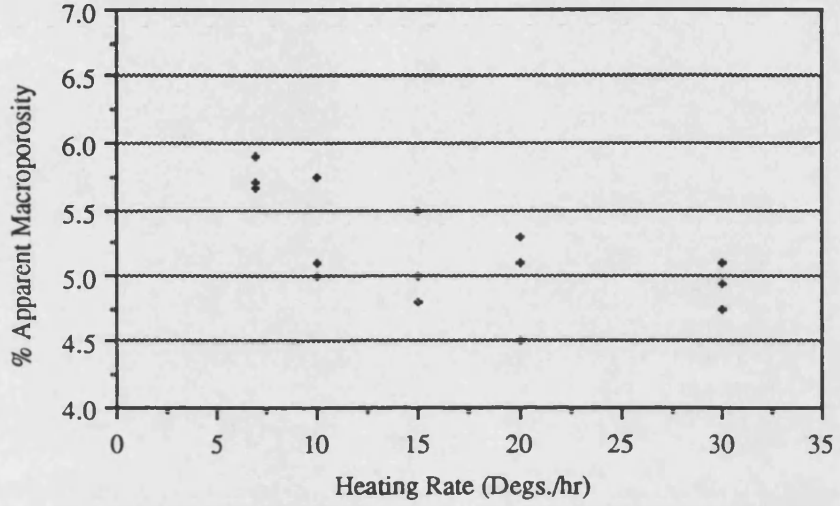

Figure 120

The effect of increasing the carbonisation dwell time on the weight loss from samples of A1 friction material carbonised to 400°C.

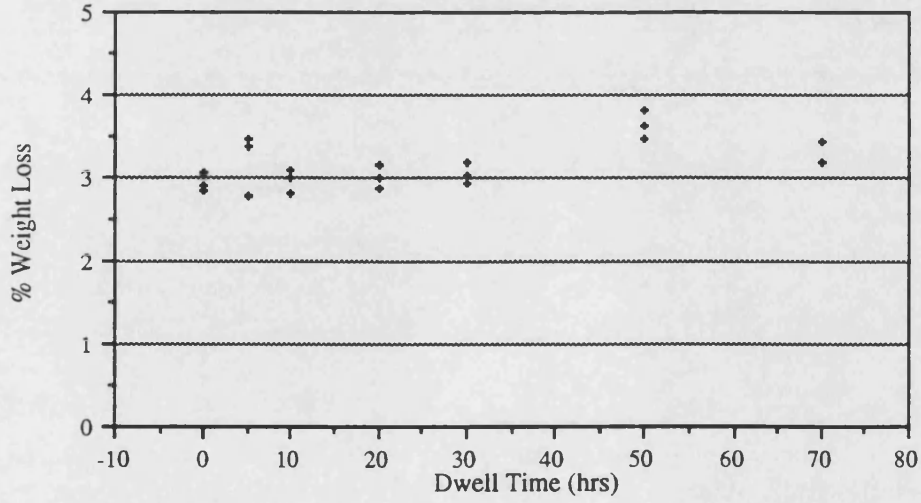

Figure 121

Bulk density vs dwell time at 400°C in samples of A1 friction material carbonised in an inert atmosphere.

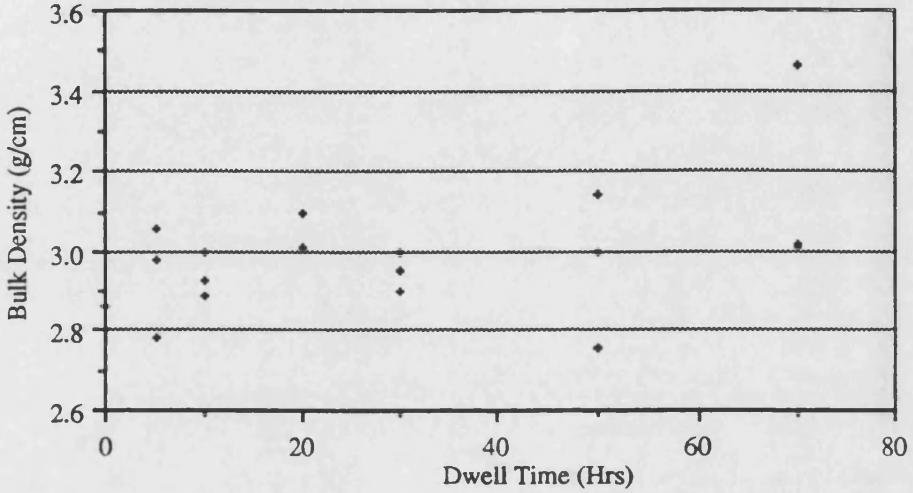

Figure 122

The effect of increasing the carbonisation dwell time on the apparent porosity of A1 friction material.

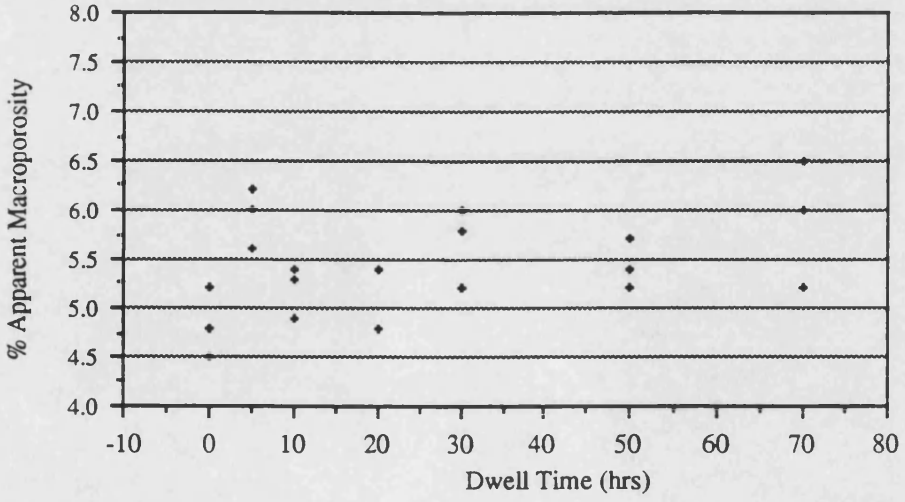

5.3 An investigation into the use of iron powders and high temperature lubricants In friction materials.

5.3.1 Introduction

The work described in this section was directed towards examining how individual constituents affect friction film formation and the overall wear behaviour of a friction material. Friction film formation has been shown to protect both the friction material and the disc surface from excessive wear (section 4.4). Friction films have been shown to contain a significant proportion of iron in the form of magnetite (Fe_3O_4), a hard wearing oxide which originates from the iron in the disc surface. At the end of chapter 4 it was suggested that iron powders could be incorporated into friction materials to encourage the formation of iron rich friction films. This work also highlighted the importance of incorporating lubricants into friction materials, because it was found that friction films were often removed by materials due to inadequate lubrication at the frictional interface. The preliminary study described in this section looks specifically at friction materials which have been formulated from iron powders, and also examines the effects of incorporating different lubricants into these formulations. The tribological properties of each formulation were then examined using a series of pin on disc tests.

5.3.2 Methods and materials.

Three different materials were formulated at the E.F.I. factory, the constituents of which are detailed in table 15 below. Each mix was divided into 150g batches which were then moulded into 152.0 x 25.4 x 10.0mm bars, at a pressure of 2MPa, using a platten temperature of 150°C, for curing time of 6 minutes. The bars were post-baked for 6 hours at 150°C in an oxygen atmosphere using a muffle furnace. Pin on disc specimens ($10mm^3$) were then fashioned from the bars using a diamond tipped circular saw.

Table 15 :The contents of the experimental iron rich formulations

Constituents	Material (X) Wt%	Material (Y) Wt%	Material (Z) Wt%
B.P. Novalac Resin	30	15	10
Sponge Iron	70	60	60
Shot Coke	--------	25	20
CaF_2	--------	--------	10

Sponge iron powder made by a hydrogen reduction process, produces an iron powder with an extremely irregular surface geometry and a large porosity, with an apparent density as low as 1.00 - 2.50 g/cm^3. During moulding of the friction material the irregularly shaped iron particles bond together by mechanical keying, and their porous structure allows resin to penetrate the particles thereby producing a strong composite. Shot coke and calcium fluoride (CaF_2) both of which have lubricating properties, were added to examine the effects of different lubricants on film formation and material wear rate.

Pin on disc testing involved 8 successive tests, each lasting 2hrs, conforming to the standard test procedure described in section 4.2.2. The first 4 tests were unheated, whilst external heating was used to raise the disc surface temperature to approximately 400°C during the last 4 tests. All tests were conducted on the outer wear track using a sample pressure of 2.7MPa, and a sliding speed of 2.06m/s. Before each material was tested the disc surface was conditioned to remove any films and to ensure that the surface Ra value was less than 0.1, in order to minimise any surface roughness effects. This was achieved by running a sample of A2 friction material against the wear track, which effectively removes all existing friction films and at the same time produces a polished disc surface. This process produces a surface which simulates the condition of a used brake disc surface, and is the method of disc conditioning used during industrial testing of friction materials.

5.3.3 Results.

Figure 123 shows the cumulative wear during successive tests for each of the three friction materials examined. All three materials produced visible friction films during the first unheated test. Material (X) wore extremely heavily during unheated testing, and quickly reached the limits of measurement for the test rig,

and as a result the ultimate wear figure is much higher than indicated in figure 123. The same behaviour was shown during the second unheated test on material (X), after which testing on material (X) was ceased. Material (Y) showed much lower wear than material (X) during the unheated part of the test regime, but, suffered very severe wear during the first heated test, which again caused the wear transducer to go off scale. The same behaviour occurred during a second hot test, and so at this point testing on material (Y) ceased. Material (Z) showed very low wear during both the unheated and heated parts of the test regime, although the edges of the test specimen did start to crumble away towards the end of testing.

5.3.4 Discussion

It was noted that all three materials formed a friction film during the first unheated test. This behaviour is not seen in other friction materials, where film formation only occurs during high temperature tests. Therefore, the formation of friction films under comparatively low temperature conditions is unique to friction materials containing a large proportion of sponge iron. It has been shown that conventional 'iron free' friction materials form friction films which contain a large proportion of iron oxide in the form of magnetite (Fe_3O_4), where the magnetite film forms by deforming and oxidising iron which originates from the cast iron disc surface. Fine grey cast iron used for brake discs has essentially a pearlitic structure which has a hardness of 200 - 250 Hv, so high temperature conditions are needed for the deformation and smearing of cast iron. In contrast low temperature film formation is possible in materials containing sponge iron because the iron present is almost pure ferrite, which has a lower hardness of approximately 80 Hv. The pure metal is easily deformed and spreads readily between the two interface surfaces, and so films form at much lower temperatures.

In figure 123 it can be seen that material (X) wore very heavily during the first two unheated tests, whereas material (Y) showed far better wear resistance during unheated tests. This is because material (X) did not contain a lubricant, whereas material (Y) contained shot coke which as a consequence of its disordered graphitic structure acts as a lubricant, thereby reducing the wear of the material. However, material (Y) did wear very severely during the first two heated tests. This is because the lubricating properties of disordered graphite found in the coke particles, are limited by decomposition and oxidation above 500°C [21]. Therefore during a heated test where the disc surface temperature reaches approximately 400°C, it can be assumed that spot temperatures generated at the rubbing interface are certainly several hundreds of degrees higher, which is well

beyond the upper temperature limit for this type of graphite lubrication. Material (Z) showed good wear resistance both at high and low temperatures. This was due to the material composition, which included calcium fluoride as well as the other three materials. Calcium fluoride is an inorganic solid with a lamellar structure and is known to possess a coefficient of friction of 0.1 up to temperatures of 1000°C [21], making it an ideal high temperature lubricant. This explains why material (Z) showed good wear resistance even at high temperatures.
It was noted that the strength of material (Z) degenerated during testing, as samples started to crumble at the edges towards the end of the high temperature testing. This problem would probably be solved by incorporating some fibrous reinforcement into the composite.

5.3.5 Conclusions

1) Friction materials formulated from iron powders were shown to form friction films at far lower test temperatures than conventional friction materials. Friction films are known to contain a significant proportion of iron oxide, which ordinarily forms from iron originating from the brake disc surface. The results suggest that by incorporating sponge iron powders into the friction pad, a more accessible source of iron is available at the sliding interface. Sponge iron deforms and spreads more easily than the harder cast iron, and so films can form at lower temperatures in these materials.

2) Shot coke has been shown to be an effective low temperature lubricant, which reduces the wear of iron based friction materials drastically during unheated tests. However, during tests where the disc surface temperature was raised to approximately 400°C, the lubricating properties of shot coke were no longer effective and heavy wear occurred.

3) The addition of calcium fluoride which possesses lubricating properties at both low and high temperatures reduced the high temperature wear of iron based friction materials drastically.

Figure 123

Cumulative wear data for the three experimental materials (X), (Y), and (Z), during successive pin on disc testing.

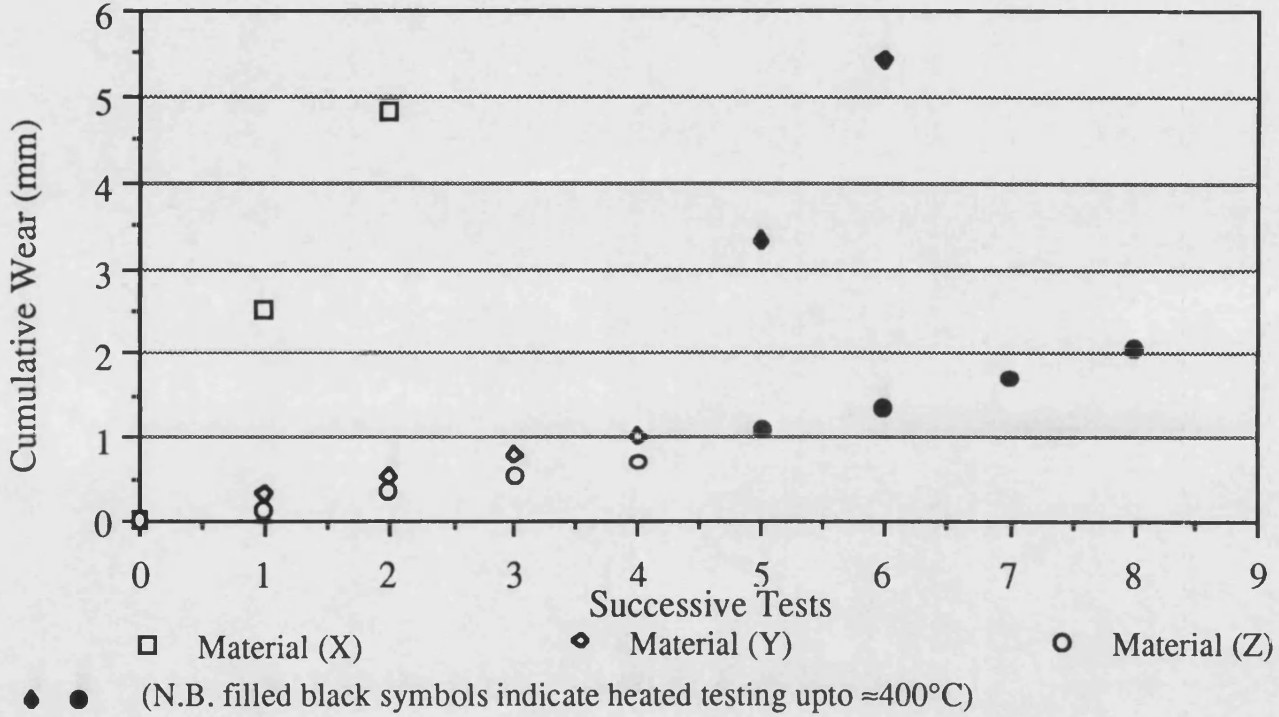

5.4 The tribological properties of carbonised iron based friction materials.

5.4.1 Introduction

A preliminary study of the tribological properties of iron based friction materials was described in section 5.3. and indicated that the incorporation of iron powders into friction materials resulted in the formation of friction films at lower test temperatures. This section of work is directed towards examining the tribological properties of carbonised iron based friction materials. The aim being to produce a friction material with an optimum set of properties, i.e. a material that demonstrates good wear resistance at both high and low temperatures, produces little or no disc wear, and demonstrates superior fade resistance.

Two iron based friction materials supplied by European Friction Industries were examined in this study, and the wear properties of each material was assessed using a series of pin on disc tests conducted at both high and low temperatures. After initial tests, the better of the two materials was carbonised to 400°C. The wear rate of the carbonised friction material and accompanying disc wear were assessed using pin on disc tests, whilst the fade resistance of the material was examined by dynamometer testing.

5.4.2 Methods and materials

i) Pin on disc testing of A3 and A4.

The wear properties of the two iron based materials are examined in this section, and are referred to as A3 and A4. The composition of each material is detailed in table 12.

Table 12 Composition of A3 and A4

Component	A3 (Wt %)	A4 (Wt %)
Phenolic Resin	6	6
Sponge Iron	42	42
Steel Wool	21	15
Shot Coke	21	21
Other Additives	10	10
Graphite Powder	----------	6

Pin on disc test samples (10mm cubes) of each material were prepared. Prior to testing, the cast iron disc was firstly conditioned so that two wear tracks were produced on the disc surface, each having a polished smooth finish, free from any surface films so that both tracks had an R_a value of less than 0.1. This eliminated any disc surface roughness effects, and also gave a surface finish which was typical of a well run-in disc. Figure 124 illustrates the testing arrangement used, where A3 was tested on the inner wear track, and A4 was tested on the outer wear track.

Figure 124

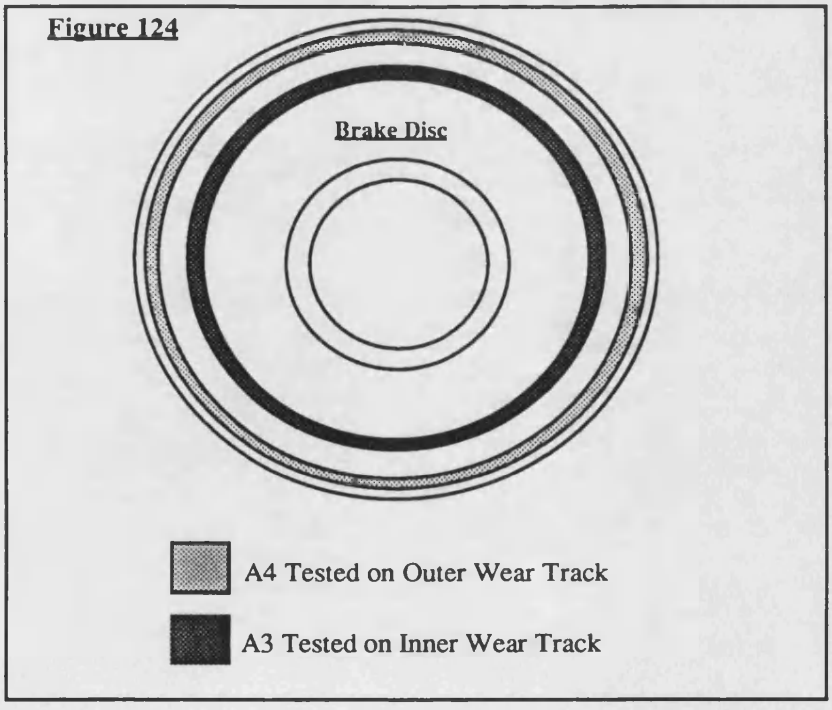

The load and disc r.p.m used during testing were adjusted to allow for the difference in circumference of the two wear tracks, thereby insuring that each test was conducted under the same conditions. The sample pressure used was 2.7MPa, and the sliding speed at the interface was 2.06m/s for all the tests conducted.
Each sample was subjected to 7 test runs, each test was 2 hrs long, and the first three were low temperature tests using no external heating. The following 4 tests were heated tests, in which the disc surface temperature was raised to approximately 400°C. The wear of the friction material and the disc surface were measured after each test in the same manner outlined in section 4.2.2.

ii) Carbonisation and testing of A3 friction material.
Following the initial tests outlined in (i) above, samples of the A3 material were partially carbonised using a Carbolite tube furnace under an inert argon atmosphere. The heating regime used is described in table 13 below.

Table 13 Heating schedule used for the carbonisation of A3 friction material

RAMP	TEMPERATURE
100°C/hr	up to 150°C
50°C/hr	up to 200°C
20°C/hr	up to 300°C
7°C/hr	up to 400°C
4hr Dwell	At 400°C

Pin on disc test samples (10mm cubes) of carbonised A3 were then prepared. The material was then tested using the same test regime and test conditions as described in (i) above.

iii) Dynamometer testing of carbonised and uncarbonised samples of A3.
A Motorcycle dynamometer was used to assess and compare the fade characteristics of both the carbonised and uncarbonised samples of A3 friction material. Two sets of motorcycle brake pads made of A3 were moulded, and one set was then carbonised using the procedure outlined in (ii) above. Each set of pads was then subjected to a full dynamometer test schedule as described in

section 5.1.2. The thickness and weight of each pad were measured before and after testing, so that wear data on each material could be obtained.

5.4.3 Results.

i) Pin on disc testing of A3 and A4.

During the testing of A3 and A4 it was noted that a friction film appeared on the disc wear track after the first test, even though this test was unheated. This behaviour was not found during earlier studies using A1 or A2 friction materials, where high temperatures were required for friction film formation. Figure 125 shows the cumulative wear of A4 during successive tests. There is an increase in the wear rate of the material during the high temperature tests, resulting in a final wear of 3.4mm. Figure 126 shows the resulting disc wear from these tests. The results presented show an interesting feature in that the cumulative wear figures recorded are not always positive, which indicates that after some of the tests the disc wear scar has not deepened but has been filled with friction film. Overall the disc wear figures presented are very low, reaching less than 1 μm after 7 tests.

Figure 127 shows the cumulative sample wear for A3 material, again there is an increase in the rate of sample wear during the high temperature tests as expected, reaching 2.4mm after 7 tests. Figure 128 is the accompanying disc wear for these tests, and shows a similar behaviour to the A4 sample, in that disc wear is very low and is not always positive due to the formation of a friction film. After 7 tests the disc wear was negligible.

Comparing the wear rates of each material, the A3 material shows greater wear resistance, wearing approximately a third less than A4 under the same conditions. For this reason the A3 material was selected for use in the carbonisation experiment described above.

ii) Carbonisation and testing of A3 friction material.

All the carbonised samples of A3 appeared to be unaffected by the carbonisation showing no signs of shrinkage, cracking, or blistering. During pin on disc testing it was again noticed that a friction film formed during the first unheated test, as was found in uncarbonised samples of A3. Figure 129 shows the cumulative wear of the carbonised material during successive pin on disc tests. The results are similar to those of uncarbonised A3 (see figure 127), with 7 tests resulting in a cumulative sample wear of 2.38mm. The cumulative disc wear for carbonised A3 is shown in figure 130, again disc wear is very low with this material, resulting in a final disc wear of less than 1μm after 7 tests.

iii) Dynamometer testing of carbonised A3.

Figures 131 and 132 show the bedding performance, and cold performance test results for both A3 uncarbonised and carbonised friction materials respectively. The average friction coefficient is shown by the thick blue line, whilst the temperature rise is shown by the red line. On comparison, both materials appear to have an average friction coefficient of 0.4. The in-stop change in friction coefficient is shown by the distance between the circular and square marker for each stop. Here there is a difference in the behaviour of the two materials, the carbonised material shows a much reduced in-stop variation in μ, compared to A3 uncarbonised. Comparing the 'cold' test results, the carbonised material shows an average friction coefficient of between 0.4 and 0.45, whereas the uncarbonised A3 pads have a reduced average coefficient of friction of between 0.3 and 0.35.

Figures 131 and 132 also shows the initial performance test results of the two materials. The diagram shows the effect of increasing sliding speed and increasing pressure on the coefficient of friction of each material. Uncarbonised A3 (figure 131) shows a very stable average coefficient of friction, which is affected very little by rising sliding speed or rising pressure at the frictional interface. The average value lies between 0.325 and 0.4. The carbonised A3 (figure132) shows a higher average coefficient of friction of between 0.36 and 0.45. The carbonised material also shows a slightly greater sensitivity to increasing sliding speed, and increasing calliper pressure.

The first and second fade test results for uncarbonised and carbonised A3 friction material are shown in figures 133 and 134 respectively. The disc surface temperature reached approximately 400°C during these tests, as indicated by the red line on the graph. The blue line represents the average coefficient of friction recorded during each test. The carbonised A3 sample (figure 134) shows a very stable coefficient of friction during the first fade test, which remains at approximately 0.4. There is also very little in-stop fluctuation in μ. In contrast the uncarbonised A3 first fade test shows a much greater fluctuation in the average friction coefficient (figure 133), ranging from 0.25 to 0.39. The in-stop fluctuation in μ is also much greater, and indicates that there is a drop in the coefficient of friction within each stop, particularly those conducted at high temperatures. This is known as in-stop fade.

The second fade test on A3 carbonised shows a higher average coefficient of friction, ranging from 0.4 to 0.56. The in-stop fluctuations in μ are all positive, i.e. μ rises showing a maximum at the end of each stop. The stability of the average friction coefficient of the A3 uncarbonised material is much improved during the

second fade test, ranging between 0.3 and 0.35. The in-stop fluctuation in μ is reduced and positive.

The final performance test results for the two materials are also shown in figures 133 and 134. Considering the carbonised A3 material first (figure 134), the coefficient of friction shows a slight fall as the calliper pressure is increased, and generally increases with increasing sliding speed. Overall the average coefficient of friction showed a greater fluctuation than in the initial performance tests, and ranged between 0.36 and 0.5. During the 20m/s part of the test there was an uncharacteristic result at the 300p.s.i. pressure level, which can not be explained at this time. The final performance characteristics of the uncarbonised A3 pads (figure 133) show a very stable coefficient of friction, which is relatively unaffected by increasing the calliper pressure, or increasing the sliding speed. The average coefficient of friction remains at approximately 0.35 for the duration of the test. This is a slightly lower value than the initial performance test results recorded for this material.

Table 14 lists the change in weight and thickness of each pad tested, so that the wear of each material can be compared.

Table 14

The weight and thickness loss from each pad during dynamometer testing.

Brake Pad	Wt Loss (g)	Thickness Loss (mm)
Left A3-Carbonised	2.6	0.63
Right A3-Carbonised	2.8	0.65
Left A3-Uncarbonised	6.57	1.65
Right A3-Uncarbonised	3.33	0.91

From the data listed in the table above it is clear that the carbonised A3 material underwent less wear than the uncarbonised pads during dynamometer testing.

5.4.4 Discussion

It was found that during the initial unheated pin on disc tests with A3 and A4 friction materials, a friction film formed. This behaviour was not seen in any friction materials which did not contain iron powder. This indicates that incorporation of sponge iron into friction materials, aids the formation of friction films, see section 5.3.4.

The disc wear due to A3 and A4 was very much lower than the disc wear generated by other friction materials. Friction film formation has been shown to reduce the rate of disc wear in brake systems (see section 4.2), so the fact that A3 and A4 both develop friction films more readily than other friction materials indicates that the disc surface is covered with a protective film at an earlier stage, thereby reducing disc wear.

It has also been shown that friction films consist mainly of Fe_3O_4, in which the iron component usually originates from the cast iron disc surface during testing with conventional friction materials. It has been shown that the process of film formation can occur more readily if iron rich friction materials are used. This is because film formation can be initiated more easily from the deformation and oxidation of the irregularly shaped particles of sponge iron rather than from a solid cast iron disc for the reasons stated in section 5.3.4. Another important consideration is that the iron particles contained within the friction material are only attached by mechanical keying, whereas detachment of an iron particle from the disc surface, involves the fracture of the metal surface. It follows that less energy is needed to extract the iron particles from the friction material than from the disc surface. These reasons explain why films formed at lower temperatures when iron rich friction materials are used. Also, the fact that friction films formed from iron which originated from the friction material rather than from the disc, explains why disc wear was reduced so drastically.

The A3 material showed superior wear resistance compared to the A4 material. The reason for this lies in the fact that the two materials have slightly different compositions; the A4 contains 6wt% graphite powder, and 6wt% less steel wool. The effect of adding graphite powder was explored in section 3.4, where it was found that a graphite powder addition of 5wt% improved the wear resistance of a friction material, but also resulted in a decrease in the strength and elastic modulus of the material. Both A3 and A4 contain 21wt% of shot coke, which has a disordered graphitic structure. In section 5.3 it has been shown that shot coke acts as a lubricant and reduces material wear markedly at low temperatures, and so the addition of extra graphite would have a negligible effect on the wear rate of a material in this temperature range. However, the addition of extra graphite and the subsequent removal of 6wt% of steel wool, may well have reduced the strength of the friction material resulting in high wear rates under high temperature test conditions where the lubricating effects of coke or graphite are negligible [82, 21].

Pin on disc testing of carbonised A3 indicated that the material behaved similarly to uncarbonised A3, showing a slightly lower sample wear rate, low disc wear, and the ability to form a friction film at low temperatures.
Comparing the dynamometer test results for each material, there was little difference in behaviour of the two materials during the bedding performance, cold performance, and initial performance tests, except that the carbonised A3 material showed a slightly higher μ value that fluctuated less during each stop.

There were important differences in the behaviour of the two materials during the first and second fade tests, in which the carbonised A3 displayed a far more stable coefficient of friction, and showed only a small rise in μ during each stop. The uncarbonised A3 material displayed a lower and more unstable average coefficient of friction, and more significantly, showed a tendency to fade during stops conducted at high temperatures. These results underline the improvements in fade resistance achieved by partially carbonising friction materials to a temperature of 400°C.
The uncarbonised A3 pads showed a marked improvement in frictional stability during the second fade test, because the pad surfaces had become conditioned during the first fade test, which effectively removed the volatiles that cause fade. The carbonised A3 pads showed an increased average coefficient of friction during the second fade test, also as a result of surface conditioning.

The weight and thickness changes reported in table 14 indicate that the carbonised A3 material possessed better wear resistance than the uncarbonised A3 material. These wear figures can be compared with the wear behaviour of carbonised and uncarbonised samples of A1 during dynamometer testing which are shown in table 10 section 5.1. Clearly the A1 friction material wore far less than the A3 material. The reasons for this is that the two materials have different compositions which cause them to behave differently during high temperature braking. The A1 material only forms a friction film at high temperatures, this film contains iron which originates from the cast iron disc surface, resulting in higher disc wear when using A1 material. The A3 material forms iron rich friction films more readily at low temperatures. In this case the iron originates from the friction material, and so the friction material wear rate is higher, and the disc surface wear rate is lower with A3 material.

5.4.5 Conclusions

1) Iron rich friction materials have been shown to produce friction films during low temperature tests. This behaviour is not seen in iron free friction materials.

2) Iron rich friction materials have been shown to produce negligible disc wear. This is due to two factors, firstly the formation of a protective friction film at low temperatures reduces disc wear, and secondly the film forms from iron which originates from the friction material rather than the disc surface, which again lessens the disc wear.

3) A4 showed a higher pad wear rate than A3 because the material contained less steel wool, and more graphite powder, reducing the strength of composite.

4) Pin on disc testing of carbonised A3 material indicated that a partial carbonisation up to 400°C had a negligible effect on the wear behaviour of A3 material.

5) Dynamometer testing of both carbonised and uncarbonised A3 indicated that carbonisation resulted in a material with a more stable coefficient of friction, and superior fade resistance, whilst retaining a good wear resistance.

6) A3 friction material had a slightly higher pad wear rate compared to A1 friction material, but produced much less disc wear.

Figure 125

The change in cumulative wear of A4 friction material during successive pin on disc tests.

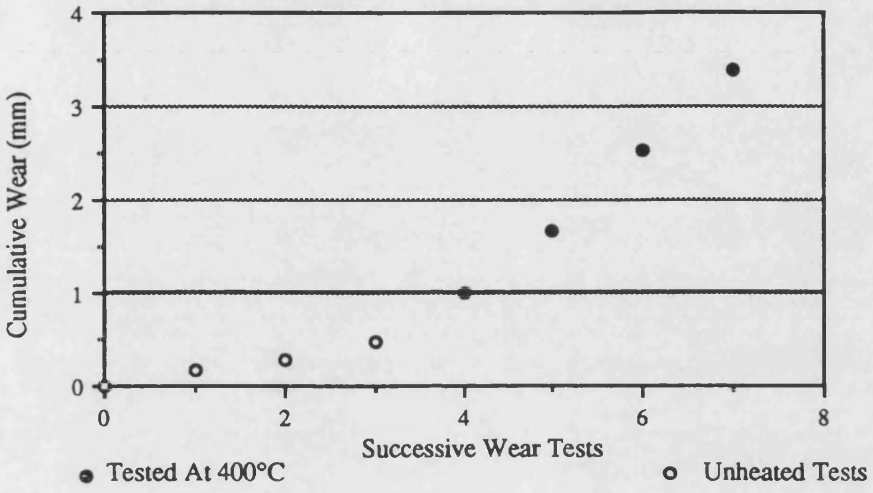

Figure 126

The change in cumulative disc wear due to A4 friction material during successive pin on disc tests.

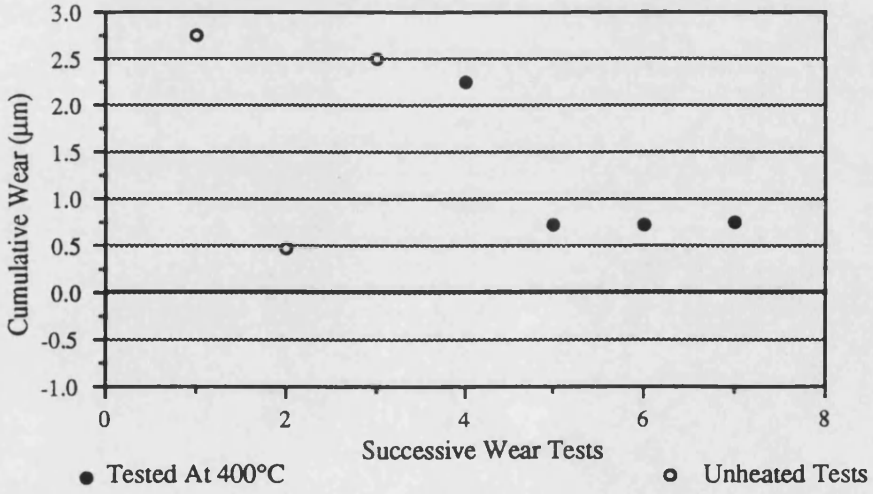

Figure 127

The change in cumulative wear of A3 friction material during successive pin on disc tests.

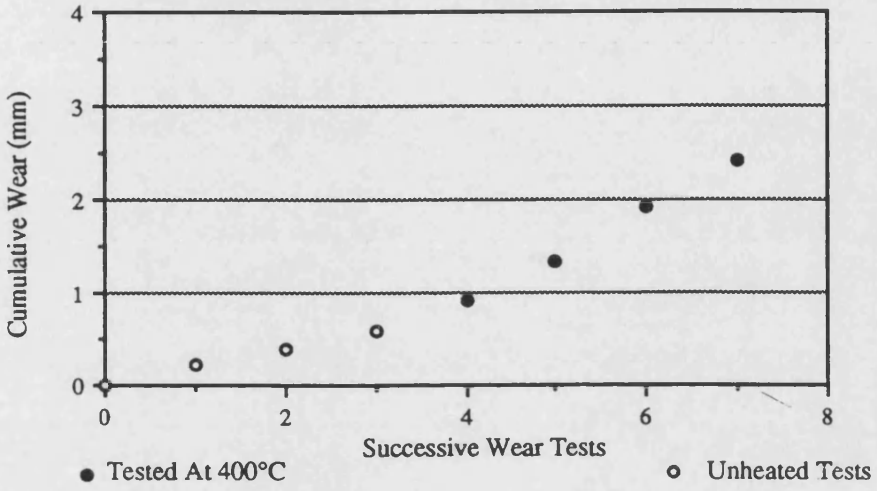

Figure 128

The change in cumulative disc wear due to A3 friction material during successive pin on disc tests.

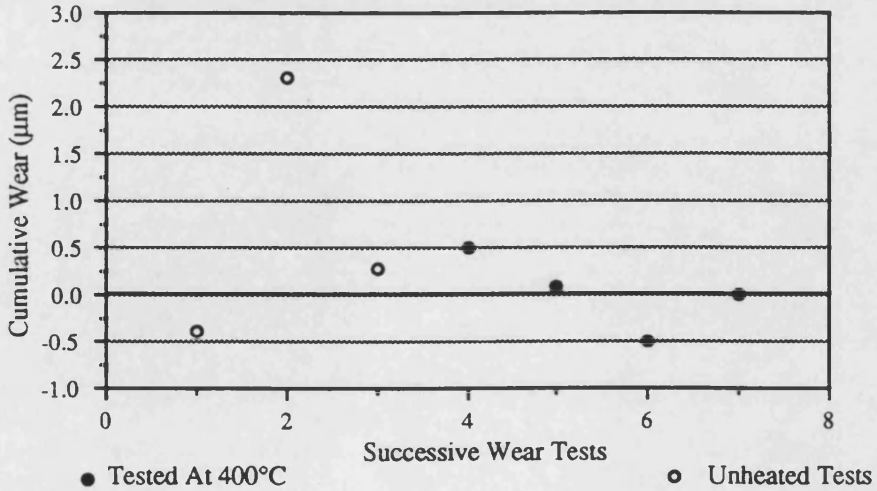

Figure 129

The change in cumulative wear of carbonised A3 friction material during successive pin on disc tests.

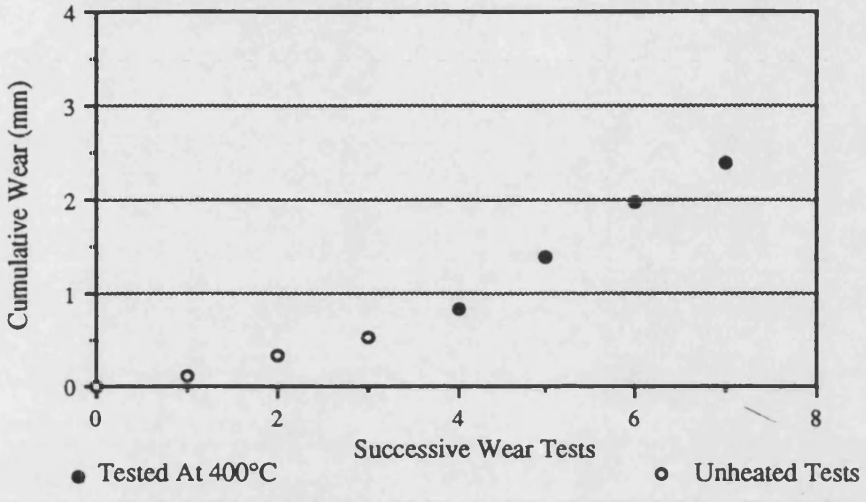

Figure 130

The change in cumulative disc wear due to carbonised A3 friction material during successive pin on disc tests.

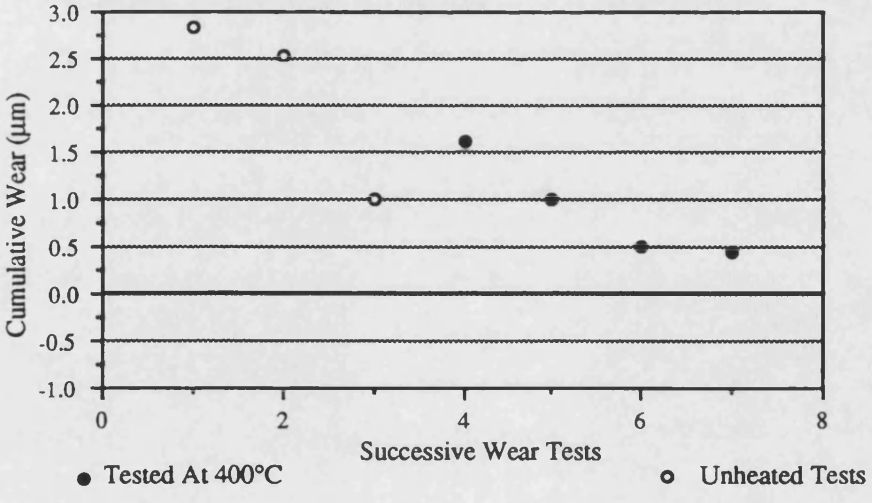

Figure 131

Dynamometer testing of samples of un-carbonised A3 friction material, showing the bedding-in, cold, and initial performance test results.

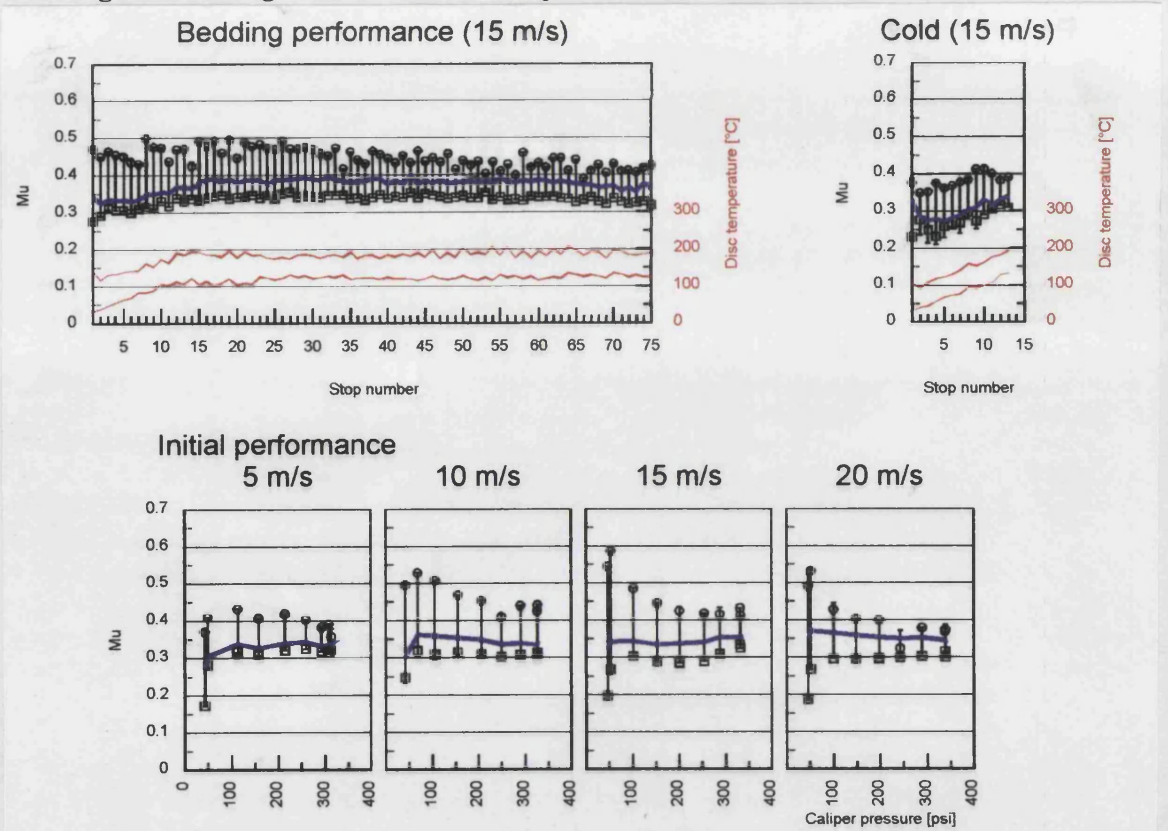

Figure 132

Dynamometer testing of samples of carbonised A3 friction material, showing the bedding-in, cold, and initial performance test results.

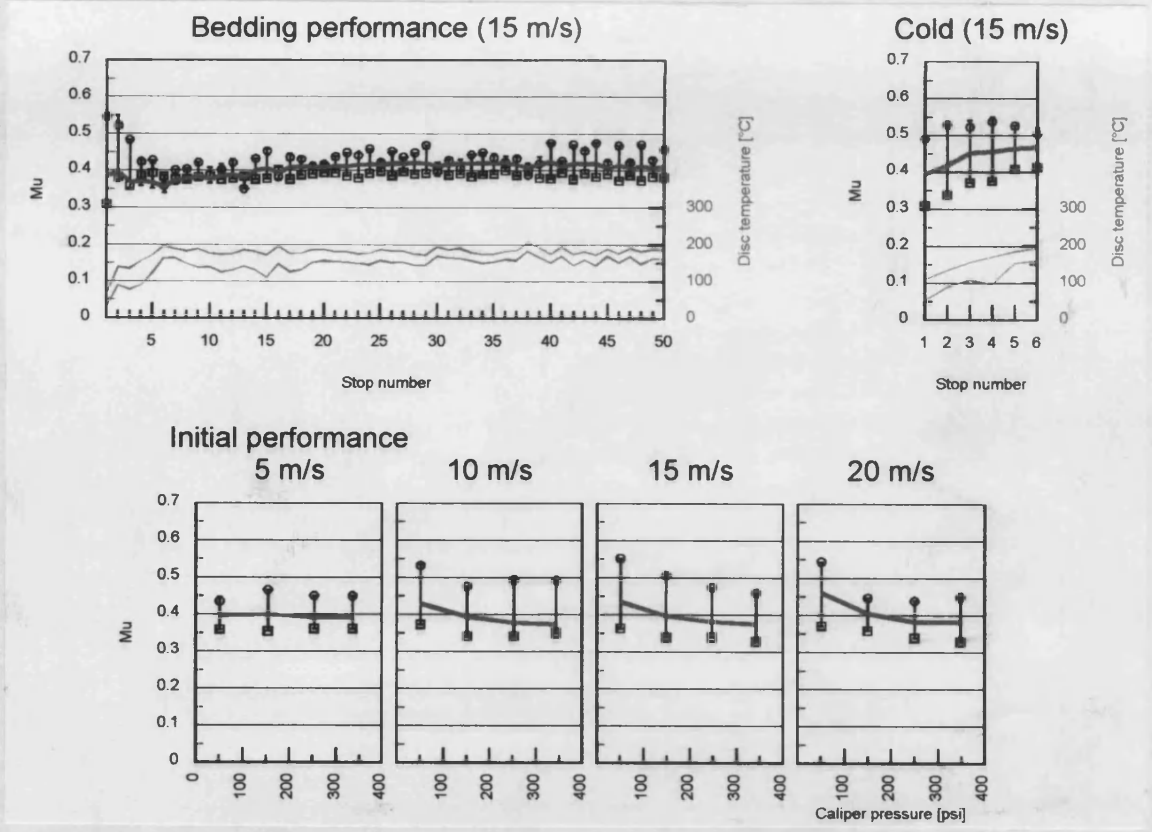

Figure 133

Dynamometer testing of samples of un-carbonised A3 friction material, showing the first and second fade tests and the final performance test results.

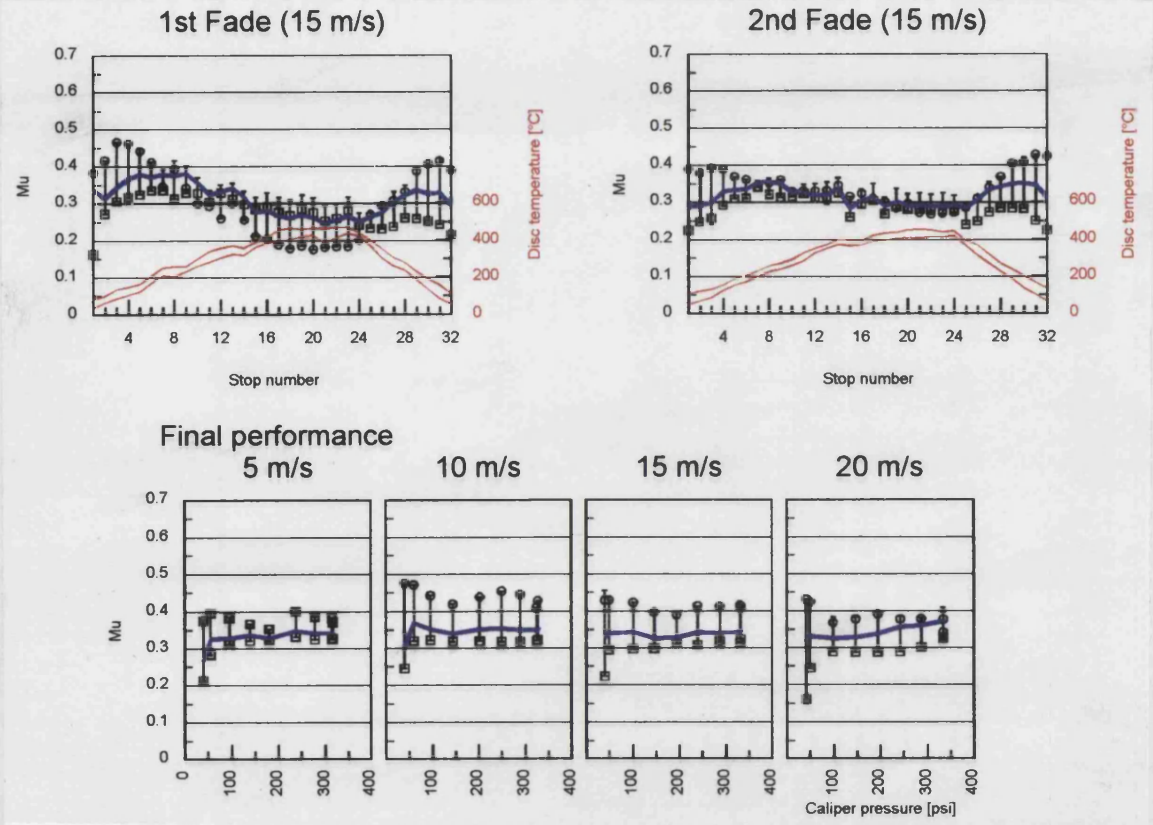

Figure 134

Dynamometer testing of samples of carbonised A3 friction material, showing the first and second fade tests and the final performance test results.

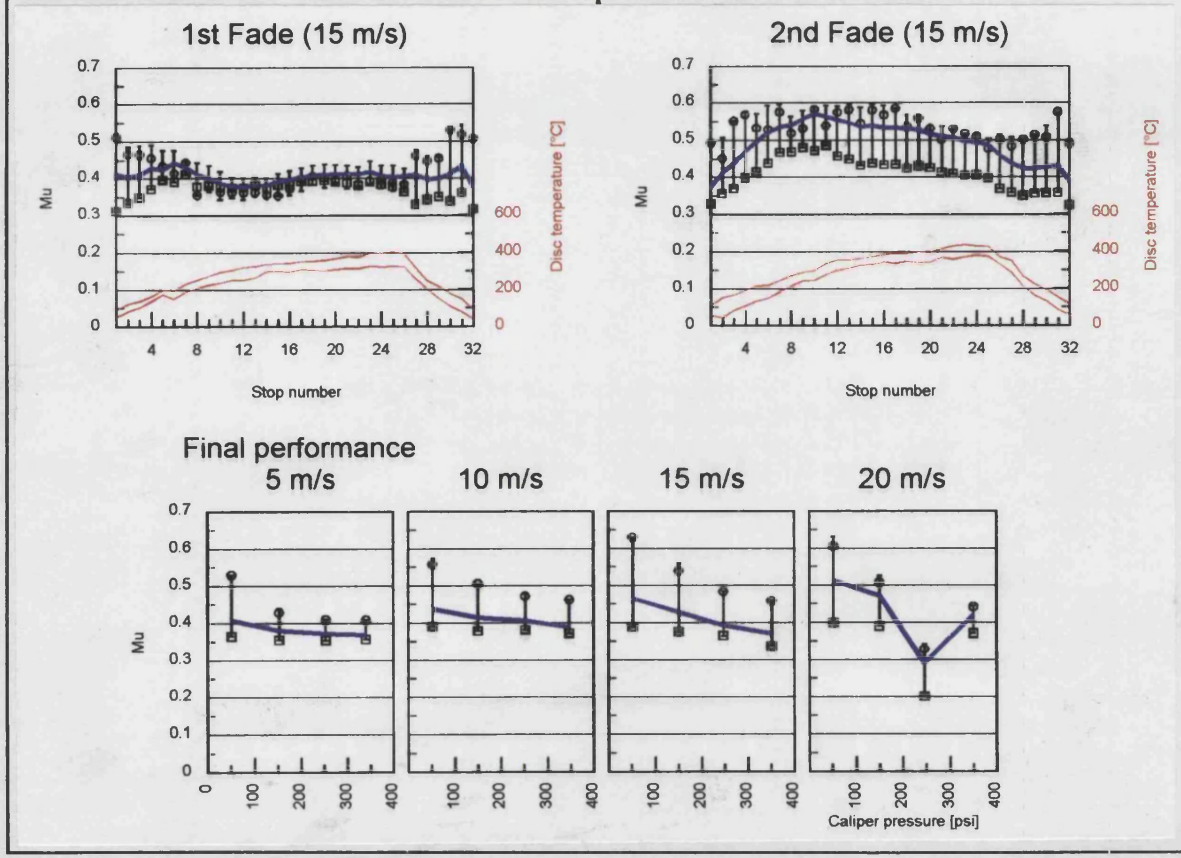

5.5 Chapter summary

In the first part of chapter 5 a hard wearing conventional friction material (A1), was carbonised to 400°C, and the wear behaviour of the material was then compared with uncarbonised A1 using pin on disc tests. Whilst it was found that the carbonisation process had little effect on either the wear rate of the material, or on its ability to form friction films, there was a significant improvement in the high temperature stability of μ the coefficient of friction.

Dynamometer testing revealed that there was also a significant improvement in "in-stop fade", which is characterised by an instantaneous fall in the coefficient of friction of a material when the brakes are applied during each stop. In uncarbonised A1 the in-stop fade was quite severe during stops conducted at high temperatures, whereas the uncarbonised material showed negligible in-stop fade. Carbonisation up to 400°C therefore markedly improves the fade resistance of friction materials.

Carbonising friction materials in order to improve their fade resistance does however increase the cost of production. Early carbonisation experiments used very slow heating rates and long dwell times, as it was thought that if the carbonisation was carried out too rapidly, the friction materials would be damaged. Clearly faster heating rates and shorter dwell times would be advantageous and such possibilities were explored in the experiments described in section 5.2.

A1 friction material was used to examine the effects of raising the heating rate from 7 to 30°C/hr, showed that faster heating rates had a negligible effect on the weight loss, density, and macroporosity of carbonised samples. A similar set of experiments examined the effect of using different dwell times of between 0 and 70hrs during carbonisation, and again it was found that the length of dwell had a negligible effect on the weight loss, density, or macroporosity of the carbonised samples. No increase in the size or amount of macroporosity, or the development of cracks within the sample which would reduce the strength and so affect the wear resistance of the friction material, was observed. These experiments indicated that samples of friction material can be safely carbonised to 400°C, using a heating rate of 30°C/hr, without a dwell at the end of the heating regime. Such a regime would reduce the time taken for carbonisation by 60%.

The problem of high wear rates in carbonised friction materials, especially at high temperatures, led to a detailed examination of the behaviour of conventional friction materials during high temperature tests, the results of which were described in chapter 4. From this work it was found that materials which form stable friction films during high temperature tests were protected from severe wear. These films were found to be made up largely of magnetite (Fe_3O_4), the iron originating from the disc surface. It was suggested that film formation could be encouraged by incorporating iron powders into friction materials, and this led to the study described in sections 5.3 and 5.4 of chapter 5.

During initial studies of three iron based friction materials an important phenomenon was observed. A friction film formed on the disc surface during the first unheated test using each of the three materials. This indicated that films form more readily using friction materials which contain sponge iron. The reasons for this are two fold, firstly the irregularly shaped particles of iron within the friction pad were easier to detach than iron derived from the brake disc. Secondly sponge iron is almost pure ferrite which is soft and can be deformed and smeared into a film far more easily than the pearlitic iron found within the cast iron disc. It follows that lower energies and hence lower temperatures are needed for film formation to proceed in materials containing sponge iron.

This study also highlighted the importance of using lubricants which can operate over the entire temperature range encountered at the frictional interface. Shot coke was shown to be a very effective lubricant under test conditions where the temperature remained below 400°C, but at higher temperatures its lubricating properties diminished. Calcium fluoride was found to be an effective lubricant during both unheated and high temperature tests and resulted in materials with much lower wear rates.

It was apparent from these studies that friction materials which contain iron powders have superior film forming properties, which could be beneficial in reducing the wear rates of carbonised friction materials. This theory was tested with samples of iron based friction materials carbonised to 400°C. The wear properties of the carbonised material were examined using a series of pin on disc tests, and compared with uncarbonised material. It was found that the carbonisation process had little effect on the wear rate of the friction material. Another important observation was that iron based friction materials produced almost zero disc wear, whereas conventional friction materials produced significant disc wear. The main reasons for this were because firstly friction films formed from the iron within the friction pads, rather than by removing iron from the brake disc, and secondly because during any given test, friction materials

containing sponge iron produced a friction film far earlier than conventional friction materials. This meant that the disc surface was covered with a protective film for a larger proportion of the test time, resulting in the lower disc wear produced by iron based friction materials.

Dynamometer testing used to compare the frictional characteristics of carbonised and uncarbonised A3 showed that the carbonisation process resulted in a material with superior fade resistance exhibiting a stable coefficient of friction, negligible in-stop fade, and superior wear resistance compared to A3 in the uncarbonised form.

Final summary

This investigation was directed towards the improvement of the high temperature frictional performance of conventional resin bonded friction materials. An ideal friction material should display a stable coefficient of friction under all conditions. Conventional materials however, often fade at high temperatures, a phenomena characterised by a fall in the coefficient of friction during braking. This effect is potentially very dangerous as it results in a severe loss in braking efficiency. The high temperatures generated at the sliding interface between the brake disc and friction material, cause the organic components within the friction pads (in particular the phenolic resin matrix material), to soften and volatilize near the sliding surface. This effectively lubricates the frictional interface reducing the real area of contact between the pad and the brake rotor, leading to the characteristic drop in friction coefficient known as brake fade. At the beginning of this investigation it was postulated that brake fade could be eliminated by the careful removal of the volatile components which are thought to be the cause of fade. It was proposed that this could be achieved by carbonising conventional friction materials in an inert atmosphere in order to drive off any volatiles present. The majority of volatiles produced emanate from phenolic resin which forms the matrix of friction materials. A detailed study on pure phenolic resin samples showed that during a carbonisation to a temperature of 800°C, the resin samples undergo an average weight loss of 30%, and volume reduction of 35%, and there was also a strong indication that the resulting structure was more ordered. However, when a similar carbonisation regime was applied to conventional friction materials, the high temperatures involved caused some of the other constituents to expand and become reactive. As a consequence the resulting carbonised product was weakened and unsuitable for use as a friction material.

A range of friction materials were formulated from only those constituents thought to remain inert over the temperature range examined. In this way carbonised materials with greater physical strength were produced. Low temperature laboratory pin on disc testing gave promising wear results for these materials, and the results of a full dynamometer test were encouraging indicating that the carbonised material possessed some fade resistance. However the higher temperatures involved in dynamometer testing caused the carbonised material to wear very heavily.

An examination of the relationship between the strength of a carbonised friction material and the carbonisation temperature, showed that as the carbonisation

temperature was increased, the weight loss from the composite increased, and the flexural strength of the composite was reduced, so that at temperatures above 500°C the material retained insufficient strength to be of use as a friction material. However, a lower temperature carbonisation to 400°C was shown to produce a composite with sufficient strength to be used as a friction material. The question was whether a partial carbonisation would remove sufficient volatiles to gain an improvement in fade resistance.

A hard wearing commercial friction material was selected and carbonised to 400°C, and the resulting material was found to possess good strength and toughness. The pin on disc wear machine was modified so that disc temperatures of 400°C+ could be produced. Testing indicated that the carbonisation process had not affected the wear resistance of the material, which showed low wear during both low and high temperature tests. Dynamometer testing confirmed that there was a significant improvement in the high temperature stability of the coefficient of friction of the material compared to uncarbonised samples. This was an important finding, and clearly proved that a partial carbonisation of 400°C was affective in reducing fade in phenolic resin based friction materials.

A large proportion of the work reported was directed towards obtaining a better understanding of how conventional friction materials behave under high temperature conditions. The behaviour of two different commercial friction materials were compared. One material was designed for use as a heavy duty industrial friction material, whilst the other material was intended for use in the automobile market. The industrial material was known to have a better wear life than the automobile material, but the specific reasons for this difference were not fully understood.

Heated pin on disc tests revealed that both materials experienced a substantial increase in wear rate at high temperatures. Arrhenius plots for each material showed a linear relationship, indicating that wear was controlled by a thermally activated process in these materials. Interestingly the wear rate of the automobile material increased markedly at test temperatures above 200°C, whereas this increase did not occur in the industrial material, until the test temperature rose to 300°C+. This difference in behaviour is reflected in the associated activation energies of the two materials, where the activation energy of the industrial material was found to be over twice that of the automobile material, this indicated that the industrial material must be exposed to a higher temperature to cause a thermally induced increase in wear.

Repeated testing at high temperatures revealed that there were fundamental differences in the way in which each material behaved. The industrial material showed much less disc and pad wear at high temperatures, because a film formed on the frictional surfaces of both the disc and the pad during high temperature testing. This behaviour was not seen in the automobile material, where lasting adherent friction films were not produced.

Analysis of the friction films produced on the rubbing surfaces of both the disc and the pad, indicated that whilst they contained many of the components found within the friction material, they were made up largely of iron oxide in the form of magnetite (Fe_3O_4), the iron originating from the cast iron disc surface. The fact that magnetite is twice as hard as pearlitic iron explains why the formation of a film reduced both disc and pad wear. These findings confirmed the importance of friction films in reducing both disc and pad wear, and it was proposed that film formation could be further encouraged by using friction materials with a high iron content. Three such materials were formulated each containing a large proportion of iron powder. Pin on disc testing showed that these materials formed friction films much more readily at much lower temperatures than conventional materials. It was argued that this was because the irregularly shaped iron particles being loosely bound within the friction material, were a more accessible source of iron than the iron of the brake disc. Also iron powder is almost pure ferrite which has a low hardness of approx. 80Hv, and will deform and smear more easily than the essentially pearlitic structure of cast iron having a hardness of 200 - 250Hv. This meant that the extraction, deformation, and oxidation processes involved in the formation of a friction film could occur more easily in materials containing iron powders. It was also found that iron based friction materials produced almost zero disc wear, whereas in conventional friction materials the amount of disc wear produced was significant.

To examine whether the fade resistance of iron based friction materials could be improved by a partial carbonisation, samples of an iron based composite were carbonised to 400°C. The resulting wear properties of the material were examined using a series of pin on disc tests, which showed that the carbonisation process had a negligible effect on the friction material wear rate, the film forming properties, or disc wear. Dynamometer testing confirmed that carbonisation up to 400°C, produced a material with a stable coefficient of friction at high temperatures, showing negligible in-stop fade.

Further studies examined how the wear rate of commercial friction materials was affected by repeated high temperature pin on disc tests. It was found that the wear rate of a sample rose after repeated high temperature tests. This was attributed to

the cumulative effects of frictional heating on the brake material, causing a high degree of carbonisation within the surface layers of friction material. Heated pin on disc tests cause the disc surface temperature to rise to approximately 400°C, and it can be assumed that spot temperatures several hundreds of degrees higher can be generated at the frictional interface between the sample and disc. It has been shown in the work reported in section 4.1 that carbonisation temperatures above 500°C will reduce the strength of a friction material, accounting for the higher wear found in samples which have been repeatedly tested at high temperatures. TGA studies of the surface layers of test samples showed that the volatile content of the surface layers fell as a function of how often the sample had been subjected to high temperature testing. This indicated that the degree of carbonisation of the surface layers of friction materials rose with repeated exposure to the high temperatures generated at the frictional interface, causing their wear rates to increase. A similar effect is known to occur in brake pads while in service, where the wear life of pads increases with use.

The work described highlighted the complexities involved in determining the wear behaviour of friction materials. Aside from the interaction of individual effects produced by differences in the physical test conditions, such as load, sliding speed, and the temperature of the system, there is also the added considerations of whether the material produces a friction film, and also how the wear rate of the material is affected by the test history of the individual sample. These latter properties are dependant on the composition of the friction material, where the use of iron powders and the incorporation of high temperature lubricants can encourage the formation of adherent friction films thereby reducing both disc and pad wear markedly.

Main conclusions

1) The carbonisation of existing formulations of phenolic resin based friction materials to a temperature of 400°C is affective in preventing brake fade during high temperature testing.

2) The use of carbonisation temperatures above 400°C will result in the removal of a larger percentage of volatiles, but are impractical as the resulting composite is then too weak and friable to be of use as a friction material.

3) The wear rate of commercial friction materials was shown to increase as disc temperatures rose above 300°C.

4) Some commercial friction materials formed adherent friction films on the rubbing surfaces of the friction couple during high temperature tests, which reduced the wear of both the friction material and the brake disc.

5) The friction films formed were found to consist mainly of iron oxide in the form of magnetite (Fe_3O_4).

6) The incorporation of iron powders into friction material formulations encourages the formation of iron oxide friction films at low temperatures, resulting in negligible wear of the brake disc surface.

7) Successive high temperature tests have been shown to cause the thermal degradation of the friction material surface, during which large amounts of volatiles are removed from the phenolic resin matrix, weakening the material leading to an increase in wear rate.

Future work

The various carbonised friction materials examined in this work performed well during continuous drag pin on disc and standard dynamometer testing, however, the carbonisation process may well have reduced the fatigue life of the friction material. This is important as friction materials are subjected to repeated compressive and shear stresses over very many cycles during their working life. Thermal fatigue can also occur as a result of the ever changing thermal conditions within the braking system, which can very from -20°C to 500°C. Clearly there is a need to assess the fatigue properties of carbonised friction materials as well as their economic viability, before they can be seriously considered as an alternative to existing friction materials.
Road testing is also advisable so that the actual wear life of carbonised materials can be gauged with some reliability, and also to ensure that the braking performance of the material is unaffected by dusty or wet conditions.

It has been shown that the inclusion of iron powders in friction materials encourages the formation of protective friction films containing iron oxide. It is worth exploring the possibility that other metal powders such as copper may also form friction films from their oxides, and if so the properties of the films produced could then be characterised.

Fade is largely caused by the lubricating action of the decomposition products of phenolic resin, used as the binder in brake pad materials. From this it followed that one solution to the problem of fade was the removal of the volatile components of phenolic resin by carbonisation, which was the approach used in this work. However, the fade problem may be solved by improving the high temperature stability of phenolic resin. A study of the literature indicates the possibility of using nitrogen modified resins, the additive being based on aniline, which produces a resin said to be stable up to 900°C [89], after an initial heat treatment up to 330°C. Other possibilities are the esterification or etherification reactions with the phenolic resin hydroxyl group. Complex formation using elements such as Ca, Mg, and Zn, or the replacement of the methylene linking group using silicon or sulphur based compounds. In general all methods outlined reduce the oxidative susceptibility of the phenolic hydroxyl or methylene group. However, most of these modifications make the resin unattractive either because

of their associated health hazards or poorer properties, although even marginal improvements in high temperature stability are worth exploring.

In recent years there has been a drive towards reducing the weight of trucks and automobiles to aid fuel economy, which has lead to the development and manufacture of light weight brake systems involving the use of metal matrix composite brake discs, made from aluminium alloys reinforced with particles of silicon carbide. Such materials will start to yield at temperatures as low as 400°C, and so the high temperatures generated in brake systems could potentially result in catastrophic disc wear. Also the use of very abrasive reinforcements like silicon carbide, may lead to heavy brake pad wear. These problems can be addressed to some extent by developing friction materials which deposit thick friction films on to the disc surface, this would then protect the friction material from the abrasive particles within the disc and also reduce temperature effects on the disc. The future development of friction materials tailored for aluminium alloy reinforced discs will present further research opportunities, looking specifically at the physics and chemistry involved in friction film formation.

There has been extensive research into the use of char forming polymer materials as ablatives for use in the aerospace industry. The process of ablation is similar to the processes that occur at a frictional interface, both involve high temperatures which cause the polymeric ablative materials to undergo carbonisation and the loss of volatiles, leaving a carbon backbone which forms a hard char layer. This layer then protects the underlying uncarbonised material for a time until it is eroded from the surface and a new char layer forms [90]. Extensive research has been conducted into the char forming properties of a range of polymeric materials a selection of which is given below:

Table 15. Thermogravimetric Analysis of Some High Temperature Polymers [90].

Type of Polymer	% Residue at indicated temperature (°C)						
	300	400	500	600	700	800	900
Phenolic	98	70	51	46	42	41	40
S- Polyimide	100	99	98	68	62	60	58
O-Polyimide	100	99	97	68	63	60	59
Polybenzimidazole	100	98	97	95	87	81	77
Polyimidazopyrrolone	100	98	95	93	90	88	86
Poly-Schiff base	100	100	99	96	92	88	86
Polysiloxane	99	98	97	95	92	89	89
Polybenzoxazole	100	100	100	95	78	76	74
Polybenzothiazole	100	100	100	98	96	93	90
Polythiazole	96	94	91	78	64	61	60
BBB	100	100	100	100	90	84	83
Polythiazone	100	100	100	100	100	100	91

Clearly some of the more recently synthesised polymers listed above have considerably higher weight residues than phenolic resin, due to the higher degree of cross-linking found in these polymers. It follows that brake materials formulated from such materials would only fade at very high temperatures, making then of great interest to the friction material manufacturer, although the economics of using such resins would also have to be considered.

The physical conditions created during the high temperature ablation of re-entry heat shields illustrated in figure 135, are similar to those produced at the rubbing interface during high temperature braking. Although there are obvious differences between the two situations in that material is removed by mechanical wear processes in friction materials, rather than by erosion, it is felt that some of the modelling techniques used in describing the physical processes which occur during the ablation of phenolic resin based heat shields, could be applied to friction materials. For example a detailed kinetic model which describes the pyrolysis of phenolic resin has been developed, from which material weight loss under a variety of heating conditions can be predicted.

Figure 135

Typical temperature and density profile in a charring ablative body [90].

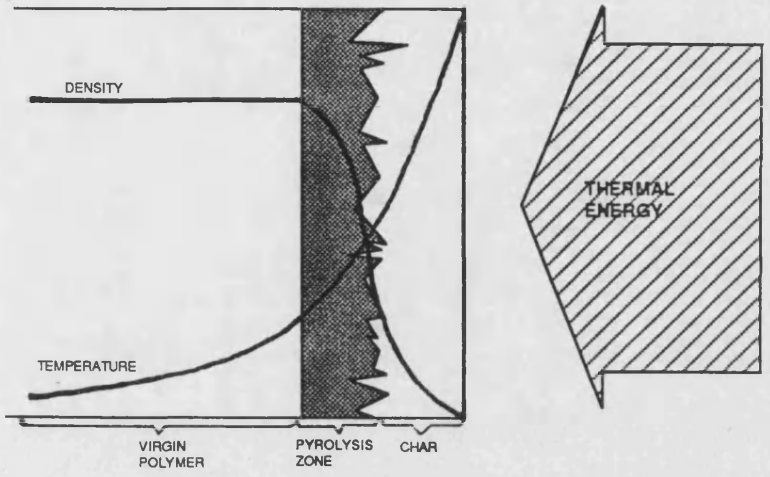

Also complex analytical prediction of the ablation process in phenolic resin has been attempted, involving the modelling of the important physical processes which occur within a char layer including: the heat conduction through the surface char layer into the underlying virgin material, heat and mass transfer due to char removal, and the heat and mass transfer associated with transpiration of the gases due to pyrolysis.

The work reported here has shown that there are a number a factors which need to be considered when attempting to model the tribological behaviour of friction materials. Many of these factors are interconnected as illustrated in figure 136:

Figure 136
Factors affecting the tribological properties of friction materials.

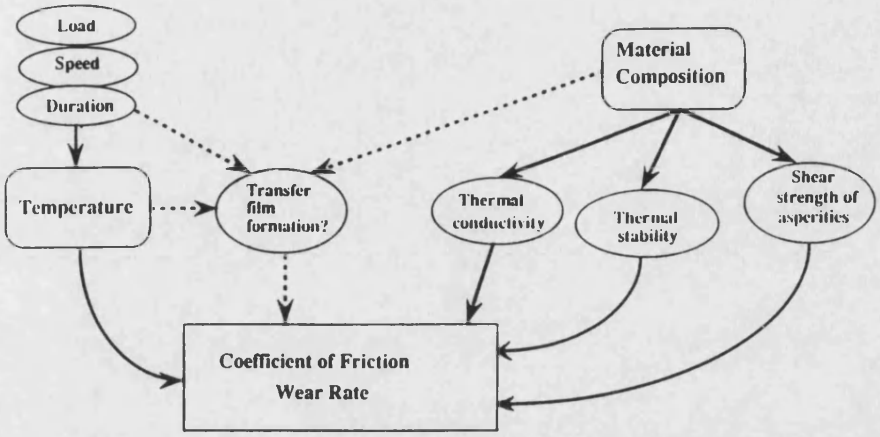

High powered computer software such as neural networks which are now available, are capable of modelling and so predicting the outcome of complex physical processes involving the interaction of many contributing factors. Such analytical techniques maybe well suited to unravelling the complexities of predicting the behaviour and ultimate wear life of friction materials under a variety of conditions, which would be most worthwhile.

Acknowledgements

Firstly I would like to thank my main sponsors the EPSRC, and also my industrial sponsors European Friction Industries who also supplied many of the test materials and arranged all the dynamometer testing.
Harry Reiter was my University supervisor throughout this project, and I'd like to thank him for his pragmatic advise and guidance. I would also like to thank Dr Keith Ellis my industrial supervisor, a busy man who showed constant interest and always managed to find the time to help.
I would also like to acknowledge the contribution made by each member of the technical staff within the department of materials science, who's individual expertise were of great assistance on many occasions. Similarly a special thanks to the Rev. Barry Chapman for his invaluable assistance in producing the x-ray diffraction data presented in this work.
Lastly I am indebted to Toby Hutton who agreed to act as my proof reader, and set about the onerous task with gullible enthusiasm, I thank him for soldiering on to the end.

References

1) Dr K. Ellis, European Friction Industries, .private communication, (Nov. 1991).

2) Kregelskii I.V.,(1965), "Friction &Wear ", Butterworths, London.

3) Herring J.M.Jr. (1967), "Mechanisms Of Brake Fade In Organic Brake Linings", Automotive Engineering Congress, Detroit Mich. pp 1 - 6.

4) Awastai S, Wood J. L. (1988), "C/C Composite Materials For Automotive Brakes", Advanced Ceramic Materials, Vol. 3, No5, pp 449 - 451.

5) Gibson D.W, Taccini G.J. (1989), "Carbon/Carbon Friction Materials For Dry & Wet Brake & Clutch Applications", 40th Annual Earthmoving Industry Conference, Peoria Illinois.

6) Ho S.W, Ho D, Wu K.F, Lin C.S, (1991), "Powder Metallurgy Conference & Exibition, Chicargo Illinois, D910 pp 609 - 612.

7) Ho T.L, Peterson M.B, Ling F.F. (1974),"Effect of Frictional Heating on Brake Materials", Wear, Vol. 30, pp 73-91.

8) Pye A. (1989), The Feasability Of Substitution, in: "Alternatives To Asbestos -The Pros andCons", pp 1 - 67, Chichister, John Wiley & Sons.

9) Ferodo LTD. (1968), "Friction Materials For Engineers", Chorley & Pickersgill, Leeds.

10) Jacko M. J. Ducharme R. T. Somers J.H. (1974), "Brake and Clutch Emissions Generated During Vehicle Operation", SAE Transactions, paper No 730548, pp 1813 - 1831.

11) Scieszka S.F. (1980), "Tribological Phenomena In Steel - Composite Brake Material Friction Pairs" Wear, Vol. 64, pp 367 - 378.

12) Halberstabt M.L, Mansfield J.A, Rhee S.K. (1977),"Effects Of Potassium Titanate Fibre on the Wear Of Automotive Brake Linings", Bendix Corporation Southfield, Michigan. . Int. Conf. on Wear Of Materials, St Louis, April 1977 ASME pp 560-568.

13) Suramaniam N, Brijnaresh R, Sinha F.D, Blum Y.R.C, Dharani L.R. (1990), "Glass Fibre Based Friction Materials", PRIVATE COMUNICATION.

14) Hettinger W.P, Newman J.W, Krock R.P, Boyer D.P. (1986) "Carboflex & Airocarb - Ashlands New Low Cost Carbon Fibre and Carbonizing Products For Future Brake applications, Soc. Automotive Engineers, paper No 860767.

15) Briscoe B.J, Tweedale P.J. (1990), "Aramid Fibre Friction : "Asbestos Replacement In High friction Materials ?", Inst. Of Physics Conference series No 111, pp 81 - 90.

16) Unknown author "Fiberflex @ Ceramic Fibre Reinforcement Of Friction Materials", (1981) The Carborundum Company, Product Applications Data.

17) Washaburgh F.J. (1986), "Encor @ 66 Ultra-Short Fibres For Asbestos-Free Friction Materials", SAE paper No 860630.

18) Lemon P.H.R.B. (1988),"Recent Developments In Phenol Formaldehyde Polymers", Polymer Paint colour Journal, Oct. 1988.

19) Dowson D. (1979), "History Of Tribology", Longman, London.

20) Bowden F.P, Tabor D. (1976), "Friction An Introduction To Tribology", Heinemann, London.

21)Huchings I.M. (1992),"Tribology Friction & Wear Of Engineering Materials", Metallurgy & Materials Science Series, Edward Arnold.

22) Bowden F.P, Tabor D. (1986), "Friction & Lubrication Of Solids (part 1)", Clarendon press Oxford.

23)Edwards C.M. Halling J. (1968), "An Analysis Into The Plastic Deformation of Asperites and It's Relevence To The Value Of Coefficient Of Friction", J Mech. Eng. Sci., No 10, pp 101 - 104.

24) Greenwood J.A, Williamson J.K.P. (1966), "Contact of Nominally Flat Surfaces", Proc. R. Soc. 295, pp 300-319.

25) Burell J.T. (1957-1958), "Surrvey of Possible Wear Mechanisms", Wear, Vol. 1 pp 119-141.

26) Archard, J.F. (1953), "Contact and Rubbing of Flat Surfaces", Jn. Applied Physics, 24 pp 981-986.

27) Halling J. (1988), "Principles Of Tribology", Maccmillan Press London.

28) Oberle T.L. (1951), "Properties Influencing Wear of Metals", Jn. Metals 3 pp 438-9.

29) Lawn B.R, Swain M.V. (1975), Jn Materials Science 10, pp 113-122.

30) Lancaster J.K. (1969), "Abrasive Wear of Polymers" Wear, vol 14, pp. 223-224.

31) Jimbo Y, Mibe T, Akiyama K, Matsui H, Yoshida M, Ozawa A. "Development of High Thermal Conductivity Cast Iron for Brake Disk Rotors", SAE paper No 900002.

32) Rhee S.K. (1971) SAE paper No 710247. Presented at Engineering Congress of Soc. of Automotive Engineers Detroit, Mich. Jan. 1971.

33) Rhee S.K. (1971), "Wear of Metal-Reinforced Phenolic Resins", Wear, Vol. 18, pp. 471-477.

34) Liu T, Rhee S.K. (1976), "High Temperature Wear of Asbestos-Reinforced Friction Materials", Wear, Vol. 37, pp. 291-297.

35) Liu T, Rhee S.K. (1978), "High Temperature Wear of Semi-metallic Disc Brake Pads", Wear, Vol. 46, pp. 213-218.

36) Todorovic J, Douboka C. (1987), "Modelling of Tribological Properties of Friction Materials Used in Motor vehicle Brakes", Inst. Mech. Eng. Conf. - "Friction Lubrication and Wear Fifty Years On", paper No C226/87, Vol. 2, pp 911-916.

37) Douboka C, Todorovic J. (1983) "Linear Wear Hypothesis for the Prediction of Brake Lining Life", Inst. Mech. Eng. Conf. paper No C15/83, pp 13-18.

38) Bros J, Scieszka S.F. (1977), "The Investigation of Factors Influencing Dry Friction In Brakes", Wear, Vol. 41, pp. 271-286.

39) Tawaka K, Ueda S, Nogucki N. (1973), "Fundermental Studies on the Friction of Resin-Based Friction Materials", Wear, Vol 23, pp. 349-365.

40) Harding P.R.J. (1983),"An Investigation into The Operational Wear Life of Disc Brake Pads", Inst. Mech. Eng. Conference Braking of Road Vehicles, Loughborough 1983, paper No C11/83, pp 7-12.

41) Rhee S.K. (1974),"Friction Coefficient of Automotive Friction Materials - It's Sensitivity to Load, Speed, & Temperature" SAE Trans. Vol. 83, paper No 740415, pp 1575-1580.

42) Jacko M.G, Tsang P.H.S, Rhee S.K. (1989),"Wear Debris Compaction and Friction Film Formation of Polymer Composites" Wear vol. 133, pp 23 - 38.

43) Metzler H. "The Brake Rotor - Friction Partner of Brake Linings" SAE paper No 900847.

44) Coyle J.P, Tsang P.H.S. (1983),"Microstructural Changes of Cast Iron Rotor Surfaces & Their Effects on Brake Performance & Wear Resistance", SAE paper No 830534.

45) Chapman B.J, Rizkallah-Ellis A.A.M. "Effect of Surface Finish of Brake Rotors on the Performance of Brakes", Wear. Vol. 57 No2 pp. 345-357.

46) Briscoe B. J, Pogsian A. K, Tabor D. (1974) "The Friction & Wear of High Density Polyethene : The Action of Lead Oxide & Copper Oxide Fillers", Wear, Vol. 27, pp. 19-34.

47) Nikolskii A.V, Kozakov A.T, Kravchenko V.N. (1988),"Dynamics of Change of Chemical State of Friction Surfaces of Metal- Polymer Pair In the Frictional Interaction Proccess", Trenie Iznos, Vol. 9, No 5 pp. 860-869.

48) Rhee S.K, Ludema K.C. (1977), "Mechanisms of Formation of Polymeric Transfer films", Poc. Int. Conf. Wear of Materials, St Louis MO, ASME pp 482-486.

49) Rigney D.A, Chen L.H, Naylor M.G.S, Rosenfield A.R. (1984)"Wear Proccesses In Sliding Systems", Wear, Vol. 100, pp 195-219.

50) Ajayi O.O, Ludema K.C. (1990),"Mechanism of Transfer Film Formation During Repeat Pass Sliding of Ceramic Materials", Wear, Vol. 140, pp. 191-206.

51) Jacko M.G. (1978) "Physical and Chemical Changes of Organic Disc Pads In Service", Wear Vol 46, pp 163 - 175.

52) Liu T, Rhee S.K, Lawson K.L. (1979),"A Study of Wear Rates and Transfer Films of Friction Materials", Proc. Int. Conf. on Wear of Materials 1979, Dearborn, Michigan. ASME New York 1979 pp 595 - 600.

53) Rhee S.K, Jacko M.G, Tsang P.H.S. (1990) "The Role of Friction Film in Friction, Wear and Noise of Automotive Brakes", Wear, Vol. 146, pp. 89-97.

54) Sinha S.K, Biswas S.K. (1992) "Friction & Wear Behaviour of Continuous Fibre as Cast Kevlar-Phenolic resin composite", Jn. Materials Science Vol. 27, pp 3085-3091.

55) Wirth A, Whitaker R. (1992) "The Role of Friction Film Chemistry in Automotive Couples", Presented at Int. Physics Conf. X-ray Optics Microanalysis, Manchester 1992, Ser. No 130, pp 455-460.

56) Wirth A, Whitaker R. (1992)" An Energy Dispersive X-ray & Imaging X-ray Photoelectron Specroscopical Study of Transfer Film Chemistry & its Influence on Friction Coefficient", Jn. of Physics D: Applied Physics Vol. 25, A38-A43.

57) Wirth A, Stone K, Whitaker R. (1992) "A Study of the Relationship Between Transfer Film Chemistry and Friction Performance in Automotive Braking Systems", 10th Annual Brake Colloquium and Engineering Display, Arlington Virginia. SAE paper No 922541.

58) Wirth A, Eggleston D, Whitaker R. (1994)," A Fundamental Tribochemical Study of the Third Body Layer Formed During Automotive friction Braking", Yet To Be Pubished.

59) Hermansson T, Kuyolenstierna C, Nilsson P.H, Borjesson M. (1993), "Some Details Concerning The Uniformity Of Disc Wear In Automotive Disc Brakes as a Function of Third Body Layer Properties", Proc. Int. Congress on Tribology, Vol. 5, pp.422-427.

60) Tsang P.H.S, Jacko M.G, Rhee S.K. (1985), "Comparison of Chase and Inertial Brake Dynamometer Testing of Automotive Friction Materials", Proc. Int. Conf. "Wear of Materials" pp 129.

61) Jacko M.G, Ducharme R.T. (1973), "Simulation & Characterisation of Used Brake Friction Materials & Rotors", SAE Trans. Vol. 82, pp 746-754. paper No 730191.

62) Bark L.S. (1977), "Polymer Changes During Friction Material Performance", Wear Vol. 41, pp 309-314.

63) Fitzer E, Mueller K. Schaefer W. (1971), Chem. Physics of Carbon 7, pp 310-313.

64) Scieszka S.F. (1980), "Tribological Phenomena in Steel-composite Brake Material Friction Pairs" Wear. Vol. 64, pp 367-378.

65) Morterra C, Low M. J. D. (1984), "I.R. Studies of Carbons -VII, The Pyrolysis of Phenol Formaldyhyde Resin", Carbon Vol. 23, No 5, pp. 525-530.

66) Jenkins G.M, Kawamura K. (1976),"Polymeric Carbons- Carbon Fibre, Glass and Char." Cambridge University Press.

67) Lancaster J.K. (1975), "The Friction & Wear of Non-graphitic Carbons", ASLE Transactions Vol. 1, pp.43-54.

68) Yoshida K, Takahashi K, Okuno K, Katagiri G, Iwaki M, Ishitani A, (1988), "Wear Reduction of Glassy Carbon by Li Implantation", Applied Physics Letters 52, (13).

69) Burton R.A, Burton R.G. (1990),"Wear Experiments on Glassy-Carbon Based Materials", Transactions of the ASME 68/Vol. 112, pp 68-72.

70) Dr L. Pardini University of Bath, private communication. (Nov. 1991).

71) Lum R, Wilkins C. W, Robins M, Lyons A.M, and Jones R.P. (1983), "Thermal Analysis of Graphite and Carbon-Phenolic Composites by Pyrolysis-Mass Spectroscopy", Carbon, Vol. 21, No 2, pp 111-116.

72) ASTM D Standard No 790-80 (1980) Standard Test Methods For Flexural Properties of Plastics & Electrical Insulating Materials.

73) Rhee S.K. (1974), "Wear Mechanisms of Asbestos Reinforced Automotive Friction Materials", Wear, Vol 29, pp 391.

74) Nelson J.B. (1967), NASA Tn D3919. (cited by Rhee 1974 ref 73).

75) Friedman H.L. (1965), "Kinetics of Thermal Degradation of Char-Forming Plastics from Thermogravimetry. Application to Phenolic Resins.", J. Polymer Sci. Part C, No 6, pp 183-195.

76) Henderson J.B, Tant M.R, Moore G. R. (1980), "Determination of Kinetic Parameters For the Thermal Decomposition of Phenolic Ablative Materials by a Multiple Heating Rate Method", Thermochimica Acta, Vol. 44, pp 253 - 264.

77) Farmer R.W. (1972), "Phenolic Resin Char-Formation During Hyperthermal Ablation", Thermochimica Acta, Vol. 4, pp 223-238.

78) Stokes E.H. (1995) "Kinetics of Pyrolysis Mass Loss From Cured Phenolic Resin", J. of Thermophysics & Heat Transfer, Vol. 9, No 2, pp 352-358.

79) Dr G Love University of Bath, Centre for Electron Optical Studies, personal communication. (April 1995).

80) Heinrich K.F.J. (1981), "Electron Beam X-ray Microanalysis", Van Nostrand Reinhold Company.

81) Cullity B. D. (1959), "Elements of X-ray Diffraction", 2nd addition, Addison-Wesley Publishing Co, Massachusetts USA.

82) Braithwaite E.R. (1964), "Solid Lubricants And Surfaces" Pergamon Press, Oxford.

83) Kofstad P. (1988), "High Temperature Corrosion", Elsevier Applied Science Publishers Ltd.

84) Borjesson M, Eriksson P, Kuylenstierna C, Nilsson P.H, Hermansson T, (1993), "The Role of Friction Films in Automotive Brakes Subjected to Low Contact Forces", Inst. Mech. Eng. pp 259-267, Paper No C44/026/93.

85) Karpenko G, Kripakevich R. (1962), "Influence of Hydrogen on Properties of Steel", Metalurgizdal, Moscow (pp 2-15).

86) Eyre T.S, Dutta K. (1974), "Some Applications of the Scanning Electron Microscope in Wear Studies", ASLE/ASME Lubrication Conference, Montreal, Canada, Oct 8-10, pp 1-8.

87) Bulk Density Measurement BS- 1902, part IC, (1967).

88) Shaw H. M, Hutton T, Ediringhe M.J. (1992), Jn. of Mat. Sci. Let., Vol. 2, pp 1075 - 1077.

89)Knop A, Pilato A. (1985), "Phenolic Resins," Chemistry Applications and Performance, Future Directions, Springer-Verlag, Berlin pp 144-155.

90) D'Alelio G.F., Parker J.A. (1971), " Ablative Plastics", Marcel Dekker Inc, New York.

91)Pickup I, McEnaney B, Bodsworth L. (1987) "Strength-Structure Relationships for Porouse Glassy Carbons" Proc. International Conf. Carbon 1987, pp 484-485.

Figure i

Inertia dynamometer. A) Front flywheel, B) Rear flywheel, C) Motor, D) Rear brake assembly, E) Drive belt.

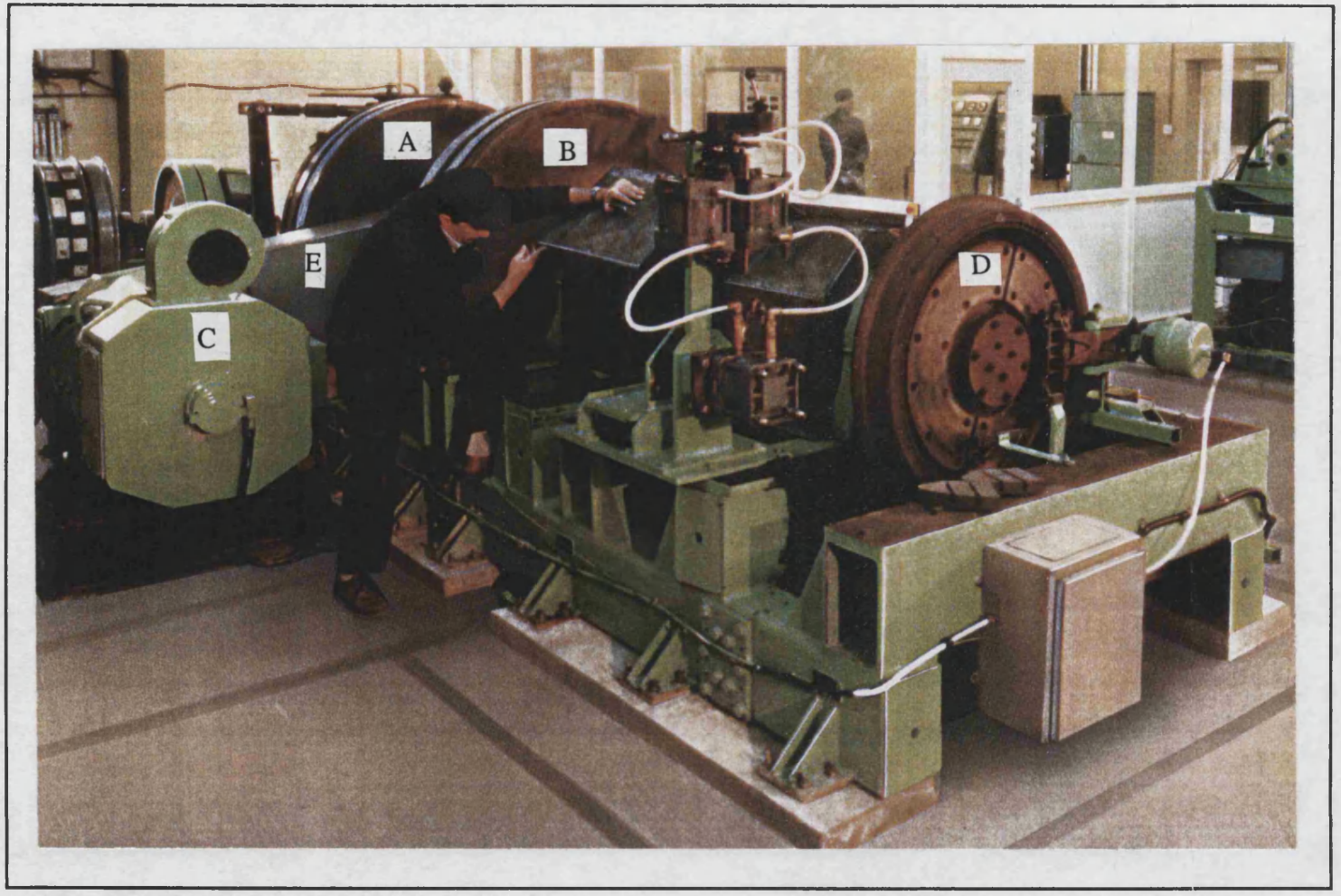

Figure ii

Plan view of a inertia dynamometer, each component marked is listed in the accompanying table (page 233).

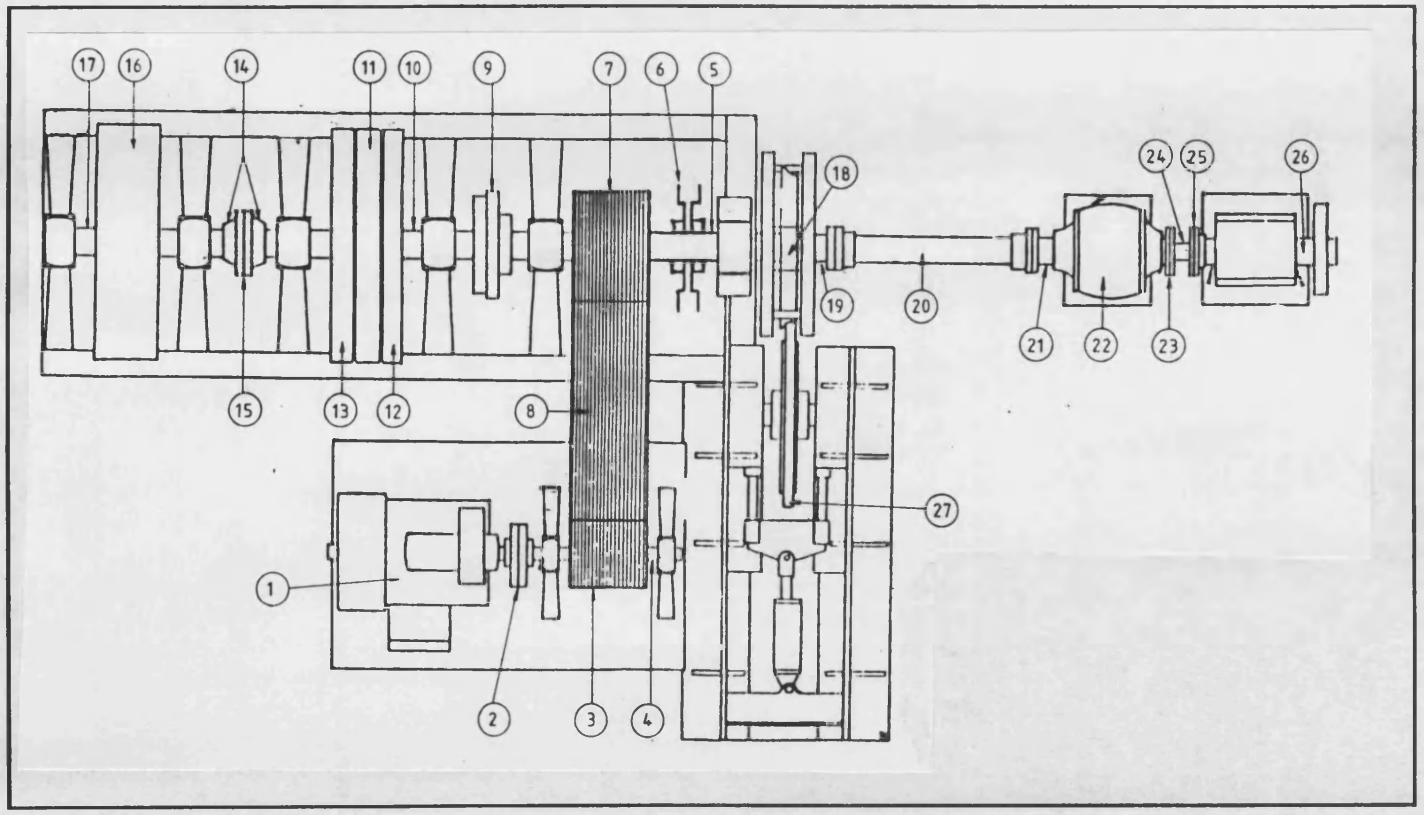

TABLE 1

ITEM NO	DESCRIPTION	INERTIA kgm^2
1	Motor (inertia supplied by manufacturer)	6.5
2	Motor coupling	1.2
3	Small motor pulley (cast iron)	8.1
4	Motor pulley shaft	0.1
5	Test head shaft	2.5
6	Emergency brake (cast iron)	32.5
7	Main shaft driving pulley (cast iron)	49.7
8	Drive belts	8.2
9	Shear pin coupling	5.6
10	Variable flywheel shaft	1.7
11	Fixed flywheel	920.1
12	Single variable flywheel (front)	916.0
13	Single variable flywheel (rear)	916.0
14	Flywheel coupling (Wellman Bibby GFD55)	3.7
15	Grease plate for GFD55 coupling	0.2
16	7.5 t Flywheel	2762.1
17	7.5 t Flywheel shaft	4.2
18	Test head extension coupling	1.1
19	Spacer	1.0
20	Cardan shaft	1.6
21	Gearbox coupling (input)	0.4
22	Gearbox	6.0
23	Gearbox coupling (output)	0.4
24	Rotary torque transducer (including 2 half couplings)	0.9
25	Tailstock coupling	0.4
26	Tailstock shaft	0.4
27	Rail wheel	128.1